

The copyright of this thesis vests in the author. No quotation from it or information derived from it is to be published without full acknowledgement of the source. The thesis is to be used for private study or non-commercial research purposes only.

Published by the University of Cape Town (UCT) in terms of the non-exclusive license granted to UCT by the author.

Dimerization of naphtha-range Fischer-Tropsch olefins
into diesel-range products over zeolite H-ZSM-5
and amorphous silica-alumina

by

Molladi Andrew Maseloane

Submitted in fulfillment of the requirements of the degree of

Master of Science in Chemical Engineering

August 2011



Centre for Catalysis Research
Department of Chemical Engineering
University of Cape Town
Cape Town
South Africa

DEDICATION

This work is entirely dedicated to the memory of my late supervisor and mentor

Dr. Chris Nicolaides.



(1953-2009)

DECLARATION

I know the meaning of plagiarism and declare that all the work in the document, save for that which is properly acknowledged, is my own.

Signed by candidate

Date

Molladi Andrew Maseloane

University of Cape Town

ACKNOWLEDGMENTS

Glory and thanks to God, for never leaving my side during the times of this work. Without His mercy and presence, completing this dissertation would have not been possible.

I extend my immeasurable gratitude to my wife, Liziwe, and my son, Bokang, for their understanding and allowing me the valuable time needed during this thesis. A big thank you to my mother, Setlhoko, and grandmother for the well-wishes and hopeful prayers in all life challenges. Also to the Maseloane family at large.

I also want to thank the following:

Dr. Chris Nicolaides, as my project leader and supervisor. Under his leadership, I have learnt much about the world of zeolite catalysis, ways of approaching research and being critical and objective in addressing issues of catalysis (logical and thoughtful). Working with Chris has taught me his ways of scrutinizing results, proof-reading of printed documents and polishing reports. I am thankful for his meticulous guidance throughout the duration of the project and for being a tremendous source of inspiration.

Michelle Huyser and Dr. Cathy Dwyer for initiating my move from Homogeneous to Heterogeneous Catalysis and providing me with the opportunity to study further.

Prof. Jack Fletcher for his role as my supervisor and providing guidance where necessary.

My co-supervisor, Walter Böhringer, for not only taking over from where Chris left off, but also thoroughly questioning and refining my thesis to withstand academic scrutiny. Also for his detailed and perceptive comments that contributed immensely to the shape and clarity of the final thesis.

Drs. Des Young and Frans Prinsloo for their managerial support.

Chantelle Crause for coordinating the supply of 1-hexene and 1-octene feeds.

Megan Kirk for her assistance in ^1H -NMR analysis and interpretation of the results using the in-house method developed by her.

Rudi Britz, Kelvin Jacobs and Mazwi Ndlovu from Sasol Fuels Research for the characterization of my products with regard to diesel properties.

Petrus Makgoba and Genevieve Joorst for their encouragement and interest in the dimerization project.

Ramabitsa Ramatsebe for his technical support.

Tebogo Manong for his support and hospitality during the write-up and thesis-polishing times.

Thebe Mokone, Tawanda Sango, Yolanda Gwagwa, Mike Sibiya and Mariam Ajam for their encouragement.

Savi Govender for always supplying the urgently requested articles needed for this thesis.

Süd Chemie, through Alan Thompson, and Albermale for supplying the H-ZSM-5 and ASA catalysts, respectively.

Sasol Technology R&D for the financial support, permission to carry out the research on this work, present and publish.

SYNOPSIS

The “straight run” diesel fuel produced by Sasol’s Low Temperature Fischer-Tropsch (LTFT) and Slurry Phase Distillate (SPDTM) processes (with most of the production capacity located in Qatar) consists mostly of linear paraffins and is, therefore, of a very high cetane number of about 70-75, but has very poor cold-flow properties and is too low in density with regard to diesel specifications. Since the South African market requires a cetane number of only 45 (South African Bureau of Standards, SABS 342) and no superior cold flow properties, “straight run” FT diesel can be used as a blending stock to upgrade petroleum-derived higher density and lower cetane number diesel fuel.

However, most of the product from the slurry-phase distillate process is in fact wax and is hydrocracked to a moderately branched diesel fuel that meets both high cetane number and cold-flow property requirements (but still lacks density).

The “straight run” diesel fraction from Sasol’s High Temperature Fischer-Tropsch (HTFT) and Sasol Advanced Synthesis (SAS) processes utilized by Sasol’s Synfuels refineries in Secunda, South Africa, after olefin hydrogenation, provides the basis of Sasol’s South African diesel pool. The HTFT diesel has a rather high content of (mono-)aromatic hydrocarbons and thus meets the current density specifications. However, the HTFT/SAS process is optimized towards naptha-range hydrocarbons and the product

constitutes about 70 wt% being C₅-C₁₂ olefins while the rest is mostly lower olefins, C₂-C₄. The selectivity to diesel-range hydrocarbons is, therefore, rather low. As a result, Sasol South Africa is short of diesel-range hydrocarbons.

Sasol Synfuels Refineries in Secunda uses a modification of UOP's Catalytic Polymerization "CatPoly" process, utilizing a "solid phosphoric acid" (SPA) catalyst, to produce higher boiling products. Even though CatPoly produces a high quality gasoline and good jet fuel SPA is not a good catalyst choice for producing good diesel since the oligomerization product is highly branched. The diesel obtained from the CatPoly process has a cetane number of only 29-30, which is much lower than the South African Bureau of Standards' minimum requirement of 45, but has excellent cold flow properties and can, therefore only be used as a blendstock.

Diesel fuel can also be produced by oligomerizing lower olefins using zeolite H-ZSM-5 as the catalyst. Oligomerization processes that are using H-ZSM-5 as the catalyst are Mobil's "Mobil Olefins to Gasoline and Distillates" (MOGD) process and PetroSA's "Conversion of Olefins to Distillate" (COD) process. Both the MOGD and the COD process are not "true" oligomerization processes in that there is both a forward and a reverse reaction, because of the rather high reaction temperatures used and conversion driven close to olefin carbon number equilibrium distribution and isomers equilibrium distribution.

However, due to the shape-selective constraints imposed by the pore system of the H-ZSM-5 zeolite oligomers are less branched and the resulting diesel fuel has, therefore, a higher cetane number than the diesel obtained from Sasol's CatPoly process. The branching in the MOGD diesel-range product is limited to an average of 2-3 methyl branches per molecule, which are more or less randomly distributed over the carbon chain, but typically at distances of about 5 carbon atoms. Cetane numbers obtained in the MOGD and COD processes are in the ranges of 55-56 and 51-54 respectively.

In this study, the dimerization of 1-hexene and 1-octene (as model compounds for Fischer-Tropsch naphtha-range olefins) into diesel-range olefins was carried out in a tubular, continuous flow fixed-bed reactor, in the liquid phase, over zeolite H-ZSM-5 and an amorphous silica-alumina (ASA) catalyst. Both catalysts were in the form of extrudates. Reaction temperatures were varied widely between 50 and up to 210 °C, reaction pressure was varied between 10 and 40 bar and WHSV was varied between 0.15 and 3.0 g/g.h. Pressure was always set high enough to keep the reaction mixture in the liquid phase at the reaction temperatures applied. Typical reaction conditions were 150-170 °C, 40 bar and WHSV of 0.5-1.0 g/g.h.

Gas chromatographic analysis of the product mixtures, ¹H-NMR analysis of selected samples (after hydrogenation) for the extent of branching, and characterization of selected product fractions (after hydrogenation) for diesel fuel properties were carried out. For instance, the C₁₆ dimerization product

from 1-octene, obtained at 50% oligomerization conversion of 1-octene had a cetane number (after hydrogenation over Pt/C at 20 bar and ambient temperature) of 57.

The average number of branches per dimer molecule was somewhat higher than 2. Values between 1.99 and 2.52 were obtained. Conversion was found to be the major parameter that determined the extent of branching. No differences in branching between dimers obtained from different catalysts and feed olefins were seen, when compared at the same temperature and similar conversions. The mostly di- or slightly higher branched dimers obtained at medium conversions resulted in high cetane numbers of around 55-60 for the hydrogenated 1-octene dimer (i.e. C₁₆) fractions. Temperature was found to have an additional effect on branching and thus on the cetane number, in that it not only boosts reaction rate and conversion but also accelerates isomerisation rates so that, at a given conversion, it produces a slightly more branched product and, therefore, a somewhat lower cetane number. Hence, an increase in temperature will come with a decrease in cetane number.

Cetane numbers of (hydrogenated) naphtha-range olefin dimers are significantly higher than those obtained from commercial synthetic diesel-producing processes such as CatPoly, MOGD and COD. The dimerization/trimerization product, after hydrogenation, meets or exceeds all South African diesel-fuel specifications except density, making it a valuable blendstock for upgrading low quality, high density (crude oil derived) diesel fractions.

As the study revealed, potential industrial scale production of dimer/trimer diesel from naphtha-range olefins will neither need to utilize an expensive zeolite catalyst nor need to charge expensive pure 1-olefins, as done in this study. Instead, a cheap amorphous silica-alumina (ASA) catalyst may be first choice, while the feed may be any naphtha-range olefin or olefin containing stream from the Fischer-Tropsch refinery, in particular the 'waste' or residual olefin streams from separation processes, e.g. those used for the recovery of specific chemicals.

The amorphous material tested in this study (a mesoporous silica-alumina with a molar silica/alumina ratio of 10) showed a higher activity than the crystalline material tested (medium pore zeolite H-ZSM-5 with a molar silica/alumina ratio of 90).

The ASA catalyst exhibited little coking and showed good long term stability (losing about 25% of its initial activity during 5 weeks on stream), comparable to the stability of the zeolite catalyst. Silica-alumina catalysts are also known to be regenerable when coked and to be fairly insensitive to moisture and oxygenates contained in the reaction mixture.

No difference was observed between the zeolite and the ASA catalyst with regard to product branching. At medium conversion slightly more than two branches per dimer molecule were obtained from α -olefins. This outcome reflects the rapid double bond isomerization of the feed olefins (to an equilibrium pool that is dominated by internal olefins). In addition, this result

suggests that, under the reaction conditions applied (liquid phase), dimerization reactions over the medium-pore acid zeolite catalyst H-ZSM-5 were “chemically controlled” and did not take place inside the shape-selectively constraining pore system, but on the external surface of the zeolite crystallites, whereas on the amorphous silica-alumina catalyst no such constraints exist. This was confirmed by poisoning the external surface sites of the zeolite crystallites with bulky organic nitrogen compounds that were not able to penetrate into the pore system to occupy the internal sites. The selective poisoning pretreatment rendered the zeolite crystallites inactive, showing that the oligomerisation reaction was catalysed by sites located on the external surface of the zeolite crystallites.

As mentioned above, long term stabilities of the ASA catalyst and the H-ZSM-5 were similar. The expected superiority of the medium pore zeolite over the amorphous material in that regard was not observed. The dimerization reaction takes place on the external surface of the zeolite crystallites where the shape-selective constraints that suppress coke formation inside the zeolite pores do not exist. Hence, the superiority of the H-ZSM-5 catalyst with regard to coking can not materialize.

However, with regard to the carbon number distribution, products from the two catalysts differed significantly. Trimer selectivity was much higher over the ASA catalyst (essentially at the expense of the dimers) compared to that over the zeolite. Correspondingly, cracking selectivity was lower. It appears that this may be related to moderate mass transfer control by the mesoporous

ASA catalyst extrudates that reduces intermediate selectivity (to the dimers) in favour of secondary products (the trimers). Over H-ZSM-5, in contrast, the pore system of the extrudates outside of the zeolite crystallites, that is all the pores and void spaces between the external surface of the zeolite crystallites and the external surface of the extrudate particles they are shaped into, is macroporous and spacious and appears not to be mass transfer controlling, or much less so.

However, a small percentage of the reacted olefins appear to have entered the micropore system of the zeolite indeed but they were cracked down, after initial dimerization, on their way out of the much more mass transfer controlling micropore environment of the zeolite. This results in the higher cracking selectivity obtained over H-ZSM-5 in contrast to ASA.

With regard to possible feedstocks it appears that any naphtha-range olefin or olefin containing feedstock, including any kind of such stream that may come from the Fischer-Tropsch refinery, may be suitable for dimerization/trimerization to diesel.

The longer carbon chain feed, octene, was found to be less reactive towards dimerization than the shorter carbon chain feed, hexene, but more reactive towards cracking, irrespective of the catalyst employed. The former could be related to the lower concentration of functional groups (the double bonds) per unit mass or volume of the longer carbon chain feed compared to the shorter carbon chain feed, while the latter appears to be related to the higher molecular mass or larger chain length of the cracking precursors, the dimers and trimers.

The best results obtained during this screening-like study (under conditions that were not optimized) were from 1-hexene conversion over the ASA catalyst. High 1-hexene conversion to other carbon number products, of almost 90%, and dimer plus trimer selectivity of almost 90 wt% at low temperatures of 150 °C and WHSV of 0.5 g/g.h was obtained when using the ASA catalyst. In addition, half of the around 10 wt% cracked products were compounds boiling higher than the original monomer, making the recycling expenditures much less. Operating pressures of less than 10 bar, with feed and products in the liquid phase and no gases to compress, as well as operating temperatures of around 150 °C, are within the range of conditions that are favourable to deal with from an engineering and operational point of view.

CONTENTS

DEDICATION.....	i
DECLARATION.....	ii
ACKNOWLEDGMENTS.....	iii
SYNOPSIS.....	vi
CONTENTS.....	xiv
TABLE OF CONTENTS.....	xv
LIST OF FIGURES.....	xxii
LIST OF TABLES.....	xxviii
LIST OF ABBREVIATIONS.....	xxxi
LIST OF SYMBOLS.....	xxxiii

TABLE OF CONTENTS

CHAPTER 1.....	1
1. BACKGROUND.....	1
1.1 References.....	6
 CHAPTER 2.....	 10
2. LITERATURE REVIEW.....	10
2.1 Olefin dimerization and oligomerization.....	10
2.1.1 Metal catalysed olefin oligomerization – the coordinative mechanism....	11
2.1.1.1 Metal catalysed olefin dimerization and oligomerization.....	12
2.1.1.2 Homogeneous catalysts for olefin dimerization and oligomerization.....	13
2.1.1.3 Carbon number distribution.....	14
2.1.1.4 Industrial processes for ethene oligomerization to α -olefins.....	17
2.1.1.5 The oligomerization of higher olefins.....	18
2.1.1.6 Industrial processes for the oligomerization of higher olefins.....	19
2.1.1.7 Dimerizing naphtha-range olefins to diesel-range products over homogeneous catalysts?.....	21
2.1.2 Acid catalysed olefin oligomerization – the carbenium ion mechanism..	22
2.1.2.1 Fundamentals of acid catalyzed olefin oligomerization.....	22
2.1.2.1.1 Mechanism of 1-hexene dimerization and typical products.....	24
2.1.2.1.2 Conjunct oligomerization.....	28
2.1.2.2 Industrial processes for the oligomerization of olefins to fuels over acid catalysts.....	30

2.1.2.2.1	The CatPoly process, using solid phosphoric acid.....	31
2.1.2.2.2	The MOGD process.....	34
2.1.2.2.3	The COD process.....	36
2.1.3	Radical induced olefin oligomerization – the free radical mechanism.....	37
2.1.4	Comparison of the different mechanisms and types of catalysis.....	37
2.2	Zeolites and other alumina-silicates.....	39
2.2.1	Zeolite structures and chemical composition.....	39
2.2.2	Zeolite channel structures and sizes.....	41
2.2.3	Aluminum content.....	43
2.2.4	Zeolite catalysis.....	44
2.2.5	Catalysis by Brønsted acid sites.....	45
2.2.6	The use of zeolite catalysts in industrial processes.....	47
2.2.7	Other alumina-silicates than zeolites.....	48
2.2.7.1	Amorphous silica-alumina.....	48
2.2.8	Shape-selectivity of zeolites and related microporous materials.....	51
2.2.9	Shape selective catalysis over external zeolite crystallite surface.....	53
2.3	The use of H-ZSM-5 as a shape-selective catalyst in olefin oligomerization...	56
2.3.1	Kinetics and thermodynamics of olefin oligomerization over H-ZSM-5...	58
2.3.1.1	Limited branching over H-ZSM-5.....	60
2.3.1.2	Rapid double bond isomerization.....	63
2.3.1.3	Effect of reaction conditions on carbon number distribution and type of products – kinetic and thermodynamic control.....	66
2.3.1.4	Effect of H-ZSM-5 silica/alumina ratio on activity and selectivity.....	72

2.3.1.5	Fouling of H-ZSM-5 catalyst	72
2.4	Dimerization/oligomerization of light and naphtha-range olefins over alumino-silicates different from H-ZSM-5 and other solid acid catalysts ..	74
2.4.1	Dimerization/oligomerization of 1-hexene over different solid acid catalysts	75
2.4.2	Rapid H-transfer over wide pore zeolites	79
2.4.3	Summary – apparent advantages of using H-ZSM-5 as catalyst in olefin oligomerization	80
2.5	Dimerization and oligomerization of olefins over external crystallite surface-modified zeolite catalysts	80
2.5.1	Crystal size effect	81
2.5.2	Selective blocking and poisoning of the external sites of zeolite crystallites	81
2.5.3	Selective poisoning of the internal sites of zeolite crystallites	89
2.6	Summary of the findings described in Sections 2.1 – 2.5	90
2.7	Effect of mass transfer control on consecutive reactions	94
2.7.1	The Thiele Modulus	94
2.7.2	Effect of mass transfer limitations on intermediate yield and selectivity ..	95
2.8	References	100
CHAPTER 3		110
3.	OBJECTIVES, HYPOTHESIS AND KEY QUESTIONS	110
3.1	The objective of this study	110
3.2	Hypothesis	112
3.3	Key questions	114
3.4	References	115

CHAPTER 4	117
4. EXPERIMENTAL AND METHODS	117
4.1 Chemicals and catalysts used in this project	117
4.2 Reactor set-up and configuration	118
4.3 Experimental procedure	121
4.3.1 Poisoning and use of poisoned H-ZSM-5 catalysts	123
4.4 Product quantification and analysis	124
4.4.1 GC analysis and GC data evaluation	124
4.4.2 ¹ H-NMR analysis	126
4.4.2.1 Sample preparation	126
4.4.2.2 Recording and evaluation of ¹ H-NMR spectra	127
4.4.3 Analysis of fuel properties	132
4.5 References	135
CHAPTER 5	137
5. RESULTS	137
5.1 Dimerization of 1-hexene over H-ZSM-5 catalyst	138
5.1.1 Searching “optimum” reaction temperature	139
5.1.2 Start-up effects and replication of experiments	142
5.1.3 Catalyst activity and deactivation as a function of time-on-stream	143
5.1.4 Effect of temperature on catalyst activity, catalyst deactivation and product branching	146
5.1.5 Effect of pressure on catalyst activity and selectivity	149

5.1.6	Effect of space velocity on catalyst activity, catalyst deactivation and product branching.....	151
5.1.7	Effect of poisoning of the external surface of the H-ZSM-5 zeolite crystallites on catalyst activity for 1-hexene dimerization.....	154
5.1.7.1	Poisoning with 2,4,6-collidine.....	154
5.1.7.2	Poisoning with 2,6-di- <i>tert</i> -butylpyridine.....	156
5.2	Dimerization of 1-octene over H-ZSM-5 catalyst.....	157
5.2.1	Searching “optimum” reaction temperature.....	158
5.2.2	Effect of time-on-stream on catalyst activity.....	159
5.2.3	Effect of varying space velocity.....	160
5.2.4	Reactivities of <i>n</i> -hexene and <i>n</i> -octene feeds over H-ZSM-5.....	160
5.2.5	Properties of the hydrogenated 1-octene dimer fraction with respect to use as diesel fuel.....	161
5.3	Dimerization over amorphous silica-alumina (ASA) compared with zeolite H-ZSM-5.....	163
5.3.1	Effect of reaction temperature on the dimerization of 1-hexene over amorphous silica-alumina.....	163
5.3.2	Catalyst activity/deactivation as a function of time-on-stream for the dimerization of 1-hexene over the ASA catalyst.....	167
5.3.3	Dimerization of 1-octene over amorphous silica-alumina.....	169
5.4	Summary of results.....	172
5.5	References.....	175

CHAPTER 6	177
6. DISCUSSION AND CONCLUSIONS	177
6.1 Comparison of catalysts	177
6.1.1 Catalyst activity	177
6.1.2 Catalyst stability	178
6.1.3 Carbon number selectivity	180
6.1.3.1 Effect of temperature on carbon number selectivity	180
6.1.3.2 Effect of conversion on carbon number distribution	183
6.1.3.2.1 Summary of the conversion effects	184
6.1.3.3 Effect of catalyst type on carbon number distribution	185
6.1.3.4 Effect of mass transfer control on carbon number distribution	196
6.1.4 Branching of the dimers	200
6.1.4.1 Effect of double bond isomerization in the feed on branching	200
6.1.4.2 Theoretical analysis of <i>n</i> -hexene dimerization and dimer branching	201
6.1.4.3 Experimental results for <i>n</i> -hexene and <i>n</i> -octene dimer branching	205
6.2 Comparison of feeds	207
6.2.1 Reactivity of the two different feeds	207
6.3 Product properties with respect to use as diesel fuel	209
6.4 Conclusions	212
6.4.1 Dimerization product properties and quality	212
6.4.2 Optimum reaction conditions	213
6.4.3 Catalyst of choice	213
6.4.4 Any naphtha-range olefins may be fed	214
6.5 References	215

CHAPTER 7	217
7. RECOMMENDATIONS	217
APPENDIX (DATA)	219
1. 1-Hexene dimerization over H-ZSM-5 catalyst	219
2. 1-Octene dimerization over H-ZSM-5 catalyst	224
3. 1-Hexene dimerization over ASA catalyst	227
4. 1-Octene dimerization over ASA catalyst	227

LIST OF FIGURES

Figure 2-1:	Coordinative olefin oligomerization mechanism in the presence of a nickel complex.....	12
Figure 2-2:	Reaction scheme for the “true” trimerization of propene over a solid acid catalyst.....	23
Figure 2-3:	Schematic representation of the mechanism for the dimerization of linear molecules with internal double bonds (here two 3-hexene molecules) over a Brønsted acid catalyst to produce a double branched dimer.....	24
Figure 2-4:	Schematic representation of the mechanism for the dimerization of 1-hexene over a Brønsted acid catalyst to produce a single branched dimer.....	25
Figure 2-5:	Examples of <i>n</i> -hexene dimerization reactions leading to monobranched, dibranched and, illustrated by a single example, tribranched C ₁₂ products.....	26
Figure 2-6:	Mechanisms of by-product formation during “conjunct” oligomerization over an acid catalyst.....	29
Figure 2-7:	Mechanism of propene oligomerization in the presence of H ₃ PO ₄ as catalyst.....	32
Figure 2-8:	Some elementary building units of zeolites: SiO ₄ and AlO ₄ tetrahedra, forming secondary building units and then different zeolite structures.....	40
Figure 2-9:	Schematic representation of the three-dimensionally interconnected channel system and projection of the structure of zeolite ZSM-5.....	42
Figure 2-10:	Diffusion in catalysis over a porous solid: the pores are occupied by adsorption from the gas or liquid phase, after which the adsorbed species diffuse to the active centres.....	45

Figure 2-11:	Formation of Lewis acid sites from two Brønsted acid sites	46
Figure 2-12:	Schematic representation of the three “classical” types of shape-selectivities	52
Figure 2-13:	Shape-selective environments in different sections of the zeolite surface structure	55
Figure 2-14:	Infrared analysis of the liquid product obtained from the conversion of propene over silica-alumina “Si/Al” compared to that obtained over H-ZSM-5	57
Figure 2-15:	MOGD model reaction path for propene feed	59
Figure 2-16:	Comparison of calculated olefin equilibrium distributions under different boundary conditions and experimentally determined distributions from conjunct oligomerization reaction over H-ZSM-5	61
Figure 2-17:	Limited methyl branching of the propene oligomerization/cracking products obtained over shape-selective H-ZSM-5 versus those expected over a non shape-selective true oligomerization catalyst	62
Figure 2-18:	Hexene isomer distribution obtained during oligomerization of 1-hexene over H-ZSM-5	65
Figure 2-19:	Model predictions for the effects of temperature and pressure on the average carbon number of the product mixture obtained from single-pass propene (conjunct) oligomerization over H-ZSM-5	67
Figure 2-20:	Effect of temperature on “restricted” olefin equilibrium distribution over H-ZSM-5	68
Figure 2-21:	Effect of temperature on the carbon number distribution of the products from propene oligomerization over H-ZSM-5	69
Figure 2-22:	Effect of space velocity on the product-carbon-number distribution from the conversion of propene over H-ZSM-5	70

Figure 2-23:	Conversions and oligomer selectivities obtained in the oligomerization of 1-hexene over different catalysts of identical $\text{SiO}_2/\text{Al}_2\text{O}_3$ ratio.....	78
Figure 2-24:	Bulky pyridine type and organophosphorus compounds used for the poisoning of the external surface acid sites of zeolites.....	83
Figure 2-25:	Effect of poisoning of the external surface of H-ZSM-23 on methyl branching in the C_{12+} fraction obtained from the oligomerization of propene.....	86
Figure 2-26:	Yield of primary product B as influenced by the ratios of reaction rate constants k , diffusivities D and catalyst particle dimensions r_{\dots}	96
Figure 2-27:	The conversion of methanol (MeOH) to dimethyl ether (DME) and hydrocarbons ($[\text{CH}_2]$) over H-ZSM-5 catalysts of different crystallite sizes but similar $\text{SiO}_2/\text{Al}_2\text{O}_3$ ratios.....	98
Figure 4-1:	The dimerization reactor set-up.....	119
Figure 4-2:	Schematic representation of a loaded reactor.....	120
Figure 4-3:	Temperature profile in the catalyst bed.....	121
Figure 4-4:	GC traces of the product mixtures obtained from the conversion of 1-hexene and 1-octene.....	125
Figure 4-5:	$^1\text{H-NMR}$ spectrum of the C_{12} paraffin sample obtained from hydrogenating the C_{12} product from 1-hexene dimerization over the H-ZSM-5 catalyst.....	128
Figure 5-1:	Volcano curve from 1-hexene dimerization (H-ZSM-5 catalyst).....	141
Figure 5-2:	Repeatability of 1-hexene conversion in dimerization experiments (H-ZSM-5 catalyst).....	142
Figure 5-3:	Performance of the H-ZSM-5 catalyst over a prolonged time on stream.....	144
Figure 5-4:	1-Hexene dimerization conversion and major product yields.....	146

Figure 5-5:	Effect of temperature on C ₆ = conversion in 1-hexene dimerization experiments.....	147
Figure 5-6:	Effect of pressure on C ₆ = conversion in 1-hexene dimerization experiments (H-ZSM-5 catalyst).....	149
Figure 5-7:	Effect of WHSV on conversion and major product yields (H-ZSM-5 catalyst).....	152
Figure 5-8:	Effect of adding 2,4,6-collidine to the 1-hexene feed.....	155
Figure 5-9:	Dimerization of poisoned 1-hexene feed over H-ZSM-5 catalyst whose external surface was pre-poisoned with 2,6-di-tert-butylpyridine	156
Figure 5-10:	“Volcano curve” from 1-octene dimerization (H-ZSM-5 catalyst).....	158
Figure 5-11:	Catalyst deactivation as a function of time-on-stream during the dimerization of 1-octene (H-ZSM-5 catalyst).....	159
Figure 5-12:	Comparison of the volcano curves obtained from 1-hexene dimerization over H-ZSM-5 and amorphous silica-alumina (ASA)....	165
Figure 5-13:	Catalyst activity/deactivation as a function of time-on-stream during the dimerization of 1-hexene over ASA.....	166
Figure 5-14:	Catalyst activity/deactivation as a function of time-on-stream during the dimerization of 1-octene over ASA.....	169
Figure 5-15	Temperature dependence of 1-octene dimerization (ASA).....	170
Figure 6-1:	Effect of reaction temperature on 1-hexene conversion and selectivity over H-ZSM-5 and amorphous silica-alumina (ASA).....	181
Figure 6-2:	Effect of reaction temperature on 1-octene conversion and selectivity over H-ZSM-5 and amorphous silica-alumina (ASA).....	182
Figure 6-3:	Effect of WHSV on 1-hexene conversion and carbon number fraction selectivity over H-ZSM-5.....	184

Figure 6-4	Product selectivities as a function of conversion from the dimerization of 1-hexene over H-ZSM-5 at 170 °C.....	186
Figure 6-5:	Product selectivities as a function of conversion from the dimerization of 1-hexene over H-ZSM-5 at 50-210 °C.....	188
Figure 6-6:	Product selectivities as a function of conversion from the dimerization of 1-hexene over ASA at 50-210 °C.....	189
Figure 6-7:	Product selectivities as a function of conversion from the dimerization of 1-octene over H-ZSM-5 at 100-210 °C.....	191
Figure 6-8	Product selectivities as a function of conversion from the dimerization of 1-octene over ASA at 150-210 °C.....	193
Figure 6-9	Degree of branching of the dimers as a function of conversion as obtained from the dimerization of the two feeds, 1-hexene and 1-octene, over H-ZSM-5 and ASA at different reaction conditions....	205
Figure 6-10	Cetane number of C ₁₆ fraction obtained from 1-octene dimerization over H-ZSM-5 (hydrogenated).....	209

LIST OF TABLES

Table 2-1:	MOGD diesel fuel (hydrogenated oligomerizate) product quality.....	36
Table 2-2:	Typical composition of the hydrogenated COD diesel fuel.....	63
Table 2-3:	Types of branching of the iso-paraffins present in the COD diesel fuel.....	63
Table 2-4:	Comparison of pentene product-isomer-distributions from different feedstocks with the equilibrium distribution.....	64
Table 2-5:	Typical composition of the hydrogenated COD diesel fuel.....	71
Table 4-1:	Chemicals and catalysts used.....	117
Table 4-2:	Percentages of protons present as CH ₃ 's, CH ₂ 's and CH's (normalized) in the hydrogenated dimers from <i>n</i> -hexenes.....	130
Table 4-3:	Fuel properties tested and definitions.....	133
Table 5-1:	Experiments conducted in this project.....	137
Table 5-2:	Simulated equilibrium isomer distribution of fed <i>n</i> -hexenes at 170 °C and 40 bar (liquid phase).....	139
Table 5-3:	Average degree of branching (1H-NMR results) of the C ₁₂ paraffin samples obtained from combining and hydrogenating all of the 1-hexene dimerization product samples collected at 150, 160 and 170 °C (H-ZSM-5 catalyst).....	149
Table 5-4:	Effect of pressure on 1-hexene dimerization during repeat pressure series (H-ZSM-5 catalyst).....	150
Table 5-5:	Average degree of branching (by ¹ H-NMR) in the distilled-off and hydrogenated C ₁₂ fractions from two 1-hexene dimerization runs (H-ZSM-5 catalyst).....	153
Table 5-6:	Simulated equilibrium isomer distribution of <i>n</i> -octenes at 170 °C and 40 bar (liquid phase).....	157

Table 5-7:	Properties of the C ₁₆ paraffins obtained from hydrogenating the C ₁₆ olefin fraction of the 1-octene dimerization product (H-ZSM-5 catalyst) and of other diesel fuels from olefin oligomerization.....	162
Table 5-8:	Trimer yields and selectivities from 1-hexene dimerization over H-ZSM-5 and ASA catalyst at equal temperature, pressure and conversion.....	166
Table 5-9:	Degrees of branching derived from ¹ H-NMR analyses of hydrogenated C ₁₂ fractions from 1-hexene dimerization over the H-ZSM-5 and ASA catalysts.....	167
Table 5-10:	Cetane numbers and degrees of branching derived from ¹ H-NMR analyses of the hydrogenated C ₁₆ fraction from 1-octene dimerization at “optimum” reaction conditions over the H-ZSM-5 and ASA catalysts.....	171
Table 6-1:	Sources of data points from 1-hexene dimerization experiments over H-ZSM-5 catalyst used to construct Figure 6-4.....	185
Table 6-2:	Sources of data points from 1-hexene dimerization experiments over ASA catalyst used to construct Figure 6-6.....	189
Table 6-3:	Sources of data points from 1-octene dimerization experiments over H-ZSM-5 catalyst used to construct Figure 6-7.....	191
Table 6-4:	Sources of data points from 1-octene dimerization experiments over ASA catalyst used to construct Figure 6-8.....	192
Table 6-5	Dimer, trimer and cracked product selectivities selectivities from 1-hexene dimerization over H-ZSM-5 and ASA catalyst at identical reaction temperature, pressure and identical conversion....	195
Table 6-6:	Reaction schemes of <i>n</i> -hexenes dimerization depicting the type of products forming and the approximate likelihood (statistically) of formation.....	202

Table 6-7	Example of a reaction scheme of possible reactions of <i>n</i> -hexene isomers with branched hexyl carbenium ions.....	204
Table 6-8	Diesel specific properties of the hydrogenated C ₁₆ olefin fraction of the 1-octene dimerization product (H-ZSM-5 catalyst) compared to other diesel fuels.....	210

LIST OF ABBREVIATIONS

ASA	Amorphous silica-alumina
ASTM	American Standard Testing Method
BEA	Zeolite Beta (International Zeolite Association, IZA, structure code for zeolite Beta)
CatPoly	Catalytic Polymerization (process)
CDCl ₃	Deuterated chloroform
CEN	Comité Européen de Normalisation (European Standards Organization)
CFPP	Cold Filter Plugging Point
CN	Cetane Number
COD	Conversion of Olefins to Diesel (process)
Et ₃ Al	Triethylaluminum
Euro	European Emissions Standard
FID	Flame Ionization Detector
FIMS	Field Ionization Mass Spectroscopy
FT	Fischer-Tropsch (process)
GC	Gas Chromatograph or Gas Chromatogram
GCMS	Gas Chromatography-Mass Spectrometry
GTL	Gas-to-Liquids
IFP	Institut Français de Pétrole
IP	Institute of Petroleum
¹ H-NMR	Proton Nuclear Magnetic Resonance Spectroscopy

HTFT	High Temperature Fischer-Tropsch (synthesis)
H-ZSM-5	Acid form of zeolite ZSM-5
LTFT	Low Temperature Fischer-Tropsch (synthesis)
MCM-41	Zeolite MCM-41 (Mobil Composition of Matter – forty one)
MCM-56	Zeolite MCM-56 (Mobil Composition of Matter – fifty six)
MFI	Zeolite Mobil Five (International Zeolite Association, IZA, structure code for zeolite ZSM-5)
MOGD	Mobil Olefins to Gasoline and Distillate (process)
MON	Motor Octane Number
RON	Research Octane Number
SABS	South African Bureau of Standards
SANS	South African National Standards
SAPIA	South African Petroleum Industry Association
SEM	Scanning Electron Microscopy
SHOP	Shell Higher Olefins Process
SiO ₂ /Al ₂ O ₃	Silica-Alumina
SPA	Solid Phosphoric Acid
SPD TM	Sasol Slurry Phase Distillate TM (process)
TON	Zeolite Theta One (International Zeolite Association, IZA, structure code for zeolite Theta-1)
UOP	Universal Oil Products Inc.
ZSM-5	Zeolite ZSM-5 (Zeolite Socony Mobil – five)

LIST OF SYMBOLS

LHSV	Liquid Hourly Space Velocity
MHSV	Mass Hourly Space Velocity
molHSV	Molar Hourly Space Velocity
WHSV	Weight Hourly Space Velocity
Å	Ångström
bar	Pressure unit
cm	Centimeter
cSt	Centistoke
d_r	Reactor diameter
d_p	Particle diameter
g	Gram
g/g.h	Grams (of feed) per gram (of catalyst) per hour
kg	Kilogram
L_b	Bed length
min	Minute
ml	Milliliter
mm	Millimeter
m^2/g	Meter squared per gram (of catalyst)
nm	Nanometer
P	Pressure

ppm	Parts per million
S	Selectivity
T	Temperature
T _{int}	Internal temperature
TOS	Time-On-Stream
wt%	Weight percent
X	Conversion
Y	Yield
μm	Micrometer
%	Percent
°C	Degree Celsius

CHAPTER 1

1. BACKGROUND

Fischer-Tropsch (FT) synthesis converts synthesis gas ($H_2 + CO$) into (mostly) hydrocarbons. The product ranges continuously from C_1 (methane) to infinity, while the molar selectivity constantly declines. The typical technical processes produce low olefins and conventional liquid fuels such as diesel, kerosene and naphtha.¹

Straight run diesel fuel makes up about 20% of the total FT product produced by the Sasol Slurry Phase Distillate (SPDTM) process as utilized by Qatar Petroleum's (51%) and Sasol's (49%) Oryx GTL plant located in Ras Laffan Industrial City, Qatar,^{2,3} which is based on Sasol's Low Temperature Fischer-Tropsch (LTFT) technology. This straight run diesel consists mostly of linear paraffins and is, therefore, of a very high cetane number of about 75-80. These linear and less-branched paraffins have, however, poor cold flow properties.^{4,5,6,7}

In order to maximise diesel fuel production, the heavier than diesel product, mostly wax, is subjected to a mild hydrocracking step, yielding about 80% diesel, 15% naphtha and 5% C_1 - C_4 gases. The diesel from wax hydrocracking has a cetane number of 70-75 and improved cold flow properties.^{5,6} Since the South African market requires both a cetane number of only 45 (SABS 342)⁸ and no superior cold-flow properties, the straight run FT and wax

hydrocracking diesel can be used as a blending stock to upgrade petroleum derived lower cetane number diesel fuel.⁴

The product from Sasol's high temperature Fischer-Tropsch (HTFT) and Sasol Advanced Synthesis (SAS) processes utilized by Sasol's Synfuels Refineries in Secunda, South Africa, is optimized towards naptha-range hydrocarbons. This product is mostly also linear and olefinic. About 70 wt% of the C₅-C₁₂ fraction are olefins.^{5,9} The high-temperature Fischer-Tropsch process derived straight-run higher carbon number (C₁₀-C₂₀) linear and mono-methyl branched olefins cannot only be blended into the diesel pool (after hydrogenation) but are also valuable chemical feedstocks that can be hydroformylated to form oxygenated products, comprising aldehydes and/or alcohols.^{10,11,12} These alcohols, which are referred to as detergent-range alcohols, can be subsequently converted into surfactants by alkoxylation or sulfonation^{4,13}. Mid-branched surfactants have been shown to be both biodegradable^{4,13,14} and to possess good cold-wash detergency.^{12,15,16}

As a result, Sasol is short in diesel-range hydrocarbons so that "solid phosphoric acid" (SPA) catalyst based polymerisation technology, the "CatPoly" process, is used, whereby "solid" refers to the phosphoric acid being adsorbed on Kieselguhr, to oligomerize some of the lower olefins. A part of the higher-carbon-number liquid products and transportation fuels, in particular diesel, but also motor-gasoline and jet fuel, leaving Secunda, is produced by oligomerization of low olefins, mostly butenes.^{9,17,18,19,20}

Even though SPA produces high quality gasoline, it is not a good choice for producing good diesel, since the oligomerization product is highly branched.^{17,19} The diesel obtained from the Sasol Synfuels Refineries' CatPoly process has a cetane number of only 29-30¹⁷, which is much lower than the South African Bureau of Standards' minimum requirement of 45⁸, but has excellent cold-flow properties^{6,17} so that SPA-derived diesel can only be used as a blendstock.

Diesel fuel can also be produced by oligomerizing naphtha-range or lower olefins using zeolite H-ZSM-5 as the catalyst. H-ZSM-5 is an acidic zeolite with medium-pore channels that allows the formation of an oligomerizate consisting of near-linear molecules.²¹ Technologies that employ the H-ZSM-5 catalyst are the "Mobil Olefins to Gasoline and Distillates" (MOGD)^{22,23} and the "Conversion of Olefins to Distillate" (COD)²⁴ processes. Oligomers from the MOGD and COD processes are less branched than those obtained from the CatPoly process. Cetane numbers obtained in Mobil's MOGD and PetroSA's COD processes, after hydrogenation of the olefin oligomers, are in the ranges of 52-56²⁵ and 51-54²⁴ respectively.

Both the MOGD and the COD processes are not "true" oligomerization processes in that there is both a forward and a reverse reaction because of the rather high reaction temperatures used and conversion driven close to olefin carbon number equilibrium distribution and isomers equilibrium distribution. As oligomerization products form in the forward reaction, say from propene (C_3) to C_6 , C_9 , C_{12} oligomers etc., the long-chain products

crack back to short-chain molecules, which in turn oligomerize forward again.²³ As a result, there is formation of an olefin “pool” with a continuous carbon number spectrum, i.e. $C_4^=$, $C_5^=$, $C_6^=$, $C_7^=$, $C_8^=$, $C_9^=$ etc. Due to the shape-selective constraints imposed by the H-ZSM-5 zeolite catalyst, the branching in the diesel-range product is limited to an average of 2-3 methyl branches per molecule that are more or less randomly distributed over the carbon chain, but typically at distances of about 5 carbon atoms.^{26,27}

Furthermore, due to the rather severe reaction conditions, there is formation of monocyclic aromatics, amounting to $\leq 5\%$ in the MOGD diesel²² and about 10% in the COD diesel.²⁴ Aromatics are in principle unwanted in diesel, but currently required to meet density specifications (SANS 342).⁸

After the oligomerization of the olefins, there is deep hydrotreatment needed to saturate the olefin oligomers, which also reduces the amount of aromatics present. The product, after hydrogenation, consists essentially of a mixture of moderately branched paraffins in the diesel-range. The diesel has both a good cetane number (higher than 50, see above) and good cold flow properties.^{22,24}

While the CatPoly, MOGD and COD processes produce a “pool” of oligomers which fall in a certain carbon number range, specifically the diesel range, there are also selective olefin oligomerization processes that produce specific products. The catalytic oligomerization of ethene is commercially applied in order to selectively produce even numbered linear α -olefins in the C_4 - C_{20+}

range.^{28,29,30,31,32,33} Recently, catalyst systems have been developed which selectively trimerize ethene to 1-hexene^{34,35,36} and, more recently, tetramerize ethene to 1-octene.^{36,37,38} Ethene dimerization and oligomerization reactions to produce α -olefins are typically carried out using homogeneous alkylaluminium or late-transition-metal catalysts, particularly nickel-based catalysts or a combination of these.³²

The olefins obtained from the FT process, are predominantly linear α -olefins, although olefins with internal double bonds and some mono-methyl branched species are also obtained, with the methyl group situated at any position along the hydrocarbon chain.^{3,32,39}

An alternative, attractive method for producing specific higher olefins would be the dimerization of low-carbon-number α -olefins, for example, conversion of 1-butene to octenes, ideally 1-octene, or conversion of 1-hexene to dodecenes, ideally 1-dodecene.^{32,39} However, despite the many catalysts known to dimerise olefins, relatively few of these systems have shown promising commercial viability due to a variety of limiting factors that include competing side reactions, catalyst activity and stability, selectivity for dimer formation and severity of the reaction conditions.⁴⁰

The introduction of microporous materials (zeolites) in the 1960's contributed to the improvement of many chemical processes.^{41,42} Interest in medium-pore zeolites has grown in the last few decades, both at academic institutions and at industrial laboratories, and molecular shape-selective zeolites have

emerged to become a significant group of industrial catalysts.⁴³ Acidic zeolites may be applicable for the dimerization of naptha-range n-olefins to moderately branched diesel-range and detergent-range olefins. It is known that the acid-catalyzed dimerization of linear α -olefins leads to linear, mono, di-, and tri-branched dimer olefins with preference for di-branched products with both the branching and the double bond close to the middle of the molecules.^{32,44,45,46}

1.1 References

- ¹ R.L. Espinoza, A.P. Steynberg, B. Jager, A.C. Vosloo, Appl. Catal. A: General, 186 (1999) 13-26.
- ² Sasol Limited, www.sasol.com, accessed 2010-12-21.
- ³ A. de Klerk, Ph.D. Thesis, University of Pretoria (2008).
- ⁴ M.E. Dry, Appl. Catal. A: General, 189 (1999) 185-190.
- ⁵ L.P. Dancuart, R. de Haan, A. de Klerk, Stud. Surf. Sci. Catal., 152 (2004) 482-532.
- ⁶ D. Leckel, Energy & Fuels, 23 (2009) 2342-2358.
- ⁷ P.W. Schaberg, P.M. Morgan, I.S. Myburgh, P.N.J. Roets, J.J. Botha, "An Overview of the Production, Properties and Exhaust Emissions Performance of Sasol Slurry Phase Distillate Diesel Fuel", Proc. 2nd International Colloquium on Fuels, Technische Akademie Esslingen, Germany, January 20-21 (1999) 587-597.
- ⁸ South African Bureau of Standards, www.stansa.co.za (SANS 342, Edition 4 (2006) 1-10), accessed 2011-01-10.
- ⁹ A. de Klerk, Energy & Fuels, 20 (2006) 1799-1805.

-
- ¹⁰ M.J. Betts, M.E. Dry, A. Geertsema, G.J.H. Rall, US 6,756,411 B2 (2004), assigned to Sasol Technology (Pty) Ltd.
- ¹¹ G.A. Olah, Á. Molnár, "Hydrocarbon Chemistry", 2nd Edition, John Wiley & Sons, New Jersey, Chapter 13 (2003) 731-732.
- ¹² I.H. Potgieter, A.E. Buck, M.J. Betts, US Statutory Invention Registration H1, 818 (1999), assigned to Sasol Technology (Pty) Ltd.
- ¹³ M.E. Dry, Catal. Today, 71 (2002) 227-241.
- ¹⁴ A.J. Ellis, S.G. Hales, N.G.A. Ur-Rehman, G.F. White, Appl. Environ. Microbiol., 68 (2002) 31-36.
- ¹⁵ M. Tsumadori, "Recent Trends of Surfactants in the Fabric & Home Care Field", Proc. 6th World Surfactant Congress CESIO, Berlin, Germany, June 21-23 (2004) paper # 196.
- ¹⁶ B. Fell, "Raw Materials and Intermediate Products for Anionic Surfactant Synthesis" in "Surfactant Science Series, Anionic Surfactants: Organic Chemistry", H.W. Stache (Ed.), Marcel Dekker Inc., New York, NY, Vol. 56 (1996) 1-52.
- ¹⁷ A. de Klerk, Energy & Fuels, 20 (2006) 439-445.
- ¹⁸ J.H. Coetzee, T.N. Mashapa, N.M. Prinsloo, J.D. Rademan, Appl. Catal. A: General, 308 (2006) 204-209.
- ¹⁹ T.N. Mashapa, A. de Klerk, Appl. Catal. A: General, 332 (2007) 200-208.
- ²⁰ A. de Klerk, US 0,108,568 A1 (2010), assigned to Sasol Technology (Pty) Ltd.
- ²¹ C.T. O'Connor, "Oligomerization" in "Handbook of Heterogeneous Catalysis", G. Ertl, H. Knözinger, F. Schüth, J. Weitkamp, (Eds.), Wiley-VCH, Weinheim, Vol. 6 (2008) 2854-2864.

-
- ²² W.E. Garwood, "Conversion of C₂-C₁₀ Olefins to Higher Olefins over Synthetic Zeolite ZSM-5" in "Intrazeolite Chemistry", G.D. Stucky, F.G. Dwyer (Eds.), ACS Symp. Ser., Vol. 218, Am. Chem. Soc., Washington, DC (1983) 383-396.
- ²³ S.A. Tabak, R.E. Holland, M.R. Ireland, Preprints, AIChE Summer National Meeting, Philadelphia, PA, August 19-22 (1984) Paper 42a.
- ²⁴ C.D. Knottenbelt, C. Dunlop, K. Zono, M. Thomas, WO 069407 A2 (2006), assigned to The Petroleum Oil Corporation of South Africa (Pty) Ltd. (PetroSA).
- ²⁵ S.A. Tabak, B.S. Wright, H. Owen, US 4,504,693 (1985), assigned to Mobil Oil Corp.
- ²⁶ S.A. Tabak, F.J. Krambeck, W.E. Garwood, J. AIChE., 32 (1986) 1526-1531.
- ²⁷ R.J. Quann, L.A. Green, S.A. Tabak, F.J. Krambeck, Ind. Eng. Chem. Res., 27 (1988) 565-570.
- ²⁸ S. Naqvi, "Process Economics Program", SRI Consulting, Report No. 12E (2008).
- ²⁹ Chemsystems, "Alpha Olefins", Report Abstract, PERP06/07-5 (2008) 1-11.
- ³⁰ R.L. Poe, D.J. Royer, US 4,455,289 (1984), assigned to Conoco Inc.
- ³¹ W. Keim, Angew. Chem. Int. Ed. Engl., 29 (1990) 235-244.
- ³² J. Skupińska, Chem. Rev., 91 (1991) 613-648.
- ³³ G. Busca, Chem. Rev., 107 (2007) 5366-5410.
- ³⁴ J.T. Dixon, M.J. Green, F.M. Hess, D.H. Morgan, J. Organomet. Chem., 689 (2004) 3641-3668.
- ³⁵ H. Mahomed, A. Bollmann, J.T. Dixon, V. Gokul, L. Griesel, C. Grove, F. Hess, H. Maumela, L. Pepler, Appl. Catal. A: General, 255 (2003) 355-359.

-
- ³⁶ E. Killian, K. Blann, A. Bollmann, J.T. Dixon, S. Kuhlmann, M.C. Maumela, H. Maumela, D.H. Morgan, P. Nongodlwana, M.J. Overett, **et al**, J. Mol. Catal. A: Chemical, 270 (2007) 214-218.
- ³⁷ A. Bollmann, K. Blann, J.T. Dixon, F.M. Hess, E. Killian, H. Maumela, D.S. McGuinness, D.H. Morgan, A. Neveling, S. Otto, M. Overett, A.M.Z. Slawin, P. Wasserscheid, S. Kuhlmann, J. Amer. Chem. Soc., 126 (2004) 14712-14713.
- ³⁸ K. Blann, A. Bollmann, H. De Bod, J.T. Dixon, E. Killian, P. Nongodlwana, M.C. Maumela, H. Maumela, A.E. McConnell, D.H. Morgan, M.J. Overett, M. Pretorius, S. Kuhlmann, P. Wasserscheid, J. Catal., 249 (2007) 244-249.
- ³⁹ R.D. Broene, M. Brookhart, W.M. Lamanna, A.F. Volpe Jr., J. Amer. Chem. Soc., 127 (2005) 17194-17195.
- ⁴⁰ B.L. Small, A.J. Marcucci, Organometallics, 20 (2001) 5738-5744.
- ⁴¹ A. Dyer, "An Introduction to Zeolite Molecular Sieves", John Wiley & Sons, New York, NY (1988) 107-113.
- ⁴² J. Weitkamp, Solid State Ionics, 131 (2000) 175-188.
- ⁴³ N.Y. Chen, W.E. Garwood, F.G. Dwyer, "Shape Selective Catalysis in Industrial Applications", Marcel Dekker Inc., New York, NY (1989) 7-30.
- ⁴⁴ C.P. Nicolaidis, M.S. Scurrrell, P.M. Semano, Appl. Catal. A: General, 245 (2003) 43-53.
- ⁴⁵ A. Corma, S. Iborra, "Oligomerization of Alkenes" in "Catalysts for Fine Chemical Synthesis, Microporous and Mesoporous Solid Catalysts", E.G. Derouane (Ed.), John Wiley & Sons, Vol. 4 (2006) 125-140.
- ⁴⁶ J.P.G. Pater, P.A. Jacobs, J.A. Martens, J. Catal., 179 (1998) 477-482.

CHAPTER 2

2. LITERATURE REVIEW

2.1 Olefin dimerization and oligomerization

Dimer has the same Greek root –*meros*, as in isomer, monomer, oligomer and polymer, meaning “part”. Mono-, di-, oligo- and poly- also come from Greek roots, *olig-* meaning a “few” and *poly-* meaning “many”. An oligomerization process is based on “growing” the oligomers by consecutive addition of monomer molecules. The joining up of two monomers produces a dimer. The process is called dimerization. Molecules formed by the combination of three or four or a few more monomers, normally up to ten, are called oligomers.¹ Oligomerization, which is a controlled form of polymerization, generally refers to the preparation of molecules consisting of only a relatively few monomer units, as opposed to polymerization which implies the combination of many monomers, leading to high molecular weight products.¹

There are two types of oligomerization reactions, namely, “true” and “conjunct” oligomerization.^{2,3} In “true oligomerization”, the product contains integral multiples of the monomer or, as in this study, olefinic species.^{4,5} In “conjunct oligomerization” many types of reactions occur simultaneously resulting in the formation of species with intermediate carbon numbers and other compounds. The extent to which these side reactions take place depends on the nature of the catalyst and the severity of the reaction conditions, especially temperature.⁶

In industrial manufacturing processes, either the one (see sections 2.1.1.4 and 2.1.1.6) or the other extreme (see Section 2.1.2.2) are usually aimed at.

Dimerization and oligomerization of olefins can be achieved by mainly three different mechanisms, the coordinative, carbenium ion and free-radical mechanisms.

2.1.1 Metal catalysed olefin oligomerization – the coordinative mechanism

Metal-catalyzed olefin oligomerization follows a coordination mechanism (Figure 2-1). The incoming olefin coordinates to a metal atom, followed by addition of the metal atom to the olefinic double bond. In the context of olefin oligomerization, this step can be regarded as the insertion of an olefinic double bond into the bond between the metal and an H- or alkyl ligand.

Metal catalyzed olefin oligomerization is a process where, by a true oligomerisation reaction, monomer units (the olefins) are successively inserted into the metal-carbon bond of an alkyl chain that is growing on a surface metal atom of a heterogeneous catalyst or, in homogeneous catalysis, the central metal atom of a catalyst complex.^{6,10,19,7} Having started from a metal hydride species (an H-ligand or surface hydrogen) the grown alkyl chain desorbs from the metal by β -hydride elimination after two or more consecutive insertion steps to yield a dimer or oligomer and simultaneously restore the original H-ligand (see Figure 2-1).^{19,8}

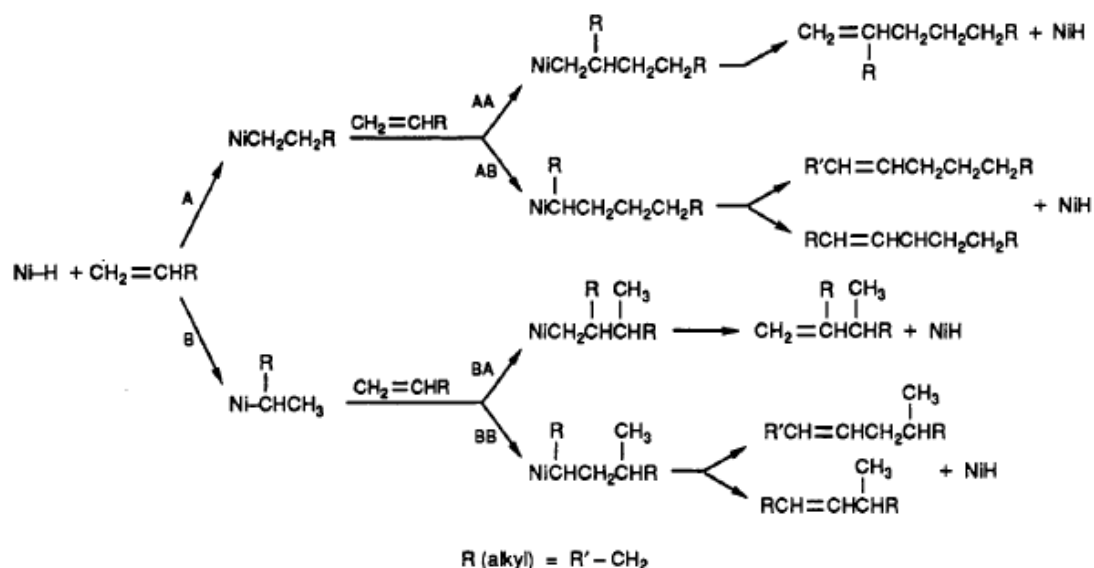


Figure 2-1: Coordinative olefin oligomerization mechanism in the presence of a nickel complex. **(A)** Addition of the olefin's α -carbon atom to the nickel atom. **(B)** Addition of the olefin's β -carbon atom to the nickel atom.¹⁹

2.1.1.1 Metal catalysed olefin dimerization and oligomerization

Metal catalysts for olefin oligomerization can be heterogeneous or homogeneous. Heterogeneous catalysts consist typically of a metal that is supported on a carrier (such as silica-alumina).^{9,6} Homogeneous catalysts are either alkyl aluminium complex-based or are a combination of a transition metal complex and a Lewis acid.^{8,9,19}

The outcome of metal catalysed coordinative dimerization and oligomerization depends on many factors. While the chain length is much controlled by conversion, temperature and the type of the metal (with Ni catalysts favouring dimerization^{8,9}), the degree of branching of the oligomers is determined by the type of reactant fed (a less branched product is obtained from 1-olefins^{9,19}), the acidity of the catalyst system (be it, for a heterogeneous catalyst, the

acidity of the carrier or be it, in case of a homogeneous catalyst, the strength of the Lewis acid ^{6,8,9,19}) and also largely by steric effects, i.e., the effect of ligand bulkiness on the orientation of the inserting olefin and the resulting orientation of the metal-ligand configuration.^{8,9,19}

In olefin dimerization via coordination mechanism (and correspondingly in oligomerisation), bulky ligands tend to force the reaction to follow route A – AA of Figure 2-1 (the topmost route) that yields dimers having a single branch per molecule.^{8,35} Hence, olefin oligomers produced by a coordination mechanism are typically less branched.^{8,9,19,35} The said steric effect of the ligands on branching selectivity is discussed in section 2.1.1.5 in more detail.

2.1.1.2 Homogeneous catalysts for olefin dimerization and oligomerization

There are, at first, the ‘classical’ Ziegler catalysts, namely tri-alkyl aluminium compounds and modifications thereof.^{6,10,19} Numerous other homogeneous catalysts, though only representing a very small number of general types, have been described in the literature. Of these other catalyst systems, the vast majority are transition metal complexes, mostly based on nickel, titanium, zirconium and chromium, with typically various phenyl, amine, phosphine, halogen and other ligands. Most of them are coordinated to a trialkyl aluminium group as a co-catalyst or activator.^{11,12,13,14,15,16,17,18,19,20,21,22,23} The literature on oligomerization catalysts up to 1989 has been extensively reviewed in 1991.¹⁹ The more recent developments have been reviewed with particular consideration of the industrially applied catalysts and processes,⁷ and focus on selective ethylene trimerization.¹⁶

Besides the Ziegler catalysts, only a few of the transition metal based catalysts described in the literature have found commercial application (see Section 2.1.1.4). The earlier processes produce a mixture of oligomers that covers a range of carbon numbers (see Section 2.1.1.3). More recently, specifically tailored catalyst systems have been developed over which, under specific conditions, high carbon number selectivity can be achieved. These catalysts are typically based on titanium or chromium complexes and catalyze the selective oligomerization of ethene to either dimers, trimers or tetramers.^{7,16,17,18,20,21,22,23}

The α -olefins obtained from homogeneously catalyzed ethene oligomerization are linear and even-numbered. Propene and higher olefins can also be oligomerized over such catalysts. However, linear oligomers only form with high selectivity in ethene oligomerization, while branched oligomers form in higher olefins oligomerization.^{7,19} It was also found that, in general, olefin oligomerization activity is highest for ethene and decreases with increasing carbon number.^{7,19}

2.1.1.3 Carbon number distribution

The formation of higher olefins from lower olefins, such as the formation of linear α -olefins from ethylene, is an oligomerization process. The carbon number distribution of the product is determined by chain growth and termination.^{6,7,10,19}

- Chain growth occurs, throughout, by repeated insertion of a monomer into the bond between the growing chain and the central metal atom of the catalyst.

- The growing chain can be bonded to the central metal atom in two different ways, namely on one of its ends (as with the 'classical' catalysts)^{6,7,10,19} or on both ends as a metallacycle (as with the more novel, carbon number selective catalysts).^{7,16,17,20,21,22,23}
- Termination of chain growth can occur, or be imposed, in three different ways, namely the following:
 - Chain growth may be terminated by random desorption of the growing chains from the central metal atom of the catalyst, which is followed by the formation of new chains that start growing from the vacant site. This competition, or balance, between chain growth and termination (the chain growth probability) results in a product carbon number distribution that follows a Schulz-Flory distribution.^{7,10} Product carbon number distributions can therefore cover a wide range (depending on the catalyst and the reaction conditions) but with the highest molar selectivity always for the dimer.
 - Operating under conditions where, simultaneous to growth, no desorption takes place, is also possible. The technical process is carried out as a two-stage process. In the first stage growth continues until it comes to a halt, for instance, by feed depletion, or is forced to end by changing conditions. In the second stage, which is operating at higher temperature and lower pressure, the grown chains are forcibly displaced by ethylene. Since no sites become vacated during chain growth and since, therefore, no new chains can start growing, a product with a more narrow carbon number distribution is obtained, with less short chain oligomers and a molar selectivity maximum at a higher

carbon number than that of the dimer. The carbon number distribution of the two stage product corresponds to a Poisson distribution.^{5,7,10,13}

- Termination of growth can also be controlled by differences in intermediate stabilities as with the more novel, carbon number selective catalysts, where the growing chain is bonded to the central metal atom of the catalyst complex on both ends as a metallacycle.^{7,16,17,18,20,21,22,23} The resulting ring grows readily but only to a certain extent, i.e., to a certain carbon number. Thereafter the ring opens, the chain desorbs and a new ring starts growing. It is assumed that the final metallacycle is energetically favored over the larger cycle and that the growth rate slows down once the said size has been reached.^{7,16,17} This results in high selectivity towards a single carbon number product. The state of the art is that ethylene dimers, trimers and tetramers can selectively be synthesized by metallacycle mechanism.^{7,10,16,17,18,20,21,22,23} In a recent review on olefin oligomerization,⁷ one of the foci is carbon number selective dimerization of ethylene and dimerization of higher olefins. Selective ethylene trimerization has also been reviewed recently.¹⁶

The importance of the ligands on the metal atom has been emphasized¹⁸. For titanium and chromium based oligomerization catalysts variation of ligands can “completely modify the reactivity of the metal center”⁷, that is, alter the reaction mechanism. For these catalysts it means turning the reaction mechanism from chain growth to ‘ring growth’, i.e. to a metallacycle mechanism (and *vice versa*). $\text{TiCl}_4/\text{AlEt}_3$, for example, is an ethylene polymerization catalyst and $\text{Ti(OR)}_4/\text{AlEt}_3$ is a selective ethylene dimerization catalyst.

2.1.1.4 Industrial processes for ethene oligomerization to α -olefins

In the industrial ethene oligomerization processes for the selective manufacture of linear α -olefins, homogeneous catalysts are applied throughout. Catalysts used are either the classical triethyl aluminium Ziegler catalysts or complexes of transition-metals as outlined in Section 2.1.1.2.^{7,10}

A 2-stage process (using a triethyl aluminium Ziegler catalyst) was developed by Albemarle (now Ethyl Corp.). The Ethyl process is operated by INEOS. In the 2-stage process, ethene oligomerization is carried out at around 120-150 °C and 140-210 bar, which step is followed by the displacement of the oligomers from the catalyst at around 260-320 °C and 10-15 bar.^{5,7,10,13} As discussed in Section 2.1.1.3, a product with a Poisson distribution of carbon numbers is obtained from the oligomerization stage. In the technical process INEOS recycle some of the light oligomers (which measure leads to the formation of branched products).

1-stage processes, using different catalysts, are operated by a number of α -olefin producers. Chevron Phillips (CP) Chemicals, who are operating an improved version of the original Gulf process, and Sasol Germany (formerly CONDEA), who are operating the Conoco process, are using a Ziegler catalyst.^{5,7,10,11,12,13,14,19} The ethylene oligomerization stage in the Shell Higher Olefins Process (SHOP) and the UOP Linear-1 process are utilizing catalysts consisting of nickel phosphine complexes.^{5,7,10,15} The Idemitsu, Linde/SABIC and IFP-Axens' Alphaselect processes are operating zirconium

based catalysts.^{7,10} As discussed in Section 2.1.1.3, a product with a Schulz-Flory distribution of carbon numbers is obtained from the oligomerization stage. Process temperatures in the 1-stage processes range, depending on the catalyst and the desired product carbon number distribution, from about 50 to 250 °C and pressures range, correspondingly, from about 25 to 250 bar.

The carbon number selective ethylene oligomerization processes are also 1-stage processes. The catalysts used promote a metallacycle mechanism in order to achieve these high carbon number selectivities. IFP's Alphabutol process for the selective dimerization of ethylene to 1-butene is employing a titanium complex catalyst. The process was commercialized in the mid 1980s.^{10,10,18} Chevron Phillips' and Sasol's selective ethylene trimerization processes and Sasol's selective ethylene tetramerization process^{16,20,21,22,23,24,25} are utilizing chromium complex catalysts. The Chevron Phillips trimerization process was commercialized in 2003.^{16,26} Sasol are currently constructing an ethylene trimerization/tetramerization unit that has been announced to come on stream in 2013.²⁷

2.1.1.5 The oligomerization of higher olefins

As mentioned above, propene and higher olefins can also be oligomerized over homogeneous catalysts. Dimers are the major product in these reactions due to the comparatively high desorption rate of the dimerized species from the catalysts. For instance, the commercial Dimersol processes yield dimer selectivities > 80%. By continuing chain growth (and also by incorporating readsorbed dimers from the product) some higher oligomers form as well.⁷

Products from propene and higher olefins oligomerization reactions are mostly branched. The extent of branching can be controlled (within limits) by the basicity and bulkiness of the ligands on the central metal atom.

Counter intuitively, bulky ligands (such as substituted phosphines) can favour the formation of dibranched dimers, such as the preferential formation of 2,3-dimethylbutenes from propene over specifically designed nickel catalysts. Bulky ligands force the methyl end of the second propene molecule to point away from the central metal atom when approaching the metal and inserting into the bond between the alkyl group and the metal atom with the α -carbon bonding to the metal and the β -carbon bonding to the alkyl group, thus creating a second branch. With less bulky ligands bonding of the β -carbon to the metal is possible, which eventually leads to the formation of monobranched dimers.^{7,19}

2.1.1.6 Industrial processes for the oligomerization of higher olefins

Dimersol processes are the prominent examples.⁷ These processes, developed by the Institut Français du Pétrole (IFP), are widely applied in the refining environment. The typical feedstocks are propene and/or *n*-butenes but suitable feedstocks range up to C₅-olefins. Mixed feeds can also be processed. The product consists of highly branched olefinic dimers. Ziegler nickel hydride catalysts are employed, which are nickel based complexes combined with an aluminium-based co-catalyst such as (Ni^{II}/AlEt₂Cl₂).^{35,15}

With about 45 licences, IFP's Dimersol G process dimerizes propene to iso-hexenes. Dimersol E is designed to co-oligomerize ethene with propene, while Dimersol X dimerizes *n*-butenes to octenes.^{5,35,15} Extension to dimerizing higher olefins is limited since the reactivity of the olefins decreases significantly with increasing carbon number.^{15,35}

Dimers from Dimersol processes are moderately branched and mostly of the vinylidene (2-alkyl-1-alkene) type. For instance, the C₆-fraction obtained from the Dimersol G propene dimerization process at 50°C consists of 22% linear, 72% monobranched and 6% dibranched olefins, which corresponds to an average degree of branching per molecule < 1. The highly branched olefinic dimers obtained are used as a blend stock for improving the octane number of gasoline, and to provide heptene and octene feedstocks for the plasticizer industry.⁷

Supported nickel catalysts, usually prepared by impregnation or ion exchange of supports such as zeolites, silica, alumina or silica-alumina, are also known to dimerize alkenes to oligomers with a comparably high content of linear 1-alkenes.^{35,76} Ni-ZSM-5 was found to be a very active and stable catalyst for the dimerization of propene at low temperatures such as 54 °C with minimal side reactions.¹⁰⁹ Adding 3 wt% Ni to a H-ZSM-5 catalyst increased conversion from 40% (H-ZSM-5 without Ni) to 98%. Addition of Ni was also shown to increase product linearity (i.e., promoting the coordinative mechanism) when compared with unloaded H-ZSM-5. However, the process, developed for dimerizing propene and higher alkenes over Ni-exchanged ZSM-5 catalyst, is not commercialized.²⁸

In the Ethyl process for the oligomerization of ethylene over a Ziegler catalyst (see Section 2.1.1.4) INEOS recycle some of the light oligomers produced, which measure also leads to the formation of branched products.⁷

Because of their low degree of branching the naphtha range olefins produced by these processes are good feedstocks for the manufacture of chemicals such as plasticizer alcohol nonanol.⁷

2.1.1.7 Dimerizing naphtha-range olefins to diesel-range products over homogeneous catalysts?

Homogeneous catalysts appear less suitable for the dimerization/trimerization of naphtha range olefins to the desired, moderately branched diesel range hydrocarbons. The reasons are the following (see Section 2.1.1.6):

- The average degree of branching of the products obtained from dimerizing C₃₊-olefins (by state of the art commercial processes) is lower than one.
- Olefin feed reactivity decreases significantly with increase in carbon number (which limits processing, currently, to C₅ olefin feedstocks).
- Selectivity towards higher oligomers decreases significantly (which is, to some extent, a consequence of the above). This limits the formation of trimers that is required for the conversion of lower naphtha range olefins (particularly pentenes) into hydrocarbons in the diesel range.

2.1.2 Acid catalysed olefin oligomerization – the carbenium ion mechanism

While the homogeneously catalyzed processes are mainly utilized to produce “true” olefin oligomers for use as chemicals, oligomerization over solid acid catalysts is primarily motivated by the need to produce quality distillate fuels from lower molecular weight olefins, such as by Mobil’s (now Exxon-Mobil’s) MOGD^{3,62,63}, Sasol’s Catpoly^{29,30} and PetroSA’s COD^{31,32,33} processes, of whom the former is not commercialized.

Acid catalysts suitable for olefin oligomerization comprise all of concentrated sulfuric acid, hydrofluoric acid, BF_3/HF , AlCl_3/HCl , “solid” phosphoric acid and solid acid catalysts such as acidic ion-exchange resins, amorphous silica-alumina, acid zeolites etc.^{2,4,5,19,34,35,36}

2.1.2.1 Fundamentals of acid catalyzed olefin oligomerization

Acid-catalyzed olefin dimerization follows a carbenium ion mechanism.^{35,37} The catalyst protonates the olefins to yield carbenium ions. The overall process is governed by the stability of the carbenium ions. Reaction rates decrease in the order tertiary > secondary > primary carbenium ions, corresponding to their stability. Thus ethylene, which can only form a primary carbenium ion, reacts poorly over acid catalysts. Reversely, reactivity increases with chain length.^{3,94,38}

Similar to metal catalysis (see Sections 2.1.1.5 and 2.1.1.6), branching is unavoidably introduced when dimerizing or oligomerizing linear olefins over acid catalysts from carbon number 3 onwards (see Figure 2-2).

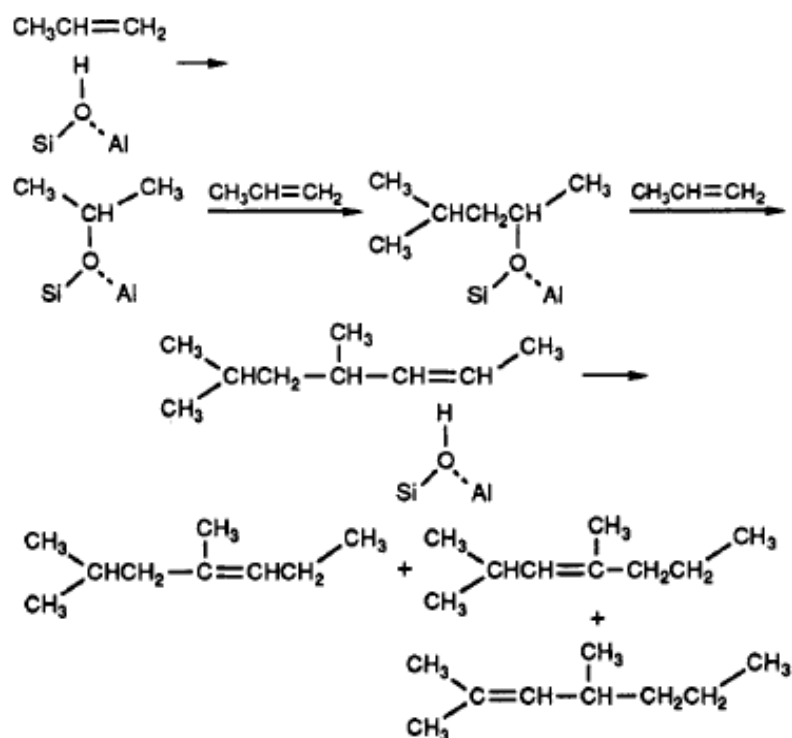


Figure 2-2: Reaction scheme for the “true” trimerization of propene over a solid acid catalyst, zeolite HY, an aluminium-silicate (taken from Skupińska).¹⁹ The reaction scheme also indicates the rapid double bond isomerisation in the C₆-olefins formed that occurs over the acid catalysts (see also Figure 2-19).

In the upper part of Figure 2-2 the reaction scheme is shown of the dimerization of propene over a Brønsted acid catalyst. Only a single pathway is possible with this small molecule. At first a carbenium ion forms whose positive charge is, as a secondary carbenium ion, located on the central carbon atom. This carbenium ion reacts with the double bond in another propene molecule, binding to the terminal carbon atom of the double bond, so that, again, a secondary carbenium ion results. In the event of desorption, a mono-branched internal C₆-olefin results. Since primary carbenium ions, due to their much lower stability, are very unlikely to form,^{38,92} the above is the only relevant pathway in the dimerization reaction of propene.

2.1.2.1.1 Mechanism of 1-hexene dimerization and typical products

Acid catalyzed dimerization of *n*-olefins such as *n*-hexene on a Brønsted acid site proceeds through a transition state, in which a C-C bond is formed between the positively charged carbon atom of a hexyl cation and a carbon atom of the double bond of a *n*-hexene molecule (Figure 2-3).¹²¹ Acid catalyzed dimerization of linear internal olefins produces two branches, in vicinal positions, per molecule formed.

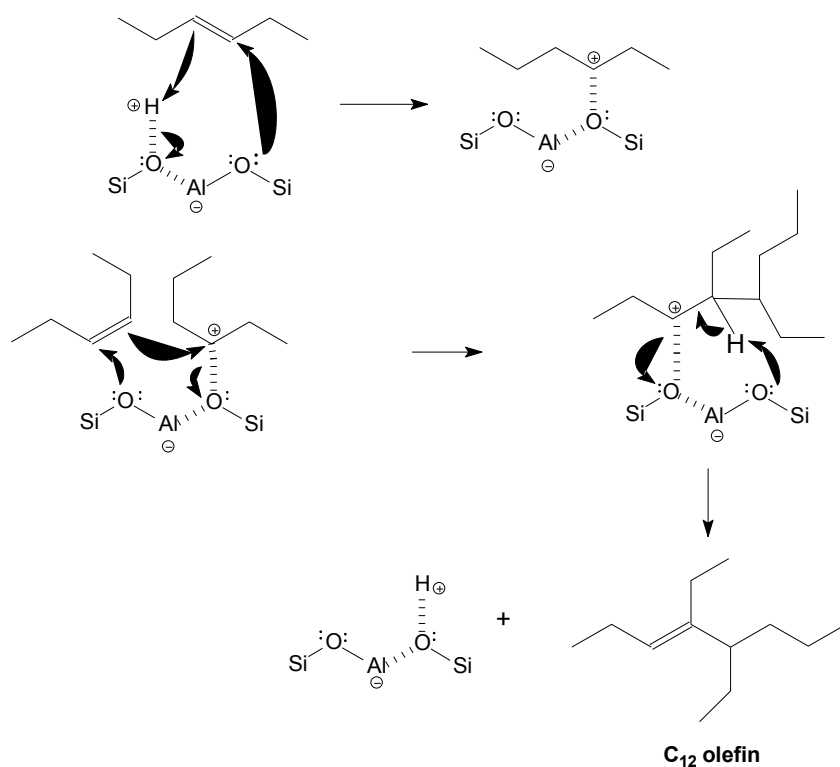


Figure 2-3: Schematic representation of the mechanism for the dimerization of linear molecules with internal double bonds (here two 3-hexene molecules) over a Brønsted acid catalyst to produce a double branched dimer.³⁹

Acid catalyzed dimerization of α -olefins (linear olefins with terminal double bonds), reacting with each other by an analogous mechanism, also tends to produce branched dimers (although with a single branch), as illustrated in

Figure 2-4. This is due to the higher stability of the secondary carbenium ion intermediates on the reaction pathway leading to the branched product compared to a reaction pathway via unfavourable primary carbenium ion intermediates (not illustrated) that would lead to a linear product.³⁹

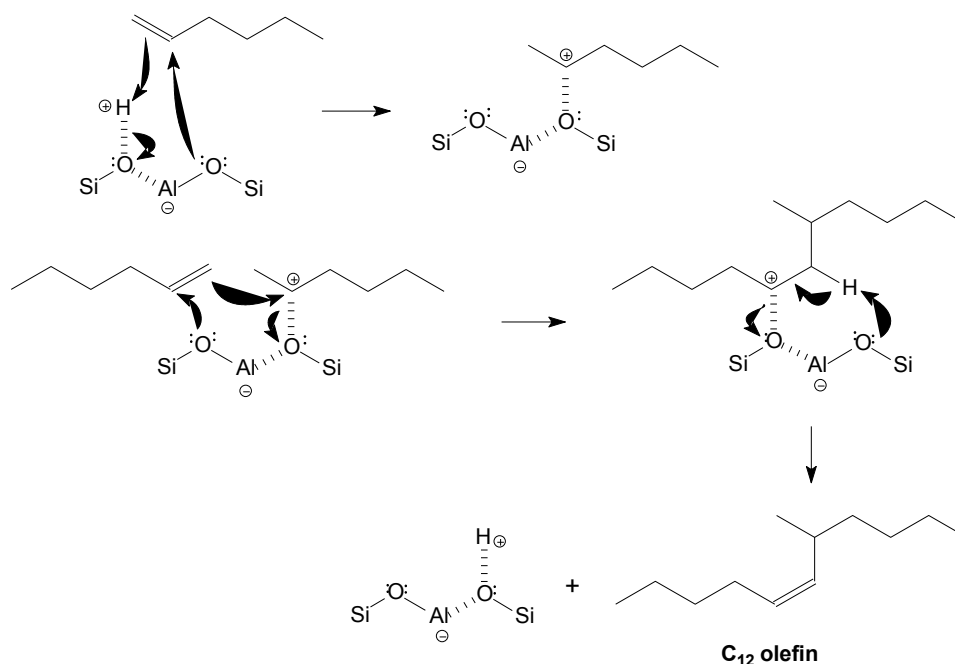


Figure 2-4: Schematic representation of the mechanism for the dimerization of 1-hexene over a Brønsted acid catalyst to produce a single branched dimer.³⁹

In 1-hexene dimerization at typical oligomerization conditions (of 100-250 °C and elevated pressures), double bond isomerization to the 2- and 3-hexenes was generally found to occur very rapidly as the first step (see Section 2.3.2.1 and Figure 2-19) usually much more rapid than skeleton isomerisation, oligomerization or cracking, so that an equilibrium or close to equilibrium pool of *n*-olefin isomers forms first, which is dominated by internal olefins.¹⁰⁶

Formation of an equilibrated pool of the double bond isomers means that, under the respective reaction conditions, the predominant species present in an

olefin oligomerization reaction mixture from linear olefin feedstock are the linear internal olefins. Internal double bonds and secondary carbenium ions are, largely, dominating the catalytic reactions as reflected in the reaction mechanism illustrated in Figure 2-5.^{3,43,106}

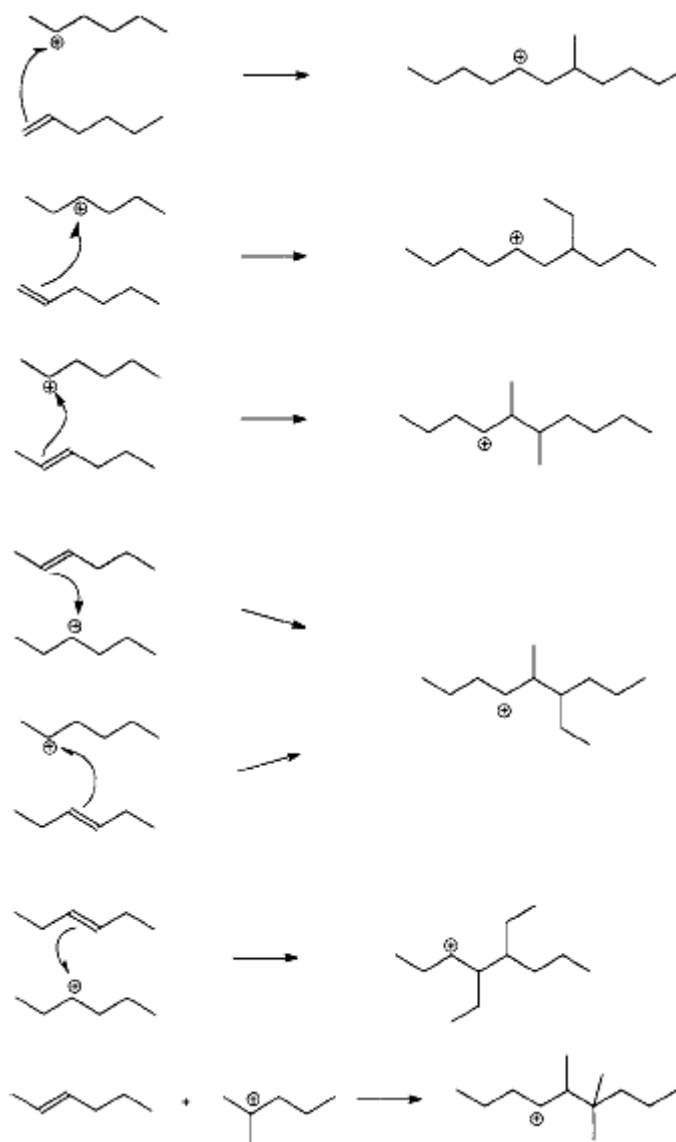


Figure 2-5: Examples (redrawn from reference) of *n*-hexene dimerization reactions leading to monobranched, dibranched and, illustrated by a single example, tribranched C₁₂ products. The latter are secondary products since an additional step, skeleton isomerization, is required. It should be noted that reactions involving primary carbenium ions are not included, since such ions are very unlikely to form.¹²¹

As can be derived from Figure 2-5, monobranched dimers could only be obtained from reactions of 1-hexene with the hexyl cations, while dibranched dimers resulted from reactions of 2-hexenes and 3-hexenes with the hexyl cations. Due to the aforementioned rapid isomerization of 1-hexene to 2-hexenes and 3-hexenes and the low equilibrium concentration of 1-hexene in the isomerized feed, see Figure 2-19, the dimers are mainly dibranched.¹²¹

Effective feed is, as discussed above, an equilibrium pool of all *n*-hexene isomers and, on the catalyst surface, the corresponding carbenium ions. As a result, the majority of the dimers formed from the equilibrated *n*-hexenes are dibranched dimers, while monobranched dimers were always found to form much less abundantly.

Since skeleton isomerization is comparatively slow (see Section 2.3.2.1 and Figure 2-19), only a small fraction of tribranched isomers forms. It was observed that, while the monobranched and dibranched dimers appeared as primary products, the tribranched dimers were secondary products.^{6,19,52,74,117,119}

In general, as illustrated in Figures 2-3 and 2-4, the double bond is close to the middle of the molecules.^{19,6,74,40,119}

The above refers to a 1-hexene dimerization product that formed without suffering from spatial constraints.

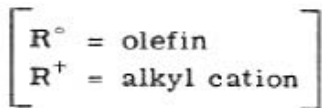
2.1.2.1.2 Conjunct oligomerization

Over acid catalysts both “true” and “conjunct” oligomerization (see introduction to Section 2.1) may occur. Examples of “true” oligomerization are given in Figure 2-2 and 2-21 for propene ($C_3=$) oligomerizing to form $C_6=$, $C_9=$, $C_{12}=$ etc. species.

In “conjunct” oligomerization many other types of reactions occur, apart from double bond isomerization and the oligomerization reaction itself, which may include skeletal isomerization, hydrogen transfer, cracking and cyclization (see Figure 2-6) to give, apart of the “true” oligomers, oligomers with intermediate carbon numbers, saturated hydrocarbons, aromatic compounds and ‘coke’.⁶

Coke, in the given context, is a relatively involatile, oligomeric or polymeric, hydrocarbonaceous residue of ill-defined chemical structure, formed on the catalyst as a result of hydrocarbon reactions, whose H/C ratio and extent of aromaticity and olefinicity depend on the reaction conditions.^{41,42} The extent to which the accompanying reactions take place depends on the nature of the catalyst and the severity of the reaction conditions, especially temperature.^{2,6}

Reaction temperature has a major influence on the outcome of acid catalyzed oligomerization reactions. For example, the conversion of propene over a solid acid catalyst, such as zeolite H-ZSM-5, leads to a true oligomerization product at low temperatures, while high temperatures, above of approximately 280 °C, lead to a conjunct oligomerization product (and a product mixture consisting of olefins, paraffins, aromatics and naphthenes).^{3,35,43}



29

2.1.2.2 Industrial processes for the oligomerization of olefins to fuels over acid catalysts

Olefin oligomerization over acid catalysts dates back to the 1930's with the commercialization (1935) of the so-called "polygas" process, developed by Universal Oil Products (UOP), to convert propene/butene mixtures over "solid phosphoric acid" (SPA), which is phosphoric acid adsorbed into the pores of Kieselguhr (diatomaceous earth), into highly branched gasoline-range (C_6 - C_{10}) olefins.^{5,35,19,6} A modified solid phosphoric acid process, "CatPoly", is operated by Sasol to produce oligomers in the diesel and jet fuel range.^{30,44,45,46,47,48}

The main disadvantages of the SPA catalyst and the polygas and CatPoly processes are the following:^{6,30}

- Short catalyst life (cannot be regenerated).
- Sensitivity to traces of water in the feed.
- Limited possibilities to tailor the catalyst properties to product demand.
- Problems with catalyst discharging from the reactor.
- Environmental issues related to its disposal.

The CatPoly process suffers an additional drawback, namely the poor self-ignition properties of the diesel fuel produced. CatPoly diesel is highly branched and therefore has a cetane number as low as 30 (raw) and 34 (after hydrogenation),⁵⁴ whereas South African market requires a cetane number of at least 45 (SABS 342)⁴⁹ and current and future European standards require at least 51.⁵⁰ CatPoly diesel can, therefore, only be used as a blend stock.

Due to the problems with and limitations of the polygas and CatPoly processes, and products, other catalysts, such as acid zeolites, were investigated for low olefin oligomerisation to gasoline and/or diesel.

Mobil developed the Methanol to Olefins, Gasoline and Distillate (MOGD) process in the early 1970's. However, the MOGD process is not commercialized. Subsequently, other companies such as Chevron and Mossgas (now PetroSA) also developed olefin oligomerization systems based on Ni-ZSM-5 (Chevron)^{51,52,53} and H-ZSM-5 catalysts (PetroSA).^{31,32,33,54} PetroSA's "Conversion of Olefins to Distillate" (COD) process is commercialized at their Mossel Bay site (commissioned in 1992).⁵⁴

2.1.2.2.1 The CatPoly process, using solid phosphoric acid

The "Catalytic Polymerization" (CatPoly) technology for manufacture of diesel is based on the polygas process for manufacture of petrol (see introduction to Section 2.1.2.2). The polygas process is operating at 150-250 °C, 18-80 bar and relatively high space velocities to limit coking.^{5,19,35,30,55}

The catalyst for this process, silicophosphoric acid or phosphoric acid, was prepared by mixing 85% orthophosphoric acid with Kieselguhr (diatomaceous earth) to form a composite material that was calcined at temperatures between 180 and 300 °C.² The final catalyst was composed, by weight, of 60% P₂O₅ and 40% Kieselguhr.^{2,35}

The specific reaction mechanism over phosphoric acid is shown in Figure 2-7). The olefinic double bond is protonated by phosphorous-bonded hydroxyl group and the resulting carbenium ion binds to the phosphorus atom via an oxygen bridge. The incoming olefin inserts into the C–O bond formed.

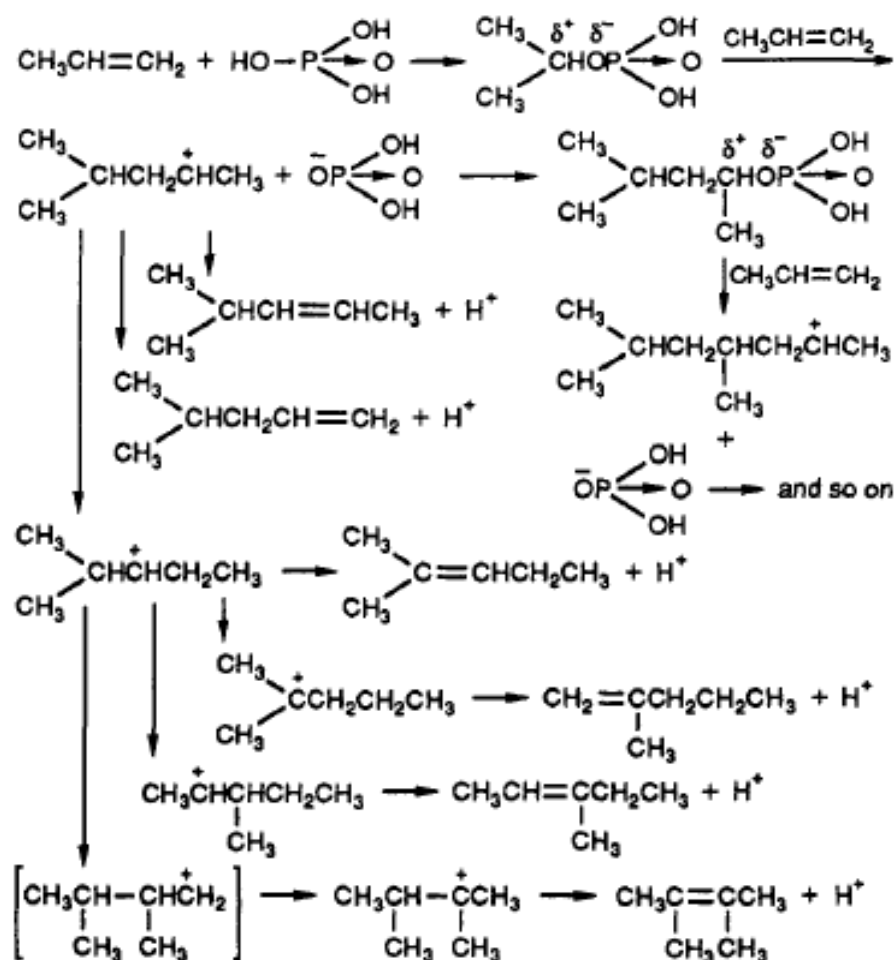


Figure 2-7: Mechanism of propene oligomerization in the presence of H_3PO_4 as catalyst (taken from Skupińska).¹⁹

Traces of water (“typically” 250-300 ppm, by mass) in the feed are known to cause structural breakdown of the catalyst, mostly due to the hydrolysis of the silicon phosphates present.⁵⁵ However, an improved SPA catalyst is known to tolerate increased water content of up to 2000 ppm (by mass).⁴⁷ Acid leaching and coking also cause deactivation.⁵⁵

A modified solid phosphoric acid process that overcomes one of the drawbacks of the original polygas process, namely its limitation to producing mainly fuels in the gasoline-range,^{5,6,35} is operated at Sasol Synfuels HTFT refineries in Secunda, South Africa, to convert low olefins from the Fischer-Tropsch process and produce oligomers in the diesel and jet fuel range.^{30,56,57,58,59,60}

Given that SPA and polygas are not primarily diesel producing catalysts and processes, the water content of the feed and the operating conditions were manipulated to produce the desired diesel-range oligomers, resulting in the diesel-specific “CatPoly” process.²⁹ The “CatPoly” process uses an SPA catalyst that is supplied by Süd-Chemie.^{46,47}

However, since there are no spatial constraints present on the SPA catalyst, the oligomers are highly branched and certain side chains are longer than methyl groups. Having a cetane number^a, therefore, of only 30 (34 after hydrogenation),⁵⁴ “CatPoly” diesel has poor self-ignition properties, but was found to have excellent cold flow properties, making it a good blending stock for straight-run Fischer-Tropsch synthesis derived diesel. Its low boiling end makes a good jet fuel.⁵⁴

^a Cetane number is a measure of how readily the fuel starts to burn (auto-ignites) under diesel engine conditions after injection. A fuel with a high cetane number starts to burn shortly after it is injected into the cylinder; it has a short ignition delay period. Conversely, a fuel with a low cetane number resists auto-ignition and has a longer ignition delay period.⁷⁸

2.1.2.2.2 The MOGD process

The Mobil Olefins to Gasoline and Distillate (MOGD) process was the first of the zeolite based olefin oligomerization processes, developed in the late 1970's. Using medium pore size zeolite H-ZSM-5 as the catalyst (channel structure and dimensions, see Figure 8), methanol is first converted into light olefins and in a second stage, also over H-ZSM-5, the olefins are converted into gasoline and diesel fuel.^{3,61,62,63,64} Mobil Oil Corporation has filed numerous patents that describe the use of zeolites, in particular H-ZSM-5, as catalysts for the conversion of low molecular weight olefins into higher molecular weight olefins and for other hydrocarbon conversion reactions.^{61,62,63,64,65,66,67,68,69,70,71,72,73,74,75,76}

The MOGD process is also widely described in the open literature. The process uses the medium pore H-ZSM-5 to convert methanol first to light olefins and then, also over H-ZSM-5, oligomerizes them into gasoline and diesel fuel (distillate).^{3,63,90,106} The catalyst in the olefin oligomerization stage has typically a silica-alumina molar ratio of 70 and is extruded with 35% alumina.^{1,64} A distillate fuel selectivity of ca. 80 wt% is obtained when operating in the distillate mode (*viz.*, fixed bed, 190-310 °C, 4-10 bar, WHSV of 0.5-1 g/g.h).¹

The limitations of the iso-olefinic structure of the MOGD product are mainly determined by the shape-selective constraints imposed by the channels of the H-ZSM-5 catalyst (see Section 2.3.1.1).^{64,91} The structure of the higher carbon number products, therefore, is primarily moderately methyl-branched olefinic chains. The average is one methyl side chain per five carbon atoms.^{64,91}

The MOGD process can produce various distillate to gasoline ratios to accommodate, for instance, seasonal swing in product demand. Due to its flexibility, the MOGD process has potential in refinery, petrochemical or synthetic fuel applications.⁶⁴ The MOGD process is, however, not commercialized.

Due to it mainly consisting of moderately branched olefins, the gasoline fraction from the MOGD process has a medium research octane number (RON) of 92^{b,77,78} (for comparison, in South Africa 95 RON is marketed at the coast and 93 RON is dominating the inland market).⁷⁷

The diesel-range product, when hydrogenated, has a rather high cetane number)^{c,77,80} of around 56 and good cold flow properties but too low a density compared to specifications (see Table 2-1).⁶⁴ With its value of 56, the cetane number of MOGD diesel is significantly above the current requirements of the South African Bureau of Standards (SANS 342/ SABS 342:2003)⁷⁹, and also above the requirements of the European Standards Organization (CEN 590)⁸⁰ and the American Society for Testing and Materials (ASTM D975)⁸⁰ requirements. The hydrogenated MOGD distillate product contains about 3 wt% aromatics.^{3,64}

^b Octane number is a measure of petrol's resistance to auto-ignition. i.e. an indicator of the fuel's anti-knock performance. The higher the octane number, the greater is the resistance of the respective petrol to knock.^{77,78}

^c Cetane number is a measure of how readily the fuel starts to burn (auto-ignites) under diesel engine conditions after injection. A fuel with a high cetane number starts to burn shortly after it is injected into the cylinder; it has a short ignition delay period. Conversely, a fuel with a low cetane number resists auto-ignition and has a longer ignition delay period.⁷⁸

Table 2-1: MOGD diesel fuel (hydrogenated oligomerizate) product quality⁶⁴
 (“Industry Standard” refers to 1980’s US standards)⁶⁴

	MOGD diesel		Industry Standard
Feed	FCC C ₃ [≡] /C ₄ [≡] ^a	C ₅ [≡] /C ₆ [≡]	
Specific gravity, g/cm ³	0.78	0.78	0.88 - 0.84
Aromatics, vol%	3	-	-
Pour Point, °C	< -51	< -51	-7
Cetane Number	52 - 56		45
90% b.p., °C	343	304	338

^a Charge stock FCC C₃[≡]/C₄[≡] was a mixture of propane/propene/butane/butene (62% olefin) pumped directly from an Fluid Catalytic Cracker unit.

- Not given in the source.⁶⁴

2.1.2.2.3 The COD process

The “Conversion of Olefins to Distillate” (COD) process was commissioned by the Moss gas Refinery (now PetroSA) in South Africa in 1992 and is operating at PetroSA’s Mossel Bay plant.^{81,82} The COD process, like the MOGD process, is based on an H-ZSM-5 type shape-selective catalyst, termed COD-9, which is supplied by Süd-Chemie.^{31,81}

The plant converts Fischer-Tropsch process derived light olefins (i.e. C₃-C₆ olefins).^{32,33} Spatial restrictions in the pore system of the H-ZSM-5 zeolite catalyst employed, similar to the MOGD process, limit branching in the product, favouring methyl branches (60-70% of total branches^{32,33}).

The COD process was designed to handle a feedstock that contains oxygenates, which includes alcohols, acids, esters and ketones, totalling 1.8 wt%.⁸¹ Since oxygenates have a negative effect on catalyst stability in

that they cause pre-mature catalyst deactivation,⁸¹ reaction conditions are comparably severe (280 °C and 50 bar). As a consequence, the raw COD distillate contains more than 10% aromatics.^{32,33} After hydrogenation of the diesel range boiling fraction to an extent that the aromatics content dropped below 0.1%, cetane numbers of 51-54 are obtained.

2.1.3 Radical induced olefin oligomerization – the free radical mechanism

The free-radical based processes are mainly of interest for polymer formation. The three steps involved are initiation, propagation and termination. In a radical polymerization reaction, propagation is initiated by the attack of a radical derived from thermal or photo-chemical decomposition of the so-called initiator on the monomer. The initiation step is followed by propagation, where the free radical end of the growing chain adds to a monomer molecule. Finally two propagating species combine or disproportionate to terminate the chain growth and to form one or two polymer molecules, respectively.³⁴

2.1.4 Comparison of the different mechanisms and types of catalysis

Of the three mechanisms discussed, only the coordinative mechanism (over metal catalysts and homogeneous metal complexes) and the carbenium ion mechanism (over acid catalysts) are relevant for olefin oligomerisation.

In acid-catalyzed olefin dimerization/oligomerization, the predominant intermediate species is the most stable carbenium ion. The mechanism takes place via

electrophilic addition of a carbenium ion to a carbon-carbon double bond, whereby the reactivities of the olefins correspond to the relative stabilities of the intermediate carbenium ions formed. Thus, short chain olefins, such as ethene and propene, are more difficult to dimerize/oligomerize.^{3,38,94} In case of acid zeolitic catalysts the reaction pathways can be altered by molecular shape-selectivity, resulting from the confinement of the reacting molecules by the zeolite microchannels (see Section 2.2).^{41,87}

In metal and metal complex catalyzed olefin dimerization/oligomerization, the predominant intermediate species is the least sterically hindered alkyl chain or alkyl ligand coordinated to the metal atom. The mechanism takes place via electrophilic addition of the metal atom to a carbon-carbon double bond (in other words, the insertion of the carbon-carbon double bond into the carbon-metal bond of the growing chain), whereby the reactivities of the olefins are largely controlled by steric hindrance, i.e. ease of access to the metal atom. Thus, long chain olefins are more difficult to oligomerize/dimerize.^{7,8,9,19,35}

In acid catalysis double bond isomerization is rapid and skeleton isomerization occurs as well (although slower), whereas in metal catalysis and catalysis over metal complexes such isomerization hardly occurs. Consequently, dimers/oligomers from acid catalysis are more branched than dimers/oligomers from metal catalysis. The trend in olefin monomer reactivity with chain length is opposite in acid and metal catalysis, namely increasing with chain length over acid catalysts and decreasing over metal catalysts. The above introduction to acid catalyzed olefin dimerization and oligomerization

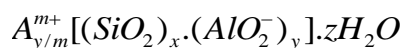
(Section 2.1.2) is followed by a brief review of the structures and properties of amorphous and crystalline aluminosilicates with focus on zeolites (see Section 2.2) and continues with a more detailed review on the use of H-ZSM-5 as a shape-selective catalyst in olefin oligomerization and the properties of the product in Section 2.3.

2.2 Zeolites and other aluminosilicates

2.2.1 Zeolite structures and chemical composition

The history of zeolites began in 1756 when a Swedish mineralogist, Cronstedt, discovered the zeolite mineral stilbite that released water vapour when heated. The name “zeolite” is, accordingly, derived from the Greek words “*zeo*” and “*lithos*”, which mean “*to boil*” and “*stone*” respectively.^{86,83} The chemical composition of zeolites is very similar to sand, as they are mainly composed of silicon and oxygen atoms. The materials look like sponges, but have very regular structures and strictly uniform pore sizes, the latter being of typical molecular dimensions.^{85,84}

The general composition of a zeolite can be represented by a formula of the type



where A is a cation with the charge m , $(x + y)$ is the number of tetrahedra per crystallographic unit cell, x/y is the framework silicon/aluminium atomic ratio and z represents the amount of water contained in the zeolite voids. The silicon and aluminium atoms of zeolites are also referred to as the T-atoms.

Löwenstein's rule states that two contiguous tetrahedra containing aluminium in the T-position, i.e. Al-O-Al linkages, are forbidden and, consequently, the Si/Al atomic ratio must be greater than or equal to 1.^{35,85,87}

Zeolites are crystalline, microporous aluminosilicates with a structure comprised of a framework based on a three-dimensional network of SiO_4 and AlO_4 tetrahedra linked together at the corners through common oxygen atoms.^{36,85,86,87,88} Using the SiO_4 and AlO_4 tetrahedra as basic building blocks, all kinds of structures can be created with pores or channels and cavities of varying dimensions (see Figure 2-8).⁸⁸

The cavities, channels and cages present in the zeolite framework have sizes typically of a few to several Angströms. At ambient temperature they are usually occupied by water molecules and extra-framework cations that are commonly exchangeable.⁸⁹

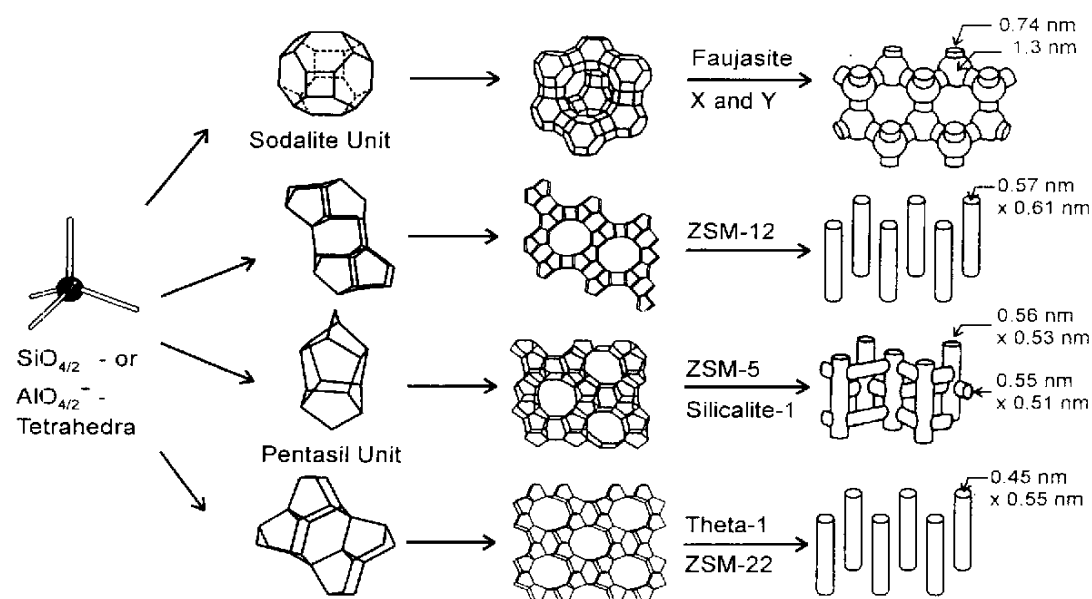


Figure 2-8: Some elementary building units of zeolites: SiO_4 and AlO_4 tetrahedra, forming secondary building units and then different zeolite structures.⁸⁵

The net formulae of the tetrahedra are SiO_2 and AlO_2^- , i.e. one negative charge resides at each tetrahedron in the framework that has an aluminium atom in its centre, and this charge is balanced by extra-framework cations.⁸⁵ The extra-framework cations (metal ions or protons) are associated to one of the bridging oxygen atoms next to an Al^{3+} ion.⁸⁸

2.2.2 Zeolite channel structures and sizes

Porous solid materials can be grouped into three classes based on their pore diameters (d) ($1 \text{ nm} = 10 \text{ \AA}$):^{85,87}

Microporous:	$d \leq 20 \text{ \AA}$
Mesoporous:	$20 \leq d \leq 50 \text{ \AA}$
Macroporous:	$d > 50 \text{ \AA}$

Referring to their channel or pore sizes, zeolites are microporous materials and are conventionally defined as ultra-large (>12 -), large (12 -), medium (10 -), or small (8-membered ring) pore-size materials depending on the smallest number of O atoms that limit the pore apertures of their largest channel. Pore diameters vary between 5 and 20 \AA .⁸⁷

Medium pore zeolites are of tremendous scientific and industrial interest due to their shape-selective properties (see Section 0). Almost all of the medium pore zeolites are synthetic in origin. Their framework structures contain 10-membered rings and they are highly siliceous.⁹⁰ Zeolite ZSM-5 has received the most attention by far, and serves as a prime example of the

uniqueness of medium pore zeolites in catalysis.^{36,85,90} Medium pore zeolites provide channel dimensions as required for the intended hexene and octene dimerization reactions.

ZSM-5 has two types of bidirectional, intersecting channels that are each formed by rings containing 10 oxygen atoms. The two intersecting channels are slightly different in their pore size. The one channel, which is sinusoidal, has an elliptical pore opening ($5.1 \times 5.5 \text{ \AA}$), the other channel, which is straight, has a nearly circular pore opening ($5.4 \times 5.6 \text{ \AA}$). These two channels intersect to form a 3-dimensional network of pores (see Figure 2-9).⁹⁰ Constantly altering between the two channel systems enables molecules to diffuse in the third dimension. This is why the ZSM-5 pore system is considered to be three-dimensionally interconnected.^{41,90}

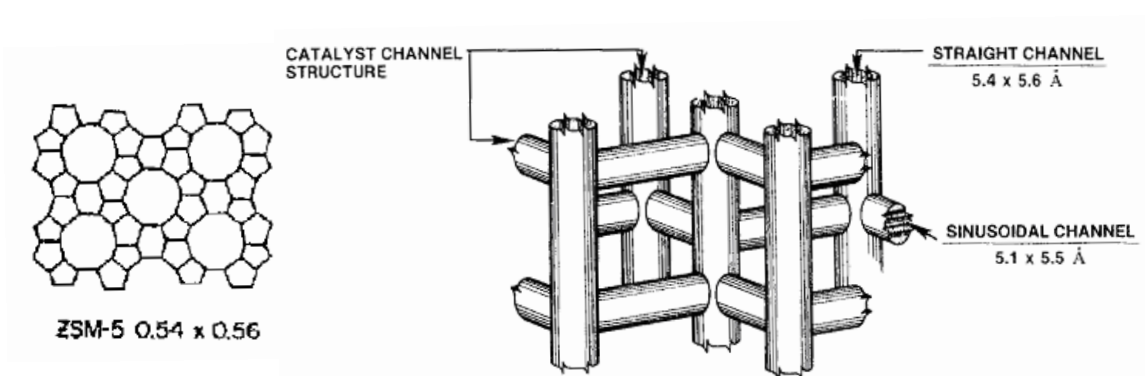


Figure 2-9: Schematic representation of the three-dimensionally interconnected channel system and projection of the structure of zeolite ZSM-5 (on the right). The shape and size of the widest channel (in nm) is indicated on the left.^{36,91}

Medium pore zeolites show remarkably low coking tendencies. These are mainly attributed to their high silica/alumina ratios and to geometrical

constraints imposed by the 10-membered ring pores.³⁶ The two factors make it sterically difficult to form the large polynuclear hydrocarbons responsible for coking inside the pore system so that coking occurs predominantly only on the outer surface of the zeolite crystals.³⁶

Highly siliceous zeolites may have ion exchange capacities in excess of their framework tetrahedral aluminium content.⁹² These aluminium-independent ion exchange sites have been identified as framework siloxy anions, which serve as counter-ions for the organic cations (templates) during synthesis, but do not contribute to the acid activity.

2.2.3 Aluminium content

The thermal stability of the crystal framework increases with increasing silica/alumina molar ratio whereby thermal decomposition temperatures of different zeolites range from ~700 °C to 1300 °C.⁸⁶

Zeolites are further grouped into families on the basis of composition, namely, the silica/alumina ratio. H-ZSM-5 is a high silica zeolite that can have a silica/alumina ratio of 12.5 to infinity (unit cell, water free: $\text{Na}_n\text{Al}_n\text{Si}_{96-n}\text{O}_{192}$ with $n < 27$). Its properties include high hydrothermal stability and, in particular, high thermal stability of the framework, high stability under acid (but low stability under basic) conditions and a low concentration of acid groups of, however, high individual acid strength.^{86,93}

Zeolites with low silica/alumina ratios have higher concentrations of acid sites than the others.⁸⁶ Zeolites with a high concentration of aluminium and balancing protons are hydrophilic and have strong affinities for polar molecules that are small enough to enter the pores (such as water molecules). Zeolites with high silica/alumina ratios, i.e. low H^+ concentrations (in the limit, practically aluminium free silicalite), are hydrophobic, taking up organic compounds (e.g. ethanol) from water-organic mixtures. The transition from hydrophilic and hydrophobic zeolites occurs at a molar silica/alumina ratio near 10.

2.2.4 Zeolite catalysis

The application of zeolites expanded in the late 1950's to commercial catalytic processes. The first commercial use of zeolites as catalysts took place in 1959 when zeolite Y was used as an isomerization catalyst by Union Carbide.^{86,88}

In catalysis, a number of consecutive steps are needed by the reactant molecules to access the catalytically active sites and to convert the reactants into products. These steps are schematically depicted in Figure 2-10 for a porous solid catalyst.

As the feed stream is in the gas or liquid phase, adsorption on the surface of the zeolite crystallites and into the zeolite pores has to take place first. In order to react, the molecules then have to be transported to the active sites inside these pores. This transport process is by diffusion.⁸⁴

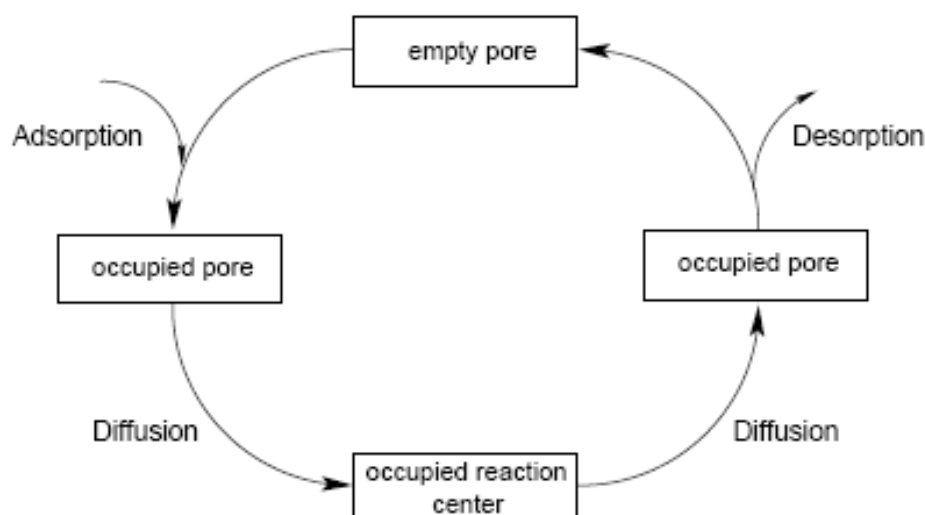


Figure 2-10: Diffusion in catalysis over a porous solid: the pores are occupied by adsorption from the gas or liquid phase, after which the adsorbed species diffuse to the active centres.⁸⁴

Once the reactants have reached the catalytically active sites, the desired (or undesired in some cases) chemical reactions can finally take place, with the conversion of the reactants into products and by-products. The catalytic sites have to be freed from the products in order to facilitate the next reaction. The products have to desorb and be transported out of the zeolite pore. Diffusion and subsequent desorption of the products from the zeolite catalyst take care of that.⁸⁴

2.2.5 Catalysis by Brønsted acid sites

The negative charge of the aluminium tetrahedra in zeolites is balanced by cations such as H^+ . The protons are associated to one of the bridging oxygen atoms next to the Al^{3+} cation (top structure in Figure 2-11).⁸⁸

The aluminium tetrahedra in the H^+ -form are Brønsted acid sites, which behave in a similar way as the protons in an acidic solution.⁸⁴ By definition⁸⁷, a solid acid catalyst having Brønsted acid sites is able to donate or at least partially transfer a proton to a reactant which then becomes associated with the resulting surface anion.

The activity of solid acid catalysts, therefore, is based on the formation of Brønsted acid sites arising from the creation of what is referred to as “bridging hydroxyl groups” within the pore structure of the zeolites, i.e. the charge balancing proton is associated to one of the oxygen atoms that form the bridges between an aluminium atom and the adjacent silicon atoms (see top structure in Figure 2-11).⁹⁴ The protons are quite mobile and at temperatures of 550 °C and higher are lost together with the bridging oxygen as water molecules resulting in the formation of Lewis acid sites, as shown in Figure 2-11.⁹⁴

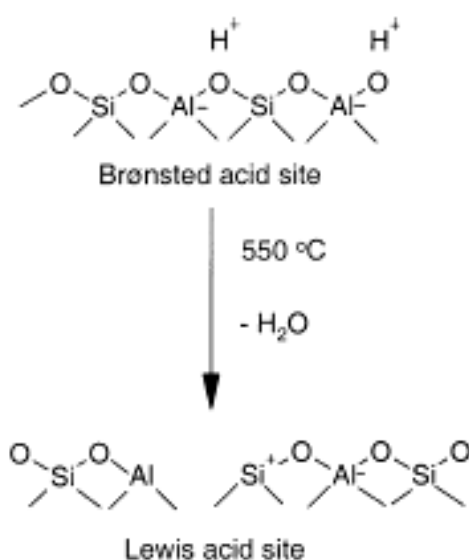


Figure 2-11: Formation of Lewis acid sites from two Brønsted acid sites (taken from Stöcker).⁹⁴

The concentration of acid sites in a zeolite is directly proportional to the concentration of aluminium in the lattice.^{85,94}

Zeolites can be used as supports for other catalytic materials. For instance, salts of metals such as platinum or palladium can be impregnated onto the zeolite crystallites and reduced, and in this way metal catalysts can be produced with a very high surface area. When using an acid zeolite, different catalytic functions can be united in a single catalyst to form a bi-functional catalyst.^{6,88}

2.2.6 The use of zeolite catalysts in industrial processes

Zeolites are the most widely used catalysts, by volume, in industry.^{6,41,85,86} These porous, crystalline materials have become extremely successful as catalysts not only for oil refining and petrochemistry, but also in the production of fine and speciality chemicals, particularly when dealing with molecules having kinetic diameters below 10 Å.⁹⁴ Upon the introduction of synthetic faujasite catalysts (zeolites X and Y) in 1962, the fluid catalytic cracking (FCC) of heavy petroleum distillates became one of the most widely used chemical processes worldwide. After 1962, zeolites were increasingly used in other processes in the fields of petroleum refining and synthesis of base chemicals.⁸⁹ Besides its application in the crude oil refining environment (e.g. as an additive to the said FCC catalysts), zeolite H-ZSM-5 has become the “work horse” amongst the zeolites used in the synthesis of small organic chemicals.^{5,41}

2.2.7 Other alumino-silicates than zeolites

Besides zeolites, which are crystalline aluminosilicates with micropores whose diameters range from 5 to 20 Å⁸⁵ (see Section 2.2.2), there are mesoporous, ordered silica-aluminas, commonly addressed as mesoporous materials, and there are also amorphous silica-aluminas with average pore diameters in the mesopore to micropore range. These materials contain Brønsted acid sites associated with the aluminium atoms and, therefore, possess catalytic activity.

However, in the amorphous materials only a part of the aluminium is located in the “ideal” environment of four tetrahedrally orientated oxygen atoms as shown in Figure 2-11 (top),^{87,55} so that the average catalytic activity per aluminium atom is lower than with zeolites.

2.2.7.1 Amorphous silica-alumina

Silica forms many different crystalline structures and structurally amorphous silica is a covalent oxide material that has many valences saturated by silanol groups. These groups have weak Brønsted acidity.⁵⁵ Amorphous silica is industrially used mostly as an absorbent and filter material.⁵⁵ In catalytic applications it can be used as a catalyst support and as a binder, but not primarily as a catalyst in its own right.⁵⁵ Alumina, on the other hand, which may exist as γ -, η -, σ -, or θ -Al₂O₃, has some catalytic activity, which is mainly related to the Lewis acidity of a small number of coordinated surface aluminium ions, and the high polarity of the surface Al-O bond.⁵⁵

However, “mixed oxides” of silicon and aluminium are catalytically active and play a relevant role in catalysis.⁵⁵ Commercial silica-aluminas can vary by composition between the extremes of pure silica and pure alumina, and the silica-rich materials are generally fully amorphous.⁹⁵ These materials are referred to as “amorphous silica-aluminas” (ASA). Amorphous silica-aluminas exhibit cation-exchange capacity and possess both Brønsted and Lewis acid sites, making ASA well suited for use as acid catalysts and supports for multifunctional catalysts.^{95,97,55}

There are a number of different, chemically unique silanol species on the ASA surface, namely bridging silanol groups [O Si-O(H)-Al] whose structures equal those of the Brønsted acid sites in zeolites (top of Figure 2-11), terminal silanol groups, bound to Al via bridging oxygen [(H)O-Si-O-Al], and pseudo bridging silanol groups of configuration [O-Si-O(H)···Al], where, for instance, the distance between the O and the Al is larger for the amorphous material than for the ideal Brønsted acid sites of a crystalline material or the bond angles distort.⁹⁵ It is unknown which species are mostly responsible for ASA’s catalytic activity.

Microporous (≤ 20 Å) and mesoporous (20-500 Å) silica-aluminas have been developed that show such catalytic activity. The mesoporous materials, although sometimes considered to be a kind of very large-pore zeolite, are mainly amorphous or semi-crystalline, with pores that are irregularly spaced and broadly distributed in size.^{96,55}

A class of layered aluminosilicates, referred to as clays which, like ASA, exhibit cation-exchange capacity, are known to be versatile and cheap catalysts for a variety of reactions of significance to the petrochemical industry.^{97,98} Clays consist of a large number of distinct structural types, based on SiO_4 tetrahedra and MO_6 octahedra (with M being Al, Mg or Fe) as building blocks. SiO_2 tetrahedra and MO_6 octahedra are each arranged individually in sheets and the individual sheets are alternately sandwiched to finally form the clay.

Partial exchange of the central cations of the octahedra or tetrahedra for cations with one unit of charge less requires balancing by another cation, which can be a proton.^{97,98} A modified montmorillonite from Süd-Chemie, designated K10, was used industrially for hydrocarbon cracking.⁹⁷

Acid-leached natural aluminosilicates, i.e. clays, were the first solid acid catalysts to be used commercially (1915). This was as cracking catalyst in the so-called Houdry process⁸⁷, which was used for some decades (1930-1960). Due to undesired impurities, such as Fe, natural clays were first replaced by synthetic aluminosilicates, referred to as amorphous silica-aluminas, until zeolites finally started to dominate solid acid catalysis.^{98,55} At present, catalytic reactions using ASA or ASA-based catalysts for industrial application include isomerization of olefins, paraffins and alkyl aromatics, alkylation of aromatics with alcohols and olefins, olefin oligomerization and cracking.^{5,6,35,30,87,98,99,55,40}

An ASA catalyst where nickel is supported on silica-alumina is used in the Hüls (now Evonic) Octol process to produce mainly chemicals via the dimerization of *n*-butenes. Linear and branched product, such as *n*-octene and methylheptenes are obtained in the dimerization step.^{5,30,40} Eni Technologies use ASA for the oligomerization of light olefins to gasoline and jet fuel.^{35,100} By Eni Technologies, propene is oligomerized to a branched olefinic gasoline product, which has a high RON (research octane number) in the range of 97 to 102.^{35,100} The IFP/Axens PolynaphthaTM process was originally also designed to use an ASA catalyst, but now uses a zeolite based catalyst.^{30,101}

The use of ASA catalysts is decreasing due to the increasing popularity of amorphous silica-aluminas with controlled pore sizes, i.e. MSA or MCM-41, and also amorphous aluminium phosphates.⁸⁷

2.2.8 Shape-selectivity of zeolites and related microporous materials

The concept of “shape-selective catalysis” was introduced in 1960 by demonstrating that CaA zeolite dehydrates 1-butanol at 260 °C, but not isobutanol.^{90,94,102,103} This observation showed that the conversion of the 1-butanol takes place inside the microporous structure of the CaA zeolite (5 Å pore diameter), which is not accessible for the branched isobutanol molecule due to its larger diameter.⁹⁴

The three “classical” and most common types of shape-selectivity occurring over zeolites and related microporous materials are schematically presented in Figure 2-12.

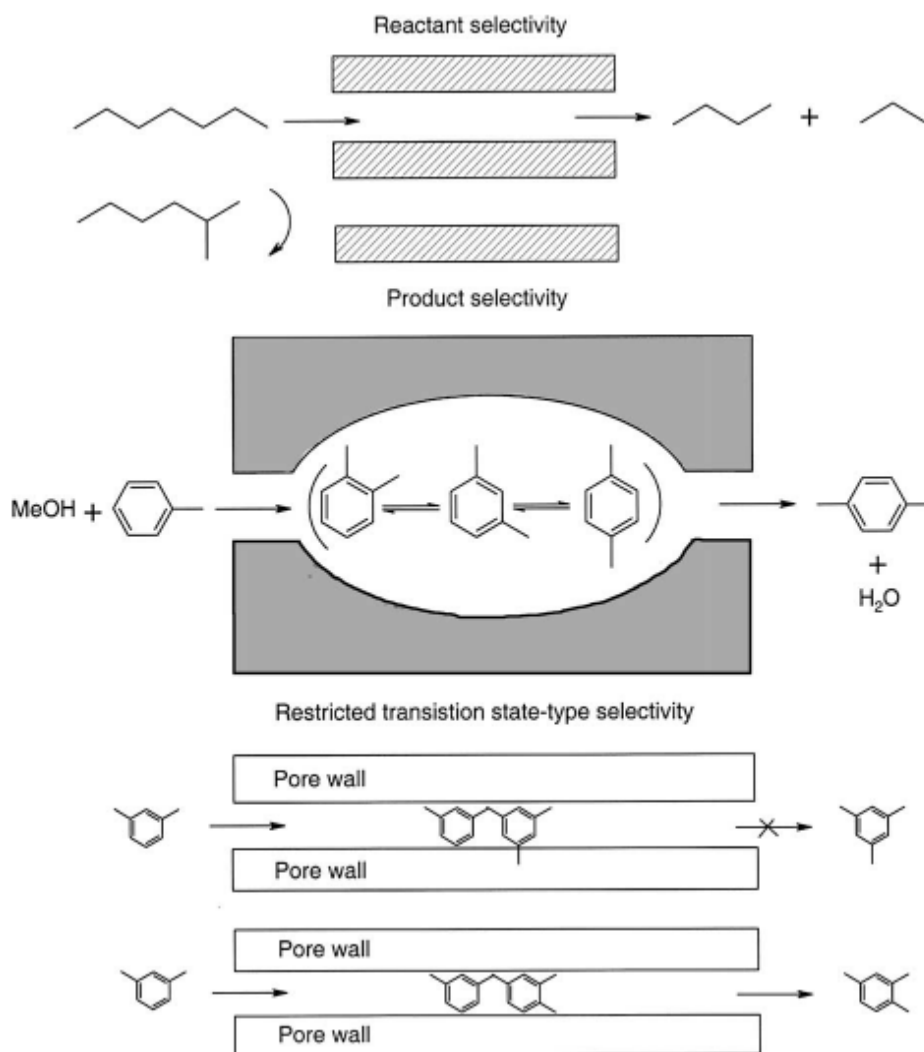


Figure 2-12: Schematic representation of the three “classical” types of shape-selectivities.^{94,104}

The mechanisms of these types of molecular shape-selective catalysis can be described and summarized as follows:¹⁰⁴

Reactant selectivity describes the phenomenon of microporous catalysts acting as molecular sieves and excluding bulky molecules from entering the intra-crystalline void-structure, while allowing smaller molecules to enter and react.^{94,103,104}

Product selectivity refers to different diffusivities of the reaction products formed inside the micropores of zeolite crystals. Sterically less hindered (“slim”) product molecules may easily leave the microporous framework, whereas bulky product molecules may stay much longer in the cavities of the zeolite but may structurally isomerize to a “slim” shape and then leave.^{94,103,104}

Restricted transition state selectivity occurs when the spatial configuration around a transition state or a reaction intermediate located in the intra-crystalline volume is such that only certain configurations are possible. This means that the formation of certain intermediates and/or transition states is more or less sterically hindered due to the shape and limited size of the pores in the microporous lattice.^{94,103,104}

Reactant selectivity and product selectivity are not necessarily yes/no effects, as Figure 2-12 may suggest, but rather often just preferences induced by different diffusivities. In so far, reactant and product selectivities are mass transfer controlled, i.e. controlled by the Thiele Modulus (see Section 2.7).^{84,94,104}

2.2.9 Shape selective catalysis over external zeolite crystallite surface

Obviously, there are no shape-selective effects visible when a reaction occurs on the external surface of the crystallites of an otherwise shape-selective zeolite. However, under certain circumstances shape selectivity occurs not only inside the pores of zeolite crystals (especially zeolite H-ZSM-5) but also at the external surface.¹⁰⁵

There are two kinds of acid sites in H-ZSM-5, which differ in their accessibility for larger molecules and the space available for catalytic transformations. The one kind is the “normal” acid site, located inside the channel system (e.g. at the intersection of two pores) that is involved in “classical” shape-selective reactions (see Sections 2.2.9 and 2.3.1). The other one is associated with special features on the external surface of the crystallites.¹⁰⁵

Schematic representations of three different types (a, b and c) of non-classical shape-selective effects are shown in Figure 2-13.

Half-cavities, that is, for instance, pore intersections that are open to the crystallite surface, are claimed to exist at the (001) plane of H-ZSM-5 (see Figure 2-13a). It is postulated that optimum van der Waals interactions exist between certain molecules adsorbed in such holes or “nests” at the external surface due to the curvature of the walls. It is further postulated that these curvatures can affect the selectivity of catalytic reactions of the adsorbed molecules.¹⁰⁵

The type of selective reaction involving the acid sites at the entrance of the pores of zeolites, where the spatial constraints are less, is termed *pore-mouth catalysis* (Figure 2-13b).⁹⁴

Another type of reaction occurs when two or more sections of a molecule match approximately the distance between pore openings at the surface of the zeolite crystallites. This is called *key-lock catalysis* (Figure 2-13 c).⁹⁴

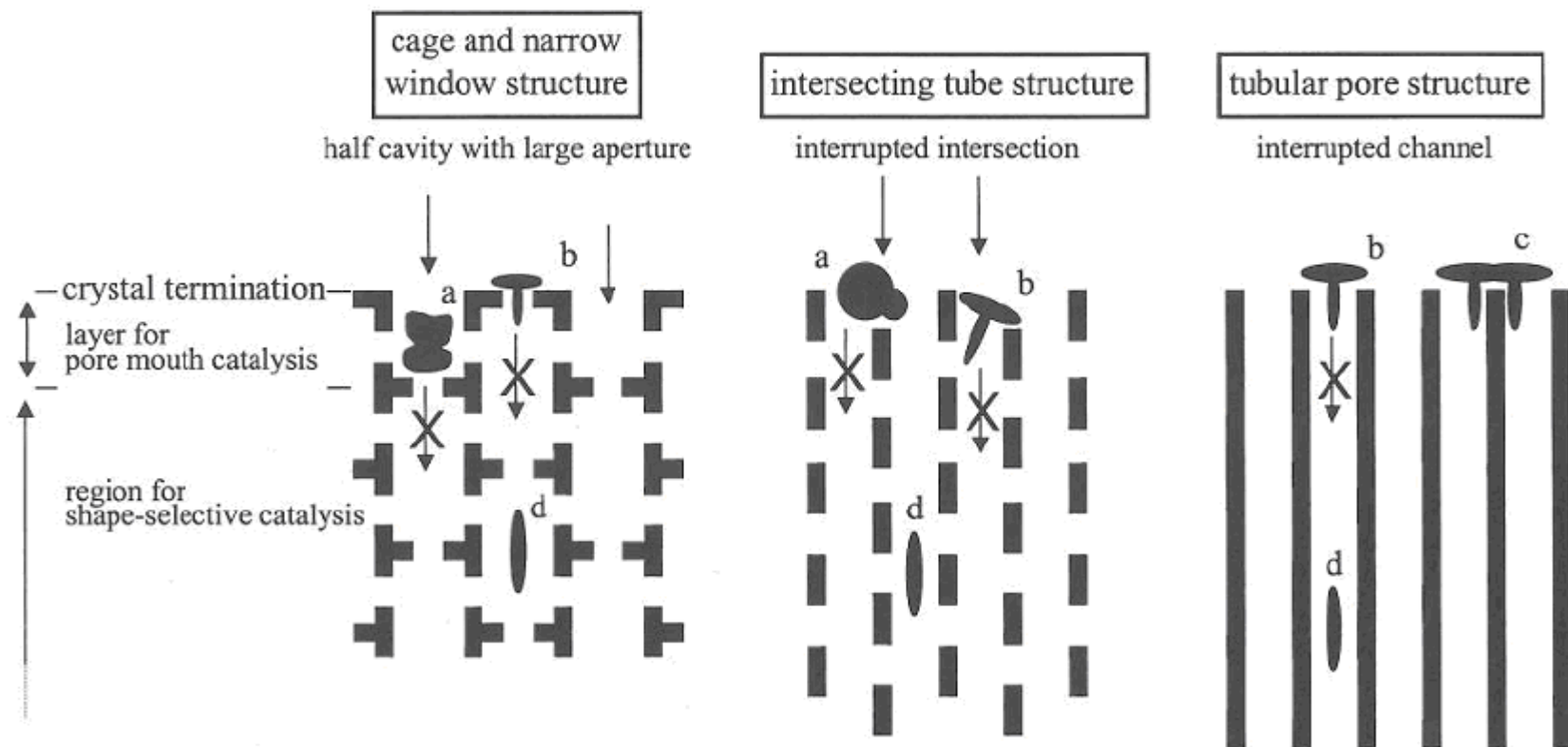


Figure 2-13: Shape-selective environments in different sections of the zeolite surface structure: (a) comparatively large molecules have access to interrupted (half) cavities and channel intersections; (b) molecules are plugged into the pore aperture for pore-mouth catalysis; (c) molecules are converted in multiple pore-mouths according to key-lock catalysis; (d) molecules are converted in the intra-crystalline, shape-selective environment (classical shape-selectivity).⁹⁴

The bottom line is that certain shape-selective effects can still be imposed on molecules that are too large to penetrate the pore system of a zeolite, since more accessible, but still constraint surface structures may provide for the catalytic activity.

2.3 The use of H-ZSM-5 as a shape-selective catalyst in olefin oligomerization

Section 2.1.2 dealt with acid catalyzed olefin oligomerization in a rather general way and Section 2.2 introduced alumino-silicates and their properties, in particular zeolite H-ZSM-5. The focus in the following is on the detailed description of the findings for olefin oligomerization over H-ZSM-5 and the kinetic, shape-selective and thermodynamic background.

In the late 1970's, the shape-selective oligomerization of C_2 - C_{10} olefins over H-ZSM-5 to olefins up to C_{30} and higher was reported.³ The reaction conditions favouring such higher molecular weight products are low temperature (200-260 °C), elevated pressure (20 bar or higher), and long contact time (WHSV less than 1 g/g.h).³ Under these conditions the reaction proceeds through the acid-catalyzed steps of 1) oligomerization, 2) isomerization/cracking to a mixture of intermediate carbon number olefins, and 3) "interpolymerization"³ to give a continuous boiling product range containing all carbon numbers. The average chain length is a function of reaction temperature and pressure.^{3,64,106} Thus, low temperature and high pressure favour the formation of distillate-range products while high temperature and low pressure favour gasoline-range products.⁶⁴

The channel system that imposes shape-selective constraints on the product configuration (limited extent of branching of the larger molecules) accounts for the difference of the product obtained from medium pore zeolite catalyst H-ZSM-5 to that from catalysts with wider pores.³ For instance, converting a propene feed over H-ZSM-5 provides long-chain hydrocarbons with, generally, a lower number of alkyl substituents (essentially methyl substituents) along the straight chain, compared to those obtained over an amorphous silica-alumina catalyst (as can be derived from Figure 2-14).

Band, cm ⁻¹	Hydrocarbon	Liquids	
		Si/Al	HZSM-5
980-965	$ \begin{array}{c} R_1 \quad H \\ \diagdown \quad \diagup \\ C=C \\ \diagup \quad \diagdown \\ H \quad R_2 \end{array} $	Weak	Medium
895-885	$ \begin{array}{c} R_1 \quad H \\ \diagdown \quad \diagup \\ C=C \\ \diagup \quad \diagdown \\ R_2 \quad H \end{array} $	Weak	V. Weak
840-790	$ \begin{array}{c} R_1 \quad H \\ \diagdown \quad \diagup \\ C=C \\ \diagup \quad \diagdown \\ R_2 \quad R_3 \end{array} $	Weak	Absent
995-985 910-905	$ \begin{array}{c} R_1 \quad H \\ \diagdown \quad \diagup \\ C=C \\ \diagup \quad \diagdown \\ H \quad H \end{array} $	Absent	Absent
1600-1590	Aromatics	Weak	V. Weak

Figure 2-14: Infrared analysis of the liquid product obtained from the conversion of propene over silica-alumina “Si/Al” compared to that obtained over H-ZSM-5 (at 232 °C, 103 bar and WHSV of 0.5 g/g.h) showing how much of the different types of double bonds is present in the respective oligomerizates.³

At 232 °C, 103 bar and WHSV of 0.5 g/g.h, the product obtained from the conversion of propene over amorphous silica-alumina contained less olefins and more aromatics, and also more highly-branched olefins, by comparison, than the product formed over H-ZSM-5, due to the shape-selective constraints imposed by H-ZSM-5.³

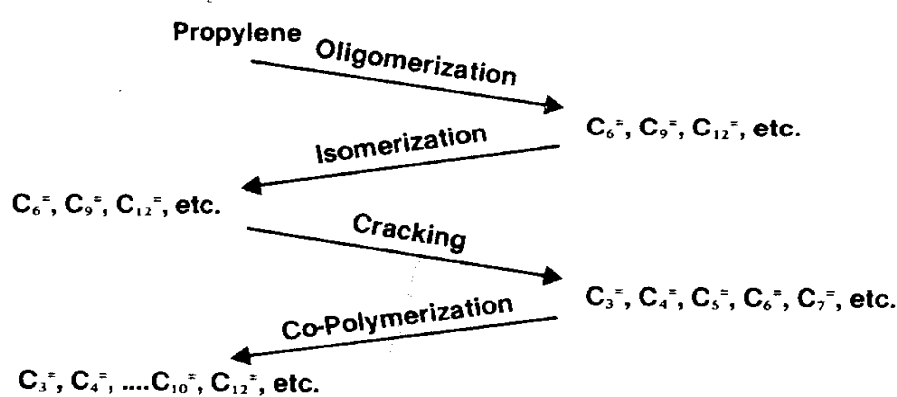
As already indicated in Section 2.2.2, H-ZSM-5 has a medium pore channel system. This channel system imposes constraints by the size of the pores within which oligomerization occurs, so that it is not physically possible to form highly branched oligomers inside.⁶⁴ The products are thus relatively straight chains with only a few methyl branches present that is, that approximately only every fifth carbon atoms of the backbone of the molecules carries a methyl group.¹⁰⁶ As a result, unique iso-olefinic products are formed.

2.3.1 Kinetics and thermodynamics of olefin oligomerization over H-ZSM-5

Mobil's MOGD process (see Section 2.1.2.2) is not a "true oligomerization" process but a "conjunct oligomerization" process (see Section 2.1.2.1) in that both the forward (oligomerization) and reverse (cracking) reactions occur simultaneously.⁶⁴ In this type of oligomerization, propene ($C_3^=$) oligomerizes in the forward direction to $C_6^=$, $C_9^=$, $C_{12}^=$, etc. and in turn, products in the higher olefin range, i.e. $C_6^=$ to $C_{12}^=$ and higher, crack back to lower olefins, which again oligomerize forward (see Figure 2-15). Consequently, the net result is a continuous carbon number product, i.e. $C_2^=$, $C_3^=$, $C_4^=$, $C_5^=$, $C_6^=$, $C_7^=$,

$C_8^=$, $C_9^=$, etc., whose carbon number distribution is a function of the reaction conditions, and whose branching is limited due to shape-selective constraints.^{64,91}

Furthermore, the olefins may undergo irreversible cyclization and hydrogen-transfer reactions during conjunct oligomerization (see Figure 2-15).²



TYPICAL PRODUCT STRUCTURE

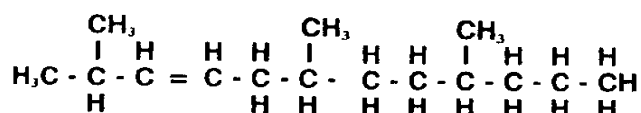


Figure 2-15: MOGD model reaction path for propene feed.⁹¹

Such reactions may lead to the formation of cycloolefins, alkyl aromatics, and paraffins.¹⁰⁶ For a conjunct oligomerization process, the structure of the product is rather independent of the olefin charge; the three potential charge streams considered for the MOGD process, namely, ethene ($C_2^=$), propene/butene ($C_3^=/C_4^=$) and pentene/hexene ($C_5^=/C_6^=$) give approximately the same product.^{64,91}

2.3.1.1 Limited branching over H-ZSM-5

The conversion of olefins over H-ZSM-5 is influenced by thermodynamic factors, kinetic limitations and shape-selective constraints.¹⁰⁶ Thermodynamic issues are important in a study on olefin oligomerization, because carbon number and isomer distributions obtained by the simultaneous oligomerization/isomerization/cracking are, with certain restrictions, equilibrated. The equilibrium product distribution is determined by the reaction conditions, e.g. temperature and pressure.³⁵

Due to the scarcity of data on the thermodynamic properties of olefin isomers containing more than six carbon atoms, thermodynamic analysis of olefin oligomerization is very difficult.^{35,106} Group thermodynamic properties were therefore employed.¹⁰⁶ Figure compares calculated (lines) equilibrium distributions for olefin oligomerization under different boundary conditions, and experimentally determined distributions (symbols) over H-ZSM-5 at a temperature of 277 °C and 0.1 bar (total olefin partial pressure).¹⁰⁶

It is seen in Figure 2-16 that the carbon number distributions for the product obtained from the conversion of different olefins in the C₂ to C₁₀ range are close to each other and also close to the calculated restricted equilibrium distribution^{3,106} (definition see figure caption of Figure 2-16), regardless of the net direction of the reaction. that is, the average molecular weight of the product grew for ethene, propene, and butene feedstocks, and decreased for 1-hexene and 1-decene.¹⁰⁶ From an in-depth product analysis it was found that the average extent of methyl branching is also independent of the

reactant and significantly lower than that from oligomerization over a non-shape-selective catalyst.¹⁰⁶

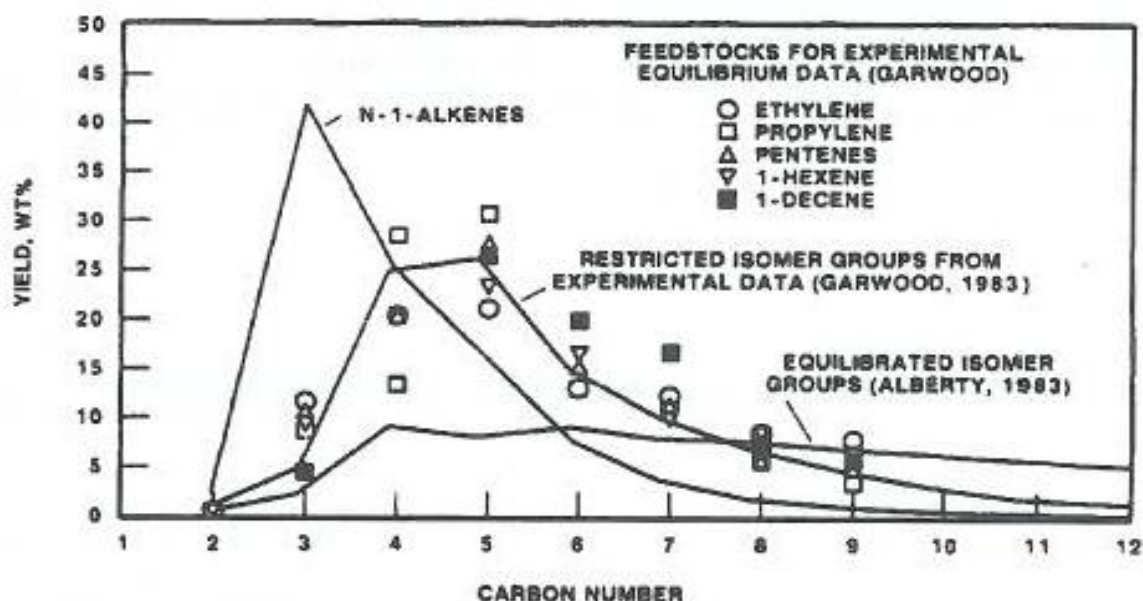


Figure 2-16: Comparison of calculated olefin equilibrium distributions under different boundary conditions (see below) and experimentally determined distributions from conjunct oligomerization reaction over H-ZSM-5 at 277 °C and 0.1 bar total olefin partial pressure.¹⁰⁶ “Equilibrated isomer groups” stands for a highly branched product, which comprises all olefin isomers possible for the respective carbon number, whereas “restricted isomer groups” stands for the limited branching observed over H-ZSM-5 where only every fifth carbon atom, on average, is methyl branched because of the shape-selective restrictions imposed by the zeolite.^{3,106} Names given in the figure refer to the bibliography in the reference (¹⁰⁶).

Narrow boiling point cuts of a hydrogenated propene oligomerization product were analysed by ¹H-NMR and FIMS (Field Ionization Mass Spectroscopy) to obtain the degree of methyl branching as a function of carbon number (see

Figure 2-17).¹⁰⁶ The “model polypropylene” structure shows one methyl side chain per two carbon atoms of the backbone of the oligomer and is therefore more branched than the real propene oligomerization product obtained over the H-ZSM-5 catalyst (“ZSM-5 polypropylene”) where, on average, only every fifth carbon atom is methyl branched. This confirms the restrictive shape-selective nature of H-ZSM-5 in forming products that are less branched.^{35,106}

Shape-selectivity in olefin oligomerization over H-ZSM-5 (towards a less branched product) could be improved by using a low, 0.1 wt% aluminium content zeolite (corresponding to a molar $\text{SiO}_2/\text{Al}_2\text{O}_3$ ratio of 450, approximately) and a hydroxylic (alcohol-containing) feed.¹⁰⁷

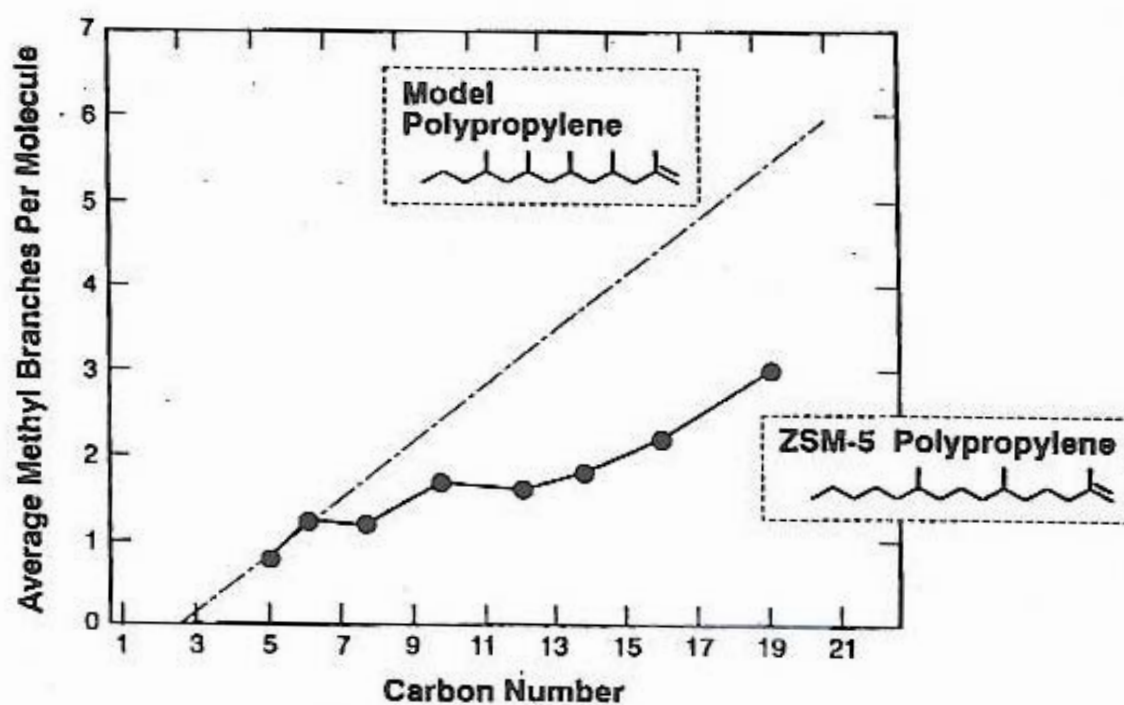


Figure 2-17: Limited methyl branching of the propene oligomerization/cracking products obtained over shape-selective H-ZSM-5 (solid line) versus those expected over a non shape-selective true oligomerization catalyst (dash-dotted line).¹⁰⁶

The commercial COD process, for instance, converts Fischer-Tropsch process derived light olefins (i.e. C₃-C₆ olefins) at 280 °C and 50 bar over a H-ZSM-5 catalyst to mostly oligomers in the diesel range. Tables 2-2 and 2-3 give the extent and types of branching in the final product.^{32,33} Due to the restrictions imposed by the shape-selective catalyst, methyl branching predominates.

Table 2-2: Typical composition of the hydrogenated COD diesel fuel.^{32,33}

Type of component	wt%
Iso-Paraffins	65.3
<i>n</i> -Paraffins	2.7
Cyclics	32.0

Table 2-3: Types of branching of the iso-paraffins present in the hydrogenated COD diesel fuel.^{32,33}

Type of branching	%
Methyl	60-70
Ethyl	2-10
Propyl	0.2-5
Butyl	0.1-5
Hexyl	0.1-2

2.3.1.2 Rapid double bond isomerization

The assumption that the oligomer isomers are equilibrated presumes that double bond and skeletal isomerization are at least as fast as the olefin oligomerization and cracking reactions.¹⁰⁶ When C₂-C₁₀ olefins were converted it was observed that pentene isomer distributions were close to equilibrium distribution (see Table 2-4).³

Table 2-4: Comparison of pentene product-isomer-distributions from different feedstocks (obtained over a H-ZSM-5 catalyst at 227 °C and sub-atmospheric olefin total pressure) with the equilibrium distribution.³

	Feed					Calculated equilibrium distribution
	C ₂ ⁼	C ₃ ⁼	C ₅ ⁼ mix	1-C ₆ ⁼	1-C ₁₀ ⁼	
Product pentene isomer, %						
1-Pentene	2	2	2	2	2	2
2-Methyl-1-butene	18	16	18	18	17	24
3-Methyl-1-butene	1	2	2	2	1	2
<i>trans</i> 2-Pentene	11	10	11	12	13	9
<i>cis</i> 2-Pentene	5	5	5	5	6	7
2-Methyl-2-butene	63	65	62	61	61	56

A detailed study on propene dimerization over H-ZSM-5 was carried out at a reaction temperature of 250 °C and 50 bar.⁴³ The primary propene dimerization product was found to be mono-methyl branched and to have a 2-methyl pentane skeleton (such as shown in Figure 2-2).

It was observed that, at 5% conversion, the distribution of the dimers, the hexene isomers, was not at equilibrium with respect to branching (the percentages of the hexenes with a 2-methyl pentane skeleton, the primary product from propene dimerization, see Figure were still higher than in equilibrium) but with respect to double bond distribution this product was equilibrated. At higher conversion of 50% the skeleton isomer distribution, including the *n*-hexene and 2,3-dimethyl butene isomers, was also close to equilibrium.⁴³

Another study on oligomerization of propene, 1-hexene and 1-hexadecene over H-ZSM-5¹⁰⁶ also established that double bond and skeletal isomerization reactions are at least as fast as olefin oligomerization and cracking reactions, see Figures 2-18 (a) and (b).

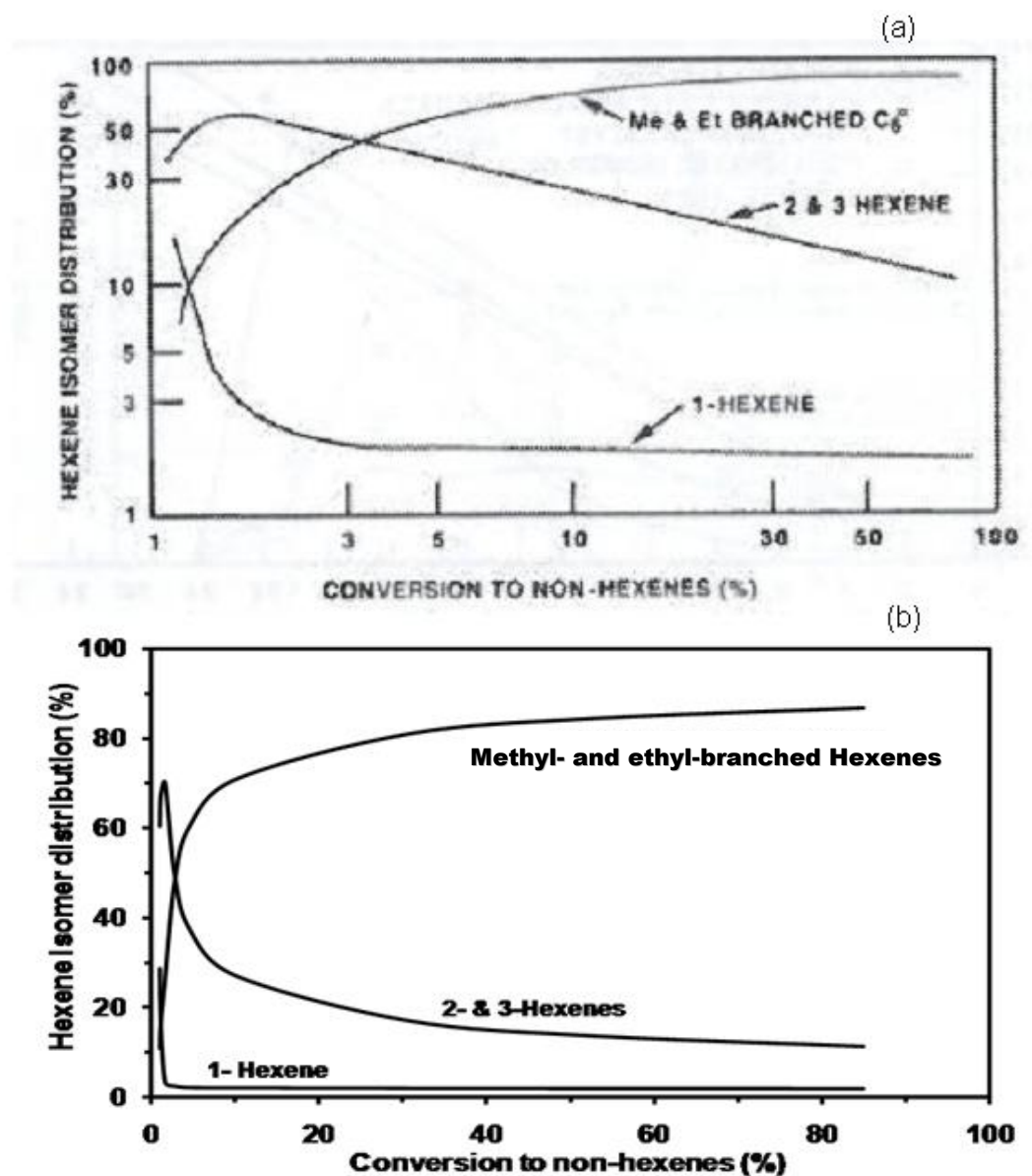


Figure 2-18: Hexene isomer distribution obtained during oligomerization of 1-hexene over H-ZSM-5 at 227 °C and 42 bar.¹⁰⁶ (a) Original graph, (b) redrawn with linear axes and normalized to 100%.

Very rapid conversion of 1-hexene to 2- and 3-hexenes occurred, which made 1-hexene to almost disappear within the time needed to convert just a few percent of the feed to non-hexenes, as shown in Figure 2-18 (b). The very rapid double bond isomerization is followed by methyl branching, while the slowest reaction, under the conditions applied, appeared to be the oligomerization.¹⁰⁶

It can be concluded that reaction rates in olefin oligomerization over H-ZSM-5 (at 227 °C) decrease as follows: double bond isomerization >> skeleton isomerization > dimerization.

2.3.1.3 Effect of reaction conditions on carbon number distribution and type of products – kinetic and thermodynamic control

Although the product structure (branching) is determined by the catalyst pores, the reaction conditions (temperature, pressure and space velocity) determine the average molecular weight and weight distribution of the product (within these limitations (see Figure 2-16)).^{35,91} The three variables, however, are interactive. The effect of reaction temperature and pressure on the olefin carbon number distribution, modelled for a single-pass conversion of propene over H-ZSM-5, is presented in Figure 2-19.

Pressure is the driving force, kinetically and thermodynamically, for oligomerization to higher-molecular weight products.^{35,106} At low reaction temperatures, higher molecular weight oligomerization products are favoured

thermodynamically, but at a given space velocity molecular-weight growth is kinetically limited (see Figure 2-19, left side of the modelled surface). Increase in reaction temperature causes the reaction rates to increase, but results in approaching thermodynamic limitation of molecular weight growth (see Figure 2-19, right side of the modelled surface).

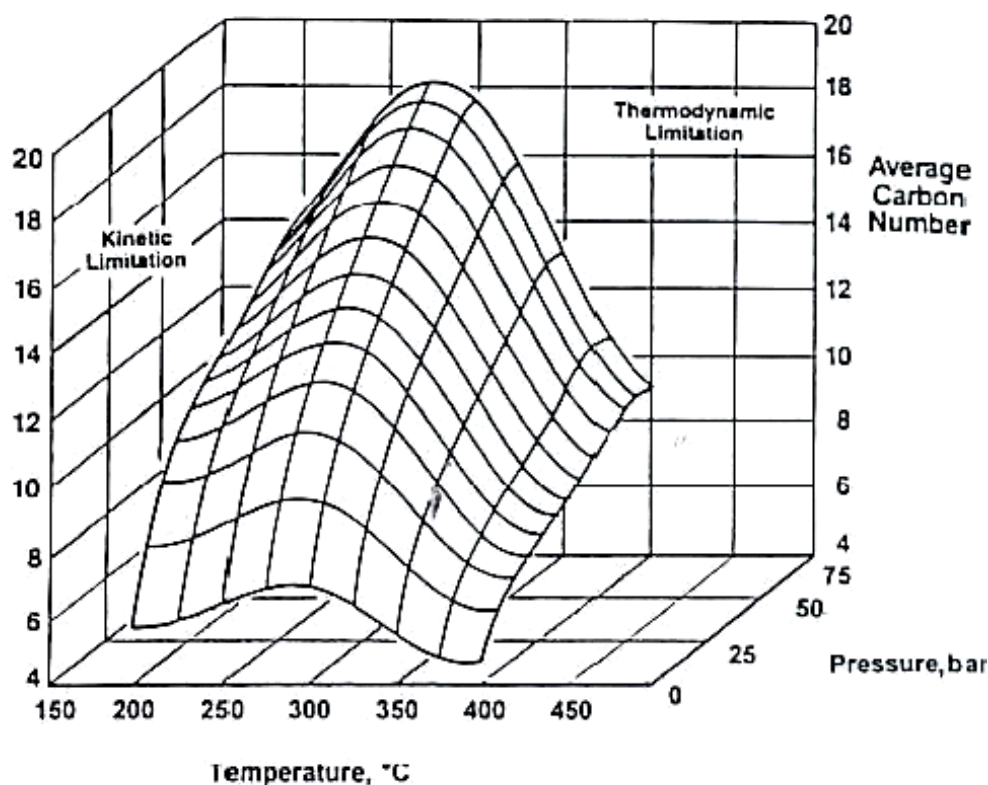


Figure 2-19: Model predictions for the effects of temperature and pressure on the average carbon number of the product mixture obtained from single-pass propene (conjunct) oligomerization over H-ZSM-5 (restricted branching, see figure caption of Figure 2-16) at constant space velocity of 1 g/gh.¹⁰⁸

At low pressure (1 bar) light olefins dominate the “restricted” thermodynamic equilibrium (see figure caption of Figure 2-16) at high temperature, while high molecular weight olefins dominate at low temperature (see Figure 2-20)¹⁰⁶.

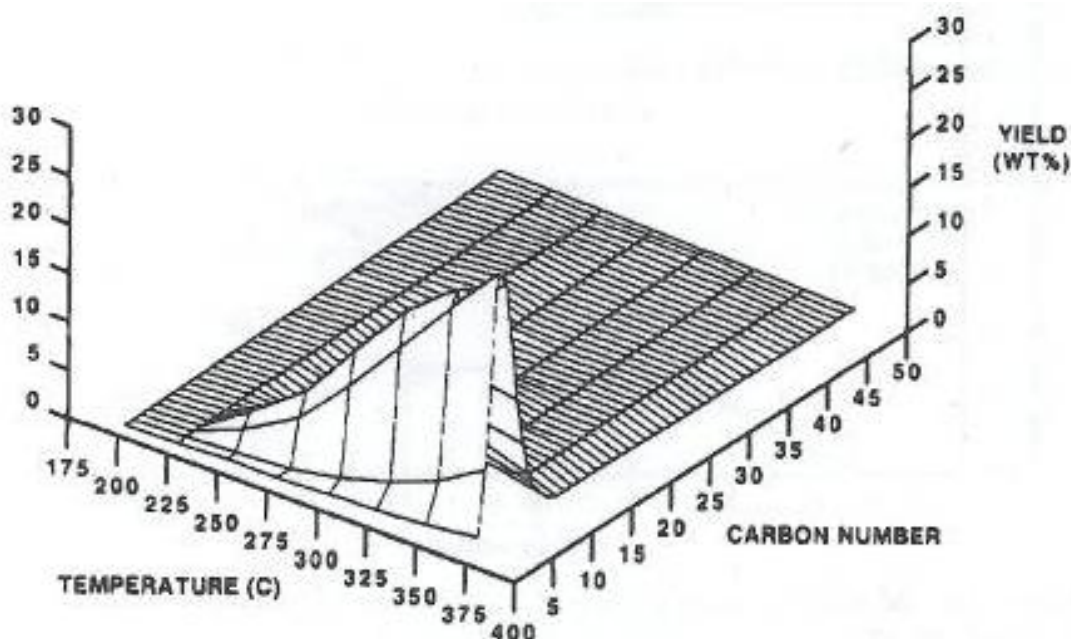


Figure 2-20: Effect of temperature on “restricted” olefin equilibrium distribution over H-ZSM-5 (restricted branching, see figure caption of Figure 2-16) at 1 bar.¹⁰⁶

Propene oligomerization under mild conditions (at 204 °C, 55 bar and a space velocity of 1.0 g/g.h), formed mainly true oligomers. The majority of the products were trimers, tetramers and pentamers (see bottom graph in Figure 2-21).^{3,90,91,106}

Randomisation occurred at intermediate temperatures, due to an increase in cracking and disproportionation rates. Due to the high olefin cracking rates, the carbon-number distribution became continuous and rather smooth.^{3,90,91,106}

At higher temperature, thermodynamic limitations come into effect and a further increase in temperature leads to a decrease in the average carbon number and an approach to carbon number equilibrium distribution^{3,90,91,106} so that light olefins eventually dominate as has been shown in Figure 2-21 (top graph).

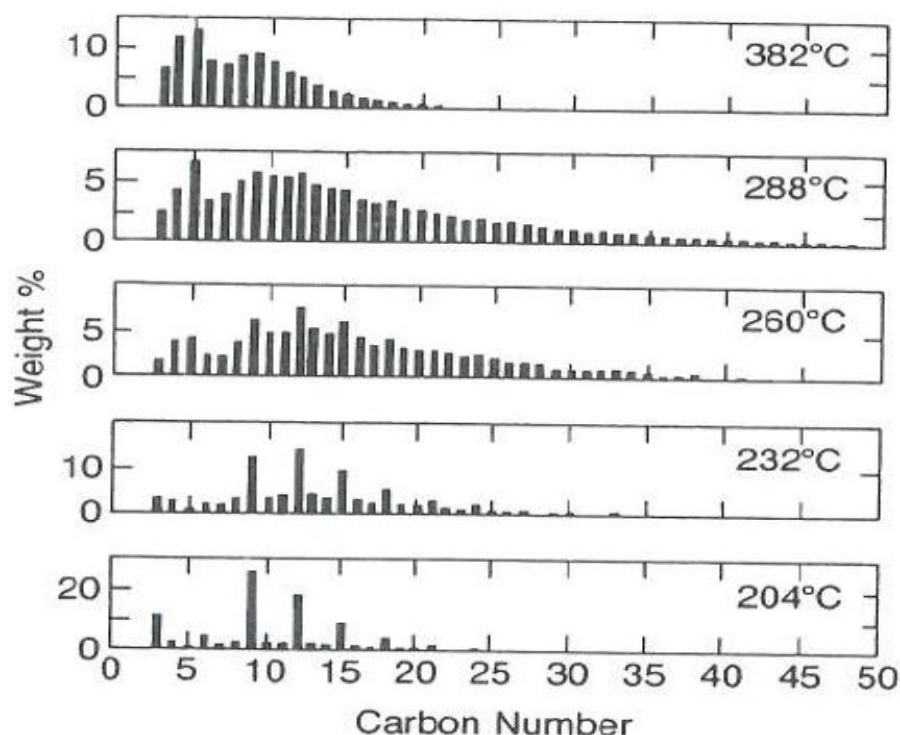


Figure 2-21: Effect of temperature on the carbon number distribution of the products from propene oligomerization over H-ZSM-5 at 204 – 382 °C, 55 bar and 1.0 g/g.h.^{3,90,91,106}

The high yields of C₃ to C₅ products, visible at the high reaction temperatures (>280 °C in Figure 2-21), that neither correspond to a true propene oligomerization product nor a conjunct oligomerization product that is equilibrated with regard to carbon number, are due to the pronounced formation of light paraffins, balancing the formation of hydrogen-deficient compounds such as cycloolefins and aromatics.¹⁰⁶

In olefin oligomerization, space velocity has a marked influence on conversion and conversion has a marked influence on selectivity. When propene was converted over H-ZSM-5 at 204 °C, 34 bar and the WHSV was varied, low WHSV of 0.4 g/g.h lead to high propene conversion of 98%, while high WHSV

of 2.7 g/g.h gave a medium conversion of 67%.³ The steps in the boiling curves (Figure 2-22) of the high-space-velocity / medium-conversion product reflect a product that consists still essentially of the true oligomers $C_6^=$, $C_9^=$, $C_{12}^=$, whilst the smooth curve obtained from the low-space-velocity / high-conversion product indicates that much cracking already occurred.³ The result reflects the influence of WHSV on the kinetics of the reaction.

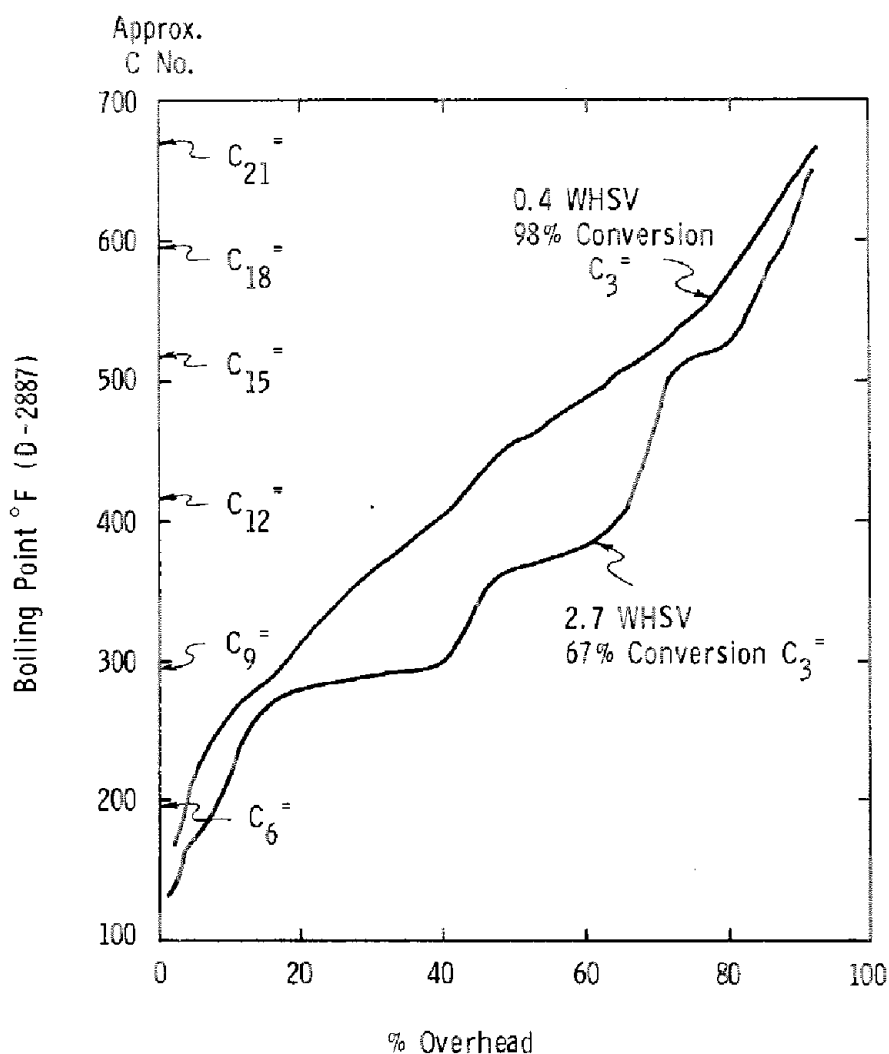


Figure 2-22: Effect of space velocity on the product-carbon-number distribution (by boiling point) from the conversion of propene over H-ZSM-5 at 204 °C and 34 bar.³

Cyclization and hydrogen transfer reactions, leading to aromatics and co-product paraffins, can play a role in olefin oligomerization over zeolites.^{6,109} This is commonly so in conjunct oligomerization, i.e., occurs at elevated temperatures and low space velocities (≥ 260 °C in Figure 2.21 and Section 2.1.2.1), but to a small extent already under comparatively mild conditions. Correspondingly, cyclization and aromatization take place under the rather severe reaction conditions of the technical olefin oligomerization processes, the MOGD and the COD process, where around 3% and >10%, respectively, of aromatics are formed.^{31,32,64,106}

The COD plant converts Fischer-Tropsch process derived light olefins (i.e. C₃-C₆ olefins) to mainly diesel range oligomers over an H-ZSM-5 catalyst.^{32,33} The process was designed to handle a feedstock that contains oxygenates, which includes alcohols, acids, esters and ketones, totalling 1.8 wt%.⁸¹ Since oxygenates have a negative effect on catalyst stability in that they cause pre-mature catalyst deactivation, operation conditions are rather severe (280 °C and 50 bar). Eventually, the raw COD diesel range boiling fraction contains more than 10 wt% aromatics and, in total, about 30 wt% of cyclic compounds as given in Table 2-5.^{32,33,81}

Table 2-5: Typical composition of the hydrogenated COD diesel fuel^{32,33}

Type of component	wt%
<i>n</i> - and iso-Paraffins	68.0
Monocycloparaffins	24.3
Dicycloparaffins	7.6
Aromatics	< 0.1

2.3.1.4 Effect of H-ZSM-5 silica/alumina ratio on activity and selectivity

High-pressure (50 bar) olefin oligomerization (of propene, 1-butene and 1-hexene) was investigated over H-ZSM-5 catalysts of different $\text{SiO}_2/\text{Al}_2\text{O}_3$ ratios at 300 °C and rather high WHSV of 12 g/g.h.¹¹⁰ Both oligomerization activity and life time increased with decreasing $\text{SiO}_2/\text{Al}_2\text{O}_3$ ratio (increasing aluminium content) of the zeolite, i.e. with increasing catalyst Brønsted acid site density.¹¹¹ Results from 1-hexene dimerization at 150-160 °C showed that the activity of the H-ZSM-5 catalyst for 1-hexene dimerization was also increased at lower $\text{SiO}_2/\text{Al}_2\text{O}_3$ ratios, i.e. higher aluminium content under milder conditions.¹²⁰

H-ZSM-5 with a $\text{SiO}_2/\text{Al}_2\text{O}_3$ molar ratio of 78 catalyzed little H-transfer reaction (limited by constraints imposed on the formation of the bimolecular H-transfer reaction complexes due to its pore system,¹⁰⁹ whereas Silicalite ('aluminium-free' H-ZSM-5) with a $\text{SiO}_2/\text{Al}_2\text{O}_3$ molar ratio of 2200, exhibited only very little H-transfer activity even at a high conversion of above 70%.¹²¹

2.3.1.5 Fouling of H-ZSM-5 catalyst

The conversion of 1-hexene over H-ZSM-5 at low temperatures of 80-120 °C and atmospheric pressure led to retained material on the catalyst in the carbon number range of $\text{C}_8\text{-C}_{15}$ with a distribution maximum at C_{12} that was largely paraffinic.⁴² The carbon number distributions of both the retained and the volatile products obtained at 120 °C reaction temperature showed the

occurrence of oligomerization and cracking reactions. Increasing the temperature to above 120 °C lead to higher molecular weight products, which included unsaturated cyclic compounds.⁴²

There was no evidence that indicated whether the residue formed at 120-240 °C was accumulated in the pores or on the external surface of the zeolite crystallites or both, though it was suggested that most was in the pores.⁴² It was also proposed that the unblocking of the pores that was achieved at 320 °C was due to the migration of the residue out of the pores to the external surface of the zeolite crystallite.⁴²

On the external surface, rather than in the pores (because of the shape-selectivity/size restrictions in the pores), part of the residue was converted to higher molecular weight products. These products were relatively involatile, because they were mainly alkylated polyaromatics. This finding was confirmed by the decrease in the formation of higher aromatics when 1-hexene was converted at 320 °C over a crystalline surface deacidified (surface dealuminated) zeolite catalyst.⁴²

It was discovered that during propene oligomerization over H-ZSM-5 (at 189 °C and above and 24 bar) olefin oligomers coated the external surface of the zeolite crystallites, thereby limiting the rate of oligomerization.¹⁰⁷

On the other hand, it appeared from the oligomerization of various low olefins over H-ZSM-5 at 227 °C and 42 bar that a substantial fraction of the pore

volume of the zeolite was filled with oligomers, and as a result the reaction occurred on the external surface of the zeolite crystallites.¹¹²

It was postulated that such retained products cannot only affect the activity and the size/shape-selectivity of the catalyst, but may also function as possible precursors in the formation of aromatic type coke, and contribute to the general deactivation of the catalyst.⁴²

Higher paraffins and aromatics that resulted from hydrogen transfer reactions were found to also block the micro- and mesopores of a US-Y zeolite, and caused deactivation of the catalyst. However, such deactivation was not observed with the mesoporous material beidellite.¹¹⁹

2.4 Dimerization/oligomerization of light and naphtha-range olefins over alumino-silicates different from H-ZSM-5 and other solid acid catalysts

Amorphous silica-alumina (ASA) catalysts are active for the oligomerization of alkenes at around 200 °C and 30 bar and selective to trimers and tetramers.³⁵

When propene was converted over an ASA catalyst under the above-mentioned reaction conditions the major dimer that formed was 3-methylpentene.

The conversion of Fischer-Tropsch olefin streams in the C₃-C₁₀ range, having low oxygenate contents, over ASA produced distillates with a density of 810 kg/m³, higher than any other oligomerization catalyst.^{44,99} Pilot scale

evaluation was done at 140-265 °C, 35-68 bar and LHSV (liquid hourly space velocity) of 0.1-2.0 g/g.h.⁴⁴ The hydrogenated distillate obtained from the ASA catalyst gave a cetane number of only 28-30,⁹⁹ which is much lower than the cetane numbers reported for the COD and MOGD diesel of around 55^{33,64}, but the flow properties were good.

The unhydrogenated naphtha fraction of the ASA oligomerizate had a RON of 92-94⁴⁴, which was higher than those obtained from olefin oligomerization over H-ZSM-5 in the COD and MOGD processes (RON of 81-95).^{30,44} It has also been reported¹¹³ that Shell employed an ASA catalyst to dimerize *n*-butenes (at 120 °C, 35 bar and WHSV of 8 g/g.h). The dimerization product (70-80% yield) was found to possess blending RON values of around 130.^{114,115} Like the low cetane numbers for the hydrogenated oligomerization diesel, high octane numbers for the olefinic oligomerization gasoline indicate a high degree of branching.

2.4.1 Dimerization/oligomerization of 1-hexene over different solid acid catalysts

Upon testing acid catalysts with different pore structures it was found that mesoporous aluminosilicate catalysts with a high specific surface area are effective catalysts for hexene dimerization. These catalysts included MCM-41 and silica-alumina co-gels, which do not contain micropores.¹²¹

When 1-hexene dimerization was studied over various zeolite and non-zeolite solid acid catalysts (e.g. ZSM-5^{106,116}; MCM-22, MCM-41, US-Y,

silica-alumina co-gel, γ -alumina, silicoaluminate, silica-magnesia co-gel¹²¹; Al-MTS, Al-MCM-41, Al-SBA-15¹¹⁶) under the typical dimerization reaction conditions (of around 100-250 °C and elevated pressures), double bond isomerization to the 2- and 3-hexenes was generally found to occur rapidly as the first step (usually much more rapid than skeleton isomerisation, oligomerization or cracking), so that the equilibrium or close to equilibrium pool of *n*-olefin isomers formed (see Section 2.3.1.2 and Figure 2-18) out of which the oligomers form.

In terms of product properties, the majority of the dimers formed from the equilibrated *n*-hexenes was dibranched with a small fraction of monobranched and some tribranched isomers and the double bond close to the middle of the molecules. It was observed that the monobranched and dibranched dimers appeared as primary products while the tribranched dimers were secondary products.^{19,6,52,74,117,119} This product represents a 1-hexene dimerization product that formed without suffering from spatial constraints.

The oligomerization of 1-hexene over crystalline mesoporous aluminium silicate H-beidellite (18-19 Å)¹¹⁸ and microporous, wide pore (7.4 Å)⁸⁵ ultrastable zeolite H-Y (US-Y) at 200 °C and 50 bar was studied in the presence of paraffinic solvents (propane, pentane, octane and dodecane) under vapour phase, liquid phase and supercritical conditions.¹¹⁹ With both catalysts improved catalyst activity and oligomerization selectivity towards the C₁₂ fraction were achieved under liquid phase reaction conditions in the presence of heavier paraffinic solvents, i.e. octane and dodecane.¹¹⁹

1-Hexene, in *n*-octane solvent, was oligomerized at 80-300 °C, 50 bar and WHSV of 0.5 g/g.h over a wide range of acid catalysts.¹²¹ Zeolite MCM-22, mesoporous material MCM-41, zeolite US-Y and silica-alumina co-gel (containing 13 wt% of Al₂O₃) exhibited high hexene oligomerization conversions at 130 °C with little deactivation during 12 hours on stream. Γ -Alumina, silicoaluminate Siralox 1.5/200 (containing 1.5 wt% of SiO₂) and silica-magnesia co-gel (containing 1 wt% MgO) were found to be less active, exhibiting oligomerization conversions of less than 60% still at 300 °C.¹²¹

The oligomerization of 1-hexene (in *n*-octane solvent) was investigated over mesoporous aluminosilicates (Al-MTS, Al-MCM-41 and Al-SBA-15, all with large BET surfaces of > 1000 m²/g) and H-ZSM-5 zeolites of both micrometer (“ μ -H-ZSM-5”) and nanometer crystallite dimensions (“n-H-ZSM-5”, crystallite diameters of 20-80 nm), all of a Si/Al atomic ratio of around 30. Oligomerization reactions were carried out at 200 °C, 50 bar, and WHSV of 0.40 g/g.h in a fixed bed reactor.¹¹⁶

All catalysts, except μ -H-ZSM-5, gave conversions above 75% with a total selectivity towards true oligomers (dimers, trimers and higher oligomers) above 95% under these conditions (see Figure 1-23).¹¹⁶ The difference between μ -H-ZSM-5 and n-H-ZSM-5 is addressed further in more detail in Section 2.5.1.

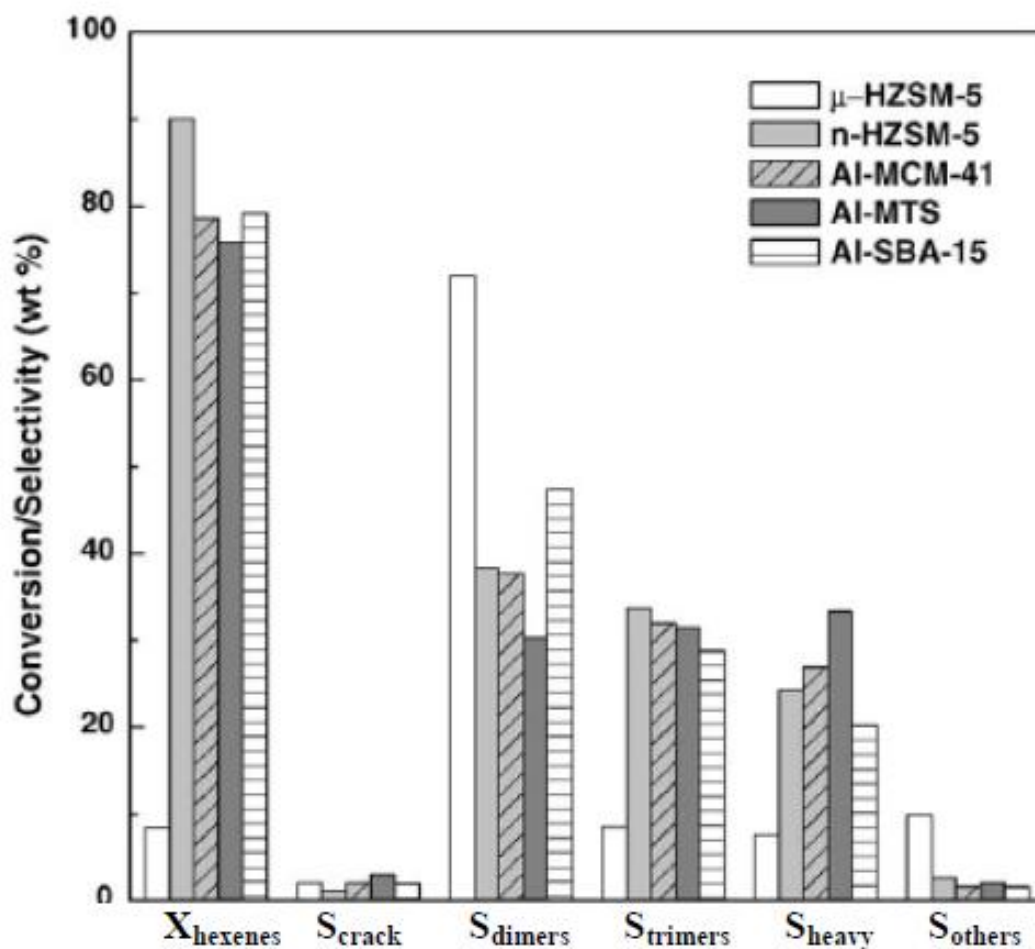


Figure 2-23: Conversions and oligomer selectivities obtained in the oligomerization of 1-hexene over different catalysts of identical $\text{SiO}_2/\text{Al}_2\text{O}_3$ ratio ($T = 200\text{ }^\circ\text{C}$, $P = 50\text{ bar}$, $\text{WHSV} = 0.40\text{ g/g.h}$, $\text{TOS} = 240\text{ min}$). “Heavy” refers to higher oligomers than the trimers.¹¹⁶

In an earlier study¹²⁰, the performance of medium pore zeolites H-ZSM-5 and H-ZSM-22 in comparison to wide pore zeolite H-beta (with molar $\text{SiO}_2/\text{Al}_2\text{O}_3$ ratios of 90, 90 and 150, respectively) and Siral 40 (amorphous silica-alumina) were evaluated for the selective dimerization of 1-hexene. The investigation was carried out in the liquid phase at low temperatures, 150-170 $^\circ\text{C}$, and pressures of 20-40 bar. The mild conditions were chosen in order to limit the

reactions to dimerization. The results indicated that dimer selectivity was largely independent of conversion even at high dimerization conversion levels (ca. 95%).¹²⁰ At the higher temperatures conversion was also found to be independent of pressure.¹²⁰

When comparing the three zeolite catalysts tested, H-ZSM-5, HZSM-22 and H-beta with regard to lifetime, all of them showed similar behaviour in terms of slowly decreasing activity with increasing time-on-stream. H-ZSM-5 appeared to be superior over the other catalysts in terms of stability, activity and dimer selectivity.¹²⁰

2.4.2 Rapid H-transfer over wide pore zeolites

In 1-hexene oligomerization it was observed that cracking of the oligomers and the formation of C₆ alkanes were the main side reactions. Cracking increased with increasing conversion. Cracking and hydrogen transfer reactions occurred mainly in wide pore zeolites beta and US-Y.¹²¹ Ultrastable zeolite Y with a SiO₂/Al₂O₃ molar ratio of 6, was very active for H-transfer in the conversion of linear hexenes (at 221 °C and 34.5 bar). With dealuminated H-mordenite (SiO₂/Al₂O₃ molar ratio of 68) H-transfer was somewhat less. In contrast, H-ZSM-5 (SiO₂/Al₂O₃ molar ratio of 78) catalyzed little H-transfer reaction. The constraints imposed by the medium pore system of H-ZSM-5 limited the formation of the bimolecular H-transfer reaction complexes.¹⁰⁹

2.4.3 Summary – apparent advantages of using H-ZSM-5 as catalyst in olefin oligomerization

At this stage, it can be summarized why H-ZSM-5 is the preferred zeolite for oligomerization processes aiming for diesel, based on the following reasons:^{3,36,86,90}

1. The strongly acidic nature of H-ZSM-5 helps catalyze oligomerization, cracking, isomerization (but also aromatization) reactions.
2. Variation of catalyst properties and process conditions enables variation between true and conjunct oligomerization.
3. In conjunct oligomerization the medium-size pore openings (5.5 Å) provide a shape-selective effect that restricts branching.
4. H-ZSM-5 is highly resistant to coking owing to the medium pore size which prevents the formation of coke precursors on the internal surfaces.
5. H-ZSM-5 is rather stable under hydrothermal conditions.

2.5 Dimerization and oligomerization of olefins over external crystallite surface-modified zeolite catalysts

It is believed that there are two different locations where the oligomerization of olefins can take place over shape-selective acidic zeolites.¹²² On Brønsted acid sites inside the channels, producing essentially linear materials, and on the outer crystallite surface, producing more branched material.

By decreasing the surface acid activity of such zeolites, products containing fewer highly branched compounds are obtained. Near linear oligomerization/dimerization products can be achieved by reducing the activity/deactivation of the external surface of the zeolite crystallites.¹²²

A number of findings indicated that the oligomerization of olefins over H-ZSM-5, in particular of the “higher” ones such as 1-hexene, takes place mostly on the external surface of the zeolite crystallites, see below.

2.5.1 Crystal size effect

The much higher activity of nano-sized H-ZSM-5 crystallites (20-80 nm) compared to H-ZSM-5 crystallites of micrometer size (see Figure 2-23) was attributed to the high external surface area ($102 \text{ m}^2/\text{g}$) of the former created by its nanometer dimension, while the reason for the low conversion exhibited by the latter, was attributed to its larger crystal size and correspondingly low external surface area ($5 \text{ m}^2/\text{g}$).¹¹⁶ However, the branching obtained over mesoporous Al-MCM-41 and nano-crystalline H-ZSM-5 (20-80 nm) catalysts was found to be similar despite the differences in acidity (density and strength of acid sites) and significantly different pore systems and textural properties.

2.5.2 Selective blocking and poisoning of the external sites of zeolite crystallites

It was discovered that during propene oligomerization over H-ZSM-5 (at 189°C and above and 24 bar) olefin oligomers coated (and deactivated) the

external surface of the zeolite crystallites, thereby limiting the rate of oligomerization on the crystallite surface (see also Section 2.3.1.5).¹⁰⁷

Shape-selectivity (towards a less branched product) was reported to have improved over external surface deactivated H-ZSM-5 crystallites.¹⁰⁷ H-ZSM-5 was silylated with hexamethyldisilane to convert the acidic surface hydroxyl groups to non-acidic trimethylsiloxyl groups. For this purpose, the H-ZSM-5 zeolite was treated for 6 hours at 250 °C in dry argon that was saturated with hexamethyldisilane, and then calcined at 400 °C. At 325 °C the silylated zeolite was not catalytically active for the oligomerization of propene. At 350 °C, at 37% conversion, the percentage of less branched oligomers (e.g. *n*-nonane and the mono-methyloctanes in the C₉ fraction, determined after hydrogenation) was found to be 57% over the silylated zeolite crystallites compared to 29% over the non-silylated zeolite crystallites.¹⁰⁷

The external zeolite crystallite surface can also be rendered substantially inactive for acidic catalysed reactions by chemisorption of, e.g., a bulky amine. Common poisons for acidic solids are ammonia, alkyl amines and pyridines. They interact with the protons of the Brønsted acid sites and form ions on the sites thus occupying/blocking the respective sites, but also depressing the activity of several of the remaining sites in the region.^{123,124} Pyridines are much stronger adsorbents than ammonia or alkyl amines. The use of other basic materials to deactivate/poison the Brønsted acid sites on the external surface of aluminosilicate crystallites has also been investigated.^{120,125,126,127,128}

These compounds must all have a diameter greater than the pore size of the zeolite to be effective. In Figure 2-24 a number of such components are shown.

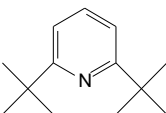
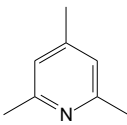
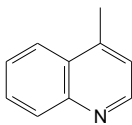
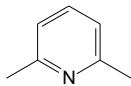
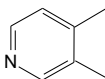
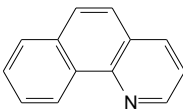
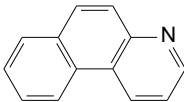
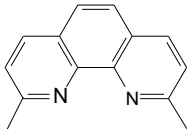
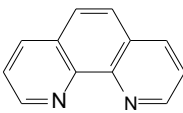
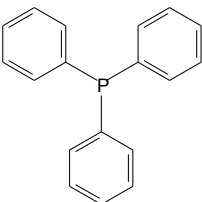
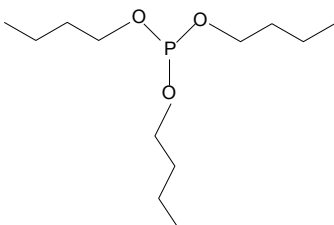
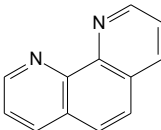
 <p>2,6-di-<i>tert</i>-butylpyridine</p>	 <p>2,4,6-collidine</p>	 <p>4-methylquinoline</p>
 <p>2,6-dimethylpyridine</p>	 <p>3,4-dimethylpyridine</p>	 <p>7,8-benzoquinoline</p>
 <p>5,6-benzoquinoline</p>	 <p>dimethylphenanthroline</p>	 <p>1,10-phenanthroline</p>
 <p>triphenylphosphine</p>	 <p>tributylphosphite</p>	 <p><i>ortho</i>-phenanthroline</p>

Figure 2-24: Bulky pyridine type and organophosphorus compounds used for the poisoning of the external surface acid sites of zeolites.^{125,129}

Zeolite crystallites of low external surface activity but with unaffected internal pore space activity can be obtained when the external acid sites are selectively deactivated by strongly basic, bulky compounds that are not able to enter the pore system and deactivate the internal sites, but block the external sites. These surface deactivating basic materials are typically bulky pyridine-type amines such as di-*tert*-butylpyridine, 2,4,6-collidine, 4-methyl-quinoline, *ortho*-phenanthroline and organophosphorus compounds like tributylphosphite and triphenylphosphine.¹²⁵

Propene, 1-decene and isobutene were oligomerized batchwise at elevated pressure in the gas phase over untreated and external-surface-deactivated H-ZSM-5 crystallites (SiO₂/Al₂O₃ molar ratio of 70).¹²² Surface deactivation was done with 2,6-di-*tert*-butylpyridine. This compound has a molecular size of 6.3 x 8.0 Å which is too large to enter the channels of medium pore zeolite H-ZSM-5 (5.4 x 5.6 Å) and thus renders only the external surface of the zeolite inactive.¹²²

When raising the temperature from 200 to 230 °C a decrease in linear product and an increase in branched product selectivity was obtained over the non-treated zeolite. This could be suppressed by adding 2,6-di-*tert*-butylpyridine to the feed.¹²² When surface-deactivated H-ZSM-5 was used as the catalyst, the oligomerization occurred inside the zeolite channels in that more linear products were produced regardless of the type of olefin feed. The shape and the size of the products were controlled by the space inside the channels and the ability of the products to diffuse out of the channels.¹²² The

product structure appeared thus to be more dependent of the location and spatial environment of the active sites than on the reaction temperature, in that more methyl branched products were obtained at higher temperatures only when the external zeolite crystallite surface was active.¹²²

High yields of low branched oligomers were obtained from the oligomerization of propene over an external-crystallite-surface-inactivated, but internally active H-ZSM-23 zeolite.¹²⁵ (H-ZSM-23 is a medium-pore zeolite having two intersecting channel systems formed by rings containing 10 oxygen atoms, and has pore sizes of $4.5 \times 5.6 \text{ \AA}$.⁹⁰) Different bulky amines were used to deactivate the external sites. For surface deactivation H-ZSM-23 crystallites were treated with a solution of 1.0 g of either 2,6-di-*tert*-butylpyridine or 2,4,6-collidine (see Figure 2-24) in 100 ml *n*-pentane. Small amounts of the solutions were also co-fed with the feed.¹²⁵

Reaction conditions for propene oligomerization of 160-225 °C, 35-43 bar and WHSV of 0.5-1.0 g/g.h were employed. A product mixture of more than 95% (by weight) oligomers was obtained. The C₁₂₊ fraction was hydrogenated for determining the methyl branching.¹²⁵ The branching of the products from the unmodified and modified zeolite catalysts is compared in Figure 2-25.

As can be derived from Figures 2-2 and 2-17, the C₁₂ product (tetramer) from true, not shape-selectively constraint or otherwise influenced propene oligomerization (e.g. by additional isomerization), has a C₉ backbone and three methyl branches. Over the unmodified (non-poisoned) H-ZSM-23 the branching was even higher¹²⁵ (see triangle shaped data points in Figure 2-25).

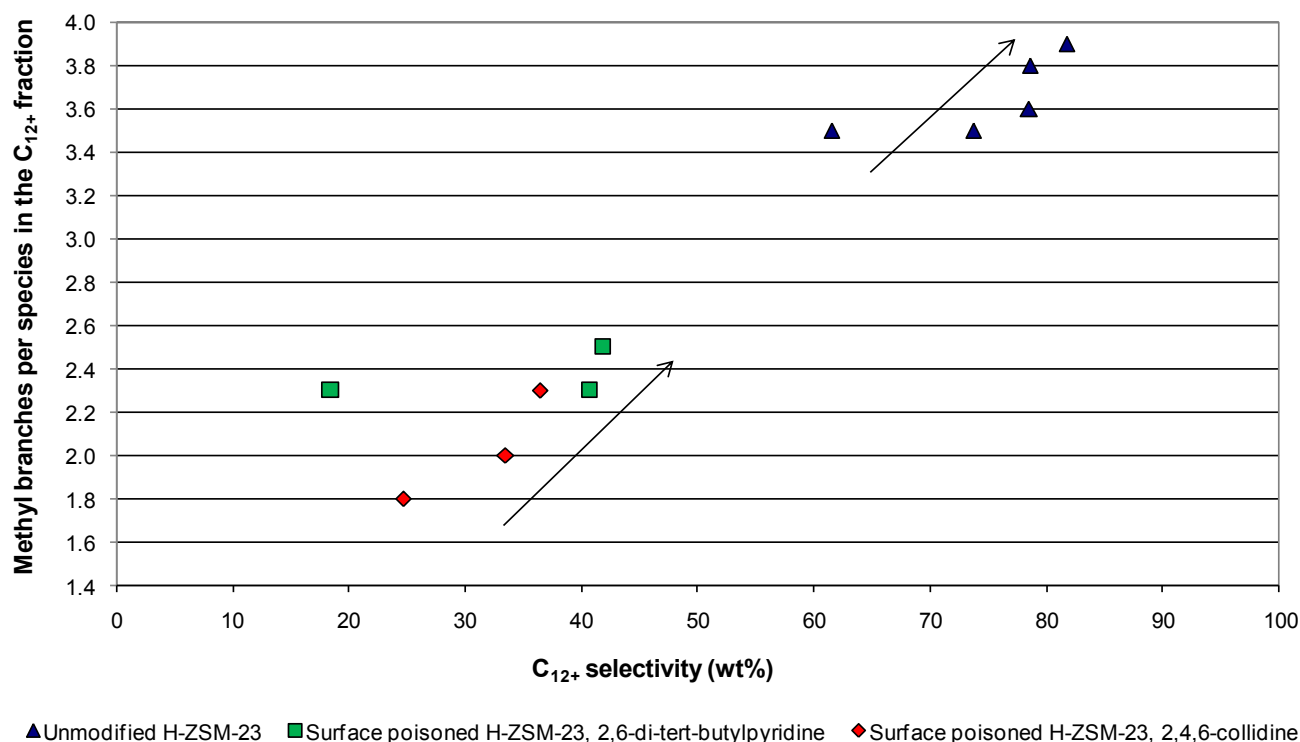


Figure 2-25: Effect of poisoning of the external surface of H-ZSM-23 on methyl branching in the C₁₂₊ fraction obtained from the oligomerization of propene. The figure is a plot of data given in the patent (arrows added).¹²⁵

However, when adding 400 ppm or more of 2,6-di-*tert*-butylpyridine or 2,4,6-collidine, both the C₁₂₊ selectivity and the extent of methyl branching of the C₁₂₊ fraction almost halved. The authors¹²⁵ concluded from the reduction of branching to almost 2 methyl groups in C₁₂₊, which is significantly below the aforementioned “natural” value of three, that this shows clearly the shape-selective effect of the pore system once the competing external crystallite surface sites were deactivated.

However, it appears that the claim by the authors that the effect is caused by the selective suppression of the oligomerization reaction on the external surface of the zeolite crystallites,¹²⁵ is questionable. Figure 2-25 is a plot of

the data given in the patent¹²⁵, namely the number of branches vs. C₁₂₊ selectivity. Other data given in the paper indicates that high C₁₂₊ selectivity comes with deep conversion of the reaction mixture. Figure 2-25 shows a clear, almost linear correlation of the increase of branching with increase in C₁₂₊ selectivity, which comes with an increase in conversion.¹²⁵ Reduced/increased branching may, therefore, be a conversion effect, i.e. caused by space velocity or catalyst activity.

During the said earlier study¹²⁰, experiments were carried out also on 1-hexene dimerization over H-ZSM-5 (SiO₂/Al₂O₃ ratio of 90), whose external surfaces were poisoned by the bulky amines 2,6-di-*tert*-butylpyridine, 2,4,6-collidine or 4-methylquinoline (see Figure 2-24), with 65 ppm added (individually) to the feed. Reactions were conducted at 170 °C and 20 bar. A rapid drop in conversion, down to almost zero, was observed upon the introduction of the poisoned feed, suggesting that the dimerization of 1-hexene occurred predominantly on the external surface of the crystallites and that most of these external sites were deactivated by the bulky amines.¹²⁰

In studies¹²⁹ on the alkylation of toluene with ethene to yield *ortho*-, *meta*- and *para*-ethyltoluenes the external surface of the crystallites of the H-ZSM-5 catalyst employed was selectively poisoned by the the addition of *ortho*-phenanthroline (kinetic diameter 7.5 Å) to the feed. 20-30 ppm (by weight) added, resulted in an increase in the percentage of *para*-ethyltoluene in the ethyltoluene fraction from 54% to 97% with only a slight decrease in toluene conversion from 97% to 94%. In comparison, other, similar or

structurally analogous nitrogen heterocycles, namely (see Figure 2-24), 7,8-benzoquinoline (7.5 Å), dimethyl phenanthroline (8.3 Å), 5,6-benzoquinoline (7.5 Å) and 4-methylquinoline (8.3 Å) were less effective in poisoning the external surface of the zeolite crystallites. 2,4,6-collidine (7.5 Å) was found to be effective only at very high concentrations.¹²⁹ It is assumed that the latter molecules were less effective due to steric hindrance with respect to accessibility of the nitrogen atoms, whereas the nitrogen atoms in *ortho*-phenanthroline are less hindered and can adsorb on the acid sites of the zeolite external surface.¹²⁹

Small heterocycles of the alkyl pyridine type, i.e. 3,4-dimethyl pyridine (7.0 Å) and 2,6-dimethyl pyridine (6.6 Å), see Figure 2-24, completely poisoned the zeolite and the conversion decreased to 2% in just 3 hours (probably due to strong adsorption on the internal surface sites).¹²⁹

In other experiments¹³⁰, hydrocarbons were converted over H-ZSM-5 at 450 °C. The external surface of the zeolite crystallites was poisoned after establishing a steady-state reaction by spiking the feed with 4-methylquinoline (see Figure 2-24), which is known to be large enough to not penetrate the pore system of H-ZSM-5. 4-Methylquinoline drastically reduced the extent of conversion of 2,2-dimethylbutane (6.2 Å molecular diameter), but had little effect on *n*-hexane (4.3 Å) conversion.¹³⁰

2.5.3 Selective poisoning of the internal sites of zeolite crystallites

It appeared from the oligomerization of various low olefins over H-ZSM-5 at 227 °C and 42 bar that a substantial fraction of the pore volume of the zeolite was filled with oligomers and, as a result, the reaction occurred on the external surface of the zeolite crystallites.¹¹²

Selective poisoning of the internal sites of a medium pore zeolite was performed.¹²⁸ Crystallites of the zeolite in its sodium form were slurried in tetrapropylammonium bromide solution to selectively exchange the sodium cations for tetrapropylammonium cations. Tetrapropylaluminium cations are too bulky to access the 10-ring pore openings of a medium pore zeolite. Therefore, only the sodium cations located on the external surface of the zeolite crystallites were, selectively, exchanged. The sites located inside the crystallites remained occupied with sodium. Then the tetrapropylammonium ions were removed by calcination in air, and left was an active acidic external surface, while the internal sites were still occupied by sodium ions and therefore inactive.¹²⁸

By this means, reactions (also of small molecules) can be studied, that occur then, selectively, only on the external surface of the zeolite crystallites. The materials prepared were used to determine the internal and external sorption capacities of zeolites.¹²³ The method was also applied successfully in a study of the *p*-selective phenol methylation over H-MCM-22 zeolite crystallites.¹³¹

2.6 Summary of the findings described in Sections 2.1 – 2.5

The findings described in Sections 2.1 – 2.5 can be summarized as follows:

- For the purpose of converting light olefins such as propene into gasoline and distillate fuel, many solid or homogeneous metal catalysts and many solid acid catalysts appear suitable.
- For the purpose of converting naphtha range olefins such as hexenes into gasoline and distillate fuel, metal catalysts are hardly suitable, while solid acid catalysts, in particular alumino-silicates and, more specifically, acid zeolites are still suitable.
- Of the acid zeolites, H-ZSM-5 appears as the catalyst of choice.
- Reaction conditions for zeolite catalysed olefin oligomerization typically range from about 150 to 300 °C at pressures from ambient to typically up to 50 bar and space velocities (WHSV), typically, around 1.0 g/g.h.
- At high temperature, say above 250 °C, conjunct oligomerization occurs.
- At low temperatures, say below 250 °C, true oligomers (dimers, trimers, tetramers, pentamers etc.) form preferentially.
- Reaction conditions for selective dimerization are the mildest.

When oligomerizing short chain to naphtha range olefins (such as propene or 1-hexene) over H-ZSM-5 into gasoline and diesel range products under comparatively severe conditions (see above), the following is observed:

- Rapid initial double bond isomerization in the olefinic feed is followed by oligomerization, skeleton isomerization, cracking, cyclization and

H-transfer reactions. The extent to which these subsequent reactions occur increases with increasing reaction severity.

- Severe reaction conditions, in particular when comparatively high temperatures are applied, lead to conjunct oligomerization and a product consisting of oligomerized and cracked isomeric olefins with carbon numbers comprising non-integral multiples of the feed olefin's carbon number, alicyclic, aromatic and aliphatic compounds.
- Smoothed carbon number distributions of the iso-olefinic product are achieved that are independent of the type and properties of the olefinic feed.
- Skeleton structures of the iso-olefinic product show moderate branching (limited to one methyl branch, approximately, per five carbon atoms of the molecule's chain – the selectivity of longer side chains is minor).
- The iso-olefinic product fraction gets to, or close to, a thermodynamically controlled state, i.e., forms a pool of compounds with equilibrated carbon number and skeleton isomer distributions (the latter within the aforementioned limitations of the branching).
- Under thermodynamical control, rather low temperatures and, particularly, high pressures of 20 bar and above favour higher molecular weight products (diesel).
- At high reaction temperature reactions on the external surface of the H-ZSM-5 zeolite crystallites become increasingly important yielding iso-olefins with a higher degree of branching and more other products.
- In the gas phase, activity itself is largely pressure independent.

Specifically upon selective dimerization the following is observed:

- Over H-ZSM-5, at temperatures below 200 °C, even at conversions > 50%, mostly dimers form.
- Other solid acid catalysts such as wide pore zeolites or mesoporous materials are also suitable for dimerization.
- Dimer selectivity decreases with increasing conversion, but slowly, while trimers form increasingly as secondary products.
- Due to the rapid initial double bond isomerization (e.g. of 1-hexene to 2-hexene and 3-hexene) the dimerization of α -olefins also leads to mainly dibranched dimers.
- Branching selectivity is similar over H-ZSM-5 and mesoporous materials indicating that the reaction over the medium pore zeolite occurs mostly on the external surface of the crystallites.
- Comparatively bulky nitrogen bases such as 2,4,6-collidine, 2,6,-tert-butylpyridine and 2,4,6-trimethylpyridine are able to selectively poison the external surface of H-ZSM-5 crystallites for hexene dimerization and improve selectivity towards less branched products.
- Catalysts with larger pore sizes than H-ZSM-5 produce oligomers with a higher degree of branching and the product also contains more alicyclic, aromatic and paraffinic compounds.
- Oligomerization activity increases with increasing aluminium content, i.e. with the catalyst's Brønsted acid site density.
- Shape-selectivity towards less branched products decreases with increasing aluminium content, i.e., improves using low aluminium content H-ZSM-5.

- Side reactions such as H-transfer and aromatization increase with increasing aluminium content.
- H-ZSM-5 appears as the most stable of the aluminium-silicate catalysts.
- At low reaction temperatures heavy materials accumulate inside the zeolite pore system and also on the external crystallite surface, plugging pores and pore mouths and blocking external surface sites.
- The said accumulation appears to be a problem more in gas phase than in liquid phase operation.

Selective poisoning of sites effects branching selectivity:

- As mentioned above, non-shape selective reactions may occur on the external surface of the H-ZSM-5 zeolite crystallites.
- Correspondingly, external crystallite surface deactivated zeolites were found to be more selective towards less branched products.
- Surface deactivation can be achieved by silylation of the external surface of the zeolite crystallites.
- Comparatively bulky nitrogen bases (such as 2,4,6-collidine, 2,6,-*tert*-butylpyridine and 2,4,6-trimethylpyridine) were shown to be able to selectively poison the external surface of H-ZSM-5 and other medium pore zeolite crystallites and improve selectivity towards less branched products.
- On the contrary, selective external crystallite surface acid catalysis can be achieved poisoning the internal active sites by selective ion exchange.

2.7 Effect of mass transfer control on consecutive reactions

2.7.1 The Thiele Modulus

The extent to which mass transfer control, that is diffusional transport inside a catalyst particle, limits the reaction of a compound can be quantified by the Thiele Modulus. For a first order reaction, the Thiele Modulus is the following:¹³²

$$\varphi \approx \varepsilon \sqrt{\frac{k \cdot r_p^2}{D_{\text{eff}}}}$$

Where:

φ Thiele Modulus

ε Geometrical factor (specifies the shape of the particle)

k Reaction rate constant (intrinsic)

r_p Critical dimension (e.g. radius of spherical or cylindrical particle)

D_{eff} Diffusivity of compound

The Thiele Modulus relates k and r^2/D , that is, it relates activity and diffusivity. Thiele Moduli > 1 indicate that internal mass transfer controls and limits the reaction rate. Consequently, the reactants are preferentially or completely consumed in a layer below the external surface of the catalyst particle and hardly or not at all get to the interior. Conversely, Thiele Moduli < 1 indicate that the chemical reaction controls the reaction rate and reactants penetrate the entire catalyst particle. The Thiele Modulus determines the effectiveness

factor (η), which quantifies the observed reaction rate of a compound as a percentage of its intrinsic rate. Accordingly, the effectiveness factor is defined as the ratio between observed and intrinsic rate constants.¹³²

2.7.2 Effect of mass transfer limitations on intermediate yield and selectivity

If diffusion of the primary reaction products out of a catalyst particle is inhibited, these products may undergo secondary reactions. The stronger this diffusional inhibition is (and the higher their reactivity), the more of the primary product will react further, resulting in an increase in yield and selectivity of the secondary product and, correspondingly, a decrease in yield and selectivity of the primary product. With increasing differences in rate constants and/or diffusivities and/or particle sizes of samples of the same catalyst, the two consecutive reactions will also have increasingly different Thiele Moduli and, consequently, increasingly different effectiveness factors for the formation of the primary and the secondary product. The yield of the primary product, the intermediate, in case of different reaction rate constants, is the following:¹³³

$$Y_B = [Q/(Q-1)] (1 - X_A) [(1 - X_A)^{-(1-1/Q)} - 1]$$

Where:

X_A = Conversion of the reactant

Y_B = Yield of the primary product (intermediate)

Q = Ratio k_1/k_2 of primary and secondary reaction rate constants

Figure 2-26 illustrates the effect of varying ratios of rate constants, diffusivities and particle sizes in a mass transfer controlled reaction system.

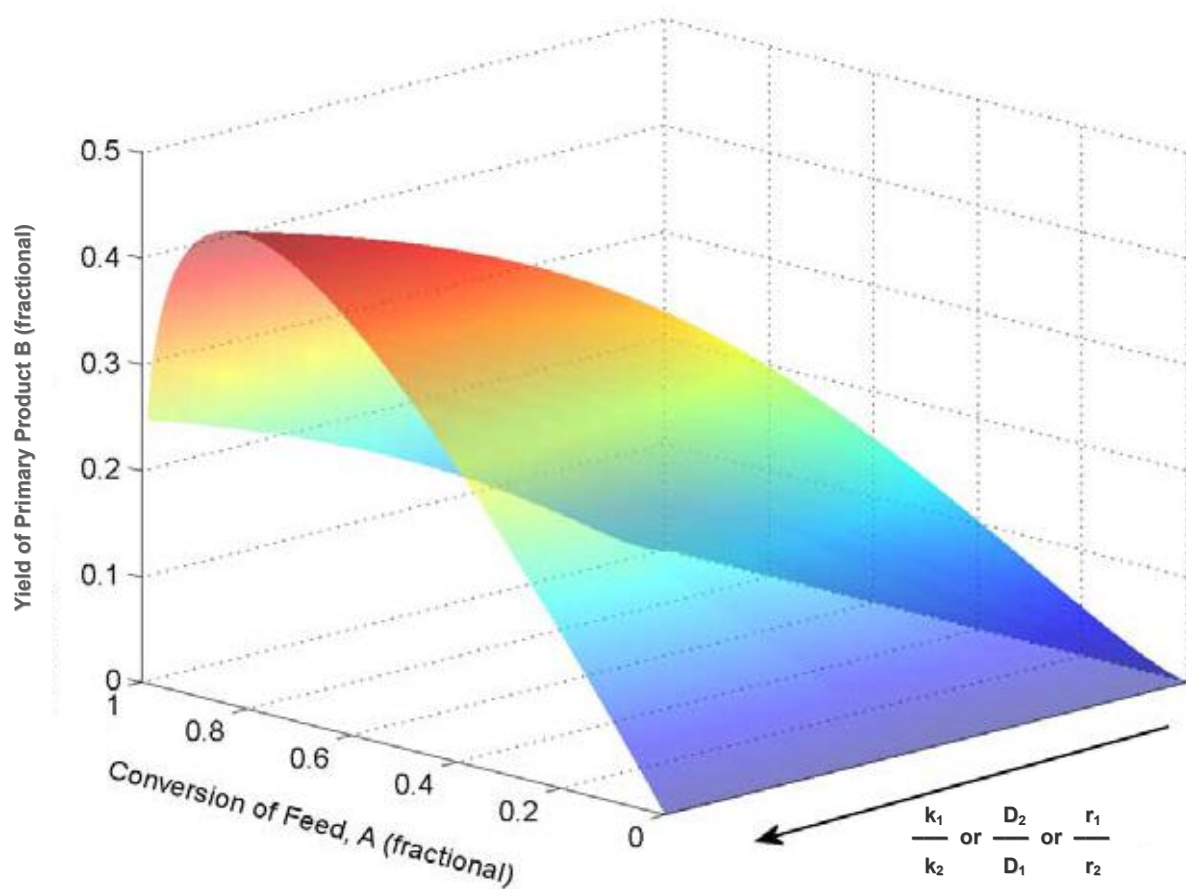


Figure 2-26: Yield of primary product B as influenced by the ratios of reaction rate constants k , diffusivities D and catalyst particle dimensions r (modified from the reference).¹³⁴

Yields of intermediate B are higher when

- (i) $k_1 \gg k_2$, that is, when the rate of formation of primary product B is significantly higher than its rate of its consumption.
- (ii) $D_2 \gg D_1$, that is, when the diffusional transport of primary product B out of the catalyst particle is significantly faster than the transport of reactant A into the particle.

- (iii) $r_2 \ll r_1$, that is, when the particles of shape 2 of the catalyst are significantly larger than those of shape 1 so that the distance of travelling of primary product B out of the particles of catalyst shape 2 is significantly shorter than the distance of travelling out of the particles of catalyst shape 1.

Obviously, with declining k_1/k_2 and D_2/D_1 ratios and declining r , a corresponding decline in the yields of primary product B is observed, because of the more rapid re-adsorption of intermediate B and formation of secondary product C.

The effect of the crystallite size of H-ZSM-5 catalysts of similar $\text{SiO}_2/\text{Al}_2\text{O}_3$ ratios on the conversion of methanol to olefins *via* intermediate formation of dimethyl ether (DME) was studied in an ideally backmixed reactor.¹³⁵ A kinetic model for the methanol-to-DME-to-olefins reaction was developed to interpret the influence of the crystal size on the individual reaction steps.

The study found that an increase in crystallite size resulted in a corresponding increase in the formation of secondary product olefins, and a decrease in the formation of the intermediate DME (see Figure 2-27). This phenomenon can be attributed to the introduction of increased diffusional resistances with an increase in H-ZSM-5 crystallite size, which increases the residence time of the DME intermediate inside the H-ZSM-5 crystals thereby providing further opportunity for the DME to be converted to olefins in a secondary reaction.¹³⁵

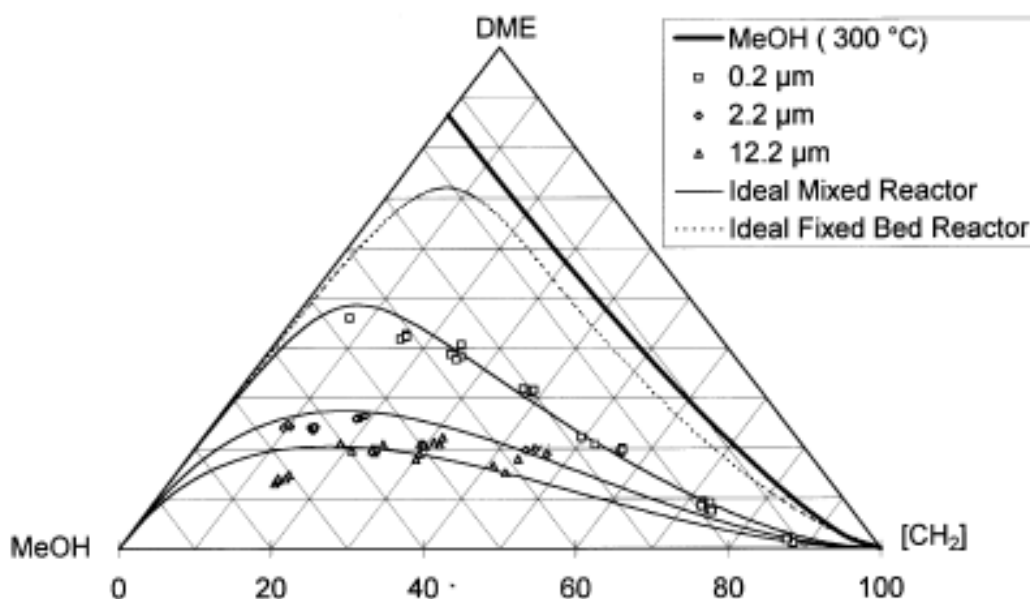


Figure 2-27: The conversion of methanol (MeOH) to dimethyl ether (DME) and hydrocarbons ([CH₂]) at 300 °C and 1 bar over H-ZSM-5 catalysts of different crystallite sizes but similar SiO₂/Al₂O₃ ratios. Curves indicate model predictions. MeOH (300 °C) refers to the thermodynamic equilibrium conversion of methanol to dimethyl ether.¹³⁵

While the above catalyst was a zeolite powder (more precisely, a zeolite crystallite agglomerates powder), mass transfer control effects on conversion and selectivity have also been observed over acid catalysts in the form of shaped mesoporous materials and zeolites shaped with a binder that produced a mesoporous matrix; typically in the form of extrudates ≥ 1 mm in diameter.

The acid catalyzed dehydration of 1-phenyl-ethanol to styrene was studied over zeolite powder that was shaped with silica binder to extrudates (1.6 mm trilobes) with the silica having formed a mesoporous matrix (10-20 Å pores).¹³⁶ In the said reaction system styrene is an intermediate that may react further

to, for instance, acetophenone and ethylbenzene, but also to styrene oligomers, which block the pores and deactivate the catalyst. It was found that both styrene selectivity and catalyst life time were maximum, when the catalyst was designed and operated such that no diffusion limitation occurred in the mesopores of the binder, that is, low zeolite content extrudates, low reaction temperature and crushed catalyst particles.¹³⁶

The acid catalyzed oligomerization of propene (conjunct oligomerization at 170 °C and 20 bar) was studied over mesoporous silica-alumina (MSA).¹³⁷ The MSA had uniform pores with a narrow pore size distribution and pore diameters around 40 Å. The MSA was either shaped in bulk to granules of 2 mm in diameter or fine MSA particles (< 50 µm) were dispersed in γ-alumina and extruded. This resulted in macroporous extrudates (2 mm in diameter) with pore diameters > 1000 Å. The apparent activation energies observed of 18 kJ/mol indicated mass transfer control of the propene oligomerization reaction over both catalysts, while the 3-fold higher conversion obtained over the macroporous MSA/γ-alumina extrudates compared to the mesoporous MSA granules (at identical WHSV_{MSA}) indicated that mass transfer control only occurred in the mesoporous MSA domain.¹³⁷

It can be summarized that increased mass transfer control of consecutive reactions reduces intermediate selectivity in favour of the selectivity of the secondary product.

2.8 References

- ¹ C.T. O'Connor, M. Kojima, *Catal. Today*, 6 (1990) 329-349.
- ² H. Pines, "Chemistry of Catalytic Hydrocarbon Conversions", Academic Press, New York (1981) 33-91.
- ³ W.E. Garwood, "Conversion of C₂-C₁₀ Olefins to Higher Olefins over Synthetic Zeolite ZSM-5" in "Intrazeolite Chemistry", G.D. Stucky, F.G. Dwyer (Eds.), ACS Symp. Ser., Vol. 218, Am. Chem. Soc., Washington, DC (1983) 383-396.
- ⁴ J. Heveling, C.P. Nicolaides, M.S. Scurrell, *Appl. Catal.*, 248 (2003) 239-248.
- ⁵ G.A. Olah, Á. Molnár, "Hydrocarbon Chemistry", 2nd Edition, John Wiley & Sons, New Jersey (2003) 723-746.
- ⁶ A. Corma, S. Iborra, "Oligomerization of Alkenes" in "Catalysts for Fine Chemical Synthesis, Microporous and Mesoporous Solid Catalysts", E.G. Derouane (Ed.), John Wiley & Sons, New York, Vol. 4 (2006) 125-140.
- ⁷ A. Forrester, H. Olivier-Bourbigou, L. Saussine, *Oil & Gas Sci. Technol. – Rev. IFP*, 64 (2009) 649-667.
- ⁸ B. Bogdanović, *Adv. Organometal. Chem.*, 17 (1979) 105-140.
- ⁹ S. Albrecht, D. Kießling, D. Maschmeyer, F. Nierlich, G. Wendt, *Chemie Ingenieur Technik*, 77 (2004) 695-709 (in German).
- ¹⁰ G.R. Lappin, L.H. Nemec, J.D. Sauer, J.D. Wagner, "Olefins, Higher" in "Kirk-Othmer Encyclopedia of Chemical Technology", Wiley Online (2010), <http://onlinelibrary.wiley.com/doi/10.1002/0471238961.1512050612011616.a01.pub2/full>.
- ¹¹ S. Naqvi, "Process Economics Program", SRI Consulting, Report No. 12E (2008).
- ¹² Chemsystems, "Alpha Olefins", Report Abstract, PERP06/07-5 (2008) 1-11.

-
- ¹³ E.O.C. Greiner, R. Gubler, Y. Inoguchi, "Chemical Handbook", SRI Consulting (2004).
- ¹⁴ R.L. Poe, D.J. Royer, US 4,455,289 (1984), assigned to Conoco Inc.
- ¹⁵ W. Keim, *Angew. Chem. Int. Ed. Engl.*, 29 (1990) 235-244.
- ¹⁶ J.T. Dixon, M.J. Green, F.M. Hess, D.H. Morgan, *J. Organomet. Chem.*, 689 (2004) 3641-3668.
- ¹⁷ D.F. Wass, *Dalton Trans.*, (2007) 816-819.
- ¹⁸ F. Speiser, P. Braunstein, L. Saussine, *Acc. Chem. Res.*, 38 (2005) 784-793.
- ¹⁹ J. Skupińska, *Chem. Rev.*, 91 (1991) 613-648.
- ²⁰ H. Mahomed, A. Bollmann, J.T. Dixon, V. Gokul, L. Griesel, C. Grove, F. Hess, H. Maumela, L. Pepler, *Appl. Catal. A: General*, 255 (2003) 355-359.
- ²¹ E. Killian, K. Blann, A. Bollmann, J.T. Dixon, S. Kuhlmann, M.C. Maumela, H. Maumela, D.H. Morgan, P. Nongodlwana, M.J. Overett, M. Pretorius, K. Hoefener, P. Wasserscheid, *J. Mol. Catal. A: Chemical*, 270 (2007) 214-218.
- ²² A. Bollmann, K. Blann, J.T. Dixon, F.M. Hess, E. Killian, H. Maumela, D.S. McGuinness, D.H. Morgan, A. Neveling, S. Otto, M. Overett, A.M.Z. Slawin, P. Wasserscheid, S. Kuhlmann, *J. Amer. Chem. Soc.*, 126 (2004) 14712-14713.
- ²³ K. Blann, A. Bollmann, H. De Bod, J.T. Dixon, E. Killian, P. Nongodlwana, M.C. Maumela, H. Maumela, A.E. McConnell, D.H. Morgan, M.J. Overett, M. Pretorius, S. Kuhlmann, P. Wasserscheid, *J. Catal.*, 249 (2007) 244-249.
- ²⁴ W.K. Reagan, EP 0417477 (1991), assigned to Phillips Petroleum Co.
- ²⁵ J.W. Freeman, J.L. Buster, R.D. Knudsen, US 5,563,312 (1999), assigned to Phillips Petroleum Co.

-
- ²⁶ Chevron Phillips press release, 2003-1-21, <http://www.cpchem.com>, accessed 2006-10-15.
- ²⁷ Sasol Media Release, 2010-12-2, http://www.sasolswla.com/pdf/Sasol%20Media%20Release_Tetramerization_Regional.pdf, accessed 2006-10-15.
- ²⁸ A.M. Al-Jarallah, J.A. Anabtawi, M.A.B. Siddiqui, A.M. Aitani, A.W. Al-Sa'doun, *Catal. Today*, 14 (1992) 1-121.
- ²⁹ N.M. Prinsloo, *Fuels Proc. Tech.*, 87 (2006) 437-442.
- ³⁰ A. de Klerk, *Green Chem.*, 10 (2008) 1249-1279.
- ³¹ C.D. Knottenbelt, C. Dunlop, K. Zono, M. Thomas, WO 069407 A2 (2006), assigned to The Petroleum Oil Corporation of South Africa (Pty) Ltd. (PetroSA).
- ³² C.D. Knottenbelt, C. Dunlop, K. Zono, M. Thomas, WO 069406 A1 (2006), assigned to The Petroleum Oil Corporation of South Africa (Pty) Ltd. (PetroSA).
- ³³ C.D. Knottenbelt, C. Dunlop, K. Zono, M. Thomas, WO 069408 A2 (2006), assigned to The Petroleum Oil Corporation of South Africa (Pty) Ltd. (PetroSA).
- ³⁴ A.G. Oblad, G.A. Mills, H. Heinemann, "Polymerization of Olefins (to Liquid Polymers)" in "Catalysis", P.H. Emmett (Ed.), Reinhold, New York, Vol. 6 (1958) 341-406.
- ³⁵ C.T. O'Connor, "Oligomerization" in "Handbook of Heterogeneous Catalysis", G. Ertl, H. Knözinger, F. Schüth, J. Weitkamp (Eds.), Wiley-VCH, Weinheim, Vol. 6 (2008) 2854-2864.
- ³⁶ W.O. Haag, N.Y. Chen, "Catalyst Design with Zeolites" in "Catalyst Design, Progress and Perspectives", L.L. Hegedus, A.T. Bell, N.Y. Chen,

-
- W.O. Haag, J. Wei, R. Aris, M. Boudart, B.C. Gates, G.A. Somorjai (Eds.), John Wiley & Sons, New York (1987) 162-213.
- ³⁷ J.A. Martens, P.A. Jacobs, *Stud. Surf. Sci. Catal.*, 137 (2001) 633-671.
- ³⁸ Sykes P., *A Guidebook to Mechanism in Organic Chemistry*, Longman Scientific and Technical, Essex, 6th ed. (1986).
- ³⁹ W. Böhringer, Centre for Catalysis Research, Department of Chemical Engineering, University of Cape Town, personal communication (2007).
- ⁴⁰ C.P. Nicolaides, M.S. Scurrall, P.M. Semano, *Appl. Catal. A: General*, 245 (2003) 43-53.
- ⁴¹ P.B. Venuto, *Microporous Mat.*, 2 (1994) 297-411.
- ⁴² J.R. Anderson, Y.F. Chang, R.J. Western, *J. Catal.*, 118 (1989) 466-482.
- ⁴³ S.J. Sealy, D.M. Fraser, K.P. Möller, C.T. O'Connor, *Chem. Eng. Sci.*, 49 (1994) 3307-3312.
- ⁴⁴ A. de Klerk, *Energy & Fuels*, 20 (2006) 1799-1805.
- ⁴⁵ T.N. Mashapa, A. de Klerk, *Appl. Catal. A: General*, 332 (2007) 200-208.
- ⁴⁶ A. de Klerk, *Energy & Fuels*, 20 (2006) 439-445.
- ⁴⁷ J.H. Coetzee, T.M. Mashapa, N.M. Prinsloo, J.D. Rademan, *Appl. Catal. A: General*, 308 (2006) 204-209.
- ⁴⁸ A. de Klerk, US 0,108,568 A1 (2010), assigned to Sasol Technology (Pty) Ltd.
- ⁴⁹ South African Bureau of Standards, www.stansa.co.za (SANS 342, Edition 4 (2006) 1-10), accessed 2011-01-10.
- ⁵⁰ 2011 Worldwide Fuel Specifications, Hart Energy Publishing, 12th Edition, (2011), www.ifgc.org (accessed 2011-06-29).
- ⁵¹ S.J. Miller, US 4,417,088 (1983), assigned to Chevron Inc.

-
- ⁵² S.J. Miller, US 5,413,695 (1995), assigned to Chevron Inc.
- ⁵³ S.J. Miller, WO 02/055633 A1 (2002), assigned to Chevron Inc.
- ⁵⁴ D. Leckel, Energy & Fuels, 23 (2009) 2342-2358.
- ⁵⁵ G. Busca, Chem. Rev., 107 (2007) 5366-5410.
- ⁵⁶ A. de Klerk, Energy & Fuels, 20 (2006) 1799-1805.
- ⁵⁷ T.N. Mashapa, A. de Klerk, Appl. Catal. A: General, 332 (2007) 200-208.
- ⁵⁸ A. de Klerk, Energy & Fuels, 20 (2006) 439-445.
- ⁵⁹ J.H. Coetzee, T.M. Mashapa, N.M. Prinsloo, J.D. Rademan, Appl. Catal. A: General, 308 (2006) 204-209.
- ⁶⁰ A. de Klerk, US 0,108,568 A1 (2010), assigned to Sasol Technology (Pty) Ltd.
- ⁶¹ E.N. Givens, C.J. Plank, E.J. Rosinski, US 3,960,978 (1976), assigned to Mobil Oil Corp.
- ⁶² W.E. Garwood, P.D. Caesar, J.A. Brennan, US 4,150,062 (1979), assigned to Mobil Oil Corp.
- ⁶³ W.E. Garwood, F.J. Krambeck, J.D. Kushnerick, S.A. Tabak, US 4,740,645 (1988), assigned to Mobil Oil Corp.
- ⁶⁴ S.A. Tabak, R.E. Holland, M.R. Ireland, AIChE Summer National Meeting, Philadelphia, PA, August 19-22 (1984) Paper 42a.
- ⁶⁵ C.J. Plank, E.J. Rosinski, E.N. Givens, US 4,021,502 (1977), assigned to Mobil Oil Corp.
- ⁶⁶ W.E. Garwood, W. Lee, US 4,227,992 (1980), assigned to Mobil Oil Corp.
- ⁶⁷ W.E. Garwood, W. Lee, US 4,211,640 (1980), assigned to Mobil Oil Corp.
- ⁶⁸ S.A. Tabak, US 4,254,295 (1981), assigned to Mobil Oil Corp.
- ⁶⁹ W.E. Garwood, US 4,547,613 (1985), assigned to Mobil Oil Corp.

-
- ⁷⁰ W.E. Garwood, J.D. Kushnerick, S.A. Tabak, US 4,717,782 (1988), assigned to Mobil Oil Corp.
- ⁷¹ C.J. Plank, E.J. Rosinski, E.N. Givens, US 4,021,502 (1977), assigned to Mobil Oil Corp.
- ⁷² W.E. Garwood, W. Lee, US 4,227,992 (1980), assigned to Mobil Oil Corp.
- ⁷³ W.E. Garwood, W. Lee, US 4,211,640 (1980), assigned to Mobil Oil Corp.
- ⁷⁴ S.A. Tabak, US 4,254,295 (1981), assigned to Mobil Oil Corp.
- ⁷⁵ W.E. Garwood, US 4,547,613 (1985), assigned to Mobil Oil Corp.
- ⁷⁶ W.E. Garwood, J.D. Kushnerick, S.A. Tabak, US 4,717,782 (1988), assigned to Mobil Oil Corp.
- ⁷⁷ South African National Standards, www.sapia.co.za (Petrol and Diesel in South Africa and the impact on air Quality – November 2008), accessed 2010-01-02.
- ⁷⁸ R. Barber, K. Carabell, J. Freel, P. Fuentes-Afflick, L. Gibbs, H. Gooch, K. Hoekman, M. Ingham, M. Johnson, D. Kohler, R. Leaper, D. Lesnini, M. Lano, W.S. Lee, M. Sztenderowicz, S. Welstand, “Motor Gasolines Technical Review (FTR-1)”, Chevron Products Company, Chevron Inc., U.S.A., (1996) 41-52.
- ⁷⁹ South African Bureau of Standards, www.stansa.co.za (SANS 342, Edition 3.2 (2003) 1-9), accessed 2008-03-04.
- ⁸⁰ J. Bacha, L. Blondis, J. Freel, G. Hemighaus, K. Hoekman, N. Hogue, J. Horn, D. Lesnini, C. McDonald, M. Nikanjam, E. Olsen, B. Scott, M. Sztenderowicz, “Diesel Fuels Technical Review (FTR-2)”, Chevron Products Company, Chevron Inc., (1998) 32-45.
- ⁸¹ C.D. Knottenbelt, Catal. Today, 71 (2002) 437-445.

-
- ⁸² E. Köhler, F. Schmidt, H.J. Wernicke, M. Pontes, H.L. Roberts, Hydrocarbon Technol. Int. Quarterly, Summer (1995) 37-40.
- ⁸³ A.F. Cronstedt, Akad. Handl. Stockholm, 18 (1756) 120 [cited from N.P. Sincadu, PhD Thesis, University of the Witwatersrand (2003)].
- ⁸⁴ D. Shuring, Ph.D. Thesis, Eindhoven University of Technology (2002).
- ⁸⁵ J. Weitkamp, Solid State Ionics, 131 (2000) 175-188.
- ⁸⁶ A. Dyer, "An Introduction to Zeolite Molecular Sieves", John Wiley & Sons, New York (1988) Chapters 1, 2, 5, 8 and 9.
- ⁸⁷ A. Corma, Chem. Rev., 95 (1995) 559-614.
- ⁸⁸ J.A. Rabo, "Zeolite Chemistry and Catalysis", ACS Monograph, Vol. 171, Am. Chem. Soc., Washington, DC (1976) 3-70.
- ⁸⁹ J. Weitkamp, lecture notes on "Zeolites I: Structures, Synthesis and Properties", Institute of Chemical Technology, University of Stuttgart, WS 2004/2005.
- ⁹⁰ N.Y. Chen, W.E. Garwood, F.G. Dwyer, "Shape Selective Catalysis in Industrial Applications", Marcel Dekker, New York (1989) Chapters 2, 3, 4 and 5.
- ⁹¹ S.A. Tabak, F.J. Krambeck, W.E. Garwood, J. AIChE., 32 (1986) 1526-1526.
- ⁹² B.C. Gates, "Catalytic Chemistry", John Wiley & Sons, New York (1992) 254-269.
- ⁹³ R. Xu, W. Pang, J. Yu, Q. Huo, J. Chen, "Chemistry of Zeolites and Related Porous Materials: Synthesis and Structure", John Wiley & Sons (Asia) Pte Ltd, Singapore (2007) Chapter 2.
- ⁹⁴ M. Stöcker, Micropor. Mesopor. Mat., 82 (2005) 257-292.

-
- ⁹⁵ <http://www.materialsdesign.com/appnote/acidity-amorphous-silica-alumina-asa-catalysts>, accessed 2011-04-13.
- ⁹⁶ C.T. Kresge, M.E. Leonowicz, W.J. Roth, J.C. Vartuli, J.S. Beck, *Nature*, 359 (1992) 710-712.
- ⁹⁷ J. M. Thomas, R.C. Theocharis, "Catalysis with Clays and Their Pillared Variants" in "Perspectives in Catalysis", J.M. Thomas, K.I. Zamaraev (Eds.), Blackwell, London, Vol. 24 (1992) 465-488.
- ⁹⁸ A. Vaccari, *Catal. Today*, 41 (1998) 53-71.
- ⁹⁹ A. de Klerk, *Energy & Fuels*, 21 (2007) 625-632.
- ¹⁰⁰ S. Peratello, M. Molinari, G. Bellussi, C. Perego, *Catal. Today*, 52 (1999) 271-277.
- ¹⁰¹ A. de Klerk, Ph.D. Thesis, University of Pretoria (2008).
- ¹⁰² P.B. Weisz, V.J. Frilette, *J. Phys. Chem.*, 64 (1960) 382-383.
- ¹⁰³ E.G. Derouane, *Stud. Surf. Sci. Catal.*, 5 (1980) 5-18.
- ¹⁰⁴ S.M. Csicsery, *Pure Appl. Chem.*, 58 (1986) 841-856.
- ¹⁰⁵ J. Weitkamp, S. Ernst, L. Puppe, "Shape-Selective Catalysis in Zeolites" in "Catalysis and Zeolites: Fundamentals and Applications", J. Weitkamp, L. Puppe (Eds.), Springer, New York (1999) 327-369.
- ¹⁰⁶ R.J. Quann, L.A. Green, S.A. Tabak, F.J. Krambeck, *Ind. Eng. Chem. Res.*, 27 (1988) 565-570.
- ¹⁰⁷ K.G. Wilshier, P. Smart, T. Western, T. Mole, T. Behrsing, *Appl. Catal.*, 31 (1987) 339-359.
- ¹⁰⁸ R.J. Quann, F.J. Krambeck, "Chemical Reactions in Complex Mixtures" in "Proceedings of Mobil Symposium", A.V. Sapre, F.J. Krambeck (Eds.), Van Nostrand Reinhold, New York (1991) 143-161.

-
- ¹⁰⁹ S.J. Miller, *Stud. Surf. Sci. Catal.*, 38 (1987) 187-197.
- ¹¹⁰ S. Schwarz, M. Kojima, C.T. O'Connor, *Appl. Catal.*, 56 (1989) 263-280.
- ¹¹¹ M.L. Occelli, J.T. Hsu, L.G. Galya, *J. Mol. Catal.*, 32 (1985) 377-390.
- ¹¹² T.J.G. Kofke, R.J. Gorte, *J. Catal.*, 115 (1989) 233-243.
- ¹¹³ R. Schmidt, M.B. Welch, B.B. Randolph, *Energy & Fuels*, 22 (2008) 1148-1155.
- ¹¹⁴ M. Golombok, J. de Bruijn, *Ind. Eng. Chem. Res.*, 39 (2000) 267-271.
- ¹¹⁵ M. Golombok, J. de Bruijn, *Appl. Catal. A: General*, 208 (2001) 47-53.
- ¹¹⁶ R. van Grieken, J.M. Escola, J. Moreno, R. Rodríguez, *Appl. Catal. A: General*, 305 (2006) 176-188.
- ¹¹⁷ C.P. Nicolaidis, M.S. Scurrrell, P.M. Semano, *Appl. Catal. A: General*, 245 (2003) 43-53.
- ¹¹⁸ J.T. Klopprogge, E. Booy, J.B.H. Jansen, J.W. Geus, *Clay Miner.*, 29 (1994) 153-167.
- ¹¹⁹ J.P.G. Pater, P.A. Jacobs, J.A. Martens, *J. Catal.*, 179 (1998) 477-482.
- ¹²⁰ M.L.O. Sumani, MSc Thesis, Department of Chemical Engineering, University of Cape Town (2006).
- ¹²¹ J.P.G. Pater, P.A. Jacobs, J.A. Martens, *J. Catal.*, 187 (1999) 262-267.
- ¹²² C.S.H. Chen, R.F. Bridger, *J. Catal.*, 161 (1996) 687-693.
- ¹²³ C. Berger, A. Raichle, R.A. Rakoczy, Y. Traa, J. Weitkamp, *Micropor. Mesopor. Mat.*, 59 (2003) 1-12.
- ¹²⁴ F. Niu, H. Hofmann, *Appl. Catal. A: General*, 128 (1995) 107-118.
- ¹²⁵ N.M. Page, L.B. Young, D.A. Blain, US 4,870,038 (1989), assigned to Mobil Oil Corp.

-
- ¹²⁶ M.R. Apelian, J.R. Boulton, A.S. Fung, US 5,284,989 (1994), assigned to Mobil Oil Corp.
- ¹²⁷ M.R. Apelian, T.F. Degnan, A.S. Fung, US 5,234,872 (1992), assigned to Mobil Oil Corp.
- ¹²⁸ A.W. Chester, A.S. Fung, C.T. Kresge, W.J. Roth, US 5,779,882 (1998), assigned to Mobil Oil Corp.
- ¹²⁹ L.D. Rollmann, *Stud. Surf. Sci. Catal.*, 68 (1991) 791-797.
- ¹³⁰ J.R. Anderson, K. Foger, T. Mole, R.A. Rajadhyaksha, J.V. Sanders, J. *Catal.*, 58 (1979) 114-130.
- ¹³¹ G. Moon, W. Böhringer, C.T. O'Connor, *Catal. Today*, 97 (2004) 291-295.
- ¹³² H.S. Fogler, "Diffusion and Reaction" in "Elements of Chemical Reaction Engineering", N.R. Amundson (Ed.), 4th Edition, Prentice Hall, New Jersey (1999) 819-823.
- ¹³³ A. Wheeler, *Adv. Catal.*, 3 (1951) 249-327.
- ¹³⁴ R. Kukard, MSc Thesis, Department of Chemical Engineering, University of Cape Town (2008).
- ¹³⁵ K.P. Möller, W. Böhringer, A.E. Schnitzler, E. van Steen, C.T. O'Connor, *Micropor. Mesopor. Mat.*, 29 (1999) 127-144.
- ¹³⁶ J.-P. Lange, C.M.A.M. Mesters, *Appl. Catal. A: General*, 210 (2001) 247-255.
- ¹³⁷ S. Peratello, M. Mollinari, G. Belusso, C. Perego, *Catal. Today*, 52 (1999) 271-277.

CHAPTER 3

3. OBJECTIVES, HYPOTHESIS AND KEY QUESTIONS

3.1 The objective of this study

As outlined in Chapter 1, Sasol is short in diesel-range products but produces low to naphtha-range olefins in abundance. Sasol is currently running a process, CatPoly,^{1,2} that, using a solid phosphoric acid (SPA) catalyst, oligomerizes such lower olefins to diesel-range products (see Section 2.1.2.2.1). Major shortcomings of this process are the limited lifetime of the catalyst^{1,3,4} and the low cetane number of the “diesel” produced, due to the high degree of branching of the CatPoly oligomerizate⁵ (see introduction to Section 2.1.2.2)

Dimerizates from naphtha-range *n*-olefins appear to be much less branched than the said CatPoly oligomerizate and, therefore, their cetane numbers will be significantly higher while still showing good cold flow properties.^{6,7,8,9}

The major objectives of this study were, on the one hand, to confirm the applicability of medium-pore width acid zeolite H-ZSM-5 for the dimerization of naphtha-range *n*-olefins into diesel-range olefins (C₁₀-C₂₀), following a previous study⁶, and, on the other hand, to test the conclusion of this previous study (see Section 2.5.2) that the dimerization reaction takes place on the external surface of the zeolite crystallites, and not inside the zeolite pore system.⁶

Following the said previous study⁶, shape-selective, medium pore channel (5.5 Å) H-ZSM-5 zeolite with a rather high molar $\text{SiO}_2/\text{Al}_2\text{O}_3$ ratio of 90 was the catalyst of choice to study the dimerization of naphtha-range *n*-olefins into moderately branched diesel-range olefins.

For comparison, and in addition to the series of zeolite catalysts investigated in the previous study, the reaction was also to be studied over a non-shape-selective catalyst, namely amorphous silica-alumina (ASA). Activities of the two catalysts were expected to be similar. An ASA catalyst with a molar $\text{SiO}_2/\text{Al}_2\text{O}_3$ ratio of 10 was chosen.

Pure 1-olefins ex-Sasol, namely 1-hexene and 1-octene, were to be used as model feed-stocks to synthesize the desired diesel-range dimers. The reaction of these olefins over the medium-pore acid zeolite catalyst was expected to produce, at medium to rather high conversions, a product of mainly dimers with moderate branching; that is, with not much more than two branches, per dimer molecule, on average.

In order to tailor the desired product composition, especially in order to control the degree of branching, reaction conditions (in particular temperature and weight hourly space velocity) were to be varied.

3.2 Hypothesis

The following was hypothesized:

1. Double bond isomerization is the most rapid reaction of the feed olefins over the acid catalyst. That is, effective feeds are the equilibrium or almost equilibrated mixtures of the respective double bond isomers of the fed 1-olefins.
2. Oligomerization under the mild conditions applied proceeds as “true” oligomerization, with dimers forming as primary products and trimers forming as secondary products, and no products with intermediate carbon numbers form.
3. Over an acid catalyst that effects no spatial restriction on the dimerization reaction, that is, over the amorphous silica-alumina catalyst to be studied, dimerization produces mostly a di-branched product.

Provided that the oligomerization reactions take place inside the pore system, the medium pore channels of the H-ZSM-5 zeolite would provide a shape-selective effect, in that they exclude bulky transition states and intermediates from forming in the pores and/or impose transport control on bulky products. These effects, if in place, would limit the degree of branching of the products to less than two.

Provided that the oligomerization reactions take place on the external surface of the H-ZSM-5 zeolite crystallites, no shape-selective effect would be present and the dimerization would also produce mostly a di-branched product.

It was, therefore, hypothesized further that:

4. Following the findings in the previous study⁶, the latter condition holds and a mostly di-branched product will be produced over zeolite H-ZSM-5.
5. With respect to branching, the product produced over the zeolite will, therefore, not differ from the product produced over the amorphous silica-alumina catalyst.
6. With respect to the carbon number distribution, the product produced over the zeolite and the amorphous catalyst may also not differ.
7. The two different model feeds, 1-hexene and 1-octene, and products thereof, do in principle not differ with respect to
 - reactivity,
 - dimer/trimer ratio at equal conversion, and
 - degree of branching.
8. Due to primary (of the feed molecules) and secondary (of the dimers) skeleton isomerization, the degree of branching increases with increasing reaction severity (conversion and temperature).
9. Since the zeolite catalyst to be used is known to be highly resistant to fouling (owing to its medium pore size, which prevents the formation of bulky olefin oligomers in the pores, and its high molar $\text{SiO}_2/\text{Al}_2\text{O}_3$ ratio of 90) it is active over prolonged times on stream.
10. Deactivation of the amorphous silica-alumina catalyst occurs more rapidly.
11. Diesel from naphtha-range olefin dimerization (after hydrogenation) has favourable properties compared to diesel from the CatPoly⁵ process in that its cetane number is much higher, while its cold flow properties are still within the required range.

12. Diesel properties are comparable to those of diesel from the other technical olefin-to-diesel oligomerization processes, the MOGD¹⁰ and the COD¹¹ process.

3.3 Key questions

The following key questions arose:

1. Are the activities of the two catalysts chosen (H-ZSM-5, molar $\text{SiO}_2/\text{Al}_2\text{O}_3$ ratio of 90, and amorphous silica-alumina, molar $\text{SiO}_2/\text{Al}_2\text{O}_3$ ratio of 10) close enough to produce similar conversions at similar reaction temperatures and within the technical limits of the test unit employed, so that selectivities can be compared?
2. Is a “true” oligomerization product, i.e. only dimers and trimers, obtained or does conjunct oligomerization also occur?
3. Do the dimerization products obtained over zeolite H-ZSM-5 and amorphous silica-alumina differ with respect to the degree of branching?
4. Is the selectivity to trimers different over zeolite H-ZSM-5 and amorphous silica-alumina?
5. Do the dimers produced over amorphous silica-alumina show the properties of a primary dimerization product, whose formation is controlled by the chemical kinetics of the reaction, that is, is it, mostly, a di-branched product?
6. Does the dimers obtained over zeolite H-ZSM-5 indicate that shape selective effects are operative, that is, is it a product with, on average, less than two branches per molecule?

7. If not, does the dimerization reaction over medium pore zeolite H-ZSM-5 indeed proceed in the channel system of the zeolite crystallites or (mostly) on their external surface?
8. Are the products from dimerizing 1-hexene and 1-octene different with respect to branching?
9. Is the zeolite catalyst reasonably stable?
10. Does the amorphous silica-alumina catalyst deactivate faster than the zeolite?
11. Does the dimerization product obtained, after hydrogenation, have properties that make it suitable as a diesel fuel?
12. Has the diesel from olefin dimerization better properties than the diesel obtained from the CatPoly⁵, MOGD¹⁰ and COD¹¹ processes?

3.4 References

- ¹ A. de Klerk, *Energy & Fuels*, 20 (2006) 439-445.
- ² N.M. Prinsloo, *Fuels Proc. Tech.*, 87 (2006) 437-442.
- ³ J.H. Coetzee, T.N. Mashapa, N.M. Prinsloo, J.D. Rademan, *Appl. Catal. A: General*, 308 (2006) 204-209.
- ⁴ A. Corma, S. Iborra, "Oligomerization of Alkenes" in "Catalysts for Fine Chemical Synthesis, Microporous and Mesoporous Solid Catalysts", E.G. Derouane (Ed.), John Wiley & Sons, New York, Vol. 4 (2006) 125-140.
- ⁵ D. Leckel, *Energy & Fuels*, 23 (2009) 2342-2358.
- ⁶ M.L.O. Sumani, MSc Thesis, Department of Chemical Engineering, University of Cape Town (2006).

-
- ⁷ J.P.G. Pater, P.A. Jacobs, J.A. Martens, J. Catal., 187 (1999) 262-267.
- ⁸ J.P.G. Pater, P.A. Jacobs, J.A. Martens, J. Catal., 179 (1998) 477-482.
- ⁹ R. van Grieken, J.M. Escola, J. Moreno, R. Rodríguez, Appl. Catal., 305 (2006) 176-188.
- ¹⁰ W.E. Garwood, "Conversion of C₂-C₁₀ Olefins to Higher Olefins over Synthetic Zeolite ZSM-5" in "Intrazeolite Chemistry", G.D. Stucky, F.G. Dwyer (Eds.), ACS Symp. Ser., Vol. 218, Am. Chem. Soc., Washington, DC (1983) 383-396.
- ¹¹ C.D. Knottenbelt, C. Dunlop, K. Zono, M. Thomas, WO 069407 A2 (2006), assigned to The Petroleum Oil Corporation of South Africa (Pty) Ltd. (PetroSA).

CHAPTER 4

4. EXPERIMENTAL AND METHODS

4.1 Chemicals and catalysts used in this project

A list of the chemicals and catalysts used in this project is given in Table 0-1.

Table 0-1: Chemicals and catalysts used

Chemical	Source	Use
1-Hexene (99.32% purity)	Sasol Secunda ^a	Reagent
1-Octene (99.29% purity)	Sasol Secunda ^a	Reagent
H-ZSM-5, SiO ₂ /Al ₂ O ₃ molar ratio = 90 ^b	Süd-Chemie (H-MFI-90)	Catalyst for dimerization
Amorphous silica-alumina (ASA), SiO ₂ /Al ₂ O ₃ molar ratio = 10 ^c	Akzo-Nobel (now Albemarle), (Silica-alumina, KF 200 carrier)	Catalyst for dimerization
Pd/C (10 wt%) ^d	Sigma-Aldrich (Product number: 20,569-9)	Catalyst for hydrogenation
1-Dodecene	Sigma-Aldrich (Product number: D22,160-0)	Peak identification
<i>n</i> -Dodecane	Sigma-Aldrich (Product number: 297879)	Peak identification
1-Hexadecene	Sigma-Aldrich (Product number: H2131)	Peak identification

^a Final product of co-monomer manufacture.

^b Extrudates, 1.6 mm in diameter, alumina binder (ca. 20 wt%¹), zeolite crystallite diameter << 0.1 µm according to SEM micrographs.²

^c Extrudates, 1.6 mm in diameter, average pore diameter of the ASA = 40 Å.

^d 10.1% Pd (dry basis by X-Ray Fluorescence), surface area of the carbon used as the support = 750 – 1000 m²/g, catalyst particle size ~ 90% < 60 µm and 10% < 5 µm.

Chemical	Source	Use
<i>n</i> -Hexadecane	Sigma-Aldrich (Product number: 296317)	Peak identification
1-Octadecene	Sigma-Aldrich (Product number: 74740)	Peak identification
2,4,6-Collidine	Sigma-Aldrich (Product number: 27690)	Selective catalyst poisoning
2,6-Di- <i>tert</i> -butyl pyridine	Sigma-Aldrich (Product number: 219584)	Selective catalyst poisoning
<i>n</i> -Pentane	Sigma-Aldrich (Product number: 158941)	Solvent for catalyst poisons
Chloroform-d, 99.8 atom% D	Sigma-Aldrich (Product number: 151823)	Solvent for ¹ H-NMR analysis
Nitrogen (99.999% purity)	Afrox	Catalyst drying and activation, auxiliary
Hydrogen (99.999% purity)	Afrox	Product hydrogenation

The dimerization experiments were carried out using the H-ZSM-5 zeolite and the amorphous silica-alumina catalysts. 1-Hexene and 1-octene feeds were used as obtained from Sasol Secunda without further purification.

4.2 Reactor set-up and configuration

The dimerization reactions were performed in a fixed-bed reactor having an internal diameter of 15 mm and a length of 252 mm. Nitrogen from a cylinder was used to pressurize the reactor during reactor leak tests, to inertise the apparatus, to activate the acid catalyst and also to keep the feed bottle under inert atmosphere during the reaction.

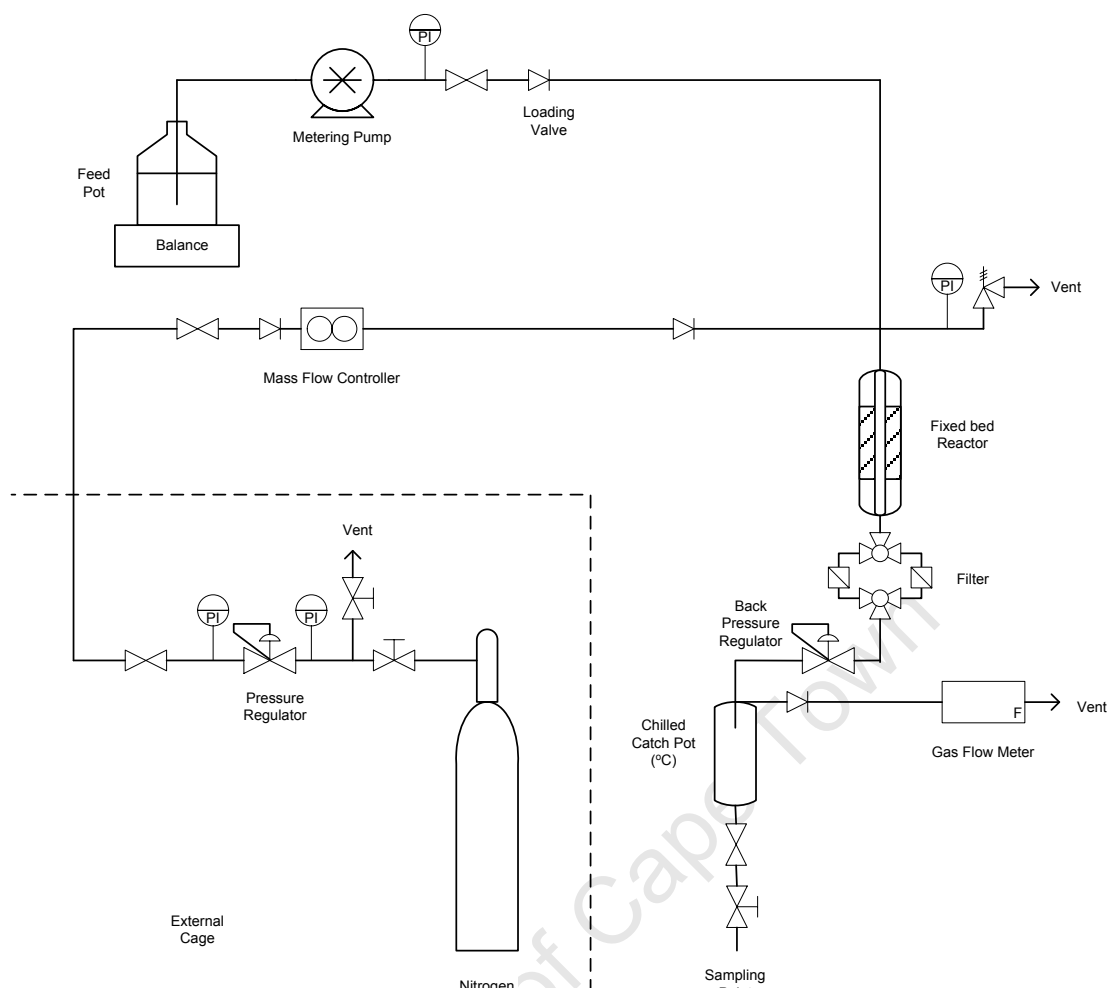


Figure 0-1: The dimerization reactor set-up.

The reactor was placed inside a temperature-controlled jacket. A movable thermocouple was placed in a thermowell that ranged co-axially through the centre of the catalyst bed. Liquid feed was fed to the reactor by an HPLC pump as can be seen in Figure 0-1. Filters were placed after the reactor to trap any solids that would otherwise collect in the sample catch-pot. A back pressure regulator was used to maintain the desired pressure of the reactor. The liquid product was collected in a catch-pot, which was cooled to 0 °C by a cooling bath. The catch-pot was emptied regularly. Samples of the liquid were taken and analyzed immediately. Possible gaseous products (i.e. crack gases possibly forming at the highest reaction temperatures applied) were vented.

The desired mass of catalyst (typically 15 g) was loaded in the middle of the reactor, as shown in Figure 4-2. Glass beads (3 mm) were used to fill up the dead volume, while glass wool was placed between the catalyst and the glass beads and also at the ends of the reactor to prevent small particles from leaving the reactor.

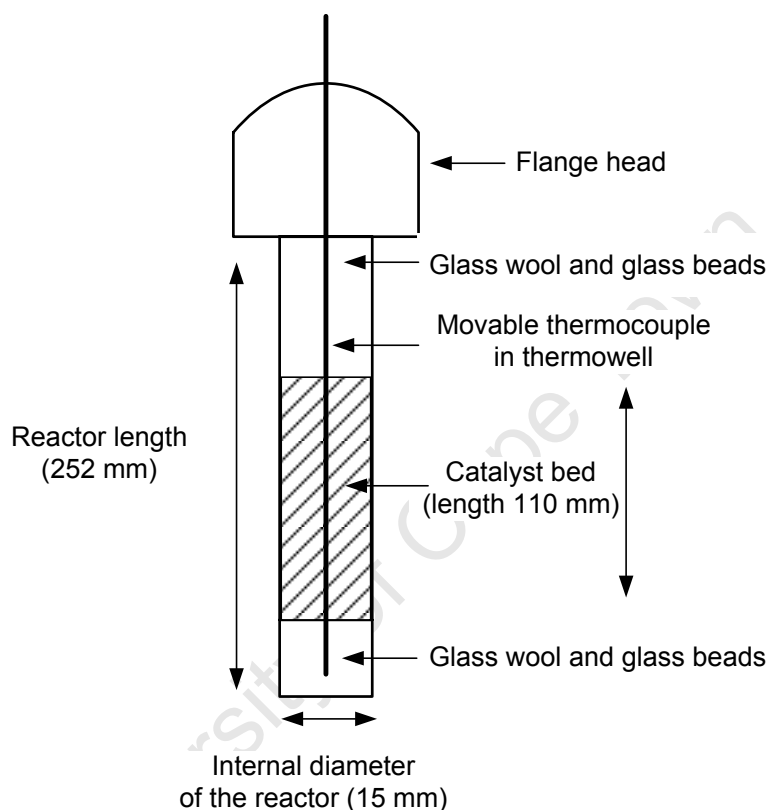


Figure 0-2: Schematic representation of a loaded reactor (mass of catalyst = 15 g, average extrudate diameter = 1.5 mm and volume of the catalyst bed in the reactor = 19 ml).

To limit the effects of channelling of the feed in the catalyst bed, the mass and size of the catalyst bed was chosen according to the rules suggested for laboratory scale heterogeneous catalyst testing, which are given in formulae (1) and (2).³

$$\frac{d_r}{d_p} = \frac{\text{reactor diameter}}{\text{particle diameter}} > 10 \quad (1)$$

$$\frac{L_b}{d_p} = \frac{\text{bed length}}{\text{particle diameter}} > 50 \quad (2)$$

The temperature profile in the catalyst bed (Figure 4-3) was measured by taking temperature readings (internal temperature, T_{int}) by the thermocouple along the thermowell from the beginning to the end of the catalyst bed. The profile was measured at steady-state operation with the temperature of the reactor oven control thermocouple at 170 °C.

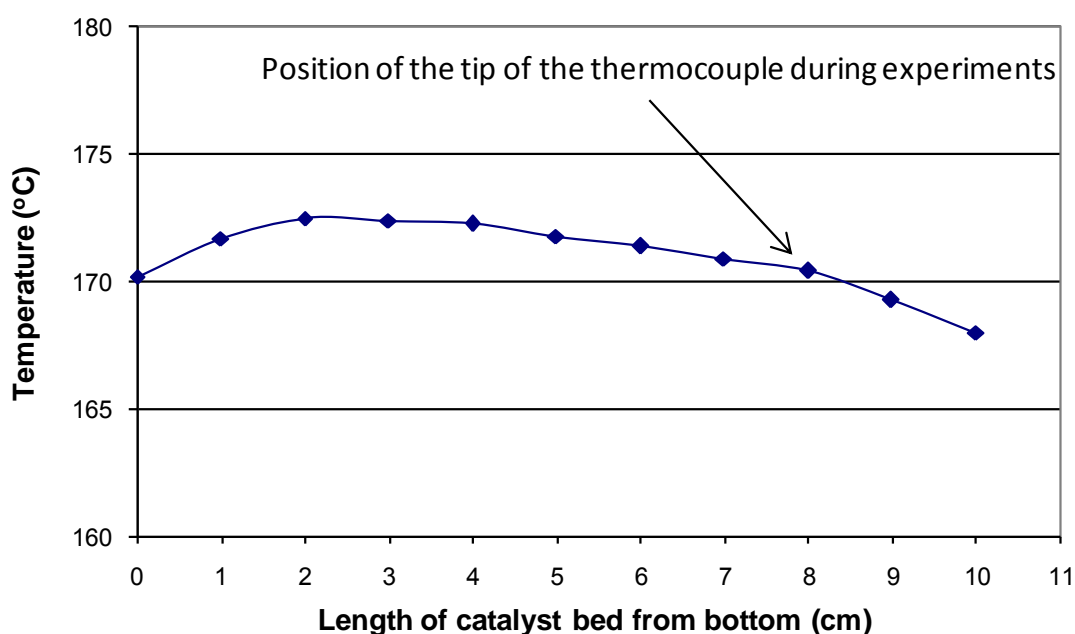


Figure 0-3: Temperature profile in the catalyst bed (measured at 170 °C of the external, reactor oven controlling thermocouple).

4.3 Experimental procedure

The H-ZSM-5 catalyst was first calcined in air (*ex-situ* in deep bed) at 500 °C (oven temperature program: oven temperature was increased at a rate of 1 °C/min from room temperature to 500 °C and was kept at this temperature

constant for 3 hours before cooling to room temperature). The amorphous silica-alumina catalyst was used without being first calcined. Both catalysts were then activated *in-situ* under flowing N₂ (to remove any moisture that might have been adsorbed during storage or after calcination) by increasing the temperature at 1 °C/min from room temperature to 250 °C and keeping this temperature constant for 2 hours before cooling to reaction temperature.

Once the reaction temperature was reached, the feed pump was started. The reactor was pressurized by first pumping the feed at a high flow rate (10 ml/min) until the reactor was filled up with feed and the desired pressure was reached. While pressurizing, the back pressure regulator (Figure 0-1) was kept closed. Then the pump was set to the desired flow rate. During this procedure, an increase of the temperature of the catalyst bed by about 50 °C was observed (caused by the compression of the nitrogen in the system). Thereafter, the temperature declined rapidly to the set reaction temperature, as soon as the liquid feed reached the position in the catalyst bed where the tip of the thermocouple was located inside the reactor's central thermowell (see Figure 4-3). Approximately 5 min were required for the thermocouple to indicate that the catalyst bed had cooled down to the set temperature. The first sample was taken after reaction temperature and pressure had stabilised at their set values.

Temperature series were carried out at 40 bar, a WHSV of 0.5 or 1.0 g/g.h and over a temperature range of typically 50 – 210 °C (see Table 5-1). To start these experiments, the reactor was filled with liquid feed at ambient temperature and, carrying the feed soaked catalyst, was pressurized to 40 bar and then heated from room temperature to 50 °C, the first reaction temperature, while

pumping feed at the set rate. The temperature was stepwise increased every 24 hours. The temperature increase was initially in 25 °C steps and later in 10 °C steps, after conversion has exceeded 50% (see e.g. Figure 5-1).

Samples at each temperature were taken hourly during the day. The operating temperature was changed at the end of the day in order to allow the temperature and the product composition to stabilize overnight before taking samples the next day.

To study the effect of pressure on 1-hexene dimerization, a continuous run was carried out where the pressure was increased in 10 bar steps from 10 to 40 bar at the fixed temperature of 170 °C and WHSV of 0.5 g/g.h. The pressure was kept constant for 24 hours before changing to the next pressure. After completing the first series, i.e. increasing stepwise from 10 to 40 bar, the pressure was taken back straight to 10 bar and again increased stepwise to 40 bar to conduct the second series.

4.3.1 Poisoning and use of poisoned H-ZSM-5 catalysts

Two different techniques were applied to deactivate the sites on the external surface of the zeolite crystals. With the first method the acid sites on the external surface of the zeolite crystals were deactivated by supplying a poisoned feed. The poisoned feed contained 0.065 g 2,4,6-collidine per 1000 g of 1-hexene, i.e. 65 ppm (wt) of this poison in the feed. The poisoned feed replaced the neat feed at the end of a “regular” dimerization experiment and was fed through the pump into the reactor loaded with the catalyst.

In another method, the H-ZSM-5 catalyst was first immersed in a mixture of 0.28 g 2,6-di-*tert*-butylpyridine dissolved in 50 g of pentane, which was a rather concentrated solution of 5600 ppm (wt). The pentane was allowed to evaporate and the poisoned catalyst was then loaded into the reactor. A poisoned feed of 65 ppm (wt) of 2,6-di-*tert*-butylpyridine in 1-hexene, prepared by adding 0.065 g of 2,6-di-*tert*-butylpyridine to 1000 g of 1-hexene, was fed according to the start-up procedure described in Section 4.3.

4.4 Product quantification and analysis

4.4.1 GC analysis and GC data evaluation

Product samples were analyzed using a gas chromatograph HP6890, with flame ionization detector (FID). A 50 m, 0.2 mm internal diameter, 0.5 μ m film thickness, Varian capillary column 190915-001 (PONA) was used for separation of compounds. Carrier gas was hydrogen at 50 ml/min with 100:1 column split ratio (50 °C). The GC oven program was as follows: Initial temperature = 50 °C, hold for 1 min, ramp at 6 °C/min to 260 °C and hold for 15 min. Typical GC traces showing the reactants and products obtained from the dimerization of 1-hexene and 1-octene over the H-ZSM-5 catalyst are shown in Figure 0-4.

For peak identification, each feed and each of the high purity standards of linear product constituents (see Table 0-1) were injected into the GC and their retention times were compared to those obtained from the reaction products. A gas chromatograph with a mass spectrometric detector (GC-MS) was used for the identification of the feed isomerization and oligomerization reaction products.

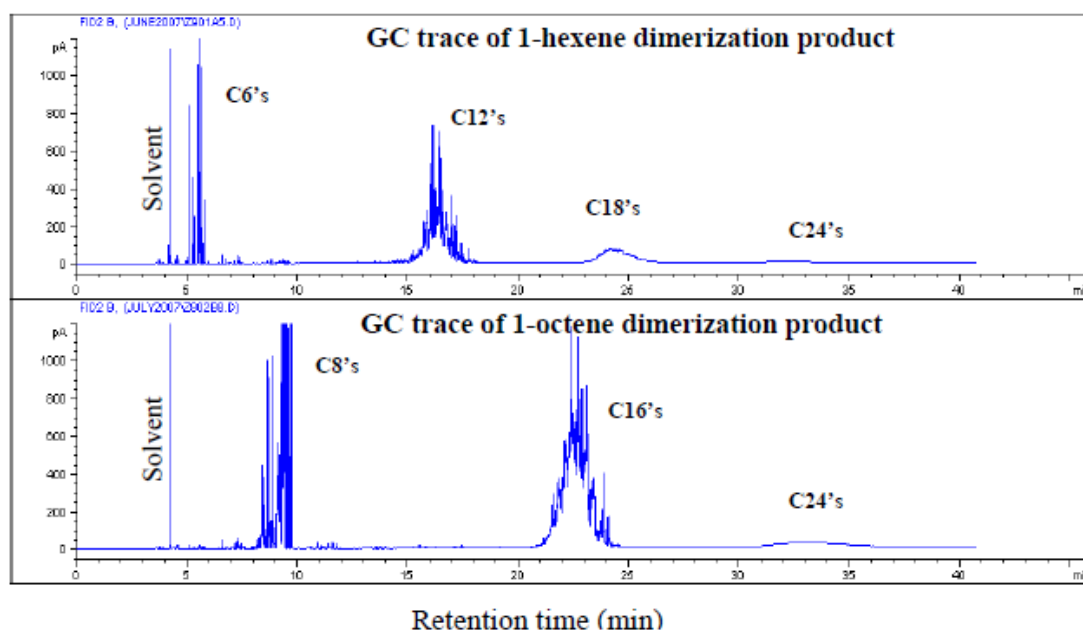


Figure 0-4: GC traces of the product mixtures obtained from the conversion of 1-hexene and 1-octene at 170 °C, 40 bar and WHSV = 0.5 g/g.h over the H-ZSM-5 catalyst. Conversions were 75% (hexene) and 50% (octene) with all $C_6^=$ and $C_8^=$ double bond isomers and skeleton isomers lumped as feed (the first peak, at about 4.2 min, is due to a trace of solvent, acetone).

Since both the feed and the products were olefins, both the carbon-specific and the mass-specific FID response factors of all components were assumed to be equal to one.

Conversion, selectivity and yield were defined as shown in the following formulae for hexene dimerization, with A = lumped peak areas (from the chromatogram report), X = conversion, S = selectivity and Y = yield. 1-Hexene and its double bond isomers and traces of skeletal isomers (iso-hexenes) were lumped together as feed “ n -hexenes”, with total peak area A_{feed} .

The feed conversion was calculated as follows:

$$X_{n\text{-hexenes}} (\text{in } \%) = \frac{A_{\text{feed-in}} - A_{\text{feed-out}}}{A_{\text{feed-in}}} \times 100 \quad (1)$$

Similarly, all peak areas of the dimers, the C₁₂ isomers in this case, were lumped together as total area A_{C12's} for the calculation of dimer selectivity (S_{C12's}) and yield (Y_{C12's}).

$$S_{C12's} (\text{in wt}\%) = \frac{A_{C12's}}{\sum (A_{C12's} + A_{\text{otherproducts}})} \times 100 \quad (2)$$

$$Y_{C12's} (\text{in wt}\%) = \frac{X_{n\text{-hexenes}} \times S_{C12's}}{100} \quad (3)$$

Selectivities and yields of trimers (S_{C18's} and Y_{C18's}) and of other products were calculated correspondingly. GC results from 1-octene conversion were evaluated analogously.

4.4.2 ¹H-NMR analysis

The C₁₂ and C₁₆ dimer fractions were analyzed for the degree of branching following an internal procedure developed for Sasol R&D.⁴

4.4.2.1 Sample preparation

In preparation for this analysis the light olefins, that is those below C₁₂ in the case of 1-hexene dimerization and those lower than C₁₆ in the case of 1-octene dimerization, were separated from the accumulated reaction products via rotavap distillation. Then the dimer fractions, C₁₂ and C₁₆ in the

case of 1-hexene and 1-octene, respectively, were distilled off from the higher oligomers. This was done individually for the product mixtures obtained at different reaction conditions applied.

The individual C₁₂ and C₁₆ olefin fractions obtained were separately hydrogenated over a Pd/C catalyst (see Table 0-1) in a 300 ml stirred autoclave reactor. The reaction was carried out at room temperature with 150 ml of liquid feed, 2.5 g of catalyst, 20 bar initial hydrogen pressure, 1000 rpm stirring rate and 2 hours reaction time, during which hydrogen consumed was replaced about four times by increasing the pressure back to 20 bar after decreasing to 5 bar.

Constancy of hydrogen pressure indicated finally that hydrogenation was complete. The low temperature was chosen in order to prevent possible skeletal isomerization of the dimers which may have flawed the results for the degree of branching.

4.4.2.2 Recording and evaluation of ¹H-NMR spectra

The resulting C₁₂ and C₁₆ paraffin samples were then analyzed by ¹H-NMR (Varian Unity Spectrometer 400 MHz instrument). For this purpose, the samples were dissolved in deuterated chloroform, CDCl₃, and a ¹H-NMR spectrum was recorded.⁴ A representative spectrum of a C₁₂ paraffin sample analyzed by ¹H-NMR is shown in Figure 0-5.

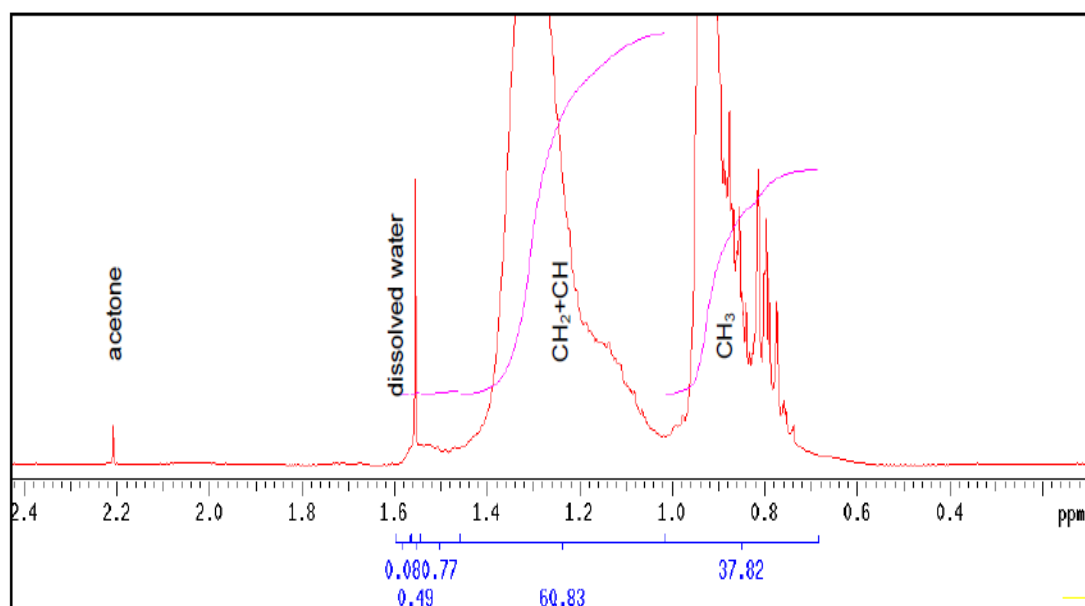


Figure 0-5: ^1H -NMR spectrum of the C_{12} paraffin sample obtained from hydrogenating the C_{12} product from 1-hexene dimerization over the H-ZSM-5 catalyst at $170\text{ }^\circ\text{C}$, 40 bar and WHSV of 0.5 g/g.h. (Acetone is a trace that was left in the NMR tube after washing, whilst the water was dissolved in the deuterated solvent, chloroform- d_3 .)

CH_3 protons resonate at a chemical shift of around $0.8 - 0.9$. The CH_2 and CH protons resonate at a chemical shift of about $1.0 - 1.5$, but cannot be separated from each other.

The spectrum was integrated. The integrals ranged from a chemical shift of $0.4 - 0.95$ (CH_3 protons) and $0.95 - 1.5$ ($\text{CH}_2 + \text{CH}$ protons). Signals of trace amounts of aromatics and olefins (due to incomplete hydrogenation) were ignored. The sum of the integrals was set to 100. The percentages of $\text{CH} + \text{CH}_2$ protons and CH_3 protons could then be read directly from the spectrum.

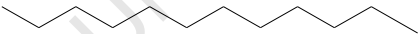
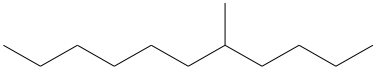
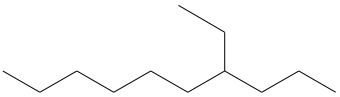
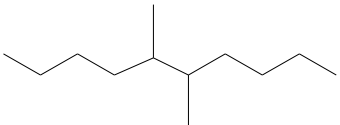
The ratio of $\text{CH}_3\text{:CH}_2\text{:CH}$ groups was calculated as follows:

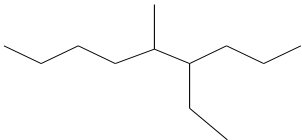
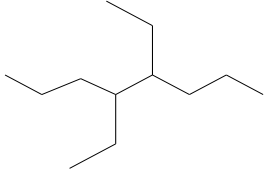
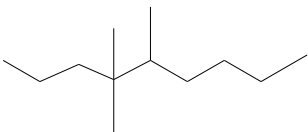
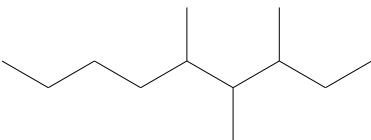
- a) The number of protons per molecule is 26 for the hydrogenated hexene dimers ($\text{C}_{12}\text{H}_{26}$) and 34 for the hydrogenated octene dimers ($\text{C}_{16}\text{H}_{34}$).
- b) The integrals of the CH_3 and $\text{CH}_2\text{+CH}$ proton signals (in percent) are taken from the ^1H -NMR spectrum.
- c) These two percentages are normalized to the numbers calculated in a), (26 or 34), so that the average numbers of CH_3 and $\text{CH}_2\text{+CH}$ protons per molecule in the dimer fractions result.
- d) The average number of branches is then calculated as follows:
 - The carbon chain of a straight chain paraffinic molecule has two terminal methyl groups. This corresponds to $2 \times 3 = 6$ CH_3 protons.
 - The said protons represent 6 out of 26 protons in the hydrogenated hexene dimers (C_{12} paraffins) and 6 out of 34 protons in the hydrogenated octene dimers (C_{16} paraffins).
 - All additional CH_3 protons originate from branching.
 - The average number of branches per molecule is then the number of additional CH_3 protons divided by 3 or the number of all CH_3 protons minus 6 and then divided by 3.
- e) From the above the following can also be determined:
 - Average number of CH groups = average number of branches (ignoring “neo” structures that may be present).
 - Average number of CH_3 groups = 2 + no of branches
 - Average number of CH_2 groups = carbon number of paraffin fraction (12 or 16) – average number of CH_3 groups – average number of CH groups.

In order to ascertain the extent of branching in the hydrogenated C₁₂ dimer fraction and to relate it to the reaction mechanism, a simple calculation reveals the expected percentage of protons of each type in each of the C₁₂ paraffin isomers that can be expected from *n*-hexenes dimerization after hydrogenation (see Table 0-2).

It should be noted that only the average number of branches, not their length (methyl-, ethyl-) or positions can be determined by ¹H-NMR. That is, this method does not allow to distinguish between products B and C (in Table 0-2) and not between products D, E and F, but allows (theoretically, if it was a pure compound) to identify quaternary carbon atoms as in product G (compared to product H).

Table 0-2: Percentages of protons present as CH₃, CH₂ and CH (normalized) in the hydrogenated dimers from *n*-hexenes.

All possible C ₁₂ isomers from <i>n</i> -hexene dimerization (hydrogenated)		Expected percentage of protons		
		Type of H	Number of H	Normalized %
(A)		CH ₃ protons	6	23.08
		CH ₂ protons	20	76.92
		CH protons	0	0.00
		Total	26	100.00
(B)		CH ₃ protons	9	34.62
		CH ₂ protons	16	61.54
		CH protons	1	3.85
		Total	26	100.00
(C)		CH ₃ protons	9	34.62
		CH ₂ protons	16	61.54
		CH protons	1	3.85
		Total	26	100.00
(D)		CH ₃ protons	12	46.15
		CH ₂ protons	12	46.15
		CH protons	2	7.69
		Total	26	100.00

All possible C ₁₂ isomers from <i>n</i> -hexene dimerization (hydrogenated)	Expected percentage of protons		
	Type of H	Number of H	Normalized %
 (E)	CH ₃ protons	12	46.15
	CH ₂ protons	12	46.15
	CH protons	2	7.69
	Total	26	100.00
 (F)	CH ₃ protons	12	46.15
	CH ₂ protons	12	46.15
	CH protons	2	7.69
	Total	26	100.00
Examples of possible C ₁₂ isomers from adding <i>n</i> -hexene and iso-hexene (mono-methyl pentene) molecules (hydrogenated)		Expected percentage of protons	
 (G)	CH ₃ protons	15	57.69
	CH ₂ protons	10	38.46
	CH protons	1	3.85
	Total	26	100.00
 (H)	CH ₃ protons	15	57.69
	CH ₂ protons	8	30.77
	CH protons	3	11.54
	Total	26	100.00

With x = percentage of CH₃ protons in the ¹H-NMR spectrum, and 23.08 the percentage of CH₃ protons in a linear C₁₂ paraffin, see row (A) in Table 0-2, it follows for the hydrogenated 1-hexene dimerization product:

$$\text{Average number of branches} = \frac{x - 23.08}{23.08 / 2} = 2 \left(\frac{x}{23.08} - 1 \right)$$

The procedure corresponds to the method developed for and used by Sasol.⁴

Analogously for the 1-octene dimerization product:

$$\text{Average number of branches} = \frac{x - 17.65}{17.65 / 2} = 2 \left(\frac{x}{17.65} - 1 \right)$$

The dimerization product at extremely low conversion, i.e. when hardly any double bond isomerization of the 1-hexene (or 1-octene) had occurred yet, will have formed from the 1-olefin (by then still the dominating constituent of the

reaction mixture) and corresponding secondary (β -) carbenium ion, according to the first example shown in Figure 2-5. The product from dimerizing the (non-double-bond-isomerized) 1-hexene molecules is shown in row (B) in Table 0-2. This product will be mono-branched and will show a 9:17 ratio of CH_3 and CH_2 plus CH protons in the ^1H -NMR spectrum, and an average number of branching of 1.0 will follow according to the equation given above.

The double bond isomerized feed consists mostly of *n*-olefins with internal double bonds (see Table 5-2 in the following chapter for exact percentages). According to examples three to six shown in Figure 2-5, double-branched dimers will have formed that eventually result in the products shown in rows (D) to (F) in Table 4-2. These products will show a 12:14 ratio of signals of CH_3 to CH_2 plus CH protons in the ^1H -NMR spectrum and an average number of branching of 2.0 will follow.

4.4.3 Analysis of fuel properties

The C_{16} paraffin fractions obtained from 1-octene dimerization at different reaction conditions and after hydrogenation were evaluated for their properties as diesel fuels at Sasol Technology's Fuels Research Laboratory. The octene dimerization product was chosen, since it (as a C_{16} fraction) is more representative for diesel than the hexene dimerization product (C_{12}). The properties of the paraffin samples were analyzed using the American Society for Testing and Materials (ASTM) methods (see Table 4-3). Details are given in Table 4-3.

Table 0-3: Fuel properties tested and definitions^{6,7,8}

Property	Test Method	Definition	Required in South Africa (SANS 342) ⁶
Flow		As a fuel is cooled its viscosity increases and it eventually reaches a temperature at which it is no longer able to flow readily and/or dissolve all of the waxy constituents, which then begin to precipitate out of solution.	
Viscosity @ 40 kin (cSt)	ASTM D445 ⁹	Viscosity is a measure of the resistive flow of a fluid through a calibrated capillary glass viscometer tube under the influence of gravity and is measured at a specific temperature. cSt @ 40 stands for the kinematic viscosity measured in centistokes at 40 °C. “Thin” liquids, like water or gasoline, have low viscosities; “thick” liquids, like syrup or motor oil, have high viscosities. The viscosity of a liquid increases as its temperature decreases. If fuel viscosity is outside the specification range, combustion may be poor, resulting in loss of power and fuel economy.	Min: 2.2 cSt Max: 5.3 cSt
Cold Filter Plugging Point (°C)	IP 309 ¹⁰	The Cold Filter Plugging Point (CFPP) refers to the highest temperature (when the sample is cooled at 40 °C per hour) at which 20 ml of the fuel fails to pass through a 45-micron wire mesh, sucked by 2 kPa (0.02 bar) vacuum, in less than 60 seconds. Cold flow improving additives lower the cold filter plugging point by changing the size and shape of wax crystals that form at cold temperatures, but do not change the cloud point.	Winter: -4 °C Summer: 3 °C

Property	Test Method	Definition	Required in South Africa (SANS 342) ⁶
Pour Point (°C)	ASTM D97 ¹¹	The pour point is the lowest temperature at which sample movement is observed when the sample container is tilted, after the sample was heated and cooled at a specific rate and observed at intervals of 3 °C. The temperature is approximately 3 to 5 °C below the cloud point (for fuels that do not contain a pour point depressant additive), when the fuel becomes so thick that it will no longer flow or freeze.	Not specified in SA (irrelevant, since SA is a warm country)
Cloud Point (°C)	ASTM D2500 ¹²	The cloud point is the temperature at which the wax just begins to precipitate and the fuel becomes cloudy. Operating at temperature lower than the cloud point will cause wax crystals to be removed by the filter and ultimately cause the filter to block.	Not specified in SA (irrelevant, since SA is a warm country)
Density @ 15 °C (g/ml)	ASTM D4052 ¹³	Density is the mass of a unit volume of material (fuel) at a specific temperature. Fuel density affects the energy content of the fuel brought into the engine at a given injector setting.	Min: 0.8000 g/ml
Cetane number	ASTM 613 ¹⁴	The Cetane number (CN) is a measure of the ignition quality of diesel fuel based on the ignition delay in a diesel engine. A fuel with a high cetane number starts to burn shortly after it is injected into the cylinder; it has a short ignition delay period. Conversely, a fuel with a low cetane number resists auto ignition and has a longer ignition delay period. The cetane number of a diesel fuel is measured using a specific standard test engine.	Min: 45

4.5 References

- ¹ J.C.Q. Fletcher, Centre for Catalysis Research, Department of Chemical Engineering, University of Cape Town, personal communication (2007).
- ² S. Nagooroo, MSc Thesis, Department of Chemical Engineering, University of Cape Town (2011).
- ³ J. Pérez-Ramírez, R.J. Berger, G. Mul, F. Kapteijn, J.A. Moulijn, *Catal. Today*, 60 (2000) 93-109.
- ⁴ M. Kirk, "Internal method for determining branching", developed for Sasol Technology R&D (Pty) Ltd., (2003) (unpublished).
- ⁵ R. M. Silverstein, G. C. Bassler, T.C. Morrill, "Spectrometric Identification of Organic Compounds", 5th Ed., John Wiley & Sons, New York, Inc., (1991) 220-221.
- ⁶ South African Bureau of Standards, www.stansa.co.za (SANS 342, Edition 4 (2006) 1-10), accessed 2011-01-10.
- ⁷ J. Bacha, L. Blondis, J. Freel, G. Hemighaus, K. Hoekman, N. Hogue, J. Horn, D. Lesnini, C. McDonald, M. Nikanjam, E. Olsen, B. Scott, M. Sztenderowicz, "Diesel Fuels Technical Review (FTR-2)", Chevron Products Company, Chevron Inc., U.S.A., (1998) 1-70.
- ⁸ South African National Standards, www.sapia.co.za (Petrol and Diesel in South Africa and the impact on air Quality – November 2008), accessed 2010-01-02.
- ⁹ American Society for Testing and Materials, ASTM D445, standard test method for determination of kinematic viscosity (2010).
- ¹⁰ International Petroleum, IP 309, standard test method for determination of cold filter plugging point (1999).

-
- ¹¹ American Society for Testing and Materials, ASTM D97, standard test method for determination of pour point (2009).
- ¹² American Society for Testing and Materials, ASTM D2500, standard test method for determination of cloud point (2009).
- ¹³ American Society for Testing and Materials, ASTM D4052, standard test method for determination of density (2009).
- ¹⁴ American Society for Testing and Materials, ASTM D613, standard test method for determination of cetane number (2010).

University of Cape Town

CHAPTER 5

5. RESULTS

A list of the experiments performed in this project is given in Table 5-1.

Table 5-1: Experiments conducted in this project (“-” indicates a series carried out within one experimental run over the same charge of catalyst; “,” indicates individual experimental runs with fresh catalyst each)

Purpose of experiment	Reaction conditions		
	Temperature (°C)	Pressure (bar)	WHSV (g/g.h)
Dimerization of 1-hexene over H-ZSM-5			
Determination of the “optimum” operating conditions (volcano curve experiments).	50-210	40	0.5
Start-up effects and experimental reproducibility of dimerization experiments.	170	40	0.5
Effect of time-on-stream on catalyst activity and deactivation.	170	10-20, 40	0.5
Effect of temperature.	150, 160, 170	40	0.5
Effect of pressure.	170	10-40	0.5
Effect of space velocity.	170	40	0.15-3.0
Effect of poisoning of the external surface of the H-ZSM-5 zeolite crystallites with 2,4,6-collidine.	170	40	0.5
Effect of poisoning of the external surface of the H-ZSM-5 zeolite crystallites with 2,6-di- <i>tert</i> -butylpyridine.	170	40	0.5
Dimerization of 1-octene over H-ZSM-5			
Determination of the “optimum” operating conditions (volcano curve experiments).	100-210	40	1.0
Effect of time-on-stream on catalyst activity.	170	40	0.25
Effect of space velocity.	170	40	0.25-2.0

Purpose of experiment	Reaction conditions		
	Temperature (°C)	Pressure (bar)	WHSV (g/g.h)
Dimerization of 1-hexene over amorphous silica-alumina (ASA)			
Determination of the “optimum” operating conditions (volcano curve experiments).	50-210	40	0.5
Effect of time-on-stream on catalyst activity and deactivation.	150	40	0.5
Dimerization of 1-octene over amorphous silica-alumina (ASA)			
Determination of the “optimum” operating conditions (volcano curve experiments).	150-210	40	0.5
Effect of time-on-stream on catalyst activity and deactivation.	150	40	0.5

5.1 Dimerization of 1-hexene over H-ZSM-5 catalyst

1-Hexene (see Table 4-1) was used as a model compound for the dimerization reaction carried out over medium-pore zeolite catalyst H-ZSM-5. Since the fed 1-olefin undergoes double bond isomerization very rapidly (see Section 2.3.2.1 and Figure 2-19), Aspen Plus 2006¹ (software suitable to simulate equilibrium data of reaction systems under given conditions) was used to predict the equilibrium double-bond isomer distribution of the isomerized feed. A condition of 170 °C and 40 bar (liquid phase) was used for the prediction of the *n*-hexene isomers liquid phase equilibrium data, which corresponds to the “optimum” reaction condition defined after the initial experiments (see Sections 5.1.1 and 5.1.2). The results are shown in Table 5-2.

All product samples showed a similar pattern of the major peaks in the C₆-group upon gas chromatographic analysis, regardless of the extent of oligomerization. The distribution reflected the data given in Table 5-2,

indicating rapid double bond isomerization, also observed by others² (see Section 2.3.1.2 and Figure 2-18).

Table 5-2: Simulated equilibrium isomer distribution of *n*-hexenes at 170 °C and 40 bar (liquid phase) (by Aspen Plus 2006¹)

Equilibrated <i>n</i> -hexene feed (mol%)	
1-Hexene	3.1
<i>trans</i> -2-Hexene	42.6
<i>cis</i> -2-Hexene	20.2
<i>trans</i> -3-Hexene	27.1
<i>cis</i> -3-Hexene	6.9

Conversion was, therefore, defined as C₆= conversion, considering all C₆ compounds as reactants (virtually the 1-hexene and all of the linear and the small percentage of branched C₆ olefins that formed), see eq. 1 in Section 4.4.1. Non-C₆ compounds are considered as products. It should be noted that the content of 1-olefin in the equilibrium mixture (the isomer that reacts to single branched dimers, see first and second example in Figure 2-5), is only 3 mol%.

5.1.1 Searching “optimum” reaction temperature

In order to establish the “optimum” operating conditions for 1-hexene dimerization, at first a “volcano curve” experiment was conducted. The aim of this experiment was to establish the “optimum” operating temperature or temperature range where there is high conversion of the hexenes and high yield of dimers and trimers, but still minimal by-product formation, i.e. both high conversion and high selectivity to the desired product.

The term “volcano” refers to the yield as a function of a varied parameter, here the reaction temperature, where increasing temperature at first results in an increase of yield due to the increase in conversion, but in the high temperature range, despite the conversion being high or still increasing, the yield decreases with increasing temperature due to the formation of more and more by-products. It is known that over H-ZSM-5 at temperatures above 200 °C, a complex product spectrum is obtained due to olefin interconversion reactions taking place, i.e. cracking, skeletal isomerization, and H-transfer reactions, see Section 2.1.2.1.2. “Optimum” is then the “summit” of the volcano (maximum yield) or, for a possible industrial application, most likely a range a little before the “summit” with somewhat lower conversion but less by-product formation.

The volcano curve experiment for 1-hexene conversion over H-ZSM-5 was conducted up to 210 °C and the results are shown in Figure 5-1. The results show that maximum conversion of $C_6=$ (> 90 wt%) was at 200 °C and maximum yield of dimers at 180 – 200 °C. As can be seen in Figure 5-1, at temperatures higher than 150 °C there was a significant increase in the formation to other products, mainly “lights” (C_4 - C_{11}). “Lights” in the context of this study are defined as all products with carbon numbers below the carbon number of the dimer, here C_{12} (but $\neq C_6$).

GC-MS analysis of the reaction product at 200 °C showed compounds that resulted from cracking, skeletal isomerization, and H-transfer reactions. These compounds included all the olefinic and paraffinic C_4 - and C_5 -compounds and also the paraffinic C_6 -compounds (that is the C_6 fraction except the C_6 -olefins) and a number of, mostly branched, olefinic C_7 - C_{11} compounds. However,

despite obtaining some paraffins, the co-products of the responsible H-transfer reactions, namely aromatic compounds, could not be found (by GC and GC-MS using PONA column, see Section 4.4.1).

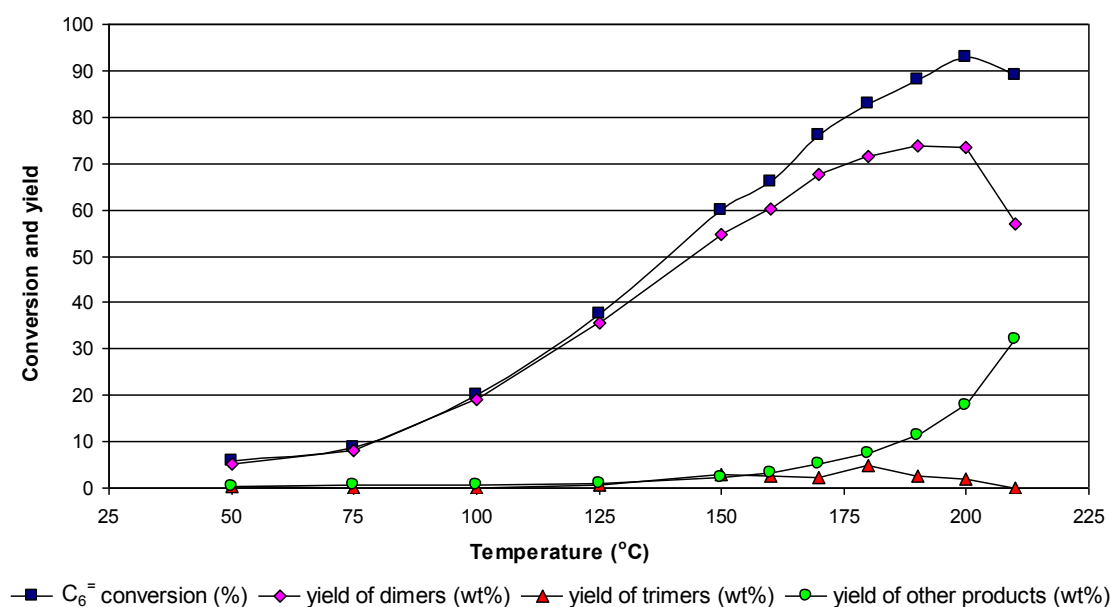


Figure 5-1: Volcano curve from 1-hexene dimerization (H-ZSM-5 catalyst, 40 bar and WHSV of 0.5 g/g.h, see Section 4.3 for the detailed procedure). “Other products” are essentially “lights” (C₄-C₁₁). “Lights” in this context are products with carbon numbers lower than that of the dimer (except C₆).

The results indicate that the “optimum” temperature range for 1-hexene dimerization at the chosen pressure of 40 bar and WHSV of 0.5 g/g.h appears to be around 150 - 170 °C. At these temperatures, the C₆= conversion is in the range of 60 - 75 %. The yield of dimers is below the maximum, but there is little by-product formation and the selectivity of dimers is, as can be derived from Figure 5-1, above 90 wt%. At the “optimum” temperature, yields and selectivities of diesel-range products, that is the combined dimer and trimer fractions, are almost as high as conversion, namely 70% and 90%, respectively, as can be derived from Figure 5-1.

5.1.2 Start-up effects and replication of experiments

Replicate experiments were conducted in order to evaluate the experimental repeatability of the 1-hexene dimerization reaction. The replicate experiment, shown in Figure 5-2 together with the corresponding first experiment, was conducted at the chosen “optimum” reaction conditions (of 170 °C, 40 bar and WHSV of 0.5 g/g.h). The replicate experiment was carried out over a fresh charge of catalyst.

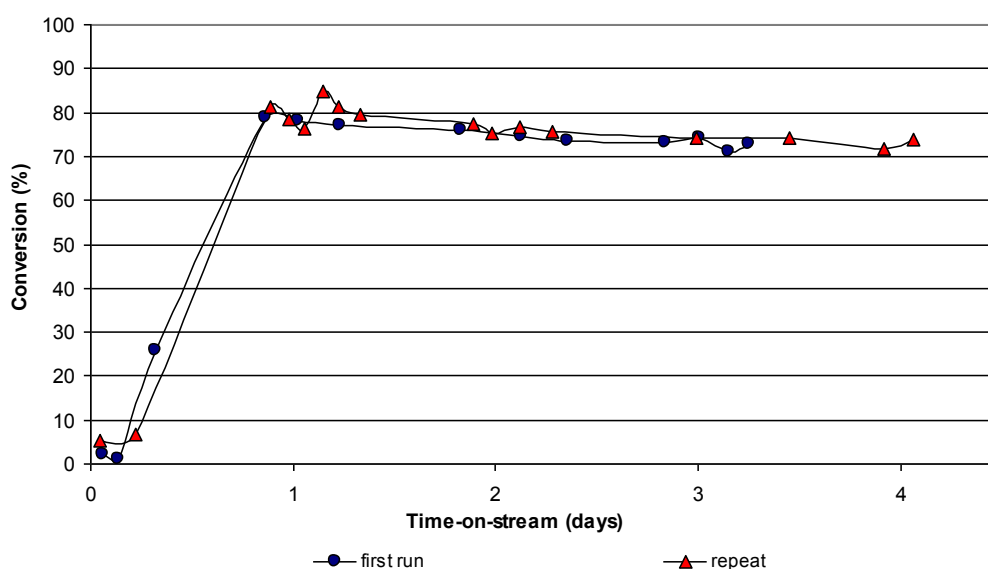


Figure 5-2: Repeatability of 1-hexene conversion in dimerization experiments (H-ZSM-5 catalyst, 170 °C, 40 bar and WHSV of 0.5 g/g.h). It should be noted that the initial increase is not an induction period, but caused by the experimental procedure (see text below).

Conversions and also dimer and trimer selectivities and trends (slow deactivation) in both experiments were equal. It is apparent that the experimental repeatability is acceptable ($\pm 2\%$ deviation in quasi steady state operation).

The seemingly low conversion at the beginning of the run shown in Figure 5-2, followed by a steep increase to quasi-steady state conversion is not indicating an induction period, but is due to (i) the hold-up of the liquid feed and product between the catalyst bed and the sampling point and (ii) the back mixing in these lines and the product catch pot, since the reactor was primed and filled with liquid feed before start up (see Section 4.3). At a WHSV of 0.5 g/g.h this results in actually 1 day of delay (see Figure 5-2). (Other such initial delays are, for instance, shown in Figures 5-3 to 5-5 further down.)

5.1.3 Catalyst activity and deactivation as a function of time-on-stream

In previous work on 1-hexene dimerization³ it was reported that, at 170 °C, there was catalyst deactivation at 20 bar but not at 40 bar. This is questionable since at 170 °C the reaction system is in the liquid phase at both the pressures and no difference should result. Other authors^{4,5,6,7,8} also reported slow deactivation of zeolite catalysts on olefin oligomerization duty. In order to investigate this, the activity of the H-ZSM-5 catalyst was evaluated as a function of time-on-stream at a number of different reaction conditions.

Figures 5-2 to 5-5 and 5-7 indicate that the conversion, i.e. catalyst activity, declines slowly but constantly with time-on-stream under all of the reaction conditions applied (150 - 170 °C, 10 - 40 bar and 0.15 - 2.0 g/g.h). In addition to the previous study³, where runs were short or conditions changed during the runs frequently, in one of the experiments carried out within this study, the reaction was allowed to continue at 170 °C, 40 bar and WHSV of 0.5 g/g.h for

a total of 48 days on-stream without any change of conditions in order to evaluate the activity of the catalyst, undisturbed, over an extended period of time, see Figure 5-3.

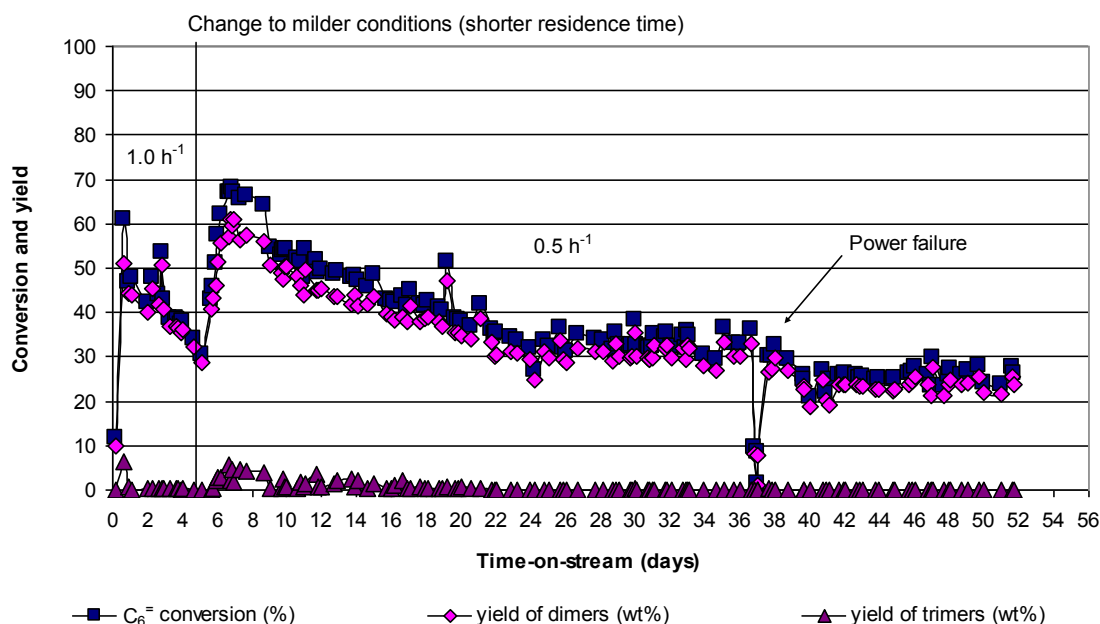


Figure 5-3: Performance of the H-ZSM-5 catalyst over a prolonged time on stream at 170 °C, 40 bar and WHSV of 0.5 g/g.h. Space velocity was 1.0 g/g.h initially, but was halved after 4 days on stream to make the long-term run decline in activity occur on higher level and be more obvious. It should be noted that the “zero” yield in trimers during most of the run is an analytical error, since the “hump” of trimers that appeared in the gas chromatograms of the low conversion products (see Figure 4-4) was too flat and small for integration.

It can be observed that conversion declined by about one third during the first 24 days on stream but became almost stable at around 35% after 24 days on stream. A power failure was experienced on the 36th day on stream (see Figure 5-3). The power failure caused the feed pump to stop and the reaction

pressure to drop to just above 1 bar, but the reactor temperature was only slowly decreasing. When the power was restored, after about 20 hours, the reaction was allowed to continue. As a result of this power failure, conversion dropped again but reached another plateau within a day (with the 1 day reflecting the hold-up and the backmixing in the experimental apparatus, i.e. still the “old” pre-power-failure product influencing the results analogous to the “start-up” effect described in Section 5.1.2). Conversion settled at an average level of 25% in the following period on stream.

The reaction product that was obtained during the first day on-stream after the power failure turned yellow in colour as compared to the normally colourless product, indicating the formation and deposition of heavy compounds (coke precursors) on the catalyst during the period of no-flow at elevated temperature (see above). Colourless liquids were only obtained again a day after the flow of 1-hexene was restored. The catalyst extrudates discharged after this extended time-on-stream were creamy in colour.

It was concluded from these observations of rather high catalyst stability that, in order to identify the most significant trends and effects of reaction conditions, it was sufficient to run most of the experiments (e.g. for the variation of WHSV) over the same charge of catalyst (see Table 5-1). Catalyst was replaced only for running the next experiment (see Table 5-1).

When operating at 20 bar (170 °C) the deactivation pattern was similar, see Figure 5-4.

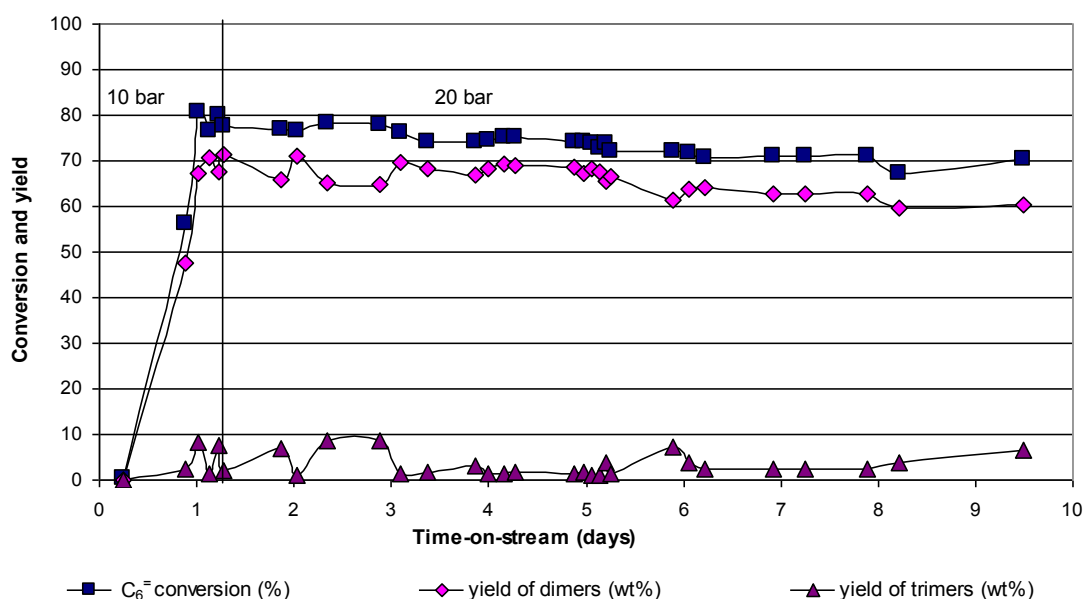


Figure 5-4: 1-Hexene dimerization conversion and major product yields at pressures of initially 10 bar and after switch to 20 bar after 32 hours on stream (H-ZSM-5 catalyst, 170 °C and WHSV of 0.5 g/g.h).

5.1.4 Effect of temperature on catalyst activity, catalyst deactivation and product branching

The effect of temperature on the dimerization of 1-hexene was investigated in the optimum temperature region (see Section 5.1.1) of 150 - 170 °C. Catalyst activity was determined as a function of time-on-stream. Fresh catalyst was loaded for each reaction temperature run and the results thereof are given in Figure 5-5.

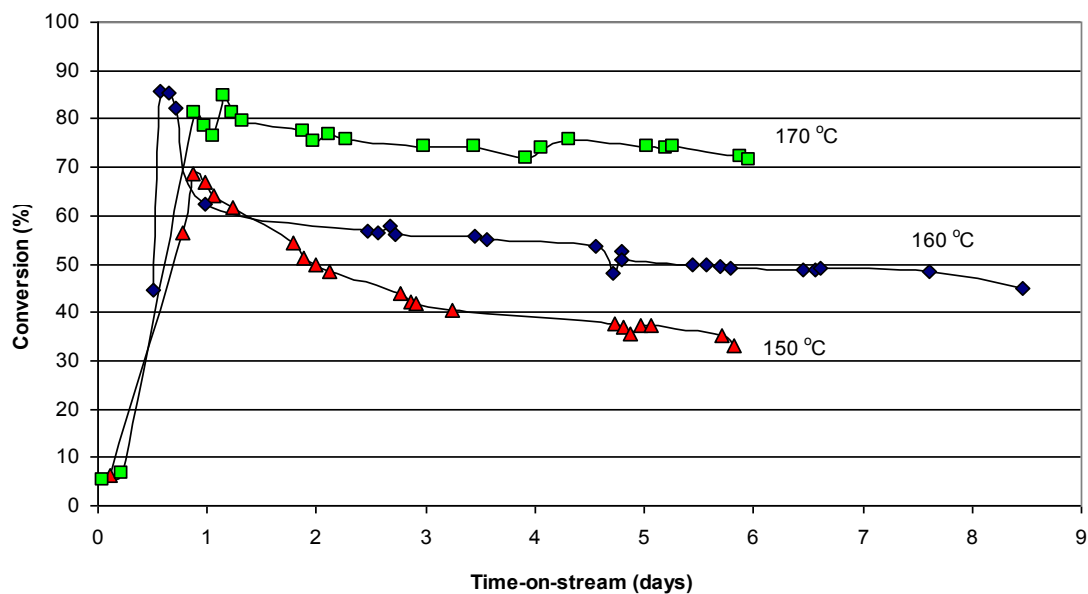


Figure 5-5: Effect of temperature on $C_6=$ conversion in 1-hexene dimerization experiments in the “optimum” temperature region of 150 - 170 °C (H-ZSM-5 catalyst, 40 bar and WHSV of 0.5 g/g.h).

While, in general, slow decrease in conversion with increasing time-on-stream (see Section 5.1.3) can be seen in all three experiments, 1-hexene dimerization at 150 and 160 °C showed a drastic decline in conversion within the first 2-3 days. This was not observed with the experiment conducted at 170 °C, which gave a rather stable conversion of around 75-80% from day one onwards. However, samples taken during day 1 represent still some start-up effects, as aforementioned (Section 5.1.2). The extent of deactivation during the 170 °C run may have been camouflaged, since at the rather high conversion of around 75-80% (see Figure 5-5) a certain loss of activity does not show as pronounced as at around 50% conversion (150 °C run). The long term run (50 days, see Figure 5-3) showed indeed, that constant deactivation also occurred at 170 °C.

Nevertheless, the results appear to indicate that operating at lower temperatures of 150 - 160 °C leads to more rapid deactivation (presumably due to blockage of the crystal surface, the pores or the active sites by higher oligomers and other heavy compounds, which are unable to readily desorb at these low temperatures as observed by others,^{4,5,6,7,8} (see Section 2.3.1.5). It can be concluded that 170 °C (instead of 150 or 160 °C) not only gives “best” conversion and selectivity (see Section 5.1.1), but also results in higher stability of the catalyst. It should be noted that the catalysts, after the end of the experiments at 150 - 170 °C and about 7 days on stream, had a similar creamy colour, indicative of a non-coked catalyst.

In Figure 5-5 only conversions are shown. The dimer and trimer selectivities in all three experiments were in the range of 85 - 95 wt% and 1.0 - 5.0 wt%, respectively, such as shown in Figure 5-2 for the 170 °C experiment during the 5 - 20 days on-stream period.

In order to determine the average degree of branching per molecule in the samples obtained at the different reaction temperatures, ¹H-NMR studies were conducted of the hydrogenated C₁₂ fractions, as described in Section 4.4.2. The results are given in Table 5-3.

It can be seen from Table 5-3 that there was an increase in branching per molecule with increasing temperature. However, it should be noted that conversions also increased significantly with temperature.

Table 5-3: Average degree of branching ($^1\text{H-NMR}$ results) of the C_{12} paraffin samples obtained from combining and hydrogenating all of the 1-hexene dimerization product samples collected at 150, 160 and 170 $^{\circ}\text{C}$ (H-ZSM-5 catalyst, 40 bar and WHSV of 0.5 g/g.h, see Figure 5-5).

Temperature ($^{\circ}\text{C}$)	Average conversion (%)	Average degree of branching per molecule
150	45	2.04
160	56	2.14
170	75	2.33

5.1.5 Effect of pressure on catalyst activity and selectivity

The effect of pressure is shown in Figure 5-6 and Table 5-4, respectively.

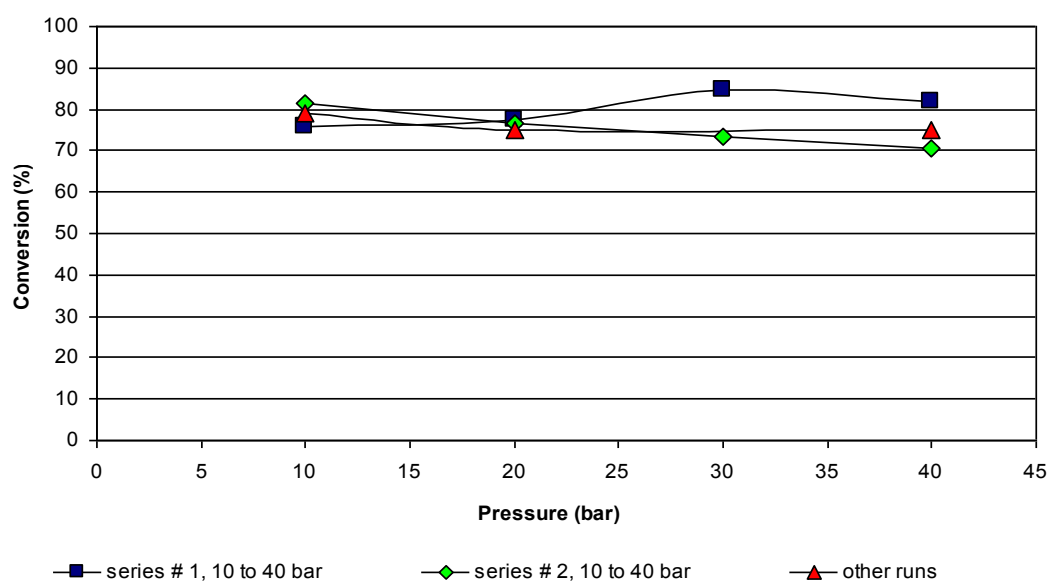


Figure 5-6: Effect of pressure on $\text{C}_6=$ conversion in 1-hexene dimerization experiments (H-ZSM-5 catalyst, 170 $^{\circ}\text{C}$ and WHSV of 0.5 g/g.h, see Section 4.3 for the detailed procedure). Series # 2 is a replicate of series # 1. Triangular data points are the averages taken from data given in Figure 5-4 (10 and 20 bar) and Figure 5-2 (40 bar).

It should be noted that under the reaction conditions applied, the reaction mixture was in the liquid phase. At 10 bar the boiling point of 1-hexene (155 °C)¹ is slightly lower than the reaction temperature of 170 °C. However, the first intermediates forming are *n*-C₆ olefins other than the 1-olefin used as the starting material. These boil somewhat higher than the 1-isomer. The final product is the dimer. The reaction mixture in the pores at 10 bar can, therefore, also be expected to be a liquid. The results obtained at 10 bar, see Figure 5-6, do not differ from the results obtained at the higher pressures.

Yields of dimers and selectivities of dimers and trimers are given in Table 5-4.

Table 5-4: Effect of pressure on 1-hexene dimerization during repeat pressure series (H-ZSM-5 catalyst, 170 °C and WHSV of 0.5 g/g.h)

Pressure (bar)	Time-on-stream (days)	Conversion (%)	Selectivity of dimers (wt%)	Selectivity of trimers (wt%)	Yield of dimers (wt%)
Series # 1					
10	3	77	92	6	70
20	4	79	83	5	65
30	5	85	81	6	69
40	6	84	88	10	74
Series # 2					
10	7	83	84	4	70
20	8	78	83	8	65
30	9	74	92	2	68
40	10	74	87	8	64
Other runs					
10	1	79	89	6	63
20	8	75	89	4	63
40	9	75	89	2	66

Branching of some of the olefins in C₁₂ fractions from pressure series (determined after hydrogenation) was analyzed by ¹H-NMR. As found earlier for other 170 °C samples from 75 - 80% conversion products, the degrees of branching were, constantly, around 2.3. The experiments show that pressure has no effect on the performance of the catalyst, i.e. conversion, carbon number selectivity and branching (as determined by ¹H-NMR). However, this may hold only as long as the reaction mixture is in the liquid phase.

5.1.6 Effect of space velocity on catalyst activity, catalyst deactivation and product branching

Further catalytic reactions were performed at 170 °C and 40 bar varying weight hourly space velocity in the range of 0.15 - 3.0 g/g.h. In addition to the long term run under constant conditions (see Figure 5-3) the outcome of this experiment did also indicate towards the rather high stability of the catalyst with time-on-stream.

The curve of conversion versus time-on-stream at the different weight hourly space velocities is shown in Figure 5-7. It was observed that 1-hexene conversion increased with decreasing space velocity, and so did the yields of dimers and, in particular, trimers. However, at the lowermost space velocity applied, at conversions around 80%, “lights” (cracking products < C₁₂, the carbon number of the dimer) yielded more than 10% (not explicitly shown).

The space velocity series was accompanied by a constant slight decline in conversion, i.e. catalyst activity. In order to complete the evaluation of space

velocity effects on 1-hexene dimerization, a second set of experiments, given as set # 2 in Table 5-5 (set # 1 was derived from Figure 5-7) was conducted at WHSV between 0.5 and 3.0 g/g.h, 170 °C and 40 bar with a fresh charge of catalyst. The C₁₂ fractions produced at each of the different space velocities during both the runs were distilled off, hydrogenated and analyzed by ¹H-NMR to analyze for branching in the products formed. The results are given in Table 5-5.

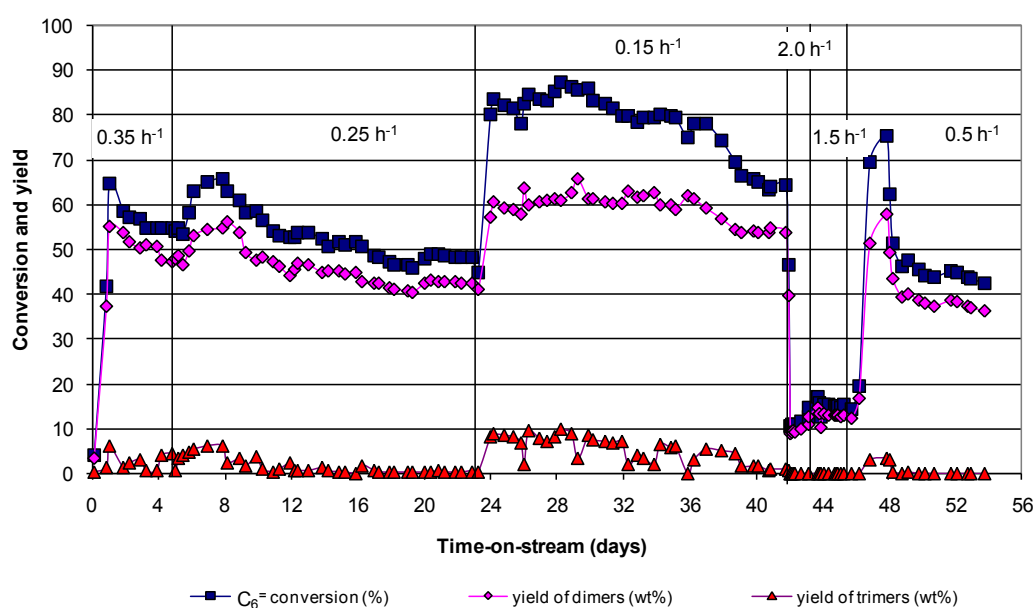


Figure 5-7: Effect of WHSV in the range of 0.15 - 2.0 g/g.h on conversion and major product yields (H-ZSM-5 catalyst, 170 °C and 40 bar). “Zero” yield of trimers means that only small amounts were formed, which could not be quantified. It should be noted that, due to the start-up effects (see Section 5.1.2), caused by backmixing and product hold-up in the experimental apparatus, the system responded with delay on changes of conditions (a day or more).

As can be seen in Table 5-5, the degree of branching per molecule decreased with increasing space velocity and decreasing conversion.

Table 5-5: Average degree of branching (by $^1\text{H-NMR}$) in the distilled-off and hydrogenated C_{12} fractions from two 1-hexene dimerization runs (H-ZSM-5 catalyst, $170\text{ }^\circ\text{C}$, 40 bar and WHSV between 0.15 - 3.0 g/g.h).

WHSV (g/g.h)	First experiment * (steady state data only)			Repeat experiment (steady state data only)		
	Average time-on-stream (days)	Average conversion (%)	Average degree of branching per molecule	Average time-on-stream (days)	Average conversion (%)	Average degree of branching per molecule
0.15	22-42	82	2.51			
0.25	5-22	56	2.37			
0.35	0-5	56	2.24			
0.50	45-55	44	2.10	0-7	73	2.42
1.00				7-10	50	2.42
1.50	43-45	15	(2.42)	10-11	34	2.39
2.00	42-43	10	1.99	11-12	28	2.09
3.00				12-14	21	2.09

* Refers to the experiment shown in Figure 5-7.

5.1.7 Effect of poisoning of the external surface of the H-ZSM-5 zeolite crystallites on catalyst activity for 1-hexene dimerization

In an attempt of limiting the reaction to occur inside the zeolite pores, the zeolite crystallite's external surface was deactivated by bulky amines. It is believed that the acid sites on the external zeolite crystallite surface can be selectively neutralized/poisoned by a bulky pyridine type compound having an effective cross-section larger than the zeolite pore¹² (see Section 2.5.2). It was therefore expected, based on other studies^{3,12,9,10,11} (see Section 2.5.2), that, since 2,4,6-collidine (kinetic diameter 7.5 Å)¹² and 2,6-di-*tert*-butylpyridine (7.0 Å),¹³ see Figure 2-24, are significantly larger in size than the 5.1 x 5.5 and 5.4 x 5.6 Å pores of the ZSM-5 zeolite (see Figure 2-9), they would only bind to the external active sites of the zeolite crystallites, deactivate the external sites, and thereby limit the 1-hexene dimerization to occur only inside the zeolite pores. It was also expected that the degree of branching may decrease due to the then increased shape-selective constraints.

5.1.7.1 Poisoning with 2,4,6-collidine

In the first experiment, the 1-hexene feed was spiked with 65 ppm by mass of 2,4,6-collidine (kinetic diameter 7.5 Å¹²), see Section 4.3.1. Switching a partially deactivated catalyst (run described in Section 5.1.6 and conversion vs. time-on-stream shown in Figure 5-7) after 55 days of converting neat 1-hexene feed to the feed poisoned with 65 ppm (wt) of 2,4,6-collidine caused a much accelerated decline in conversion from about 40% to zero over a period of 4 days, i.e. a complete loss of activity (see Figure 5-8).

It should be noted that the molar amount of collidine fed during the 4 days corresponded to only 1/10 of the number of aluminium atoms (= acid sites) present in the zeolite catalyst.

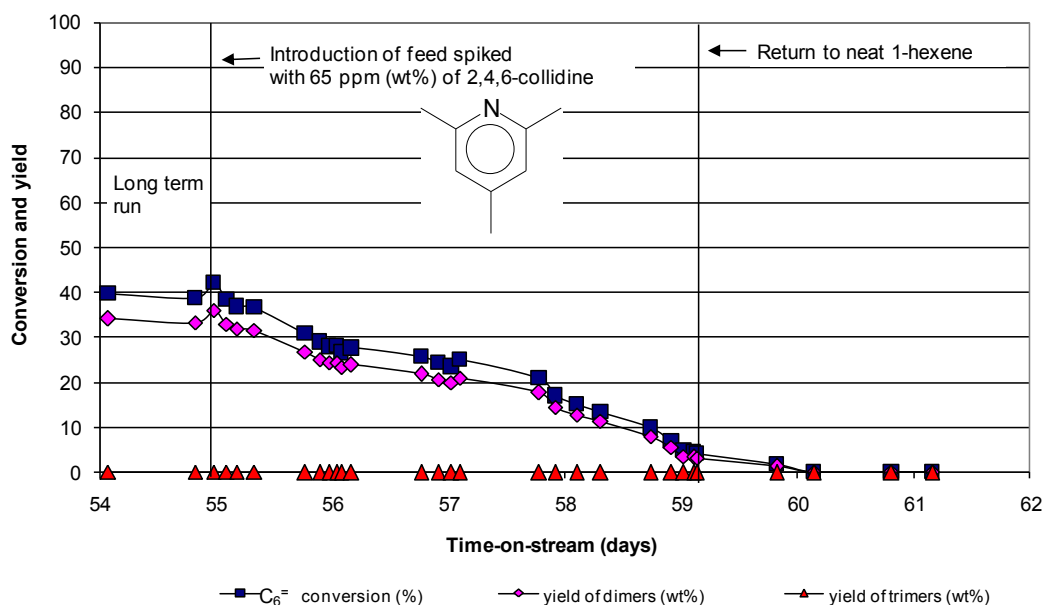


Figure 5-8: Effect of adding 2,4,6-collidine to the 1-hexene feed (65 ppm by mass) at the end of the long term run described in Section 5.1.6 and shown in Figure 5-7 (H-ZSM-5 catalyst, 170 °C, 40 bar and WHSV of 0.5 g/g.h). “Zero” yield of trimers means small amounts were still formed, but could not be quantified.

In continuation of this experiment, neat feed was introduced to the reactor again in an attempt to wash the poison off the catalyst. However, upon the return to neat feed, there was no recovery. It should be noted that the delay in response to a switch in conditions (due to the holdup and backmixing in the unit downstream the catalyst bed) is about 1 day at a WHSV of 0.5 g/g.h (see, for instance, Figure 5-2).

5.1.7.2 Poisoning with 2,6-di-*tert*-butylpyridine

In another experiment, under the same reaction conditions, another bulky pyridine-type poison, 2,6-di-*tert*-butylpyridine (kinetic diameter 7.0 Å)¹³, was evaluated for the effect of poisoning the external sites of the zeolite crystallites. In this case, fresh H-ZSM-5 catalyst (12 g of zeolite) was pre-poisoned *ex-situ* with 0.28 g of 2,6-di-*tert*-butylpyridine (see Section 4.3.1). This amount corresponds to 1/3 of the aluminum content of the zeolite sample. The pre-poisoned catalyst was then loaded into the reactor. Upon this, poisoned feed (65 ppm by mass of 2,6-di-*tert*-butylpyridine, see Section 4.3.1) was fed at 170 °C reaction temperature. The results thereof are shown in Figure 5-9.

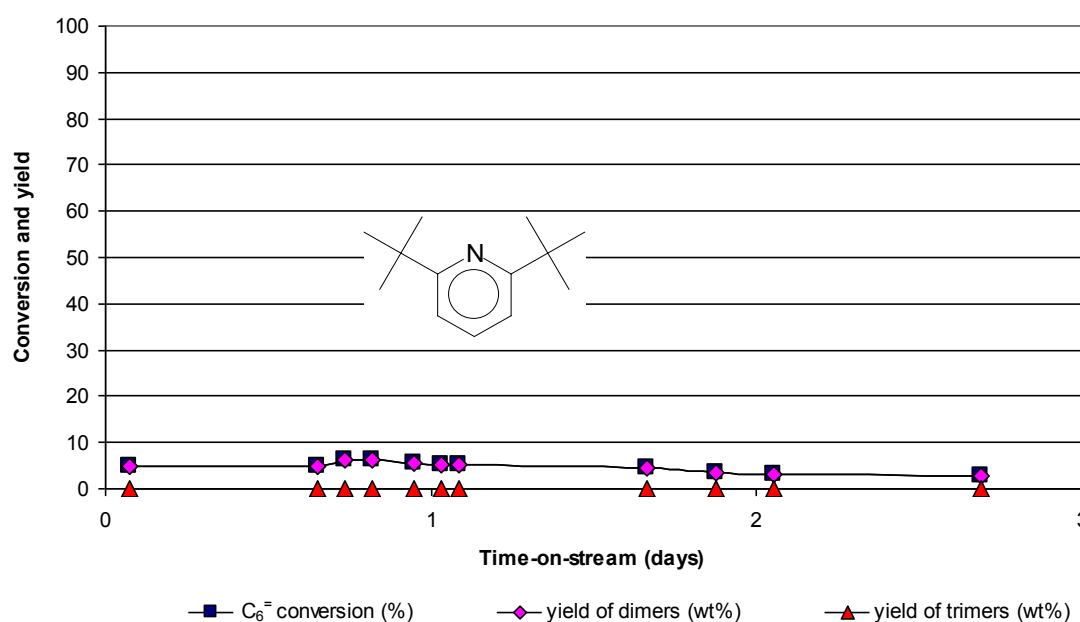


Figure 5-9: Dimerization of poisoned 1-hexene feed (2,6-di-*tert*-butylpyridine, 65 ppm by mass) over H-ZSM-5 catalyst whose external surface was pre-poisoned with 2,6-di-*tert*-butylpyridine (170 °C, 40 bar and WHSV of 0.5 g/g.h).

There was hardly any activity right from the beginning of the run when feeding the slightly poisoned feed to the pre-surface deactivated catalyst.

5.2 Dimerization of 1-octene over H-ZSM-5 catalyst

In addition to 1-hexene, 1-octene was used as a model compound and dimerized over H-ZSM-5 to produce diesel-range C₁₆ compounds for fuel quality testing. 1-Octene (see Table 4-1) was used and the same catalyst as in 1-hexene dimerization, namely H-ZSM-5 with a SiO₂/Al₂O₃ molar ratio of 90 (see Table 4-1). Since 1-octene also underwent rapid double bond isomerization, like 1-hexene, another Aspen Plus¹ simulation was carried out to calculate the *n*-octenes equilibrium distribution, see Table 5-6.

Table 5-6: Simulated equilibrium isomer distribution of *n*-octenes at 170 °C and 40 bar (liquid phase) (by Aspen plus 2006¹)

Equilibrated <i>n</i> -octene feed (mol%)	
1-Octene	0.7
<i>trans</i> -2-Octene	32.9
<i>cis</i> -2-Octene	6.4
<i>trans</i> -3-Octene	33.1
<i>cis</i> -3-Octene	7.4
<i>trans</i> -4-Octene	15.7
<i>cis</i> -4-Octene	3.7

All product samples showed a similar pattern of the major peaks in the C₈-group upon gas chromatographic analysis, regardless of the extent of oligomerization. The distribution reflected the data given in Table 5-6. Conversion was, therefore, defined as C₈⁼ conversion considering all C₈ compounds (virtually all of the linear and the small percentage of branched C₈ olefins that formed) as reactants (analogous to eq. 1 in Section 4.4.1). It should be noted that the equilibrium content of 1-octene is < 1%.

5.2.1 Searching “optimum” reaction temperature

Similar to the 1-hexene experiments, 1-octene was dimerized at first by ramping the reaction temperature up in order to determine the “optimum” operating conditions for the production of C₁₆ dimers. The “volcano curve” experiment was conducted by increasing the temperature from 100 - 210 °C in steps of at first 20 °C, then 10 °C every 24 hours at a pressure of 40 bar and a WHSV of 1.0 g/g.h. The results of the volcano curve experiment are shown in Figure 5-10.

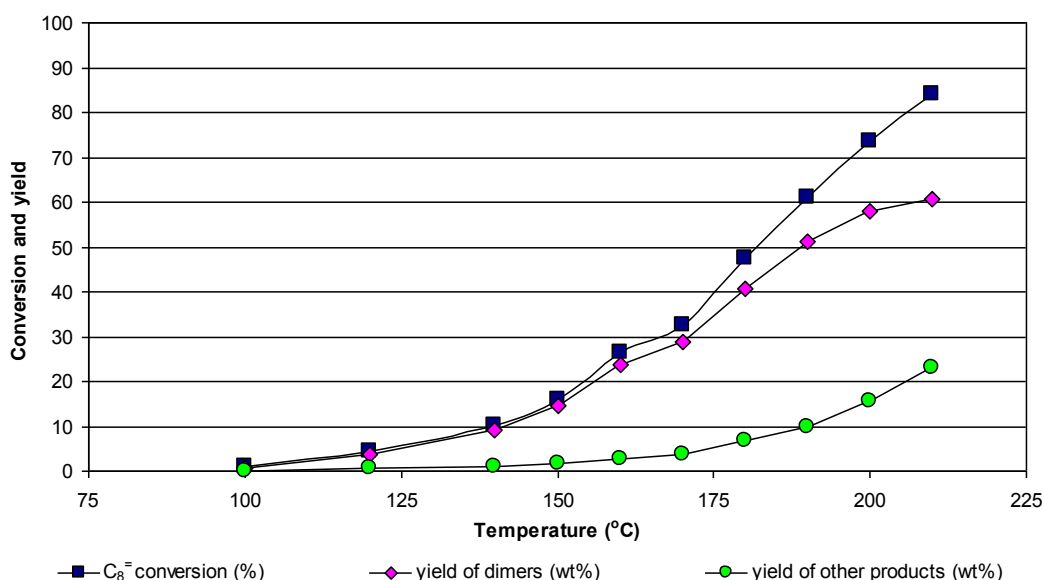


Figure 5-10: “Volcano curve” from 1-octene dimerization (H-ZSM-5 catalyst, 40 bar and WHSV of 1.0 g/g.h). “Other products” are essentially “lights” (C₄-C₁₅). “Lights” in this context are products with carbon numbers lower than that of the dimer (except C₈). It should be noted that small amounts of trimers were also formed, which could not be quantified (see text).

With 1-octene and under the chosen reaction conditions, the amount of by-products (other) increased over the whole temperature range. Small

amounts of trimers were formed (not shown). Due to the multitude of isomers present, the gas chromatogram only showed a very flat and broad hump for the trimers (see Figure 4-3), which could not be integrated.

Subsequent investigations were performed under the same reaction conditions (170 °C, 40 bar) used for 1-hexene dimerization.

5.2.2 Effect of time-on-stream on catalyst activity

The stability/deactivation of H-ZSM-5 in 1-octene dimerization was evaluated at 170 °C, 40 bar and a WHSV of 0.25 g/g.h. The results are given in Figure 5-11.

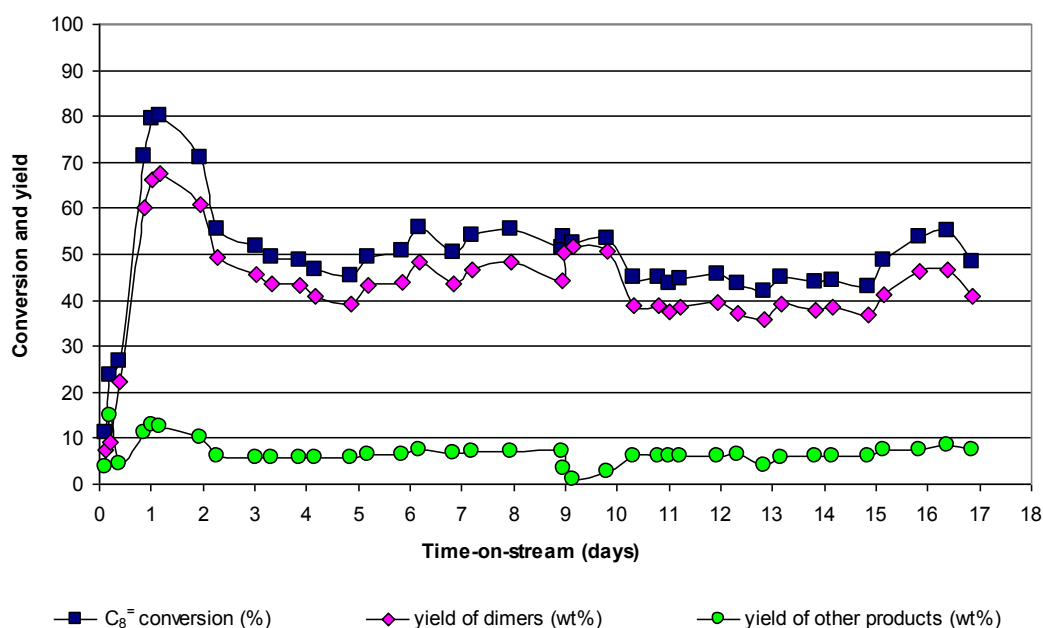


Figure 5-11: Catalyst deactivation as a function of time-on-stream during the dimerization of 1-octene (H-ZSM-5 catalyst, 170 °C, 40 bar and WHSV of 0.25 g/g.h). “Other products” are essentially “lights” (C₄-C₁₅). “Lights” in this context are products with carbon numbers lower than that of the dimer (except C₈). It should be noted that small amounts of trimers were also formed, which could not be quantified.

In general, data from 1-octene conversion showed larger scatter than data from 1-hexene conversion (which is probably due to larger analytical error).

As with 1-hexene, 1-octene conversion showed a tendency to stabilize after 3 to 4 days, in this case at around 50%, with average yields of C₁₆ dimers of more than 40%. Almost 10% of “other products” were formed, mainly “lights”. (“Lights” in this context are products with carbon numbers lower than that of the dimer, except C₈). Small amounts of trimers formed throughout the run, but the yields could not be quantified.

Dimers obtained from 1-octene, C₁₆, have a carbon number and boiling points in the middle of the typical carbon number and boiling range of diesel (viz. “Cetane Number”). They formed under the “optimum” conditions with about 40% yield and around 85% selectivity as can be derived from Figure 5-11.

5.2.3 Effect of varying space velocity

Space velocity was varied at the temperature of 170 °C and pressure of 40 bar. Conversion increased with decreasing space velocity. Space velocities and resulting conversions are presented in Table 5-7, 2nd and 3rd column.

5.2.4 Reactivities of *n*-hexene and *n*-octene feeds over H-ZSM-5

Quasi-steady state conversions of 1-hexene and 1-octene over H-ZSM-5 at identical reaction temperatures and pressures (170 °C and 40 bar), but half the space velocity for octene, are similar, see Figure 5-2 and Figure 5-11,

indicating that the thermodynamically equilibrated mixture of the *n*-octene isomers is about half as reactive over H-ZSM-5 as the thermodynamically equilibrated mixture of the *n*-hexene isomers.

5.2.5 Properties of the hydrogenated 1-octene dimer fraction with respect to use as diesel fuel

C₁₆ diesel samples were obtained by combining all samples obtained from 1-octene dimerization over H-ZSM-5 at 170 °C, 40 bar and at a specific space velocity, distillative separation of the C₁₆ olefin fraction and subsequent hydrogenation over Pd/C as described in Section 4.4.2. The C₁₆ paraffins obtained at each WHSV were submitted to Sasol Technology's Fuels Research Laboratory for testing as a diesel fuel. The results are given in Table 5-7.

As in the dimerization of 1-hexene (see Table 5-5) the degree of branching of the 1-octene derived dimers was slightly above 2 and increased slightly with decreasing WHSV (increasing conversion), see Table 5-7, 3rd and 4th column.

It can be derived from Table 5-7 that the cetane numbers of the hydrogenated C₁₆ product fractions reached values between 55 and 60 and increased with decreasing degree of branching. These cetane numbers are higher than those obtained from other olefin oligomerization processes, as shown in Table 5-7.

Table 5-7: Properties of the C₁₆ paraffins obtained from hydrogenating (see Section 4.4.2) the C₁₆ olefin fraction of the 1-octene dimerization product (H-ZSM-5 catalyst, 170 °C, 40 bar, WHSV of 0.25 - 2.0 g/g.h) and of other diesel fuels from olefin oligomerization

Product	WHSV (g/g.h)	Conversion (%)	Average degree of branching per molecule ^e	Cold Filter Plugging Point (CFPP), (°C) ^f	Density (g/ml) at 15 °C ^f (* at 20 °C)	Pour Point (°C) ^f	Kinematic viscosity at 40 °C (cSt) ^f	Cetane number ^f
C ₁₆ ^a	0.25	49	2.46	-27	0.7813	< -42	2.26	56.9
C ₁₆ ^a	0.35	34	(2.09)	-29	0.7800	< -42	2.24	59.0
C ₁₆ ^a	0.50	31	2.31	-27	0.7838	< -42	2.42	60.9
C ₁₆ ^a	1.00	20	2.19	-27	0.7813	< -42	2.31	60.0
C ₁₆ ^a	2.00	14	2.13	-27	0.7687	< -42	1.70	61.9
MOGD ^b	-	-	- ^g	-	0.7800*	< -50	2.5	56
COD ^c	-	-	-	-45	0.796*	< -42	2.7	51-54
CatPoly ^d	-	-	-	-	0.797-0.798*	-	2.1	29-30

^a Hydrogenated C₁₆ olefin fraction from 1-octene dimerization.

^b Mobil's Olefins to Gasoline and Diesel process (see Section 2.1.2.2.2 and Table 2-1).

^c PetroSA's Conversion of Olefins to Diesel process (see Section 2.1.2.2.3).

^d UOP's Catalytic Polymerization ("CatPoly") process as applied at Sasol's Secunda refineries, hydrogenated (see Section 2.1.2.2.1).

^e Determined by ¹H-NMR (see Section 4.4.2).

^f See Table 4-3 for determination of respective fuel properties and definition.

^g On average, every 5th carbon atom in the chains is methyl branched (see Sections 2.1.2.2.2 and 2.3.1.1 and Figure 2-17). This would translate in an average degree of branching of a C₁₆ paraffin of close to 3.

5.3 Dimerization over amorphous silica-alumina (ASA) compared with zeolite H-ZSM-5

Amorphous silica-alumina (ASA) is known to have Brønsted acid sites and to catalyze hydrocarbon transformation reactions. Olefin oligomerization is such a reaction.¹⁴ In order to establish the effect of restricted pore size on the dimerization of 1-hexene and 1-octene, the results obtained from using non-surface poisoned and non-pore mouth blocked H-ZSM-5 (approximate pore diameters 5.5 Å) were compared to results obtained from using an ASA (mean pore diameter 40 Å) catalyst (see Table 4-1).

5.3.1 Effect of reaction temperature on the dimerization of 1-hexene over amorphous silica-alumina

To obtain the “optimum” operating conditions for 1-hexene dimerization over ASA, reaction temperature was varied at a fixed pressure of 40 bar and a WHSV of 0.5 g/g.h, that is, at conditions identical to those used for H-ZSM-5 (see Section 5.1). Temperature was increased from 50 to 210 °C in 24 hour steps, at first at 25 °C per step and at 10 °C per step once conversion has exceeded 50%. The resulting volcano curve is shown in Figure 5-12 (b) together with the volcano curve obtained using H-ZSM-5, Figure 5-12 (a).

As can be seen in Figures 5-12, the ASA catalyst employed is more active than the H-ZSM-5 catalyst employed. For the ASA catalyzed reaction, maximum conversion of 1-hexene of 90% was achieved already at 150 °C

while over the H-ZSM-5 employed 190 °C was required. However, over ASA, at temperatures higher than 150 °C there was a significant increase in the formation of cracked products (carbon number range of C₄-C₁₁).

The yield of dimers reached a plateau of 65% already at 100 °C and declined with increasing cracking conversion from 150 °C onwards. However, from 100 °C up to 150 °C, an increase in trimer formation was observed, which then also plateaued, at about 25%, and finally also decreased with increasing cracking conversion (from 180 °C onwards). At temperatures higher than 190 °C even a decrease in conversion was observed. This is possibly due to coking of the catalyst at the high temperature achieved at the end of the run.

With H-ZSM-5 as the catalyst, the maximum conversion of 1-hexene (> 90%) was only achieved at 200 °C and the formation of cracked products took also up later than over ASA. Yields of cracked products at higher reaction temperatures were very similar with the two catalysts.

The results indicate that the “optimum” temperature for 1-hexene dimerization over the given ASA catalyst and under the given other reaction conditions (40 bar, WHSV of 0.5 g/g.h) appears to be around 150 °C. 1-Hexene conversion is around 90% and less than 10% of cracked products form. Over H-ZSM-5, under equal reaction conditions, the “optimum” temperature was around 170 °C with a 1-hexene conversion of around 70% and similar yields of cracked products.

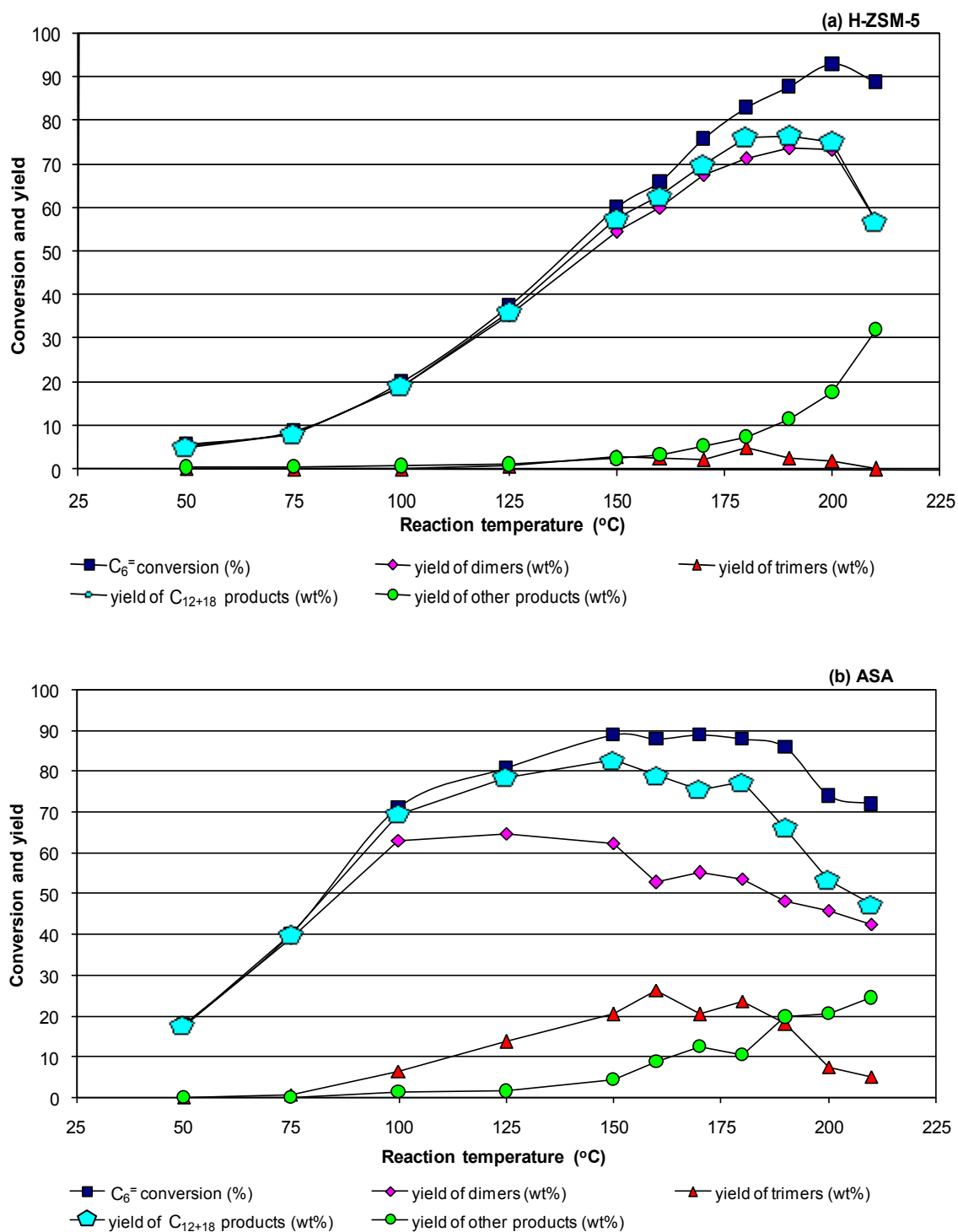


Figure 5-12: Comparison of the volcano curves obtained from 1-hexene dimerization at 40 bar and WHSV of 0.5 g/g.h over (a) H-ZSM-5 and (b) amorphous silica-alumina (ASA). “Other products” are essentially “lights” (C₄-C₁₁). “Lights” in this context are products with carbon numbers lower than that of the dimer, except C₆.

Figure 5-12 also shows that H-ZSM-5 is more selective for the formation of dimers than ASA, while the latter, at equal conversion (but achieved at lower temperatures) produces significantly more trimers. However, the difference in trimer yield and selectivity is not a temperature effect, but also shows at identical reaction temperatures and similar conversions achieved fine-tuning space velocities (see Table 5-8).

Table 5-8: Trimer yields and selectivities from 1-hexene dimerization over H-ZSM-5 and ASA catalyst at equal temperature (170 °C), pressure (40 bar) and conversion (around 85%)

Catalyst	WHSV (g/g.h)	Conversion (%)	Yield of trimers (wt%)	Selectivity to trimers (wt%)
H-ZSM-5	0.15	85 ^a	8 ^a	9.5
ASA	0.50	88 ^b	24 ^b	27.5

^a Average data from Figure 5-7, covering 24 – 32 days on stream period, 170 °C.

^b Average data from Figure 5-12 (b), 160-180 °C (plateau).

The total yield of products in the diesel-range ($C_{12} + C_{18}$) from the two catalysts is also compared in Figure 5-12 (a) and (b), showings higher yields at lower temperatures for the ASA catalyst. The degrees of branching of some of the hydrogenated C_{12} fractions obtained from the two catalysts are given and compared in Table 5-9.

Table 5-9: Degrees of branching derived from ^1H -NMR analyses of hydrogenated C_{12} fractions from 1-hexene dimerization over the H-ZSM-5 and ASA catalysts (150 °C, 40 bar and WHSV of 0.5 g/g.h).

Catalyst	Reaction temperature (°C)	Conversion (%)	Average degree of branching
H-ZSM-5	150	60	2.04
ASA	150	68	2.31

On first sight, Table 5-9 indicates a difference in the degree of branching of the products from H-ZSM-5 and ASA. It should, however, be noted that the difference in the average degree of branching between H-ZSM-5 and ASA comes with a difference in conversion and indeed, data given in Table 5-5 indicate that conversion has a significant effect on the degree of branching.

5.3.2 Catalyst activity/deactivation as a function of time-on-stream for the dimerization of 1-hexene over the ASA catalyst

In Section 5.3.1 it was shown (Figure 5-12) that, under identical reaction conditions, a higher conversion and yield of diesel (of similar degree of branching) could be obtained from reacting 1-hexene over the ASA catalyst in comparison to H-ZSM-5. The stability of ASA with time-on-stream in the conversion of 1-hexene was, therefore, also investigated. 1-Hexene was dimerized at the “optimum” conditions of 150 °C, 40 bar and at a WHSV of 0.5 g/g.h. The run was allowed to proceed over 31 days and the results are shown in Figure 5-13.

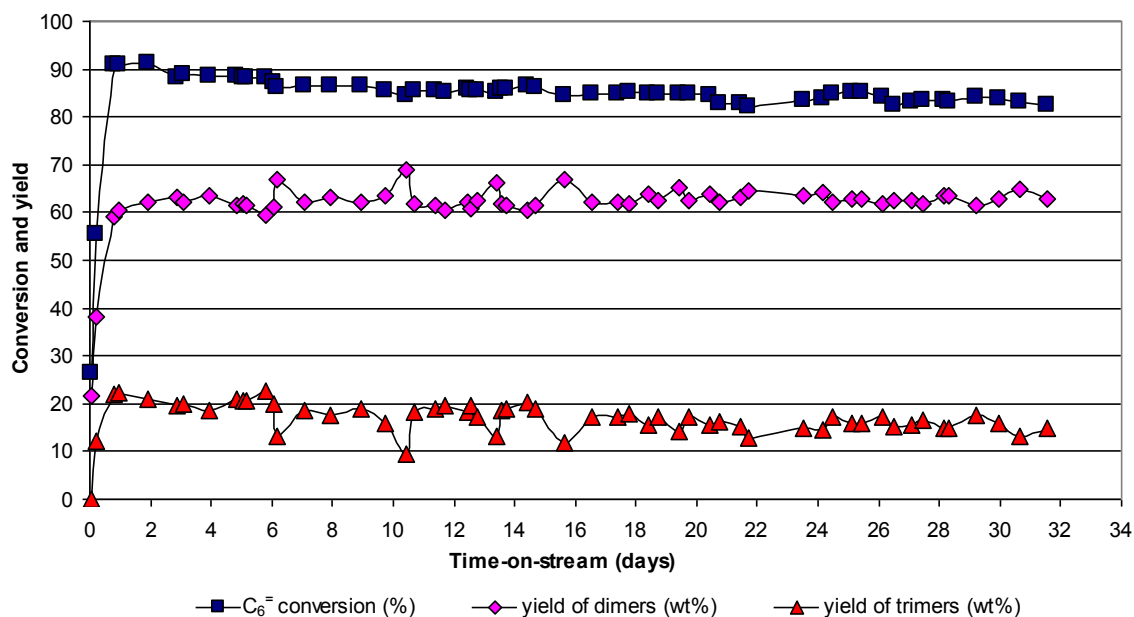


Figure 5-13: Catalyst activity/deactivation as a function of time-on-stream observed during the dimerization of 1-hexene over the ASA (150 °C, 40 bar and WHSV of 0.5 g/g.h).

The results (Figure 5-13) suggest on first sight that the activity of the ASA catalyst was fairly stable during time-on-stream; there was seemingly only minor catalyst deactivation under the above-mentioned reaction conditions. However, at conversions of around 85% this observation does not tell much. At high conversion or proximity to equilibrium conversion < 100% (as may also be the case here) even significant changes in catalyst activity will hardly reflect in the level of conversion. The yield of trimers, the consecutive product also shown in Figure 5-13, tells more about deactivation. The initial yield of trimers was about 20 wt%, i.e., in a range very sensitive to changes in catalyst activity, and declined by 25% during the run. This decline reflects the true loss in catalyst activity. Yields of dimers and trimers of, on average, 62 and 18 wt% were achieved, i.e. a diesel yield being around 80 wt%, corresponding to almost 90 wt% diesel selectivity.

5.3.3 Dimerization of 1-octene over amorphous silica-alumina

In order to compare with the products obtained from the dimerization over H-ZSM-5, 1-octene was also dimerized over ASA to produce C₁₆ olefins. A short activity/deactivation study was conducted under the same conditions as used for the dimerization of 1-hexene, namely 150 °C, 40 bar and WHSV of 0.5 g/g.h. The results are shown in Figure 5-14.

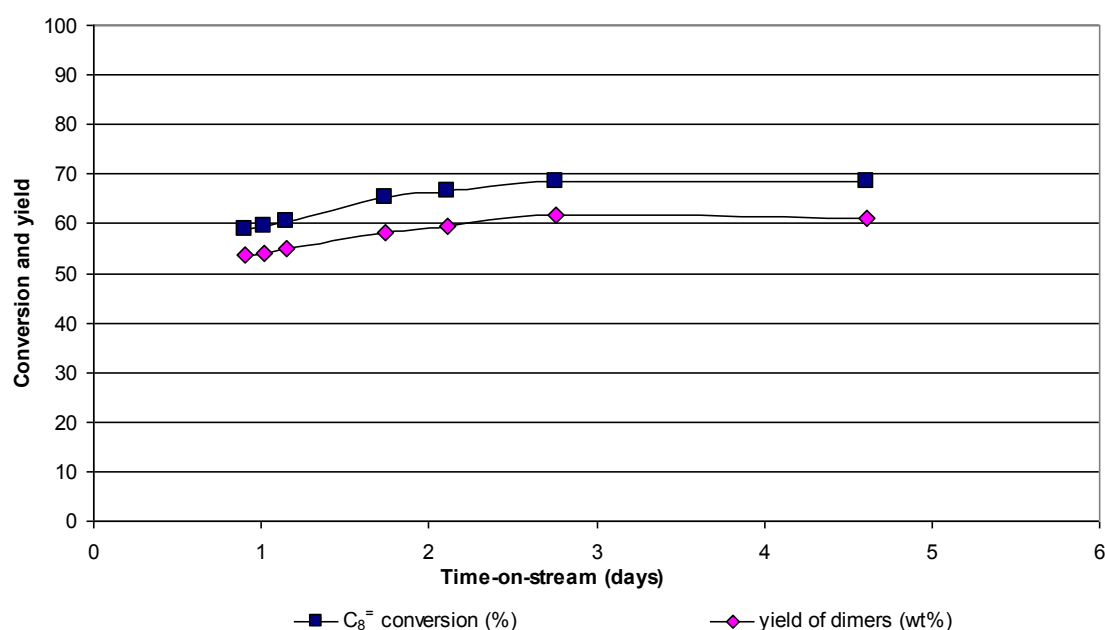


Figure 5-14: Catalyst activity as a function of time-on-stream observed during the dimerization of 1-octene over ASA at 150 °C, 40 bar and WHSV of 0.5 g/g.h. It should be noted that small amounts of trimers were also formed, which could not be quantified.

As observed for H-ZSM-5 (see Section 5.2.4), over ASA the thermodynamically equilibrated mixture of the *n*-octene isomers is about half as reactive as the thermodynamically equilibrated mixture of the *n*-hexene isomers, i.e. little less than 70% conversion of 1-octene are obtained after a few days on stream (see

Figure 5-14) compared to almost 90% conversion of 1-hexene (see Figure 5-13). As can also be seen in Figure 5-14, the yield of dimers is around 62 wt% at a 1-octene conversion of 68%. As in the case of the H-ZSM-5 catalyst (see Figure 5-10), no significant formation of trimers was observed in the 1-octene dimerization reaction. No catalyst deactivation could be observed during the short period of 5 days the ASA catalyst was on stream.

The effect of reaction temperature on 1-octene dimerization over ASA was studied in the temperature range 159 – 210 °C (see Figure 5-15).

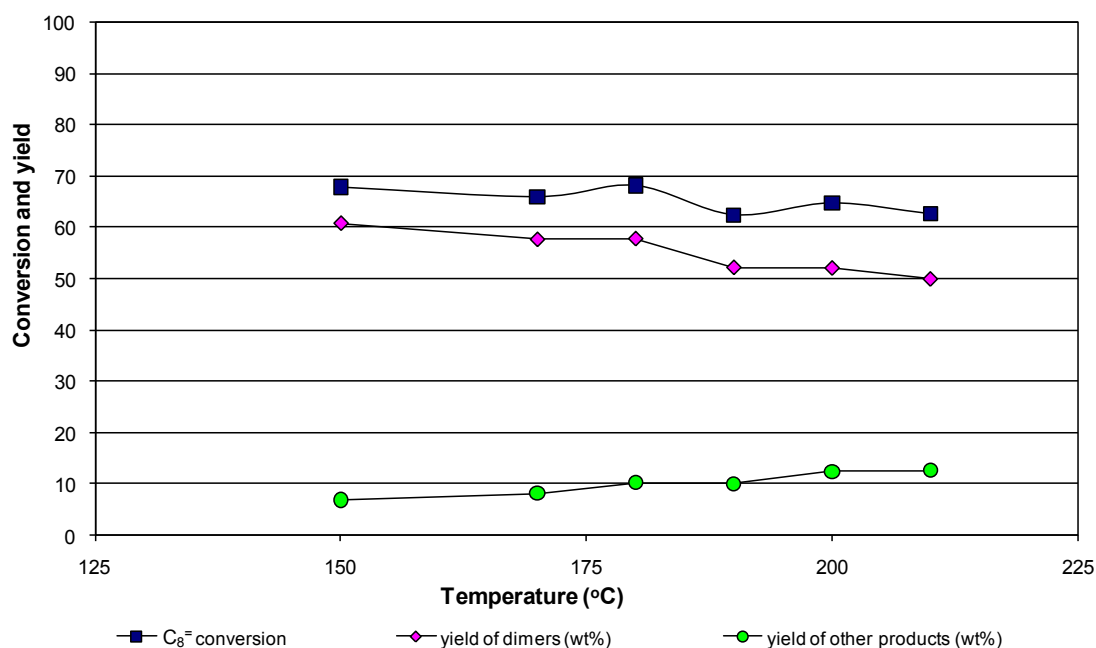


Figure 5-15: Temperature dependence of 1-octene dimerization (ASA catalyst, 40 bar and WHSV of 0.5 g/g.h). “Other products” are essentially “lights” (C₄-C₁₅). “Lights” in this context are products with carbon numbers lower than that of the dimer, except C₈. It should be noted that small amounts of trimers were also formed, which could not be quantified (see text).

As with 1-hexene (see Figure 5-12 (b)), higher yields of dimers (but lower than those from 1-hexene) were observed at 150 °C, declining slightly at higher temperatures.

A hydrogenated sample of the combined C₁₆ fractions, collected at 150 °C (see Figure 5-14), was analyzed by ¹H-NMR for its degree of branching. Results in comparison with those of a sample from dimerization over H-ZSM-5 are given in Table 5-10.

Table 5-10: Cetane numbers and degrees of branching derived from ¹H-NMR analyses of the hydrogenated C₁₆ fraction from 1-octene dimerization at “optimum” reaction conditions over the H-ZSM-5 and ASA catalysts (40 bar and WHSV of 0.5 g/g.h).

Catalyst	Reaction temperature (°C)	Conversion (%)	Average degree of branching	Cetane number ^a
H-ZSM-5	170	31	2.31	60.9
ASA	150	89	2.37	(73.9) ^b

^a See Table 4-3 for the definitions of various fuel properties.

^b This result appears to be very high for an iso-paraffinic diesel, comparable to the cetane numbers of about 75 – 80 of the straight run diesel (hydrogenated) from Sasol’s low temperature Fischer-Tropsch processes, the Sasol SPDTM (Slurry Phase Distillate) process and the Sasol LTFT (Low Temperature Fischer-Tropsch) process, which is essentially *n*-paraffinic.^{15,16,17} Unfortunately the cetane number test could not be repeated since the sample was consumed by the test.

1-Octene dimerization over H-ZSM-5 and ASA at the “optimum” temperatures of 170 and 150 °C, respectively, proceeds at significantly different conversions, but the average degree of branching, measured by the ¹H-NMR method, is similar (see Table 5-10).

The sample obtained from the ASA catalyst was found to have a very high cetane number of 73.9, much higher than the 60.9 which were obtained for the samples from the H-ZSM-5 catalyst, despite the similar degrees of branching (see Table 5-10). However, the correctness of this value is questionable (see Table 5-10, footnote ^b).

5.4 Summary of results

Studies on 1-hexene and 1-octene dimerization that were conducted over zeolite H-ZSM-5 and an amorphous silica-alumina (ASA) catalyst showed the following results:

- Double bond isomerization was the most rapid reaction in the system. As a consequence, the 'real' feeds to the oligomerization reaction were the thermodynamically equilibrated mixtures of the *n*-hexene and *n*-octene isomers, respectively.
- Therefore, conversion had to be defined as C₆ and C₈ conversion, lumping all C₆ and C₈ compounds present in the reaction mixtures as reactants (virtually the 1-hexene and 1-octene and all of the linear and the small percentage of branched C₆ and C₈ olefins that formed).
- Conversion was independent from variations of pressure, in the range of 10-40 bar at 170 °C (where the reaction mixture is assumed to be in the liquid phase, at least in the catalyst pores)..
- The "optimum" operating temperature for the dimerization of both 1-hexene and 1-octene over the H-ZSM-5 catalyst employed, at a weight hourly space velocity of 0.5 g/g.h, was found to be around 170 °C (the criterion for

“optimum” was high conversion but still very low selectivity to cracked products).

- Conversions of above 75% with the 1-hexene feed and around 50% with the 1-octene feed were achieved over the H-ZSM-5 catalyst at the “optimum” conditions of 170 °C, 40 bar, WHSV of 0.5 g/g.h and 170 °C, 40 bar, WHSV of 0.25 g/g.h, respectively.
- Small amounts of trimers formed from 1-hexene and 1-octene during dimerization over H-ZSM-5.
- Yields of diesel (under the “optimum” conditions) are, therefore, reflected in the yields of the C₁₂₊₁₈ and the C₁₆ fractions of about 75% and 45%, i.e. selectivities of >95% (for hexene dimers + trimers) and around 90% (for octene dimers).
- The amount of C₈ converted to other carbon numbers was about half the amount of C₆ that could be converted under identical conditions.
- Yields of cracking products were similar, i.e. cracking selectivity was higher in case of *n*-octene feed.
- The activity of the H-ZSM-5 catalyst declined very slowly with time-on-stream. After seven weeks on-stream, the catalyst had lost about 50% of its initial activity.
- Lower catalyst stability, i.e. more rapid decline of conversion, with time-on-stream (1-hexene feed) seems to occur at lower reaction temperatures (150 and 160 °C compared to 170 °C), probably due to blockage of the crystal surface, the pores or the active sites by higher oligomers and other heavy compounds, which are unable to readily desorb at these low temperatures.

- External surface poisoning of the H-ZSM-5 zeolite with bulky nitrogen bases completely and irreversibly destroyed the activity of the catalyst.
- The amorphous silica-alumina (ASA) catalyst was more active than the H-ZSM-5 catalyst.
- High conversions of around 85-90% and 70% were obtained reacting 1-hexene and 1-octene, respectively.
- The “optimum” operating temperature for the dimerization of 1-hexene and 1-octene over ASA at a weight hourly space velocity of 0.5 g/g.h was found to be around 150 °C.
- Only a minor decline of activity with time-on-stream was observed with the ASA catalyst.
- As over H-ZSM-5, C₈ conversion was about half of the C₆ conversion.
- Yields of diesel-range olefins (C₁₂₊₁₈, from 1-hexene and C₁₆ from 1-octene) of around 82% and 65%, respectively, were obtained over the ASA catalyst.
- Almost “true” dimerization / trimerization of 1-hexene and 1-octene could be achieved under the “optimum” reaction conditions over both catalysts, with high selectivity to the dimer of > 85%, some trimerization, minimal cracking and very little paraffin formation and no (observable) aromatization.
- The average degree of branching per dimer molecule was somewhat higher than 2, similar over both catalysts and with both feeds. Values between 1.99 and 2.52 were obtained. Differences between catalysts and feed streams, when compared at similar conversions, were small.
- The average degree of branching increased slightly with increasing conversion (the afore-mentioned lowest value observed of 1.99 was obtained at 11% conversion).

- The dimers (and trimers in case of the 1-hexene dimerization products), when hydrogenated, make a good diesel fuel blend stock.
- High cetane numbers of 55-60 for the hydrogenated 1-octene dimer fractions obtained from both catalysts are significantly higher than those obtained from commercial oligomerization processes, such as CatPoly, MOGD and COD.
- Other properties relevant for diesel fuels, such as flow properties and viscosity, were well above the minimum specifications.
- However, the density was below specifications.

5.5 References

-
- ¹ Aspen Plus User Interface, Aspen Technology, Inc, (2006).
 - ² R.J. Quann, L.A. Green, S.A. Tabak, F.J. Krambeck, Ind. Eng. Chem. Res., 27 (1988) 565-570.
 - ³ M.L.O. Sumani, MSc Thesis, Department of Chemical Engineering, University of Cape Town (2006).
 - ⁴ J.R. Anderson, Y.F. Chang, R.J. Western, J. Catal., 118 (1989) 466-482.
 - ⁵ J.P.G. Pater, P.A. Jacobs, J.A. Martens, J. Catal., 179 (1998) 477-482.
 - ⁶ J.P.G. Pater, P.A. Jacobs, J.A. Martens, J. Catal., 187 (1999) 262-267.
 - ⁷ K.G. Wilshier, P. Smart, T. Western, T. Mole, T. Behrsing, Appl. Catal., 31 (1987) 339-359.
 - ⁸ T.J.G. Kofke, R.J. Gorte, J. Catal., 115 (1989) 233-243.
 - ⁹ N.M. Page, L.B. Young, D.A. Blain, US 4,870,038 (1989), assigned to Mobil Oil Corp.
 - ¹⁰ C.S.H. Chen, R.F. Bridger, J. Catal., 161 (1996) 687-693.

-
- ¹¹ J.R. Anderson, K. Foger, T. Mole, R.A. Rajadhyaksha, J.V. Sanders, J. Catal., 58 (1979) 114-130.
- ¹² L.D. Rollmann, Stud. Surf. Sci. Catal., 68 (1991) 791-797.
- ¹³ J.A. Lercher, A. Jentys, Stud. Surf. Sci. Catal., 168 (2007) 435-476.
- ¹⁴ A. Corma, Chem. Rev., 95 (1995) 559-614.
- ¹⁵ M.E. Dry, Appl. Catal. A: General, 189 (1999) 185-190.
- ¹⁶ L.P. Dancuart, R. de Haan, A. de Klerk, Stud. Surf. Sci. Catal., 152 (2004) 482-532.
- ¹⁷ D. Leckel, Energy & Fuels, 23 (2009) 2342-2358.

CHAPTER 6

6. DISCUSSION AND CONCLUSIONS

6.1 Comparison of catalysts

The two catalysts employed were very fine crystalline zeolite H-ZSM-5 and mesoporous amorphous silica-alumina (ASA), see Table 4-1.

6.1.1 Catalyst activity

It was intended when choosing the two catalysts that activities were not too different. However, it was found that the ASA catalyst was more active. At equal reaction conditions of 40 bar, WHSV of 0.5 g/g.h and 170 °C hexene conversion over H-ZSM-5 was around 75 to 80% (Figures 5-1, 5-2, 5-3 and 5-12(a)) while over ASA it was between 85 and 90% (Figures 5-12(b) and 5-13). ASA produced 80% conversion at 125 °C already. Similar conversions of 85 and 88%, respectively, at 170 °C and 40 bar, were achieved at WHSV of 0.15 g/g.h over H-ZSM-5 and 0.5 g/g.h over ASA (Table 5-8), indicating that the ASA catalyst was about four times as active as the H-ZSM-5. With 1-octene feed differences were similar. At 40 bar, WHSV of 0.25 g/g.h and 170 °C, octene conversion over H-ZSM-5 was around 50% (Figure 5-11) while over ASA almost 70% conversion were reached already at 150 °C and WHSV of 0.5 g/g.h (Figure 5-14). Variation of space velocity allowed of adapting conversions. Activities were similar enough, in line with key question no. 1, to compare selectivities.

6.1.2 Catalyst stability

The activity of H-ZSM-5 goes through a settling-in period of, typically, between one and a few days on stream and thereafter constantly declines. In the long term experiment on 1-hexene conversion (at 170 °C in the liquid phase, see Figure 5-3) about half of the activity reached at the end of the settling-in period was lost within the next two weeks on stream, after which catalyst activity continued declining – but much more slowly – in comparison (see Figure 5-3, 10-24 and 25-52 days on stream periods). After the end of the settling-in period only little further loss in activity was observed within 2 weeks on stream (from day 3 to day 18 on stream, see Figure 5-11) during 1-octene conversion over H-ZSM-5 under identical conditions. For H-ZSM-5 this was as expected and confirms point 8 of the hypothesis (see Section 3.2).

It was hypothesized (see Section 3.2, points 9 and 10) that the stability of H-ZSM-5 would be higher than the stability of the ASA. This hypothesis was based on the expectation that (i) the formation of bulky oligomeric compounds ('coke' in the widest sense, see Sections 2.1.2.1.2 and 2.3.1.5) that would fill pores and block sites and eventually cause catalyst fouling and deactivation (see Section 2.3.1.5), was limited in the shape-selective channel system of the micro-porous H-ZSM-5 zeolite in contrast to the spacious pore system of the meso-porous ASA (see Sections 2.2.2 and 2.3.1.5) and that (ii) the higher $\text{SiO}_2/\text{Al}_2\text{O}_3$ ratio of the H-ZSM-5 catalyst also helped limiting the build-up of such highly unsaturated, heavy compounds (see Section 2.2.2).

In contrast to the hypothesis (see Section 3.2, points 9 and 10) the ASA catalyst appeared much more stable than the H-ZSM-5 (Figures 5-12(b), 5-13 and 5-14). However, as explained in Section 5.3.2 in detail, the level of conversion of around 85% obtained during the long term run shown in Figure 5-13, was too high to be sensitive enough an indicator for catalyst stability or deactivation, but the yield of around 20% of the secondary product, the trimers, was in the sensitive range and, therefore, indicative. This yield was also rather stable and declined only by about 25% (from 20 to 15 percentage points) during 30 days on stream (see Figure 5-13), while H-ZSM-5 lost almost 50% during 20 days (see Figure 5-3). Superior stability of the ASA catalyst compared to H-ZSM-5 was not expected and proves point 9 of the hypothesis (see Section 3.2) wrong.

The reason for H-ZSM-5 not showing its usual superiority with respect to stability is that this property results from restricted transition state selectivity that is imposed on polycyclics formation in the micropore system of the zeolite as addressed in the literature review (see references to the respective sections of Chapter 2 in the previous paragraph). Restricted transition state selectivity suppresses internal coke formation in H-ZSM-5. However, the suppressing effect on internal coke and coke precursor formation and the resulting difference with respect to deactivation between H-ZSM-5 and catalysts with larger pores, such as ASA, is much pronounced only at elevated temperatures (say $> 350\text{ }^{\circ}\text{C}$), where the 'classical' polyaromatic, black coke forms. In contrast, reaction temperatures applied in this study were too low to facilitate coking in the classical sense; the used catalyst was not black but of a creamy

colour. At low reaction temperatures catalyst fouling is caused by bulky oligomers that are blocking the pore systems of the catalysts and that form regardless of the dimensions of the pores (see references to the respective sections of Chapter 2 in the previous paragraph). Consequently, at low temperatures H-ZSM-5 does not show its superiority with respect to inhibiting the formation of bulky species inside the pore system that block the pores.

The absence of significant differences in the degree of branching of the dimers obtained over H-ZSM-5 and ASA (see data given in Tables 5-3, 5-5, 5-7, 5-9 and 5-10 for comparison) and the apparent restriction of the dimerization reaction to the external surface of the H-ZSM-5 crystallites where no shape-selective restrictions exist (as demonstrated by the selective poisoning of the external surface of H-ZSM-5, shown in Section 5.1.7 and discussed in detail in Sections 6.1.3.3, 6.1.4.4 and 6.1.5) indicate that there is no difference (such as different spatial restrictions) in the environment for the dimerization reaction and in the environment for coking or fouling and therefore no different influence on the stability of the two catalysts.

6.1.3 Carbon number selectivity

6.1.3.1 Effect of temperature on carbon number selectivity

In Figures 5-1, 5-10 and 5-12 and Figures 6-1 and 6-2 conversion, yields and selectivities from 1-hexene and 1-octene dimerization over both the catalysts are shown as a function of temperature. Yields and selectivities of the “other products” were low and, at WHSV of 0.5 g/g.h, only started increasing from

150 °C (ASA) and 170 °C (H-ZSM-5) onwards but did not exceed 10% yield until 90% of hexene conversion was reached.

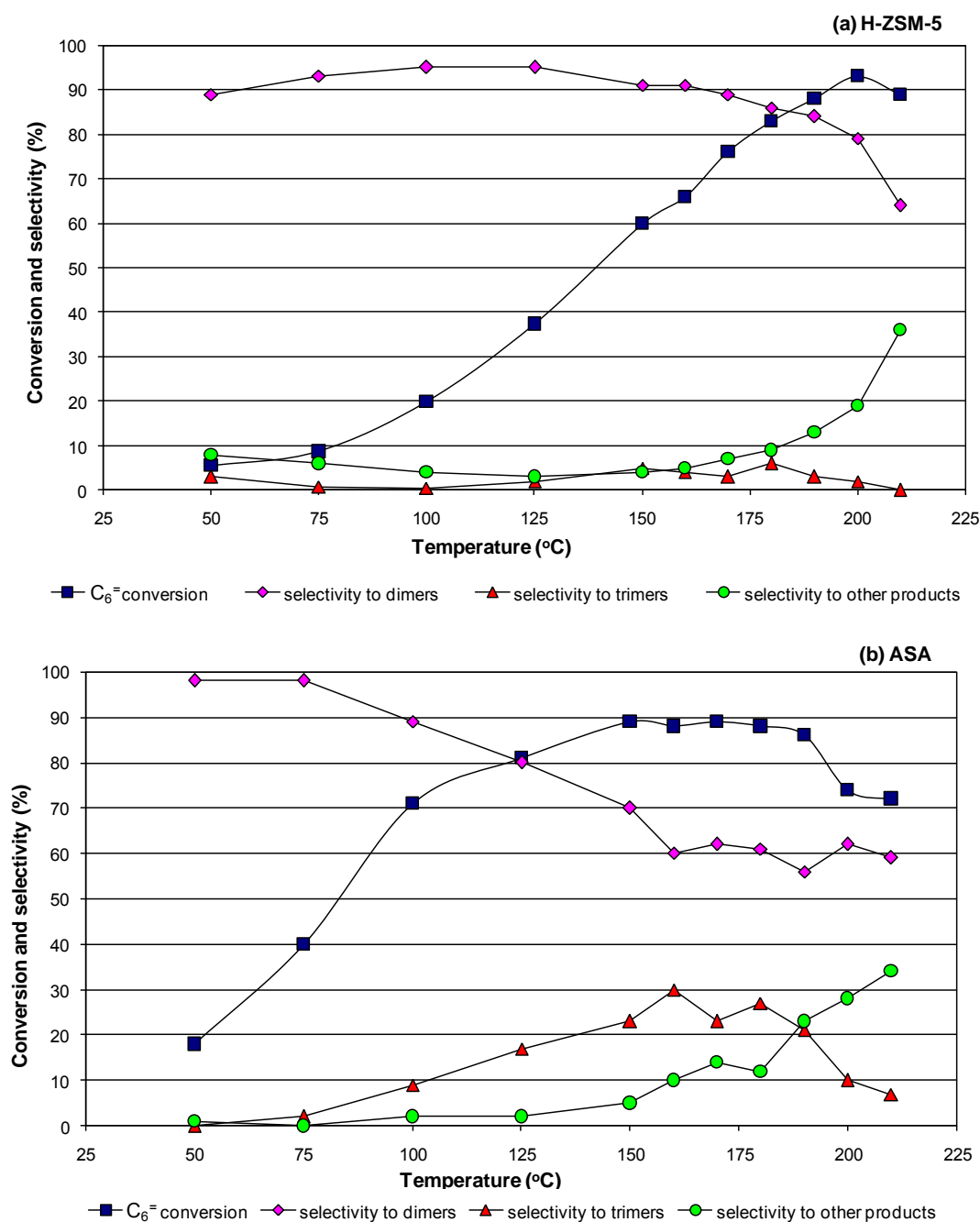


Figure 6-1: Effect of reaction temperature on 1-hexene conversion and selectivity at 40 bar and WHSV of 0.5 g/g.h over (a) H-ZSM-5 and (b) amorphous silica-alumina (ASA). "Other products" are essentially lights ($C_4 - C_{11}$). "Lights" in the context of this study are defined as all products with carbon numbers below the carbon number of the dimer, here C_{12} (but $\neq C_6$).

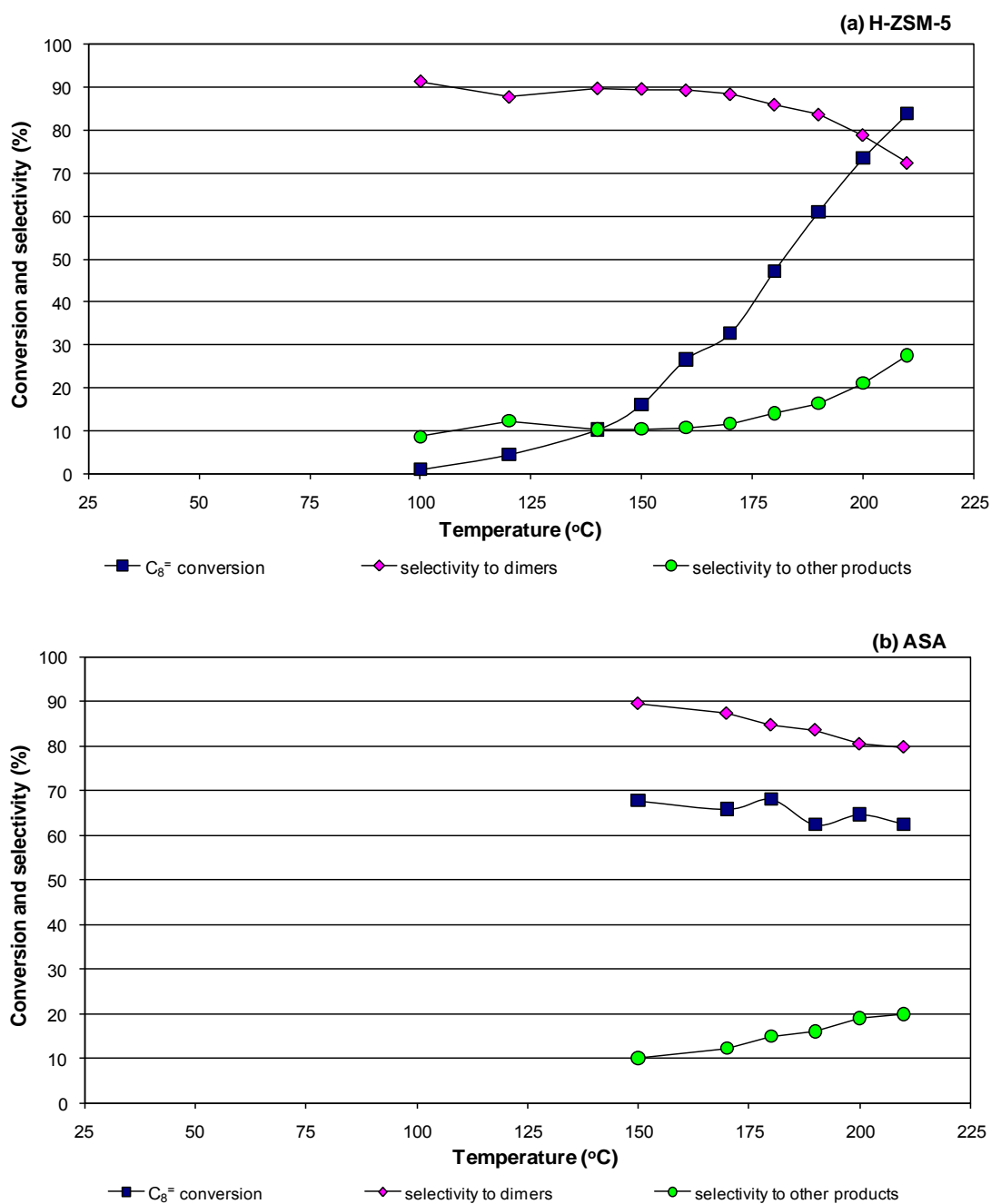


Figure 6-2: Effect of reaction temperature on 1-octene conversion and selectivity at 40 bar over (a) H-ZSM-5, WHSV of 1.0 g/g.h and (b) amorphous silica-alumina (ASA), WHSV of 0.5 g/g.h. "Other products" are essentially lights (C_4 - C_{15}). "Lights" in the context of this study are defined as all products with carbon numbers below the carbon number of the dimer, here C_{16} (but $\neq C_8$). It should be noted that small amounts of trimers were also formed, which could not be quantified.

The major product over both catalysts, H-ZSM-5 and ASA, and with both feeds, 1-hexene and 1-octene, was the dimers. Trimers formed to a lesser extent. “Other products” (as indicated in figures) formed only with very low selectivity, in particular over ASA. “Other products” comprises everything whose carbon number is different from the carbon numbers of the feed, the dimers and the trimers. Chromatograms showed (see Figure 4-4) that these were mostly lights. “Lights” in the context of this study are defined as products with carbon numbers below the carbon number of the dimer (but different from the carbon number of the feed), that is, cracked products, or dimerized and then cracked products.

As expected (see hypothesis, Section 3.2, point 2), with both the feeds, 1-hexene and 1-octene and over both the catalysts tested, H-ZSM-5 and ASA, mainly “true” oligomerization occurred as long as reaction conditions were not too severe and conversion was not too high.

6.1.3.2 Effect of conversion on carbon number distribution

Mechanistically, dimers form as primary products and trimers as secondary products. Over both the catalysts, H-ZSM-5 and ASA, cracked products (“other”) formed. “Others” comprised, in the case of *n*-hexene feed, all of C₄ to C₁₁ compounds except C₆ (feed) (see figure captions Figures 5-1 and 5-12) and in the case of *n*-octene feed all of C₄ to C₁₅ compounds except C₈ (feed) (see figure captions, Figures 5-10, 5-11 and 5-15). These carbon number ranges indicate that the cracking products resulted (mainly) from cracking of dimers, i.e. are also secondary products.

Figure 6-3 shows the effect of space velocity on carbon number fraction selectivity for 1-hexene conversion over H-ZSM-5 at 170 °C.

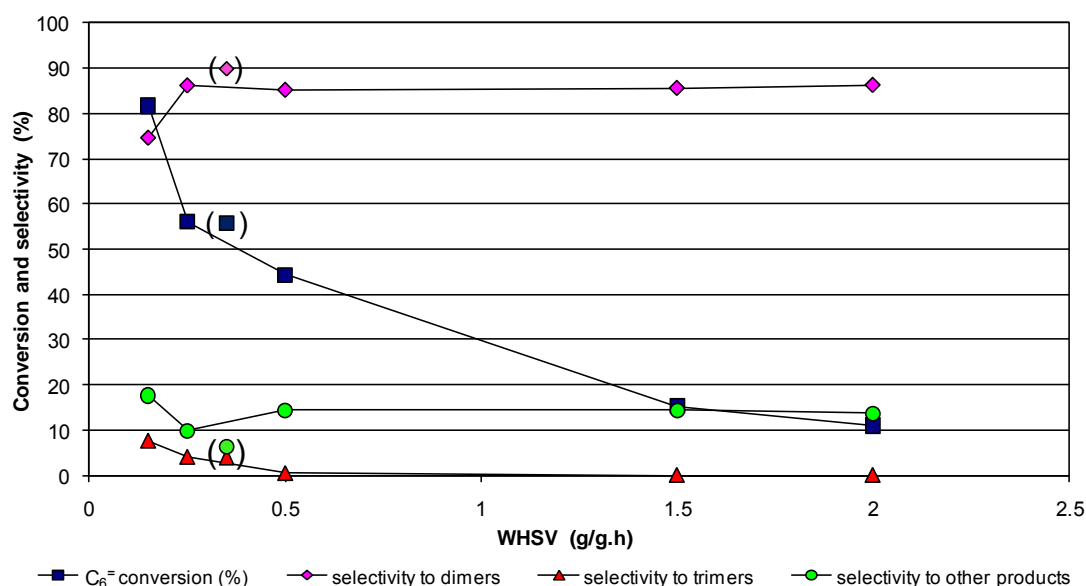


Figure 6-3: Effect of WHSV on 1-hexene conversion and carbon number fraction selectivity at 170 °C and 40 bar over H-ZSM-5. "Other products" are essentially lights (C₄-C₁₁). "Lights" in the context of this study are defined as all products with carbon numbers below the carbon number of the dimer, here C₁₂ but ≠ C₆. Data points represent the quasi-steady state averages of the data obtained from space velocity series (see Figure 5-7). Data points in brackets represent the averages of the data obtained in the beginning of the experimental run, from 1 to 5 days on stream, i.e. during the initial rapid catalyst deactivation stage before quasi-steady state has been reached.

It can be seen from Figure 6-3 that selectivity is a function of space velocity, i.e., conversion. This is as expected since both trimers and cracking products ("others") are secondary products, as discussed above. Down to a WHSV of 0.5 g/g.h, corresponding to about 50% hexene conversion, the effect is minor but at lower space velocities, that is with longer contact times and,

correspondingly, higher conversion, there is a marked increase in trimer (and cracked products) with a corresponding decrease in dimer selectivity.

Table 6-1 gives the sources (the respective figures) of the data points plotted in Figure 6-4, including reaction conditions.

Table 6-1: Sources of data points from 1-hexene dimerization experiments over H-ZSM-5 catalyst used to construct Figure 6-4 (condition values separated by “,” refer to experimental runs carried out over the same charge of catalyst).

H-ZSM-5; 1-hexene feed; 170 °C		
Source of data	Pressure (bar)	WHSV (g/g.h)
Figure 5-1	40	0.5
Figure 5-2	40	0.5
Figure 5-3	40	0.5, 1.0
Figure 5-4	10, 20	0.5
Figure 5-5	40	0.5
Figure 5-6, series # 1 and # 2	10, 20, 30, 40	0.5
Figure 5-7	40	0.15, 0.25, 0.35, 0.5, 1.0, 1.5, 2.0
Figure 5-8*	40	0.5
Figure 5-9**	40	0.5

All data points considered were derived from the individual samples taken at stable activity (quasi steady state data) and not the averages calculated.

* Feed poisoned with 2,4,6-collidine.

** Feed poisoned with 2,4-di-*tert*-butylpyridine.

Figure 6-4 shows the selectivities of dimers, trimers and cracked products (“other”) as a function of conversion for 1-hexene oligomerization over H-ZSM-5 at constant temperature (170 °C). The only parameters changed or changing were pressure, which has neither influence on conversion nor selectivity (see Figure 5-6, Table 5-4 and Section 6.3), space velocity and activity of the catalyst (time-on-stream and poisoning).

In most of the previous figures (see Chapters 5 and 6), except for plots vs. time-on-stream, data points shown represent averages of a number of individual data points obtained at steady state operation. The data points in Figure 6-4 represent the individual data points obtained at steady state conditions, including those that were used to calculate the average data shown in the previous figures.

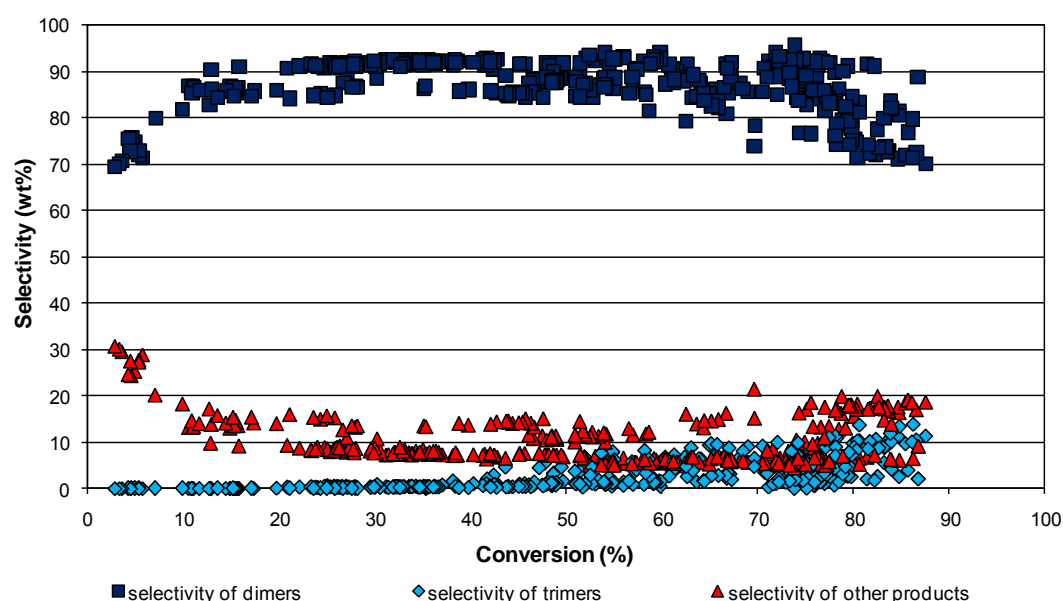


Figure 6-4: Product selectivities as a function of conversion from the dimerization of 1-hexene over H-ZSM-5 at 170 °C, 10-40 bar and WHSV of 0.15-2.0 g/g.h. "Other products" are essentially lights, C₄-C₁₁. "Lights" in the context of this study are defined as all products with carbon numbers below the carbon number of the dimer, here C₁₂ but ≠ C₆. The data points (at steady state) were taken from data given in Figures 5-1 to 5-9.

It can be observed in Figure 6-4 that at 1-hexene conversions below 50%, selectivity to trimers remained at almost zero. Only at higher than 50% conversion, trimers were obtained at a percentage that could be quantified.

Trimer selectivity increased and reached 10 wt% at 80% conversion with concomitantly decreasing selectivity to dimers. The trend of trimer and dimer selectivity with conversion reflects the behaviour of a consecutive reaction $\text{hexene} \rightarrow \text{dimer} \rightarrow \text{trimer}$ with the second reaction being comparatively slow.

Data points at < 10% conversion reflect the product over the externally pre-poisoned zeolite (see Figure 5-9) and from the end of the transition period after having switched to poisoned feed (see Figure 5-8). As discussed in detail in Section 6.1.3.3, these are dimerization products, originally, formed over the internal surface of the zeolite but forced to crack due to transport control imposed on the dimers in the zeolite pore system (product shape selectivity).

No explanation can be given for the significant scatter. However, the individual 'strings' or 'series' of data points showing in Figure 6-4 can by and large be assigned to different runs with individual charges of catalyst each and are probably due to limits in the replicability of catalyst charging and/or start-up.

Figure 6-5 shows the effect of temperature on selectivity. The effect of temperature on the selectivity of cracked products (as indicated already in Figure 5-1), confirms that the apparent activation energy for cracking is higher than the apparent activation energy for the reverse reaction (dimerization/oligomerization).

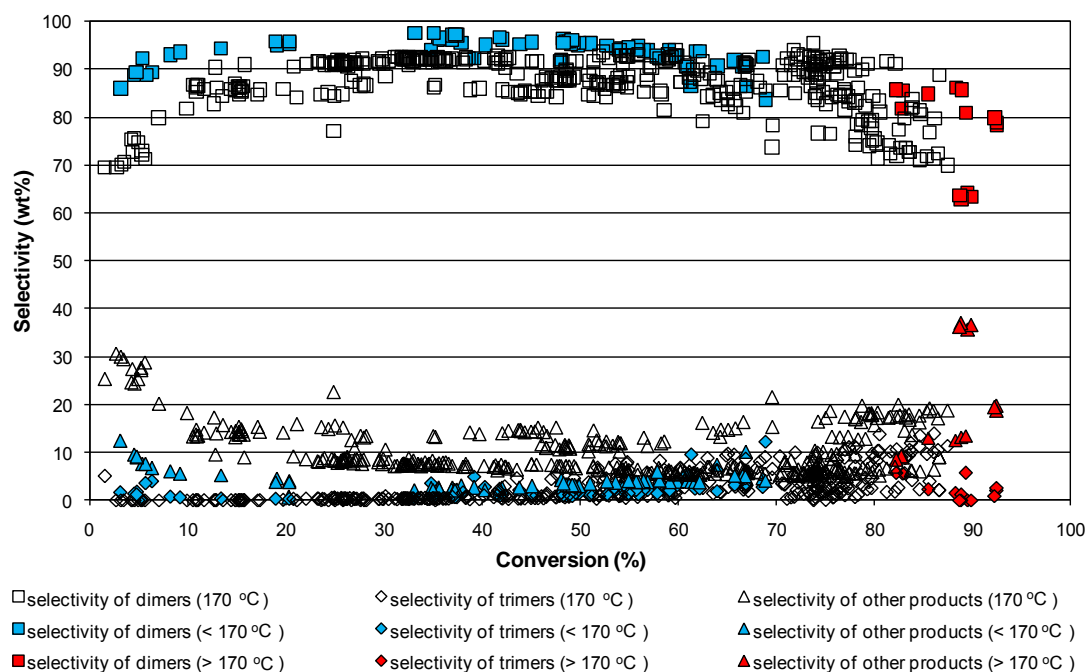


Figure 6-5: Product selectivities as a function of conversion from the dimerization of 1-hexene over H-ZSM-5 at 10-40 bar, WHSV of 0.15-2.0 g/g.h and 50-210 °C. "Other products" are essentially lights, C₄-C₁₁. "Lights" in the context of this study are defined as all products with carbon numbers below the carbon number of the dimer, here C₁₂ but ≠ C₆. The data points (at steady state) were taken from data given in Figures 5-1 to 5-9.

Figure 6-6 shows the selectivities of dimers, trimers and cracked products ("other") as a function of conversion for 1-hexene dimerization over ASA at varying temperatures (50-210 °C), 40 bar and WHSV of 0.5 g/g.h. It should be noted that with 1-hexene over the ASA catalyst, most experiments were conducted at the "optimum" temperature for ASA of 150 °C (instead of 170 °C as with H-ZSM-5) as derived from Figure 5-12. Table 6-2 gives the sources (the respective figures) of the data points plotted in Figure 6-6, including reaction conditions. The data points in Figure 6-6 represent the individual data points

obtained at steady state conditions including those that were used to calculate average data and to show average data points in the respective figures.

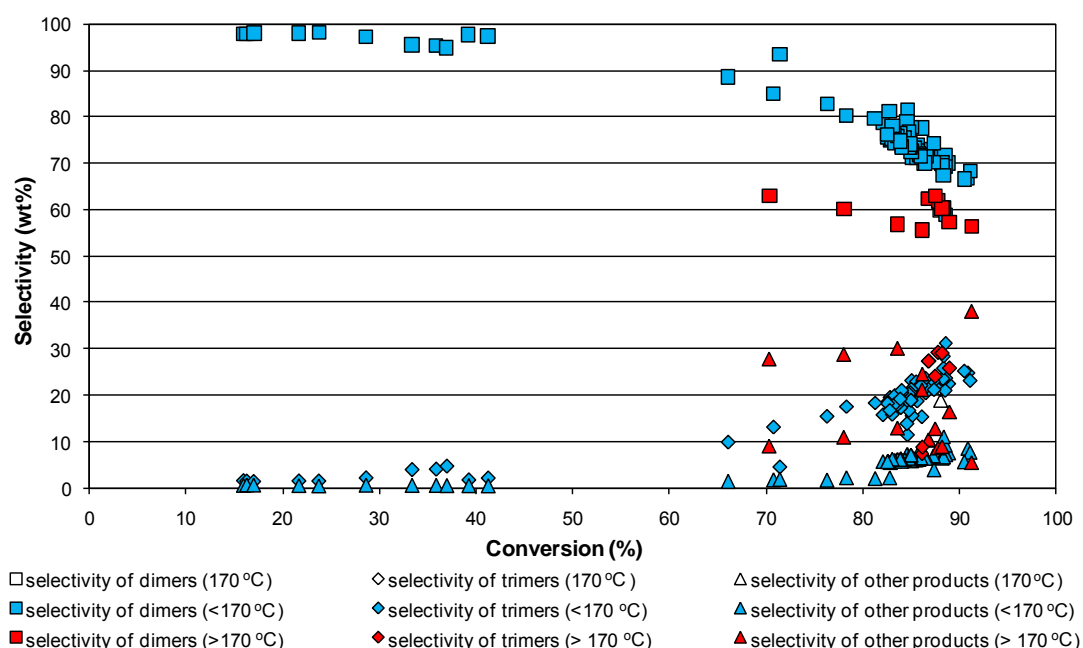


Figure 6-6: Product selectivities as a function of conversion from the dimerization of 1-hexene over ASA at 40 bar, WHSV of 0.5 g/g.h and 50-210 °C. "Other products" are essentially lights, C₄-C₁₁. "Lights" in the context of this study are defined as all products with carbon numbers below the carbon number of the dimer, here C₁₂ but ≠ C₆. The data points (at steady state) were taken from data given in Figures 5-12 and 5-13.

Table 6-2: Sources of data points from 1-hexene dimerization experiments over ASA catalyst used to construct Figure 6-6.

ASA; 1-hexene feed; 50-210 °C		
Source of data	Pressure (bar)	WHSV (g/g.h)
Figure 5-12 (b)	40	0.5
Figure 5-13	40	0.5

All data points considered were derived from the individual samples taken at stable activity (quasi steady state data) and not the averages calculated.

As was observed with 1-hexene over H-ZSM-5 (see Figure 6-5), dimerization of this feed over ASA shows a similar trend in trimer selectivity and the selectivity to cracked products (“other”) reflecting their formation as secondary products. Selectivity of trimers and cracked products only rises at higher than 50% conversion. Correspondingly, the effect of temperature on the selectivity of cracked products (as indicated already in Figure 5-12), confirming that the apparent activation energy of cracking over ASA is higher than the apparent activation energy of the reverse reaction (dimerization/oligomerization).

1-Octene was also dimerized over the H-ZSM-5 catalyst and the selectivities of dimers, trimers and cracked products (“other”) as a function of conversion at 100-210 °C, 40 bar and WHSV of 0.25-2.0 g/g.h are shown in Figure 6-7.

Table 6-3 gives the sources (the respective figures) of the data points plotted in Figure 6-7, including reaction conditions. The data points in Figure 6-7 represent the individual data points obtained at steady state conditions including those that were used to calculate average data and to show average data points in the respective figures.

It can be observed in Figure 6-7 that selectivity to trimers remained at almost zero, irrespective of conversion. As mentioned in Section 5.2.1, only small amounts of trimers formed from octene feed, which could not be quantified. The selectivity to cracked products “others” was around 10 wt% at below 55% conversion and increased towards 30 wt% with increasing reaction severity, i.e. conversion and temperature, with concomitantly decreasing selectivity to dimers.

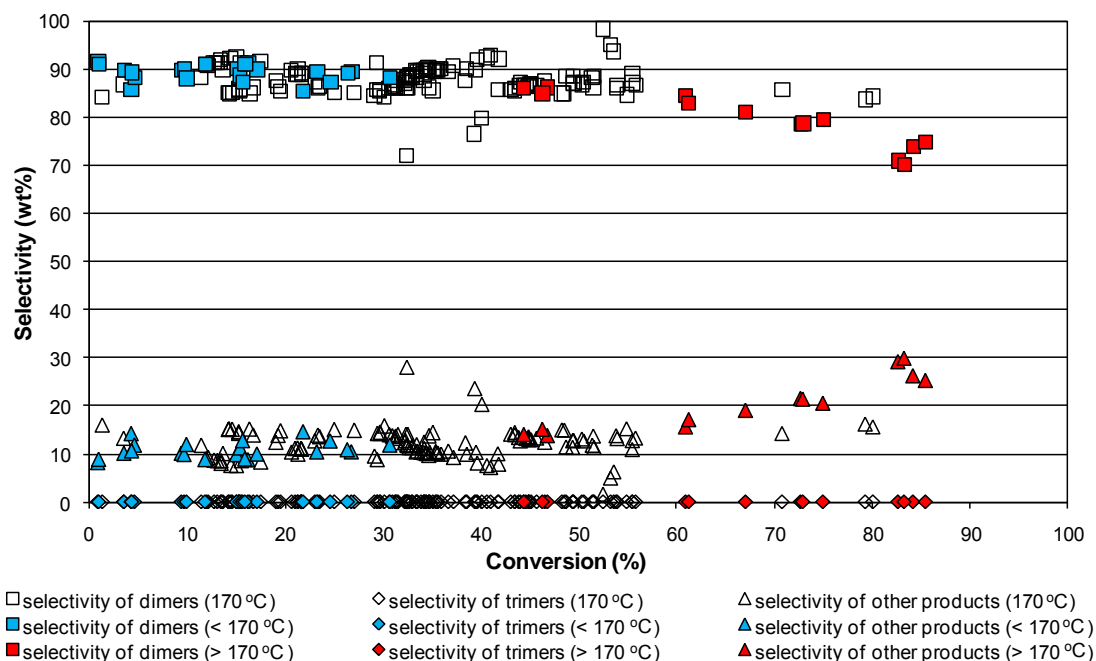


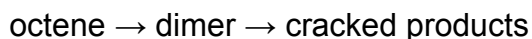
Figure 6-7: Product selectivities as a function of conversion from the dimerization of 1-octene over H-ZSM-5 at 40 bar, WHSV of 0.25-2.0 g/g.h and 100-210 °C. "Other products" are essentially lights, C₄-C₁₅. "Lights" in the context of this study are defined as all products with carbon numbers below the carbon number of the dimer, here C₁₆ but ≠ C₈. The data points (at steady state) were taken from data given in Figures 5-10, 5-11 and Table 5-7.

Table 6-3: Sources of data points from 1-octene dimerization experiments over H-ZSM-5 catalyst used to construct Figure 6-7 (condition values separated by "," refer to experimental runs carried out over the same charge of catalyst)

H-ZSM-5; 1-octene feed; 100-210 °C		
Source of data	Pressure (bar)	WHSV (g/g.h)
Figure 5-10	40	1.0
Figure 5-11	40	0.25
Table 5-7	40	0.25, 0.35, 0.5, 1.0, 1.5, 2.0

All data points considered were derived from the individual samples taken at stable activity (quasi steady state data) and not the averages calculated.

Only at higher than 50% conversion, trimers were obtained at a percentage that could be quantified. The trend of dimer and cracked product selectivity with conversion reflects the behaviour of a consecutive reaction, namely:



with the second reaction being comparatively slow.

Similar to H-ZSM-5, the ASA catalyst was also used to dimerize 1-octene and the selectivities of dimers and cracked products (“other”) as a function of conversion at 150-210 °C, 40 bar and WHSV of 0.5 g/g.h are shown in Figure 6-8.

Table 6-4 gives the sources (the respective figures) of the data points plotted in Figure 6-8, including reaction conditions. The data points in Figure 6-8 represent the individual data points obtained at steady state conditions including those that were used to calculate average data and to show average data points in the respective figures.

Table 6-4: Sources of data points from 1-octene dimerization experiments over ASA catalyst used to construct Figure 6-8.

ASA; 1-octene feed; 150-210 °C		
Source of data	Pressure (bar)	WHSV (g/g.h)
Figure 5-13	40	0.5
Figure 5-15	40	0.5
Figure 6-2	40	0.5

All data points considered were derived from the individual samples taken at stable activity (quasi steady state data) and not the averages calculated.

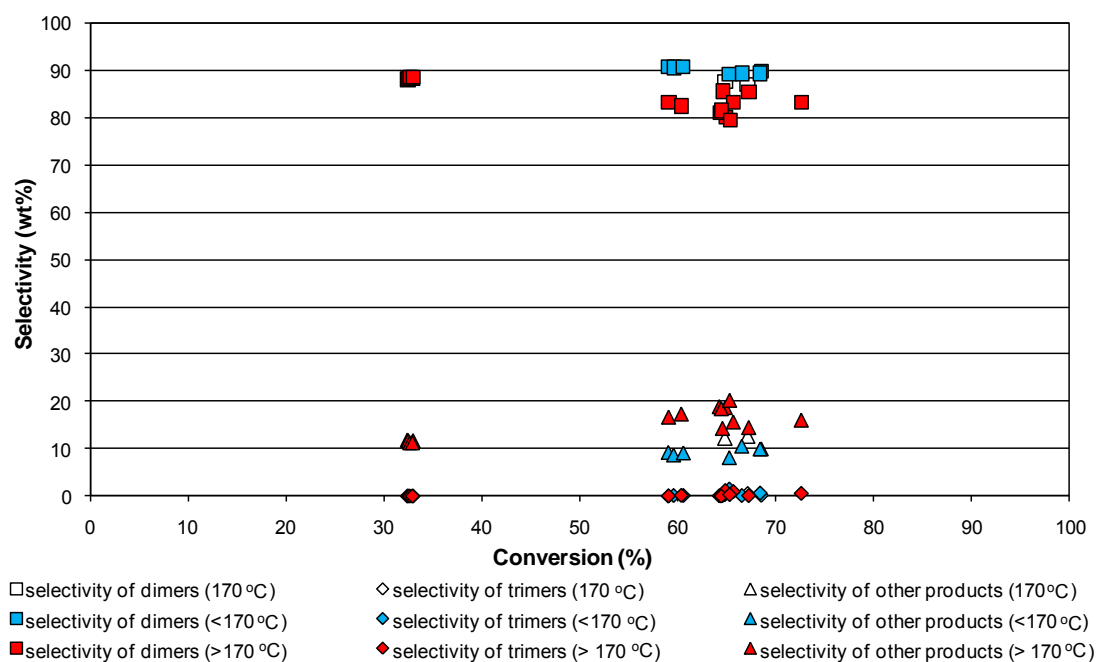
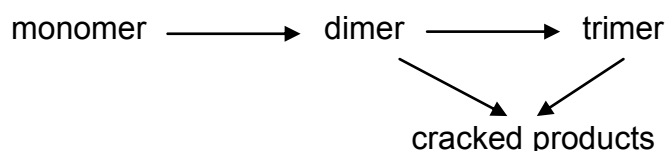


Figure 6-8: Product selectivities as a function of conversion from the dimerization of 1-octene over ASA at 40 bar, WHSV of 0.5 g/g.h and 150-210 °C. "Other products" are essentially lights, C₄-C₁₅. "Lights" in the context of this study are defined as all products with carbon numbers below the carbon number of the dimer, here C₁₆ but ≠ C₈. The data points (at steady state) were taken from data given in Figures 5-13, 5-14 and 6-2.

It can be observed in Figure 6-8 that at the lower temperatures of <170 °C, higher selectivities of dimers, i.e. around 90 wt%, were obtained at conversions above 60%. Dimer selectivities decreased with increasing temperature and more cracking products formed.

6.1.3.2.1 Summary of the conversion effects

Figures 6-1 to 6-3 and 6-4 to 6-8 suggest (and confirm) a general reaction route that comprises essentially a number of consecutive steps, namely the following.



The selectivity vs. conversion plots (Figures 6-4 to 6-8) indicate that, in general, regardless of the type of catalyst applied and the feedstock, the first step in the above sequence, namely dimerization, is significantly more rapid than the subsequent steps of trimerization and cracking.

Differences between catalysts and feedstocks with respect to their effects on product selectivities are more subtle than the similarities in major trends and the orders of magnitude indicate on first sight. These effects are discussed in detail in Sections 6.1.3.2, 6.1.3.3, 6.2.1 and 6.2.2.1.

It is also indicated in the figures, in particular in Figure 6-5, that the cracking selectivity is lower at lower temperatures, confirming that the temperature sensitivity of the cracking reaction, i.e. its activation energy, is higher than that of the oligomerization reaction.

6.1.3.3 Effect of catalyst type on carbon number distribution

The two catalysts employed, H-ZSM-5 and ASA, differed with regard to product carbon number selectivities as shown in Figures 6-4 to 6-8. Tables 5-8 and 6-5 clearly show, by direct comparison of yields and selectivities at identical temperatures and conversions, that more trimers were produced over ASA than over H-ZSM-5. However, H-ZSM-5 produced more cracked products than ASA.

Table 6-5: Dimer, trimer and cracked product selectivities from 1-hexene dimerization over H-ZSM-5 and ASA catalysts at identical reaction temperature and pressure (170 °C and 40 bar) and identical conversion (around 85%). H-ZSM-5 data are derived from Figure 5-7, average of the 24-32 days on stream data, while ASA data are derived from Figure 5-12(b), average of the 160-180 °C data.

Catalyst	WHSV (g/g.h)	Conversion (%)	Selectivity (wt%) to			
			Dimers	Trimers	Dimers + Trimers	Cracked products ^a
H-ZSM-5	0.15	85	73	9.5	82.5	17.5
ASA	0.50	88	61.5	27.5	88.5	11.5

^a “Other products” in Figures 5-7 and 5-12(b).

It was expected, point 6 of the hypothesis, Section 3.2, that carbon number distributions of products obtained from the two catalysts do not differ. However, the significant differences observed prove point 6 wrong.

6.1.3.4 Effect of mass transfer control on carbon number distribution

It can be speculated that the drastic difference in trimer selectivity may come from more severe mass transfer control imposed by the ASA catalyst compared to the zeolite catalyst. It is known, see Section 2.7, that mass transfer control imposed on a consecutive reaction reduces the selectivity to the intermediate, in this case the dimer, in favour of the secondary product, in this case the trimer.

How can the amorphous catalyst (ASA) impose more transport control on low temperature olefin oligomerization than the medium pore zeolite?

Experimental results from selectively poisoning the external surface sites of the zeolite crystallites in this study, see Sections 5.1.7 and 6.1.5 and Figures 5-8 and 5-9, the results of the previous study¹ on 1-hexene oligomerization over H-ZSM-5, and findings reported in the literature (see Section 2.5.2) show that, under mild reaction conditions, the dimerization/oligomerization of olefins over H-ZSM-5 takes place on the external surface of the zeolite crystallites.

The H-ZSM-5 catalyst used consisted of small, $\ll 0.1 \mu\text{m}$ zeolite crystallites (see Table 4-1, "H-ZSM-5"). The small crystallites provided a high external crystallite surface area and, consequently, high external surface activity, both comparable to that of the highly active "nano" *n*-H-ZSM-5 catalyst mentioned in Sections 2.4.1 (Figure 2-23) and 2.5.1. The crystallites were agglomerated to larger aggregates and these aggregates were embedded, as extrudates, in a matrix of about 20 wt% of alumina binder (see Table 4-1, "H-ZSM-5").

In order to achieve maximum effectiveness, extruded zeolite catalysts for industrial application (such as the one applied in this study) are designed for minimum mass transfer inhibition outside of the micropores of the zeolite, that is, inside the aggregates of zeolite crystallite agglomerates and in the surrounding matrix of the extrudate. This means that all of the pores outside, between and around the zeolite crystallites, i.e. inside the crystallite agglomerates and in the matrix, are macropores which, in addition to the large pore size, have a significant pore volume and a large total cross sectional area of the pores in order to allow of rapid diffusional transport of the products that have formed inside the zeolite crystallites or on the external crystallite surface back into the fluid phase and avoid mass transfer limitations.²

It was reported for propene oligomerization (for details see the second last paragraph of section 2.7.2) that dispersing small particles ($< 50\ \mu\text{m}$) of the catalyst, a mesoporous silica-alumina (pore diameter $40\ \text{\AA}$) into γ -alumina and shaping the mixture by extruding produced a macroporous matrix with the catalyst particles embedded in. The macroporous extrudates imposed no mass transfer control on the reaction. In contrast, if the mesoporous silica-alumina catalyst was extruded in bulk, significant mass transfer control occurred.³

Over extrudates from zeolites embedded in a mesoporous silica matrix (pore diameter $10\text{-}20\ \text{\AA}$), only the samples with low zeolite content, operated at low reaction temperature, as well as samples crushed to smaller size, did show no mass transfer control on the reaction performed⁴ (for details see the third last paragraph of section 2.7.2).

The ASA catalyst used in this study consisted of mesoporous extrudates (average pore diameter = 40 Å, see Table 4-1) that may provide less space (in particular less total pore volume and less cross sectional area) for diffusion and may, therefore, have imposed significant transport control on the oligomerization reaction, forcing the primary product, the dimers, towards secondary reactions, i.e. trimerization (see the two previous paragraphs and Section 2.7: Effect of mass transfer control on consecutive reactions.)

Cracking products, the “other products” or “lights” shown in the figures, are also secondary products. This is indicated by (i) the carbon number distribution of the “other products”, C₄-C₁₁, in case of 1-hexene dimerization. This fraction comprises constituents larger than the feed, as detailed in the figure captions. These compounds can only have formed from cracking dimers, that is, they are secondary products. It is also indicated by (ii) the increase in selectivity of cracking products with increasing conversion (by reducing WHSV at constant temperature), as shown in Figures 6-4 to 6-8. The selectivity to cracking products could therefore be expected to follow the same trend as the trimer selectivity, that is, higher selectivity over ASA than over H-ZSM-5. However, as can be derived from Table 6-5 and the said figures, the trend was opposite, although less pronounced, and more cracking products formed over H-ZSM-5 at identical reaction temperatures, pressure and conversions than over the ASA catalyst.

It was found that cracking selectivities from 1-hexene dimerization over H-ZSM-5 were rather constant at a level of around 10% over a wide range from medium to low conversion (see Figure 6-4), while those obtained over ASA were lower

and declined constantly with decreasing conversion (see Figure 6-6), suggesting that there might be an “inherent” cracking activity of H-ZSM-5 (inside the micropore system) that produced these cracking products.

The higher cracking specificity of the zeolite may indeed indicate towards some feed molecules penetrating the micropore system and dimerizing but not to grow further to trimers and desorb as trimers rather than crack before leaving the zeolite crystallites due to much enhanced diffusion inhibition in the micropores.

This explanation is strongly supported by the selectivities obtained over the H-ZSM-5 catalysts whose external crystallite surface was selectively poisoned (see Section 5.1.7 and Figures 5-8 and 5-9). In Figure 6-4, the $\leq 10\%$ conversion data points represent the product from these external crystallite surface pre-poisoned catalysts by charging a pre-poisoned catalyst (see Section 4.3.1 and Figure 5-9) or switching to poisoned feed during the run, so that the catalyst became increasingly surface-poisoned with time-on-stream (see Section 4.3.1 and Figure 5-8). Of these catalysts, the sites in the internal micropore system are supposed to be untouched, while the external sites are poisoned or are increasingly disappearing due to poisoning. The decline in dimer selectivity and significant increase in cracking product selectivity upon external poisoning (these are the highest cracking product selectivities obtained within all the experiments) suggest that the origin of (most of) the cracking products is the internal (micro-)pore system of the zeolite catalyst. Obviously, mass transfer control in the micropores is severe – and it is that severe that the cracking products even appear as pseudo primary products (see Section 2.7.1).

Consequently, the higher cracking specificity of the H-ZSM-5 catalyst appears not to contradict but rather confirm that the higher trimer selectivity from 1-hexene feed over the ASA catalyst is due to enhanced mass transfer control in the meso-pore system of the ASA extrudates as compared to the macro-pore system of the zeolite extrudates. It appears that the causes of the observed effects, the reasons behind the phenomena of higher cracking selectivity over H-ZSM-5 and higher trimer selectivity over ASA, are the same, namely mass transfer control, just less over the ASA catalyst, so that the trimers formed survive, whereas they react further (by cracking) in the H-ZSM-5 crystallites.

6.1.4 Branching of the dimers

6.1.4.1 Effect of double bond isomerization in the feed on branching

As literature (see Section 2.3.2.1, Figure 2-19) and the experiments within this study (see the introductions to Sections 5.1 and 5.2 and product chromatograms, Figure 4-4) showed, double bond isomerization in the feed olefins occurs much more rapidly than dimerization. Consequently, the “real” feeds in this study were mixtures of the thermodynamically equilibrated *n*-hexene or *n*-octene double bond isomers, i.e., a *n*-olefin isomers equilibrium pool. This confirms point 1 of the hypotheses (see Section 3.2).

Under the reaction conditions applied, the thermodynamically favoured *n*-hexene isomers are the 2-hexenes as given in Table 5-2. The abundance of the 2-hexenes in the equilibrated reaction mixture is twice that of the 3-hexenes while the percentage of the 1-hexene isomer is negligible (3%). In the

equilibrated octene feed, the percentage of the 1-isomer is even lower, < 1% (see Table 5-6). Therefore, the formation of dimers involving a 1-hexene or 1-octene feed molecule will only occur with very little likelihood and, consequently, the respective dimers will only form with negligible selectivity (see Section 6.1.4.2). The same holds for products whose formation would involve a primary carbenium ion as the co-reactant in the dimerization step.

6.1.4.2 Theoretical analysis of *n*-hexene dimerization and dimer branching

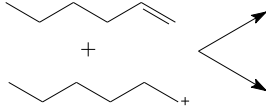

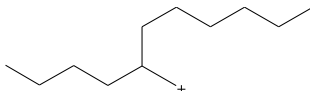
In Table 6-6 the possible products of *n*-hexene dimerization are shown. It appears clearly from this table that products “x 2”, followed by products “x 1” (see last column in Table 6-6), are the most likely ones to form and to occur in the *n*-hexene dimerization product mixture, since their formation involves the most abundant species in the reaction mixture, namely the internal olefins and, correspondingly, the internal carbenium ions (first column). These products will all be di-branched (with both, methyl and ethyl side chains) and they will show a 12:14 ratio of CH₃ and CH₂ plus CH signals in the ¹H-NMR spectrum once hydrogenated (see Section 4.4.2 and Table 4-2). Di-branched products D, E and F are not distinguishable in the ¹H-NMR spectrum, with all of them having the same number of CH₃ (12) and CH₂ plus CH (14) protons, corresponding to a degree of branching of 2.0.

Formation of the non- and mono-branched products (A, B and C) involves either the 1-hexene isomer or a primary carbenium ion or both. Under kinetic control of the dimerization reaction and considering rapid double bond isomerization (see Section 6.1.4.1), all linear and mono-branched dimerization

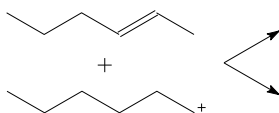
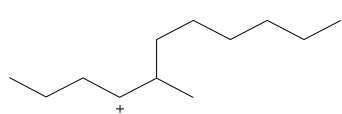
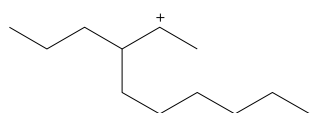
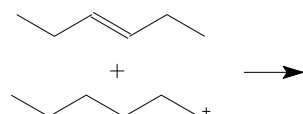
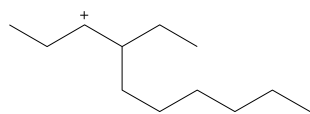
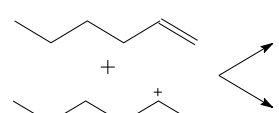
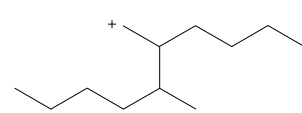
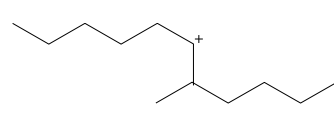
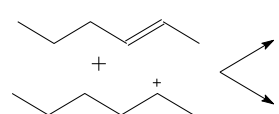
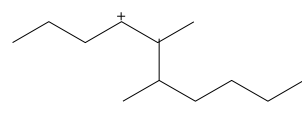
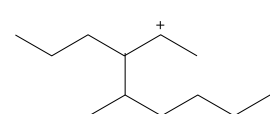
products will, therefore, only be formed at a very small/negligible extend (likelihood “unlikely” or “negligible” in Table 6-6). These products would show a 6:20 (A) or 9:17 (B and C) ratio of CH₃ and CH₂ plus CH signals in the ¹H-NMR spectrum (see Section 4.4.2 and Table 4-2), corresponding to a degree of branching of 0.0 or 1.0.

Dimerization products with structures such as (G) and (H), with three side chains (see Table 6-7), require an additional skeletal isomerization step, be it of one of the hexene monomers or of the dimer. This means that, with respect to the *n*-olefin isomers equilibrium feed pool, tri-branched dimers are secondary products. The selectivity of such tri-branched compounds can, therefore, be expected to be low at low dimerization conversion. Products would show a 15:11 ratio of CH₃ and CH₂ plus CH signals in the ¹H-NMR spectrum (see Section 4.4.2 and Table 4-2).

Table 6-6: Reaction schemes of *n*-hexenes dimerization, assuming equilibrium distributions of the *n*-hexene double bond isomers in the reaction mixture and similar stabilities and prevalences of the *n*-hexyl carbenium ions, depicting the type of products forming and the approximate likelihood (statistically) of formation.

<i>n</i> -Hexene isomers reactions with <i>n</i> -hexyl carbenium ions		Product type	Likelihood
		A	Unlikely ¹
		B	Unlikely

¹ Unlikely: involves a primary carbenium ion on the reactant or product side.

<i>n</i>-Hexene isomers reactions with <i>n</i>-hexyl carbenium ions		Product type	Likelihood
		B	Unlikely
		C	Unlikely
		C	Unlikely
		D	Unlikely
		B	Negligible ²
		D	x 2 ³
		E	x 2

² Negligible: involves the 1-hexene isomer, which is only 3% in the equilibrated mixture of *n*-hexenes (see Table 5-2).

³ x 2: involves the 2-hexene isomers which are twice as abundant as the 3-hexenes (x 1) in the equilibrated mixture of *n*-hexene isomers (see Table 5-2).

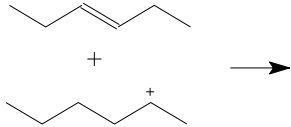
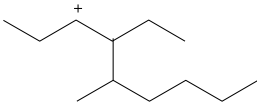
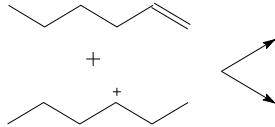
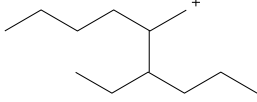
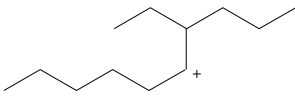
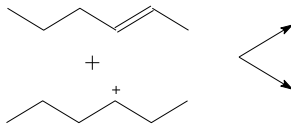
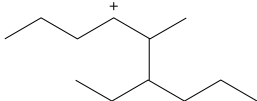
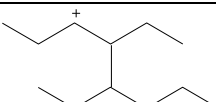
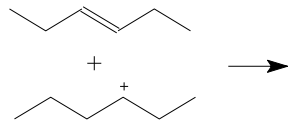
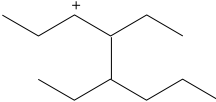
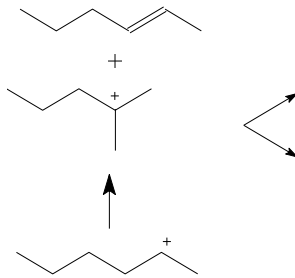
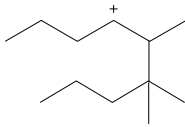
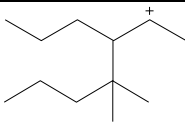
<i>n</i>-Hexene isomers reactions with <i>n</i>-hexyl carbenium ions		Product type	Likelihood
		E	x 1
		E	Unlikely
		C	Negligible
		E	x 2
		F	x 2
		F	x 1

Table 6-7: Example of a reaction scheme of possible reactions of *n*-hexene isomers with branched hexyl carbenium ions

Reaction of 3-hexene with 2-methyl pentyl carbenium ion		Product type	Likelihood
		G	Little ⁴
		H	Little

⁴ Little: involves a (comparatively slow) skeleton isomerization step, i.e. a secondary product with low likelihood in particular at low conversion.

Consequently, the vast majority of products could be expected to be di-branched, i.e. the average degree of branching would be larger than 2 but still close to 2.

6.1.4.3 Experimental results for *n*-hexene and *n*-octene dimer branching

Figure 6-9 shows the degree of branching obtained from both the feeds and both the catalysts as a function of conversion.

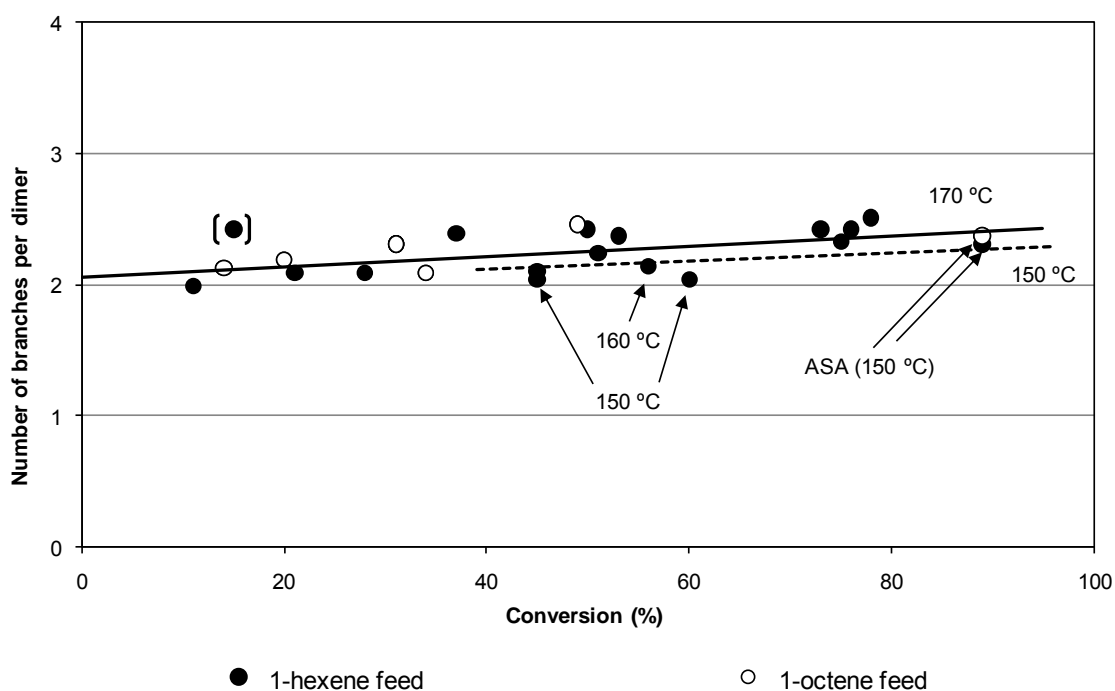


Figure 6-9: Degree of branching of the dimers as a function of conversion as obtained from the dimerization of the two feeds, 1-hexene and 1-octene, over H-ZSM-5 and ASA at different reaction conditions (solid line = 170 °C trend line, dotted line = 150 °C trend line). Data taken from Tables 5-3, 5-5, 5-7, 5-9 and 5-10.

The results shown in Figure 6-9 prove the hypothesis in points 3 to 5 (see Section 3.2), in that the resulting branching of in the dimers is not determined

by shape-selective constriction effects, since there is no noticeable difference between the two catalysts studied (the medium pore zeolite and the amorphous catalyst) and confirms the hypothesis in point 7, namely, that dimerization proceeds, effectively, on the external surface of the H-ZSM-5 zeolite crystallites.

This was confirmed by the selective poisoning of the external sites of H-ZSM-5 (see Section 4.3.1), which left hardly any activity behind for the dimerization of 1-hexene (see Section 5.1.7 and Figures 5-8 and 5-9), clearly indicating that the dimerization reaction, under the conditions applied, hardly penetrated into the pore system of the zeolite (except for the small percentage that ended cracked). This clearly proves the basis of point 4 of the hypothesis (see Section 3.2) right.

Extrapolation of the trendlines in Figure 6-9 to zero conversion results in a branching of 2 per dimer molecule, irrespective of the catalyst or feed applied. This confirms the approach and result of the theoretical analysis (see Section 6.1.4.2) and again proves points 3 and 4 of the hypothesis correct. The observations also suggest that, to some extent, the degree of branching is a function of reaction severity, that is, of temperature and conversion (and space velocity), proving point 8 of the hypothesis correct. At identical conversions the higher temperature product appears slightly more branched (see Figure 6-9).

Data collected at 170 °C (all data points in Figure 6-9 not pointed to by an arrow) show that at 80% conversion the degree of branching of the dimers is around 2.4. That is, about 40% of the dimers (or one of the monomer precursors of each dimer, corresponding to a maximum of 20% of the monomers) have

undergone skeletal isomerization. The data indicates that skeletal isomerization, under this condition, is less than half as rapid as dimerization.

Chromatograms (see Figure 4-4) showed additional peaks in the C₆- and C₈-monomer ranges, other than the five or seven peaks, respectively, for the linear olefin isomers, which were identified as branched olefins. Chromatograms showed that at higher conversions the branched isomers were also consumed.

6.2 Comparison of feeds

6.2.1 Reactivity of the two different feeds

The reactivities of the two feeds, *n*-hexene and *n*-octene appear to differ. At equal reaction conditions (170 °C, 40 bar and WHSV of 0.5 g/g.h) conversion of 1-hexene over H-ZSM-5 was at around 75-80% (Figures 5-1, 5-2, 5-3 and 5-12(a)), while conversion of 1-octene was only at around 30% (Table 5-10). Over amorphous silica-alumina (150 °C, 40 bar and WHSV of 0.5 g/g.h) conversion of 1-hexene was around 85-90% (Figures 5-12(b) and 5-13), while conversion of 1-octene hardly rendered 70% (Figure 5-14).

However, given the relative concentrations of double bonds in the feed, it appears that reactivities are in fact rather similar. Hexenes carry one C=C double bond per molecule and four C-C single bonds while octenes carry one C=C double bond per molecule and six C-C single bonds. 1 kg of hexene

contains, therefore, 1000/84 moles, while 1 kg of octene contains only 1000/112 moles (with 84 and 112 being the respective molecular masses in g).

Consequently, at equal $WHSV_{olefin}$ the molar space velocities of 1-hexene and 1-octene, here abbreviated “molHSV”, and, consequently, the molar space velocities of the double bonds, $molHSV_{double\ bonds}$, differed:

$$\frac{molHSV_{1-hexene}}{molHSV_{1-octene}} = \frac{molHSV_{double\ bonds, 1-hexene}}{molHSV_{double\ bonds, 1-octene}} = \frac{112}{84} = \frac{4}{3}$$

On the other hand, applying fundamental reaction kinetics, that is a second order rate equation for the bimolecular dimerization reaction, such as

$$r = k \times C_{double\ bonds}^2$$

leads to

$$\frac{r_{1-hexene}}{r_{1-octene}} = \left(\frac{4}{3} \right)^2$$

so that for the ratio of conversions X

$$\frac{X_{1-hexene}}{X_{1-octene}} = \frac{r_{1-hexene}}{r_{1-octene}} \bigg/ \frac{molHSV_{1-hexene}}{molHSV_{1-octene}} = \left(\frac{4}{3} \right)^2 \bigg/ \left(\frac{4}{3} \right) = \frac{4}{3} = 1.33$$

Consequently, one would expect almost 1.5 times higher a conversion of the 1-hexene feed. This ratio corresponds to the differences observed, see e.g. Tables 5-5 and 5-7: $X_{1-hexene} = 50\%$ and $X_{1-octene} = 31\%$ (H-ZSM-5, 170 °C, 40 bar, $WHSV_{olefin} = 1.0\ g/g.h$) and Figures 5-13 and 5-14: $X_{1-hexene} = 85\%$ and $X_{1-octene} = 68\%$ (ASA, 150 °C, 40 bar, $WHSV_{olefin} = 0.5\ g/g.h$).

In other words, reactivities of the 1-hexene and the 1-octene feed differ. This confirms point 7 of the hypothesis wrong with respect to reactivity. However, with respect to double bonds' reactivity differences are little.

6.3 Product properties with respect to use as diesel fuel

The ultimate objective of the study was the dimerization of naphtha-range olefins into diesel-range products and finally, by hydrogenation of these, into diesel fuel. Figure 6-10 shows the cetane numbers of the hydrogenated C_{16} dimers from 1-octene dimerization as a function of their average degrees of branching.

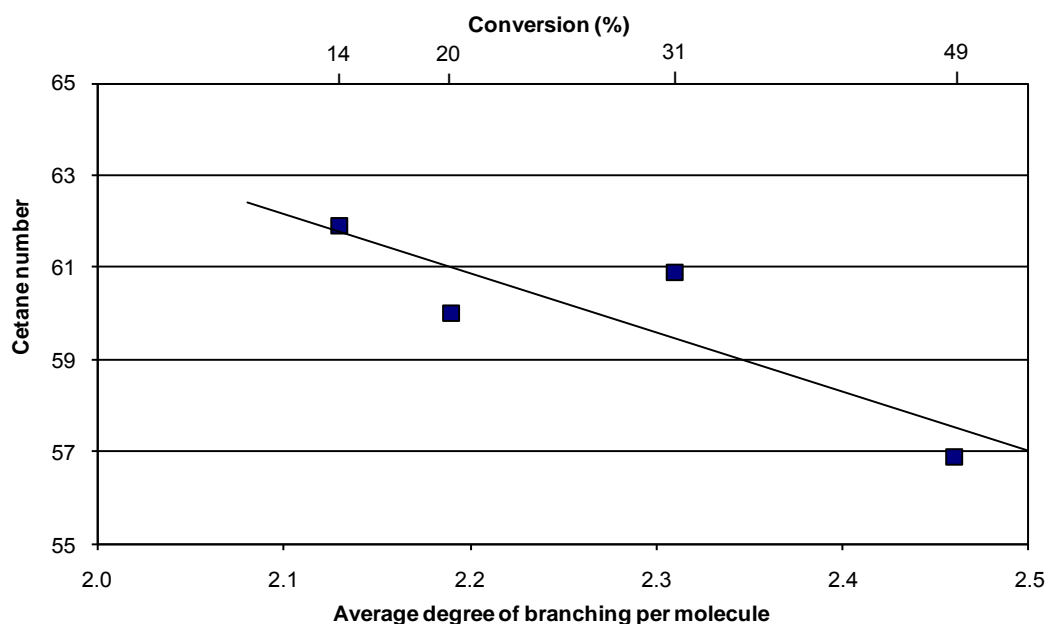


Figure 6-10: Cetane number of C_{16} fraction obtained from 1-octene dimerization over H-ZSM-5 (170 °C, 40 bar, WHSV = 0.25-2.0 g/g.h, hydrogenated) as a function of degree of branching (and conversion). Data taken from Table 5-7.

The results indicate that the cetane number decreases with increasing degree of branching. Higher conversions, as a result of decreasing space velocity, i.e. longer contact times of the octene feed over the catalyst or higher temperatures led to an increased degree of branching, see Table 5-7, 3rd and 5th column, and Figures 6-9 and 6-10, and, consequently, led to lower cetane numbers. In Table 6-8 diesel specific properties of dimerization and other synthetic diesel fuels are compared and juxtaposed to current and future standards.

Table 6-8: Diesel specific properties of the hydrogenated C₁₆ olefin fraction of the 1-octene dimerization product (H-ZSM-5 catalyst, 170 °C, 40 bar, WHSV of 0.25 and 0.5 g/g.h, see Table 5-7) compared to other diesel fuels from olefin oligomerization, Fischer-Tropsch synthesis, Fischer-Tropsch wax hydrocracking and compared to SA and European standards.

Product	Implementation year	Conversion (%)	Average degree of branching per molecule ^j	Cold Filter Plugging Point (CFPP), (°C) ^k	Density (g/ml) at 15 °C ^k (* at 20 °C)	Pour Point (°C) ^k	Kinematic viscosity at 40 °C	Cetane number ^k	Sulphur content (ppm)
C ₁₆ ^a	-	49	2.46	-27	0.7813	< -42	2.26	56.9	-
C ₁₆ ^a	-	31	2.31	-27	0.7838	< -42	2.42	60.9	-
MOGD ^{b,5}	-	-	-	-	0.7800*	< -50	2.5	52-56	-
COD ^{c,6}	-	-	-	-45	0.796*	< -42	2.7	51-54	< 2
CatPoly ^{d,7}	-	-	-	-	0.797-0.798*	-	2.1	29-30	-
Sasol SPD TM and LTFT diesel ^{e,8,9,10,11}	-	-	-	-19	0.777	-	2.4	>73	< 5
FT wax hydrocracking ^{f,12,13}	-	-	-	-23	0.762*	-	3.3	>70	< 5
Sasol HTFT diesel ^{g,10}	-	-	-	-6	0.829	-	2.2	55	< 5
Current South African specifications (Euro 3) ^{h,14}	2008	-	-	-4 or 3	0.800-0.860*	-	2.2-5.3	49	500/50
Future South African specifications (Euro 4) ^{14,15}	2014	-	-	-8	0.820-0.845	-	2.0-4.5	51	50/15
Current European specifications (Euro 5) ^{i,16}	2009	-	-	-8	0.820-0.845	-	2.0-4.5	51	10
Future European specifications (Euro 6)	2014	-	-	-10	0.820-0.845	-	2.0-4.5	51	< 10

^a Hydrogenated C₁₆ olefin fraction from 1-octene dimerization.

^b Mobil's Olefins to Gasoline and Diesel process (see Section 2.3.2).

^c PetroSA's Conversion of Olefins to Diesel process (see Section 2.3.3).

^d UOP's Catalytic Polymerization process as applied at Sasol's Secunda refineries, hydrogenated (see Section 2.3.4).

^e Sasol Slurry Phase DistillateTM and Sasol Low Temperature Fischer-Tropsch processes' straight run diesel (hydrogenated) (Qatar and Sasolburg).

^f Iron-based slurry reactor wax, hydrocracked over sulfided NiMo/SiO₂-Al₂O₃.

^g Sasol High Temperature Fischer-Tropsch (HTFT) process' straight run diesel (Secunda), aromatic content ~25 wt%.¹⁰

^h Arabic numerals in Euro stages are for light-duty vehicles.¹⁶

ⁱ Polycyclic aromatic hydrocarbons (PAH) content max. 8 wt% (from 2011).¹⁶

^j Determined by ¹H-NMR (see Section 4.4.2).

^k See Table 4-3 for determination of respective fuel properties and definition.

As can be derived from Table 6-8 and Figure 6-10 and generalized with respect to the catalysts and feeds, diesel obtained from naphtha-range olefin dimerization (here, exactly, the hydrogenated C₁₆ dimer fraction) will, depending on the extent of per pass conversion and the resulting degree of branching per molecule, have cetane numbers between 55 and 60. These cetane numbers, and the other properties, are not too different from those obtained from the MOGD and COD processes, and cold flow properties are still above the minimum requirements. Compared to those of CatPoly diesel cetane numbers are much better.

Cetane numbers of dimerization-diesel are, however, not as high as the cetane numbers of *n*-paraffinic straight run low temperature Fischer-Tropsch synthesis derived diesel (hydrogenated) and slightly isoparaffinic FT wax-hydrocracking diesel but similar to the (partially aromatic) straight run diesel derived from high temperature Fischer-Tropsch synthesis and MOGD and COD oligomer diesel (see Table 6-8). Nonetheless, cetane numbers of dimerization-diesel are higher than the cetane numbers required for diesel fuel in South Africa and Europe, currently and in future (see Table 6-8).

Naphtha-range olefin dimerization diesel is only insufficient in density. The current density specification is not met (see Table 6-8). However, future legislation will also comprise significant reductions in the contents of polyaromatic hydrocarbons (PAH) and aromatic hydrocarbons with the percentage of the former already limited to 8 wt%, since 2011, by the Euro 5 legislation.¹⁶ These limitations will, naturally, require extending or shifting the density window to lower levels.

Naphtha-range olefin dimerization diesel appears to be particularly suitable, under the present regulations, as a blending stock for high density, low cetane number below-diesel-standard gas oil fractions derived from crude oil.

6.4 Conclusions

6.4.1 Dimerization product properties and quality

Dimerization/trimerization of naphtha-range *n*-olefins produces a mixture of moderately branched diesel-range hydrocarbons that, after hydrogenation, has properties similar to MOGD (Mobil) or COD (PetroSA) oligomer diesel, but is superior to Sasol's current CatPoly oligomer diesel in terms of density and cetane number (see Table 6-8). Dimerization derived diesel meets or exceeds all current South African and European diesel fuel specifications as well as those intended to be implemented in the near future, except density (see Table 6-8).

Under the present regulations olefin dimerization/trimerization diesel was a good blending stock for high density, low cetane number gas oil fractions derived from crude oil that are below diesel standards. However, worldwide legislation, for instance the Euro 5 (2009) to Euro 6 (from 2014 onwards) standards¹⁶, tends towards lower limits for polyaromatics and aromatics, which will, ultimately, result in a shift of the future density window to lower levels, so that density specification will eventually be met as well.

6.4.2 Optimum reaction conditions

Acid catalyzed naphtha-range olefin dimerization can be performed in the liquid phase under rather mild conditions. At 150 °C, the ASA catalyst, the catalyst of choice, is sufficiently active for operating at space velocities around 0.5 g/g.h, but still hardly active for undesired cracking reactions. The minimum operating pressure required with a hexene feed at 150 °C is less than 10 bar (see Section 5.1.5).

6.4.3 Catalyst of choice

Potential industrial scale production of dimer/trimer diesel from naphtha-range olefins will not require utilization of an expensive zeolite catalyst. As the study reveals, a comparatively cheap amorphous silica-alumina (ASA) catalyst is well suitable. The ASA catalyst used in this study shows a higher activity than the H-ZSM-5 zeolite tested (see Section 6.1.1) and similar long term stability (see Section 6.1.2). Both types of catalyst are known to be fairly insensitive to moisture and oxygenates in the reaction mixture under conditions such as the applied and regenerable once fouled or coked.

The degrees of branching of the dimers obtained at identical reaction temperatures and identical conversions from the two catalysts, H-ZSM-5 and ASA, are identical, controlled by conversion and, to a lesser extent, reaction temperature. Degrees of branching range from 2.0 at 'zero' conversion up to 2.5 at about 80 – 90% conversion (see Figure 6-9). The degrees of branching provide a product that is well balanced with regard to cetane number and cold

flow properties, similar to those of the olefin oligomer diesel fuels from the MOGD and COD processes (see Table 6-8).

However, with regard to carbon number distribution, products from H-ZSM-5 and ASA differ significantly. Trimer selectivity is much higher over the ASA catalyst (essentially at the expense of the dimers), while the selectivity to cracked products is higher over the zeolite (see Table 6-5). With regard to technical application this was a difference in favour of the ASA catalyst.

All of the aforementioned makes ASA superior a catalyst for naphtha-range olefin dimerization and trimerization to diesel fuel, not only in comparison with medium pore zeolite H-ZSM-5 but even more so in comparison with solid phosphoric acid, the CatPoly catalyst.

6.4.4 Any naphtha-range olefins may be fed

Rates per mass of feed decline with increasing carbon number, but rates per double bond stay constant. Double bond and skeleton isomerized feed constituents form and are consumed in the dimerization reaction. Paraffinic feed constituents can be expected to be inert, just lowering olefin concentrations.

The above suggests that any naphtha-range olefins containing stream was a suitable feedstock for ASA (or zeolite) catalyzed olefin dimerization/trimerization to diesel. Consequently, every such stream from the Fischer-Tropsch refinery (for instance residual streams from chemicals extraction processes) was a suitable feedstock for dimerization/trimerization.

6.5 References

- ¹ M.L.O. Sumani, MSc Thesis, Department of Chemical Engineering, University of Cape Town (2006).
- ² J.C.Q. Fletcher, Centre for Catalysis Research, Department of Chemical Engineering, University of Cape Town, personal communication (2007).
- ³ S. Peratello, M. Mollinari, G. Belusso, C. Perego, *Catal. Today*, 52 (1999) 271-277.
- ⁴ J.-P. Lange, C.M.A.M. Mesters, *Appl. Catal. A: General*, 210 (2001) 247-255.
- ⁵ S.A. Tabak, R.E. Holland, M.R. Ireland, AIChE Summer National Meeting, Philadelphia, PA, August 19-22 (1984) Paper 42a.
- ⁶ C.D. Knottenbelt, C. Dunlop, K. Zono, M. Thomas, WO 069407 A2 (2006), assigned to The Petroleum Oil Corporation of South Africa (Pty) Ltd. (PetroSA).
- ⁷ D. Leckel, *Energy & Fuels*, 23 (2009) 2342-2358.
- ⁸ L.P. Dancuart, R. de Haan, A. de Klerk, *Stud. Surf. Sci. Catal.*, 152 (2004) 482-532.
- ⁹ A. de Klerk, *Energy & Fuels*, 21 (2007) 625-632.
- ¹⁰ B.I. Kamara, J. Coetzee, *Energy & Fuels*, 23 (2009) 2242-2247.
- ¹¹ D. Lamprecht, *Energy & Fuels*, 21 (2007) 2846-2852.
- ¹² D. Leckel, *Energy & Fuels*, 21 (2007) 1425-1431.
- ¹³ D. Leckel, *Energy & Fuels*, 23 (2009) 32-37.
- ¹⁴ South African National Standards, www.sapia.co.za (Petrol and Diesel in South Africa and the impact on air Quality – November 2008), accessed 2010-01-02.

-
- ¹⁵ Department of Energy, Republic of South Africa, “Draft Position On Fuel Specifications and Standards”, Government Gazette No. 34089, Vol. 549, (March 2011).
- ¹⁶ 2011 Worldwide Fuel Specifications, Hart Energy Publishing, 12th Edition, (2011), www.ifgc.org (accessed 2011-06-29).

CHAPTER 7

7. RECOMMENDATIONS

The outcome of the study suggests a number of additional investigations to be carried out over the ASA catalyst. These may comprise the following:

- Operation at low pressure in the gas phase (which may ease operation but accelerate coking or cracking).
- Conversion of naphtha-range iso-olefin model compounds (to compare to *n*-olefin reactivities). The iso-olefins may essentially be methyl branched olefins as found in Fischer-Tropsch product streams.
- Dimerization of naphtha-range olefins of carbon numbers higher and lower as C₈ and C₆ (to confirm and more accurately quantify carbon number effects on reactivity).
- Operation with different carbon number olefins also at low pressure in the gas phase (which may result in reversed olefin carbon number reactivity ranking).
- Dimerization of samples of technical olefinic or olefin containing residual streams from the Fischer-Tropsch refinery (such as those left from α -olefin recovery).
- Evaluation of ASA catalysts of different silica/alumina ratios, pore diameters and particle size (with respect to activity, stability and selectivity with specific focus on mass transfer control effects, i.e. dimer, trimer and crack product selectivities).

- Optimization of reaction conditions, with particular foci on temperature effects on reaction rate, branching, cetane number and per pass conversion on branching and cetane number.
- Long term tests lasting over several months.

Additional investigations may be carried out over H-ZSM-5 in order to finally answer the questions about the location of the dimerization reaction and the accelerated cracking reaction on the zeolite crystallites. These investigations may comprise the following:

- Selective poisoning of the internal sites of the zeolite crystallites, see Section 2.5.3. This measure should (i) hardly affect conversion and rate in the dimerization reaction but reduce cracking selectivity, and (ii) hardly affect trimer selectivity (to confirm (i) that cracking takes place inside the zeolite pore system, and (ii) confirm the different effects of mass transfer control on trimer selectivities over ASA and H-ZSM-5.
- Studies in the gas phase (to investigate whether or not the dimerization reaction is still confined to the external zeolite crystallite surface under such conditions).

APPENDIX (DATA)

1. 1-Hexene over H-ZSM-5 catalyst

Reaction conditions and reference:	1-Hexene feed, H-ZSM-5 catalyst, 50-210 °C, 40 bar and WHSV of 0.5 g/g.h; Figure 5-1																		
	50 °C					75 °C				100 °C					125 °C				
TOS (days)	0.1	0.3	0.5	0.9	1.0	1.1	1.3	1.5	1.7	2.1	2.2	2.2	2.3	2.5	3.0	3.1	3.2	3.3	3.5
% conversion	5.4	3.2	6.4	5.7	4.9	4.5	4.7	8.2	9.2	13.4	19.1	20.4	20.4	19.0	37.9	39.2	37.0	35.6	34.8
% selectivity to dimers	92.4	86.0	89.3	88.9	89.3	88.9	89.5	93.0	93.6	94.3	95.0	95.4	95.9	95.9	95.6	92.4	96.1	96.1	94.0
% selectivity to trimers	0.0	1.6	3.9	3.5	1.7	1.4	1.3	0.8	0.7	0.4	0.4	0.5	0.3	0.4	1.4	4.9	1.4	1.3	3.5
% selectivity to others	7.6	12.4	6.8	7.6	9.0	9.7	9.3	6.2	5.7	5.3	4.6	4.1	3.8	3.8	3.0	2.7	2.6	2.6	2.5
	150 °C					160 °C					170 °C					180 °C			
TOS (days)	4.0	4.1	4.1	4.2	4.4	5.0	5.1	5.1	5.2	5.4	6.0	6.1	6.1	6.2	6.3	7.0	7.2	7.5	8.0
% conversion	59.9	60.9	59.1	61.3	58.1	68.9	66.6	66.9	65.8	58.1	74.9	73.9	74.1	76.3	76.6	75.9	82.9	82.8	82.3
% selectivity to dimers	92.9	90.5	94.1	86.5	92.4	83.7	90.5	90.6	91.8	92.4	85.2	91.0	89.9	84.8	92.0	90.7	85.5	81.8	85.8
% selectivity to trimers	3.1	5.4	2.1	9.5	3.6	12.3	4.3	4.5	3.1	3.6	4.8	0.4	0.7	8.3	1.5	0.6	5.5	8.9	5.6
% selectivity to others	4.0	4.1	3.9	4.0	4.0	4.0	5.2	5.0	5.1	4.0	10.0	8.6	9.4	7.0	6.6	8.7	9.1	9.3	8.6
	190 °C				200 °C				210 °C										
TOS (days)	8.1	8.3	8.5	9.0	9.1	9.1	10.0	10.2	10.3	10.3	10.6								
% conversion	85.6	88.4	88.9	89.4	92.5	92.5	92.3	89.6	89.9	88.9	88.8								
% selectivity to dimers	84.8	86.1	85.7	80.9	78.4	78.8	79.9	64.3	63.3	62.9	63.7								
% selectivity to trimers	2.2	1.4	1.1	5.6	2.0	2.5	0.8	0.0	0.0	0.0	0.0								
% selectivity to others	13.0	12.5	13.2	13.5	19.7	18.6	19.4	35.7	36.7	37.1	36.3								

Reaction conditions and reference:	1-Hexene feed, H-ZSM-5 catalyst, 170 °C, 40 bar and WHSV of 0.5 g/g.h; Figure 5-2									
TOS (days)	0.9	1.0	1.2	1.8	2.1	2.4	2.8	3.0	3.2	3.3
% conversion	78.8	78.0	77.0	75.9	74.6	73.6	73.2	74.2	71.2	72.8
% selectivity to dimers	79.5	89.7	81.6	90.7	91.2	91.3	88.4	87.4	92.3	89.4
% selectivity to trimers	0.8	0.6	1.0	0.6	1.2	1.0	3.7	5.4	0.2	4.9
% selectivity to others	19.7	9.7	17.4	8.7	7.6	7.7	8.0	7.2	7.5	5.7

Reaction conditions and reference:	1-Hexene feed, H-ZSM-5 catalyst, 170 °C, 40 bar and WHSV of 1.0 and 0.5 g/g.h; Figure 5-3																		
	WHSV = 1.0 g/g.h																WHSV = 1.0 g/g.h		
TOS (days)	0.2	0.7	0.9	1.1	2.0	2.2	2.7	2.8	2.9	3.2	3.7	3.8	3.9	4.0	4.7	5.1	5.7	5.8	5.9
% conversion	11.8	60.9	46.9	48.0	42.1	48.0	44.1	53.6	43.0	38.5	38.5	38.4	37.2	38.1	34.0	30.4	43.0	45.6	50.9
% selectivity to dimers	83.6	84.0	94.1	91.6	94.9	94.6	95.0	94.5	94.9	95.5	95.5	94.7	95.3	95.2	95.2	95.1	95.0	94.7	90.6
% selectivity to trimers	0.0	10.4	1.6	0.1	0.9	0.7	0.8	0.6	0.8	0.7	0.7	1.0	0.4	0.6	0.4	0.0	0.3	1.1	4.1
% selectivity to others	16.4	5.6	4.3	8.3	4.2	4.8	4.2	4.9	4.3	3.8	3.8	4.4	4.3	4.3	4.4	4.9	4.7	4.1	5.3
	WHSV = 1.0 g/g.h																		
TOS (days)	6.0	6.2	6.7	6.8	6.9	7.0	7.3	7.7	8.7	9.0	9.7	9.8	9.9	10.0	10.6	10.8	10.9	11.1	11.7
% conversion	57.3	62.0	67.0	67.0	68.1	66.9	65.6	66.4	64.0	54.7	53.0	53.8	54.2	54.2	52.0	51.4	47.9	54.4	51.8
% selectivity to dimers	89.7	89.8	85.2	91.1	87.5	91.4	86.0	86.6	87.6	92.8	92.2	88.3	92.9	92.8	92.9	89.5	91.8	91.1	86.9
% selectivity to trimers	5.2	4.7	8.6	3.0	6.7	2.5	7.2	6.6	6.2	0.5	1.0	4.9	1.0	1.1	0.9	3.7	1.1	2.4	6.7
% selectivity to others	5.1	5.5	6.2	6.0	5.9	6.0	6.8	6.7	6.2	6.7	6.8	6.8	6.1	6.1	6.2	6.9	7.1	6.4	6.4
	WHSV = 1.0 g/g.h																		
TOS (days)	11.8	12.0	12.7	12.9	13.7	13.8	14.1	14.6	15.0	15.7	15.9	16.2	16.7	16.9	17.1	17.7	17.9	18.1	18.7
% conversion	48.9	49.6	48.6	49.4	47.7	48.1	47.1	45.6	48.6	42.7	42.4	42.4	43.6	41.4	45.1	41.7	41.6	42.4	41.3
% selectivity to dimers	91.8	91.8	89.6	88.4	87.6	91.3	88.3	91.6	89.9	92.5	92.0	90.2	89.1	91.5	91.7	91.3	92.8	92.1	92.4
% selectivity to trimers	1.2	1.5	3.3	4.5	5.3	1.6	4.4	1.0	3.1	0.9	1.0	2.8	4.5	1.2	0.9	2.0	1.0	0.9	0.7
% selectivity to others	7.1	6.6	7.1	7.1	7.1	7.1	7.3	7.4	7.0	6.6	7.0	6.9	6.3	7.3	7.4	6.7	6.2	7.0	7.0
	WHSV = 1.0 g/g.h																		
TOS (days)	19.0	19.2	19.7	19.9	20.0	20.6	21.1	21.7	21.9	22.0	22.8	23.2	23.9	24.2	24.7	25.0	25.7	25.9	26.0
% conversion	40.3	51.4	38.6	38.4	38.1	37.0	42.0	36.2	35.1	35.3	34.2	33.5	32.1	26.9	33.6	32.4	36.6	32.0	31.1
% selectivity to dimers	91.9	91.8	92.3	92.4	91.4	92.1	92.1	92.3	86.2	86.8	91.6	92.0	91.9	91.9	92.4	92.2	92.0	92.1	92.6
% selectivity to trimers	1.0	1.1	0.7	0.7	1.6	0.7	0.5	0.5	0.4	0.0	0.5	0.4	0.4	0.4	0.4	0.4	0.3	0.3	0.4
% selectivity to others	7.1	7.1	7.0	6.9	6.9	7.1	7.4	7.2	13.4	13.2	7.9	7.6	7.7	7.7	7.2	7.4	7.6	7.6	7.1
	WHSV = 1.0 g/g.h																		
TOS (days)	26.7	27.7	28.1	28.7	28.9	29.1	29.7	29.8	29.9	30.1	30.7	30.8	30.9	31.0	31.7	31.8	32.1	32.7	32.9
% conversion	35.0	33.9	33.8	31.4	35.5	32.7	32.3	32.5	38.4	32.6	32.3	31.9	32.1	35.3	34.5	35.5	32.2	34.7	31.9
% selectivity to dimers	91.3	92.1	92.5	92.6	92.5	92.4	92.4	92.4	92.0	92.4	92.3	92.4	92.2	92.2	92.3	92.3	92.3	92.1	92.4
% selectivity to trimers	0.4	0.4	0.5	0.2	0.4	0.4	0.4	0.4	0.5	0.3	0.4	0.4	0.4	0.4	0.3	0.4	0.4	0.3	0.3
% selectivity to others	8.2	7.5	7.1	7.1	7.2	7.3	7.3	7.2	7.6	7.3	7.3	7.3	7.4	7.4	7.4	7.3	7.3	7.6	7.3
	WHSV = 1.0 g/g.h								power failure										
TOS (days)	33.0	33.1	33.9	34.7	35.1	35.7	36.0	36.7	36.8	37.0	37.0	37.7	37.8	38.0	38.7	39.6	39.7	40.0	40.7
% conversion	35.7	34.7	30.5	29.5	36.3	33.1	32.9	36.1	9.4	1.6	8.7	30.2	30.0	32.6	29.6	25.8	25.0	20.8	27.1
% selectivity to dimers	91.9	92.1	91.8	91.8	91.8	91.4	91.7	91.8	87.5	69.6	89.1	88.6	91.1	91.0	91.3	91.2	91.2	90.6	91.3
% selectivity to trimers	0.4	0.3	0.3	0.3	0.3	0.4	0.4	0.3	0.8	5.0	1.0	0.8	0.3	0.3	0.3	0.3	0.4	0.3	0.3
% selectivity to others	7.7	7.6	7.9	7.9	7.9	8.3	7.9	7.9	11.7	25.4	9.9	10.6	8.6	8.7	8.4	8.5	8.4	9.1	8.4

Reaction conditions and reference:	1-Hexene feed, H-ZSM-5 catalyst, 170 °C, 40 bar and WHSV of 1.0 and 0.5 g/g.h; Figure 5-3 (continued)																		
	WHSV = 1.0 g/g.h																		
TOS (days)	40.9	41.1	41.7	41.9	42.0	42.7	42.8	43.0	43.7	44.0	44.7	44.9	45.7	45.8	46.0	46.8	46.9	47.0	47.7
% conversion	22.1	24.9	25.9	26.0	26.3	26.0	25.3	25.7	25.0	25.0	24.7	25.0	26.1	26.6	27.8	25.8	23.4	29.9	23.3
% selectivity to dimers	91.1	77.1	91.3	91.0	90.6	91.4	91.9	91.3	91.2	91.3	90.9	91.3	91.4	91.5	92.1	91.7	91.7	92.2	91.5
% selectivity to trimers	0.3	0.3	0.3	0.3	0.3	0.3	0.4	0.5	0.6	0.5	0.5	0.5	0.4	0.4	0.3	0.3	0.3	0.3	0.3
% selectivity to others	8.5	22.6	8.4	8.7	9.0	8.3	7.8	8.3	8.2	8.2	8.7	8.3	8.2	8.1	7.5	8.0	8.0	7.5	8.1

Reaction conditions and reference:	1-Hexene feed, H-ZSM-5 catalyst, 170 °C, 10-20 bar and WHSV of 0.5 g/g.h; Figure 5-4																		
	10bar										20 bar								
TOS (days)	1.0	1.1	1.2	1.3	1.9	2.0	2.3	2.9	3.1	3.4	3.9	4.0	4.2	4.3	4.9	5.0	5.1	5.1	5.2
% conversion	80.5	76.7	79.9	77.5	77.0	76.5	78.2	78.0	76.2	74.3	74.1	74.6	75.1	75.2	74.2	74.1	73.8	72.9	73.7
% selectivity to dimers	83.3	92.2	84.4	91.9	85.3	92.9	83.5	83.1	91.5	91.8	90.1	91.6	92.1	91.9	92.3	90.7	92.2	92.9	88.9
% selectivity to trimers	10.2	1.6	9.6	2.5	8.8	1.4	10.8	11.2	2.0	2.2	4.1	1.7	1.7	2.2	2.1	2.5	1.6	1.3	5.4
% selectivity to others	6.4	6.1	5.9	5.6	5.9	5.8	5.6	5.7	6.5	6.1	5.8	6.7	6.2	5.9	5.6	6.8	6.2	5.8	5.7
	20 bar																		
TOS (days)	5.3	5.9	6.1	6.2	6.9	7.2	7.9	8.2	9.5	9.8	10.5	10.8	11.4	11.6	11.8	12.4	12.6	12.7	12.8
% conversion	72.1	72.0	71.8	70.7	70.9	70.9	70.9	67.2	70.4	68.9	68.4	66.7	67.0	67.2	66.8	63.8	52.4	15.8	12.9
% selectivity to dimers	92.2	85.0	88.9	90.8	88.7	88.7	88.7	88.8	85.6	85.5	86.1	91.5	90.8	92.0	90.6	88.1	93.6	91.0	90.4
% selectivity to trimers	2.1	9.9	5.3	3.4	3.2	3.4	3.2	5.5	9.1	8.9	8.0	2.2	3.1	1.9	3.5	6.3	1.4	0.0	0.0
% selectivity to others	5.7	5.1	5.9	5.8	8.0	7.9	8.0	5.7	5.3	5.6	5.9	6.3	6.0	6.1	6.0	5.6	5.0	9.0	9.6
	20 bar																		
TOS (days)	13.4	13.5	13.6	14.4	14.7	14.8	15.4	15.6	15.7	15.8	16.4	16.6	16.7	16.8	17.4	17.7	17.8	18.4	18.6
% conversion	60.3	62.6	59.8	61.5	61.7	62.3	61.0	60.7	59.7	59.8	59.1	59.3	59.1	61.2	58.1	59.1	60.3	57.1	56.9
% selectivity to dimers	87.3	91.6	94.1	90.0	88.8	88.0	90.7	91.5	92.9	92.7	92.1	92.7	93.0	87.5	92.3	92.4	87.4	90.7	87.7
% selectivity to trimers	6.7	2.5	0.5	4.4	5.6	6.7	3.7	2.7	1.6	1.5	2.1	1.3	1.0	7.2	0.9	1.3	6.5	3.7	0.9
% selectivity to others	6.0	5.9	5.4	5.7	5.5	5.3	5.6	5.9	5.5	5.8	5.8	6.1	6.0	5.3	6.8	6.4	6.2	5.6	11.4

Reaction conditions and reference:	1-Hexene feed, H-ZSM-5 catalyst, 150 °C, 40 bar and WHSV of 0.5 g/g.h; Figure 5-5																		
TOS (days)	0.9	1.0	1.1	1.2	1.8	1.9	2.0	2.1	2.8	2.9	2.9	3.2	4.7	4.8	4.9	5.0	5.1	5.7	5.8
% conversion	68.7	67.0	64.1	61.8	54.3	51.1	49.8	48.3	43.9	42.1	41.9	40.4	37.5	37.0	35.7	37.3	37.3	35.1	33.2
% selectivity to dimers	92.6	86.4	90.7	93.7	94.4	95.4	95.3	96.3	95.1	96.3	96.6	95.0	97.2	97.1	96.5	97.2	97.3	97.5	97.6
% selectivity to trimers	2.7	3.4	1.8	2.4	2.1	1.6	1.7	0.8	2.1	1.0	0.8	2.8	0.5	0.5	1.1	0.6	0.6	0.3	0.2
% selectivity to others	4.7	10.2	7.5	3.9	3.4	2.9	3.0	2.9	2.8	2.7	2.5	2.2	2.3	2.3	2.4	2.2	2.1	2.2	2.2

Reaction conditions and reference:	1-Hexene feed, H-ZSM-5 catalyst, 160 °C, 40 bar and WHSV of 0.5 g/g.h; Figure 5-5																		
TOS (days)	1.0	2.5	2.6	2.7	2.7	3.4	3.6	4.6	4.7	4.8	4.8	5.4	5.6	5.7	5.8	6.5	6.6	6.6	7.6
% conversion	62.2	56.9	56.5	57.9	56.0	55.7	55.0	53.6	48.1	52.7	51.0	49.9	49.9	49.4	49.1	48.6	48.9	49.2	48.3
% selectivity to dimers	93.8	94.1	93.9	92.7	95.0	94.1	94.6	94.3	92.0	94.9	95.4	95.1	95.6	95.5	95.4	95.9	95.8	96.0	95.5
% selectivity to trimers	2.3	2.0	2.0	1.3	1.1	2.0	1.3	2.0	3.6	1.1	1.1	1.7	1.4	1.3	1.5	0.9	1.0	0.7	0.9
% selectivity to others	3.8	3.9	4.1	5.9	3.9	3.9	4.1	3.7	4.3	4.0	3.6	3.2	3.1	3.2	3.1	3.2	3.2	3.2	3.6

Reaction conditions and reference:	1-Hexene feed, H-ZSM-5 catalyst, 170 °C, 40 bar and WHSV of 0.15-2.0 g/g.h; Figure 5-7 and Table 5-5 (set#1)																		
	WHSV = 0.35 g/g.h									WHSV = 0.25 g/g.h									
TOS (days)	1.1	1.9	2.2	2.9	3.3	3.9	4.2	4.9	5.0	5.2	5.4	5.8	6.2	7.0	7.8	8.1	8.9	9.2	9.9
% conversion	64.9	58.7	57.3	56.9	55.0	54.8	54.8	54.9	54.1	55.0	53.6	58.2	63.0	65.1	65.8	63.2	61.2	58.3	58.6
% selectivity to dimers	85.3	91.7	90.2	88.8	92.7	92.7	87.2	86.1	88.6	88.6	87.2	85.5	84.3	83.8	83.6	89.2	88.3	84.8	81.4
% selectivity to trimers	9.4	2.7	4.1	5.8	1.4	1.3	7.6	8.0	1.3	6.3	7.6	8.2	8.8	9.7	9.5	3.9	5.8	3.3	6.3
% selectivity to others	5.3	5.6	5.7	5.4	5.9	6.0	5.1	5.9	10.1	5.1	5.1	6.3	6.9	6.5	6.9	6.9	5.9	11.8	12.2
	WHSV = 0.25 g/g.h																		
TOS (days)	10.3	10.9	11.3	11.9	12.2	12.4	13.0	13.9	14.2	14.9	15.2	15.9	16.3	17.0	17.2	17.9	18.2	19.0	19.3
% conversion	56.5	54.2	53.4	52.7	52.7	54.0	53.9	52.5	50.9	52.0	51.0	51.7	50.9	48.6	48.5	47.5	46.6	46.6	46.1
% selectivity to dimers	85.3	87.2	86.8	84.2	86.7	87.0	86.5	85.8	88.7	87.3	87.7	87.3	84.6	87.7	88.0	87.8	88.5	88.0	87.6
% selectivity to trimers	1.7	1.0	1.9	4.6	1.1	1.2	1.4	2.9	1.2	1.0	1.0	0.3	3.8	1.3	0.6	0.8	0.7	1.1	0.8
% selectivity to others	13.0	11.8	11.3	11.2	12.2	11.8	12.1	11.3	10.1	11.7	11.3	12.4	11.6	11.0	11.5	11.4	10.8	10.9	11.6
	WHSV = 0.25 g/g.h									WHSV = 0.15 g/g.h									
TOS (days)	20.1	20.4	20.9	21.2	21.9	22.2	22.9	23.3	24.0	24.2	24.9	25.4	25.8	26.0	26.3	27.0	27.4	27.9	28.2
% conversion	47.9	49.0	49.0	48.9	48.6	48.5	48.4	45.1	80.4	83.7	82.3	81.7	78.1	82.5	84.7	83.6	83.2	85.4	87.5
% selectivity to dimers	88.6	88.2	87.6	87.9	88.2	87.8	87.6	91.7	71.4	72.7	72.0	72.4	74.1	77.4	71.1	72.7	73.5	71.8	70.0
% selectivity to trimers	0.9	1.1	1.3	0.7	1.0	1.0	1.2	0.9	10.3	10.5	10.6	10.2	9.0	2.6	11.3	9.4	8.8	9.7	11.3
% selectivity to others	10.6	10.7	11.1	11.4	10.7	11.3	11.2	7.4	18.3	16.7	17.4	17.4	16.9	19.9	17.6	17.9	17.7	18.5	18.7
	WHSV = 0.15 g/g.h																		
TOS (days)	28.9	29.3	29.9	30.2	30.9	31.4	31.9	32.3	32.9	33.3	33.9	34.2	34.9	35.2	35.9	36.2	37.0	38.0	38.8
% conversion	86.6	85.7	86.1	83.3	82.7	81.5	80.1	79.8	78.7	79.8	79.5	80.3	79.8	79.5	75.1	78.2	78.1	74.3	69.7
% selectivity to dimers	72.4	76.9	71.3	73.6	73.6	74.2	75.5	79.3	78.4	77.7	79.1	74.6	75.0	74.0	82.8	78.7	76.0	76.7	78.2
% selectivity to trimers	10.5	3.9	10.1	9.1	8.7	8.6	8.9	2.5	5.3	4.5	2.8	8.3	7.2	7.9	0.1	4.0	7.1	6.9	6.5
% selectivity to others	17.1	19.2	18.6	17.2	17.7	17.2	15.6	18.2	16.3	17.7	18.0	17.1	17.8	18.1	17.1	17.3	16.9	16.4	15.2

	WHSV = 0.15 g/g.h						WHSV = 2.0 g/g.h									WHSV = 1.5 g/g.h			
TOS (days)	39.2	39.8	40.2	40.8	40.9	41.8	41.9	42.1	42.1	42.1	42.2	42.3	42.8	43.2	43.2	43.7	43.8	43.9	44.1
% conversion	66.7	65.9	65.2	63.6	64.3	64.4	46.7	10.8	10.5	10.9	11.1	10.9	11.7	12.9	14.9	17.4	15.7	12.7	15.5
% selectivity to dimers	80.9	82.2	82.6	84.5	85.1	83.7	85.2	86.3	86.8	86.7	86.6	85.3	85.9	86.1	86.9	85.8	86.4	82.8	85.6
% selectivity to trimers	2.9	2.8	2.8	1.4	1.7	1.6	1.4	0.0	0.0	0.0	0.0	0.0	0.0	0.0	0.0	0.0	0.0	0.0	0.0
% selectivity to others	16.3	15.0	14.6	14.0	13.2	14.7	13.4	13.7	13.2	13.3	13.4	14.7	14.1	13.9	13.1	14.2	13.6	17.2	14.4
Reaction conditions and reference:	1-Hexene feed, H-ZSM-5 catalyst, 170 °C, 40 bar and WHSV of 0.15-2.0 g/g.h; Figure 5-7 and Table 5-5 (set#1)																		
	WHSV = 1.5 g/g.h						WHSV = 0.5 g/g.h												
TOS (days)	44.3	44.7	44.8	44.9	45.1	45.3	45.8	46.2	46.9	47.9	48.1	48.3	48.8	49.2	49.8	50.1	50.8	51.8	52.1
% conversion	15.5	15.3	15.2	15.2	14.9	15.3	14.4	19.7	69.6	75.6	62.5	51.4	46.3	47.6	45.7	44.4	44.0	45.4	45.0
% selectivity to dimers	85.2	86.2	86.4	85.7	85.6	86.4	85.8	85.9	73.8	76.6	79.1	84.5	85.5	84.3	84.5	85.5	85.3	85.2	85.3
% selectivity to trimers	0.0	0.0	0.0	0.0	0.0	0.0	0.0	0.1	4.7	4.8	4.8	1.0	0.4	0.6	0.4	0.4	0.3	0.4	0.4
% selectivity to others	14.8	13.8	13.6	14.3	14.4	13.6	14.2	14.1	21.5	18.6	16.1	14.5	14.2	15.1	15.1	14.1	14.4	14.3	14.3

Reaction conditions and reference:	1-Hexene feed, H-ZSM-5 catalyst, 170 °C, 40 bar and WHSV of 0.5-3.0 g/g.h; Table 5-5 (set#2)																		
	WHSV = 0.5 g/g.h																		
TOS (days)	0.1	0.2	0.3	0.4	0.9	1.5	2.7	2.5	2.9	3.1	3.2	3.9	4.1	4.9	5.0	5.3	5.4	5.9	6.3
% conversion	71.7	14.9	24.5	66.2	78.1	71.9	71.7	69.3	73.1	75.2	72.9	74.3	75.6	74.1	73.4	73.2	71.7	72.9	75.0
% selectivity to dimers	44.0	7.5	92.3	86.7	89.7	92.8	87.1	93.3	89.4	83.9	90.4	90.0	84.6	92.2	90.9	92.5	91.4	91.5	82.8
% selectivity to trimers	0.0	0.0	0.5	5.7	2.7	0.2	2.4	2.9	4.5	9.7	1.5	3.2	9.2	1.8	2.8	1.5	0.4	1.3	11.0
% selectivity to others	56.0	92.5	7.2	7.6	7.6	7.1	10.5	3.9	6.1	6.4	8.1	6.8	6.3	6.0	6.3	6.0	8.2	7.3	6.2
	WHSV = 1.0 g/g.h						WHSV = 1.5 g/g.h									WHSV = 0.5 g/g.h			
TOS (days)	6.9	7.1	7.3	7.9	8.0	8.1	8.2	8.3	8.9	9.1	9.3	9.9	10.0	10.0	10.1	10.2	10.2	10.5	10.9
% conversion	71.3	71.2	69.6	81.5	52.9	49.3	45.4	49.7	49.4	49.8	50.5	49.6	30.9	57.1	40.3	34.1	31.7	32.9	32.1
% selectivity to dimers	92.0	87.7	91.3	74.2	92.9	94.2	94.8	93.2	94.3	93.0	93.3	93.1	95.4	91.8	93.3	95.0	92.2	90.9	95.6
% selectivity to trimers	1.4	6.3	1.8	8.6	2.1	0.8	0.0	2.1	0.8	1.7	1.6	1.0	0.1	2.3	1.4	0.2	0.6	0.6	0.3
% selectivity to others	6.6	6.0	6.8	17.2	5.0	5.1	5.2	4.7	4.9	5.3	5.1	5.9	4.5	5.9	5.3	4.9	7.2	8.5	4.1
	WHSV = 2.0 g/g.h						WHSV = 3.0 g/g.h									WHSV = 0.5 g/g.h			
TOS (days)	11.3	11.5	11.9	12.1	12.3	12.4	12.9	13.0	13.0	13.2	13.2	13.3	13.9	14.0	14.0	14.1	14.2	14.9	15.0
% conversion	30.3	28.8	30.0	28.9	29.0	24.3	26.1	26.0	20.6	21.5	21.8	20.9	18.8	19.5	19.8	17.7	51.9	52.3	71.5
% selectivity to dimers	95.2	95.7	95.6	94.9	95.5	95.8	95.8	95.7	95.2	95.4	95.3	95.2	95.2	95.3	95.4	94.1	90.4	91.2	84.6
% selectivity to trimers	0.2	0.0	0.1	0.5	0.2	0.0	0.0	0.0	0.0	0.0	0.0	0.0	0.0	0.0	0.0	0.0	1.0	2.6	4.0
% selectivity to others	4.6	4.3	4.2	4.6	4.3	4.2	4.2	4.3	4.8	4.6	4.7	4.8	4.8	4.7	4.6	5.9	8.7	6.2	11.4

Reaction conditions and reference:	1-Hexene feed, H-ZSM-5 catalyst, 170 °C, 40 bar and WHSV of 0.5-3.0 g/g.h; Table 5-5 (set#2)					
	WHSV = 0.5 g/g.h					
TOS (days)	15.1	15.3	15.9	16.1	16.2	16.3
% conversion	72.4	69.9	69.3	70.2	69.0	68.3
% selectivity to dimers	84.0	91.1	85.3	91.4	89.4	90.4
% selectivity to trimers	9.7	1.6	7.9	2.7	3.6	2.9
% selectivity to others	6.3	7.3	6.8	5.9	6.9	6.7

Reaction conditions and reference:	1-Hexene feed, H-ZSM-5 catalyst, 170 °C, 40 bar and WHSV of 0.5 g/g.h; 2,4,6-collidine (65ppm) co-fed in the 1-hexene feed; Figure 5-8								
TOS (days)	2.8	2.9	3.1	3.3	3.8	3.9	4.0	4.1	4.2
% conversion	21.1	17.1	15.2	13.6	9.9	7.1	4.9	4.6	4.2
% selectivity to dimers	84.1	84.7	84.7	84.3	81.8	79.9	74.7	75.7	75.4
% selectivity to trimers	0.0	0.0	0.0	0.0	0.0	0.0	0.0	0.0	0.0
% selectivity to others	15.9	15.3	15.3	15.7	18.2	20.1	25.3	24.3	24.6

Reaction conditions and reference:	1-Hexene feed, H-ZSM-5 catalyst, 170 °C, 40 bar and WHSV of 0.5 g/g.h; 2,4-di- <i>tert</i> -butylpyridine (65ppm) co-fed in the 1-hexene feed; Figure 5-9								
TOS (days)	0.7	0.8	0.9	1.0	1.1	1.7	1.9	2.1	2.7
% conversion	6.3	6.2	5.7	5.3	5.3	4.4	3.5	3.3	2.8
% selectivity to dimers	64.9	68.8	71.3	72.1	72.9	72.7	70.6	70.1	69.4
% selectivity to trimers	0.0	0.0	0.0	0.3	0.0	0.0	0.0	0.0	0.0
% selectivity to others	35.1	31.2	28.7	27.6	27.1	27.3	29.4	29.9	30.6

2. 1-Octene over H-ZSM-5 catalyst

Reaction conditions and reference:	1-Octene feed, H-ZSM-5 catalyst, 170 °C, 40 bar and WHSV of 1.0 g/g.h; Figure 5-10				
TOS (days)	5.1	5.2	5.3	5.4	5.6
% conversion	33.0	32.4	32.5	32.7	32.9
% selectivity to dimers	88.2	88.1	88.2	88.7	88.7
% selectivity to trimers	0.0	0.0	0.0	0.0	0.0
% selectivity to others	11.8	11.9	11.8	11.3	11.3

Reaction conditions and reference:	1-Octene feed, H-ZSM-5 catalyst, 170 °C, 40 bar and WHSV of 0.25 g/g.h; Figure 5-11 and Table 5-7																		
TOS (days)	0.9	1.0	1.2	2.0	2.3	3.0	3.3	3.9	4.2	4.9	5.2	5.8	6.2	6.8	7.2	8.0	8.9	10.3	10.8
conversion	71.2	79.3	80.1	70.8	55.5	51.6	49.4	48.7	46.5	45.1	49.5	50.5	55.8	50.3	53.9	55.5	51.5	44.9	44.9
% selectivity to dimers	84.4	83.7	84.3	85.7	89.0	88.6	88.6	88.5	87.5	87.0	87.1	87.2	86.6	86.8	86.7	87.2	86.2	86.6	86.3
% selectivity to trimers	0.0	0.0	0.0	0.0	0.0	0.0	0.0	0.0	0.0	0.0	0.0	0.0	0.0	0.0	0.0	0.0	0.0	0.0	0.0
% selectivity to others	15.6	16.3	15.7	14.3	11.0	11.4	11.4	11.5	12.5	13.0	12.9	12.8	13.4	13.2	13.3	12.8	13.8	13.4	13.7
TOS (days)	11.0	11.2	11.9	12.3	12.8	13.2	13.8	14.2	14.8	15.2	15.8	16.4	16.9						
% conversion	43.5	44.6	45.7	43.5	41.7	44.9	43.9	44.4	43.1	48.5	53.8	54.9	48.3						
% selectivity to dimers	85.9	86.7	86.6	85.4	85.7	87.0	86.5	86.5	85.8	85.0	86.1	84.7	84.9						
% selectivity to trimers	0.0	0.0	0.0	0.0	0.0	0.0	0.0	0.0	0.0	0.0	0.0	0.0	0.0						
% selectivity to others	14.1	13.3	13.4	14.6	10.1	13.0	13.5	13.5	14.2	15.0	13.9	15.3	15.1						

Reaction conditions and reference:	1-Octene feed, H-ZSM-5 catalyst, 170 °C, 40 bar and WHSV of 0.35 g/g.h; Table 5-7																		
TOS (days)	0.9	1.1	1.5	1.6	1.7	1.9	2.1	2.6	2.9	3.0	3.6	4.6	5.6	6.6	7.4	8.2	8.8	9.1	9.7
% conversion	28.2	51.3	39.5	3.5	1.3	21.3	34.4	34.7	29.4	20.6	34.6	35.4	35.6	38.5	36.6	35.3	37.2	31.4	35.9
% selectivity to dimers	89.1	88.3	89.7	86.8	84.1	90.1	90.0	89.8	91.2	89.7	90.4	89.8	89.9	90.1	89.5	89.6	90.8	87.7	90.1
% selectivity to trimers	0.0	0.0	0.0	0.0	0.0	0.0	0.0	0.0	0.0	0.0	0.0	0.0	0.0	0.0	0.0	0.0	0.0	0.0	0.0
% selectivity to others	10.9	11.7	10.3	13.2	15.9	9.9	10.0	10.2	8.8	10.3	9.6	10.2	10.1	9.9	10.5	10.4	9.2	12.3	9.9
TOS (days)	10.1	10.7	11.7	12.0	12.7	12.8	13.7	14.4	15.2	15.4	16.1	16.5							
% conversion	31.2	34.4	34.1	33.8	33.5	34.2	33.3	29.1	33.4	40.1	39.3	32.4							
% selectivity to dimers	86.8	89.8	89.8	89.7	89.5	89.0	89.6	84.5	88.1	79.8	76.5	72.1							
% selectivity to trimers	0.0	0.0	0.0	0.0	0.0	0.0	0.0	0.0	0.0	0.0	0.0	0.0							
% selectivity to others	13.2	10.2	10.2	10.3	10.5	11.0	10.4	9.5	11.9	20.2	23.5	27.9							

Reaction conditions and reference:	1-Octene feed, H-ZSM-5 catalyst, 170 °C, 40 bar and WHSV of 0.5 g/g.h; Tables 5-7 and 5-10																		
TOS (days)	0.7	0.9	1.1	1.3	1.7	2.0	2.8	3.7	4.0	4.8	5.1	5.8	6.1	6.8	7.1	7.8	8.0	8.2	8.9
% conversion	50.8	49.4	44.0	38.4	34.2	32.2	32.3	27.0	31.3	35.1	34.7	30.6	29.4	29.7	30.1	30.9	29.7	31.5	32.3
% selectivity to dimers	84.9	87.2	87.2	87.6	87.5	87.5	87.1	85.1	86.3	85.5	86.2	85.9	85.7	85.7	84.2	86.2	85.5	86.0	85.9
% selectivity to trimers	0.0	0.0	0.0	0.0	0.0	0.0	0.0	0.0	0.0	0.0	0.0	0.0	0.0	0.0	0.0	0.0	0.0	0.0	0.0
% selectivity to others	15.1	12.8	12.8	12.4	12.5	12.5	12.9	14.9	13.7	14.5	13.8	14.1	14.3	14.3	15.8	13.8	14.5	14.0	14.1

Reaction conditions and reference:	1-Octene feed, H-ZSM-5 catalyst, 170 °C, 40 bar and WHSV of 1.0 g/g.h; Table 5-7																		
TOS (days)	0.9	0.9	1.6	1.8	1.9	2.1	2.6	2.7	2.9	2.9	3.7	4.0	4.6	5.0	5.6	6.0	6.6	7.0	7.6
% conversion	17.6	15.3	14.3	14.2	16.8	23.1	16.4	14.6	15.3	15.3	23.5	25.0	23.4	19.6	19.3	21.3	21.0	19.1	21.6
% selectivity to dimers	85.4	85.5	84.9	85.0	86.2	87.4	85.0	85.0	85.8	85.8	86.5	85.1	86.2	85.3	86.3	88.8	88.9	87.7	89.0
% selectivity to trimers	0.0	0.0	0.0	0.0	0.0	0.0	0.0	0.0	0.0	0.0	0.0	0.0	0.0	0.0	0.0	0.0	0.0	0.0	0.0
% selectivity to others	14.6	14.5	15.1	15.0	13.8	12.6	15.0	15.0	14.2	14.2	13.5	14.9	13.8	14.7	13.7	11.2	11.1	12.3	11.0

Reaction conditions and reference:	1-Octene feed, H-ZSM-5 catalyst, 170 °C, 40 bar and WHSV of 2.0 g/g.h; Table 5-7														
TOS (days)	0.1	0.3	0.4	1.0	1.2	1.3	1.3	1.5	2.0	2.2	2.3	3.0	3.2	3.6	4.0
% conversion	15.9	28.6	13.9	11.4	12.1	14.4	13.4	13.6	15.0	17.5	15.5	12.7	11.9	13.0	13.4
% selectivity to dimers	89.1	90.4	89.2	88.3	90.7	92.3	91.9	89.9	92.4	91.7	91.4	91.3	91.0	91.4	91.4
% selectivity to trimers	0.0	0.0	0.0	0.0	0.0	0.0	0.0	0.0	0.0	0.0	0.0	0.0	0.0	0.0	0.0
% selectivity to others	10.9	9.6	10.8	11.7	9.3	7.7	8.1	10.1	7.6	8.3	8.6	8.7	9.0	8.6	8.6

Reaction conditions and reference:	1-Octene feed, H-ZSM-5 catalyst, 100-210 °C, 40 bar and WHSV of 1.0 g/g.h; Figure 5-10																			
	100 °C			120 °C				140 °C					150 °C					160 °C		
TOS (days)	0.2	0.4	0.5	1.1	1.1	1.3	1.4	2.0	2.1	2.2	2.3	2.4	3.0	3.1	3.2	3.3	3.4	4.0	4.1	
% conversion	1.7	0.9	1.0	3.6	4.3	4.6	4.3	9.4	11.8	9.7	9.9	15.1	15.4	15.7	16.2	17.2	15.9	23.3	24.6	
% selectivity to dimers	88.5	91.7	91.1	89.8	85.8	88.1	89.3	89.8	91.1	90.1	88.0	90.1	88.7	87.2	91.2	90.0	91.0	89.5	87.3	
% selectivity to trimers	0.0	0.0	0.0	0.0	0.0	0.0	0.0	0.0	0.0	0.0	0.0	0.0	0.0	0.0	0.0	0.0	0.0	0.0	0.0	
% selectivity to others	11.5	8.3	8.9	10.2	14.2	11.9	10.7	10.2	8.9	9.9	12.0	9.9	11.3	12.8	8.8	10.0	9.0	10.5	12.7	
	160 °C			170 °C							180 °C					190 °C				
TOS (days)	4.2	4.3	4.4	5.0	5.1	5.1	5.2	5.3	5.4	5.6	6.0	6.1	6.2	6.4	6.6	7.2	7.4	7.6		
% conversion	21.9	26.8	26.4	30.7	33.5	33.0	32.4	32.5	32.7	32.9	38.1	46.8	44.4	46.3	51.7	60.9	61.3	67.1		
% selectivity to dimers	85.4	89.5	89.1	88.1	88.5	88.2	88.1	88.2	88.7	88.7	84.2	86.2	86.0	84.9	86.7	84.4	82.9	81.0		
% selectivity to trimers	0.0	0.0	0.0	0.0	0.0	0.0	0.0	0.0	0.0	0.0	0.0	0.0	0.0	0.0	0.0	0.0	0.0	0.0		
% selectivity to others	14.6	10.5	10.9	11.9	11.5	11.8	11.9	11.8	11.3	11.3	15.8	13.8	14.0	15.1	13.3	15.6	17.1	19.0		
	200 °C					210 °C														
TOS (days)	8.0	8.1	8.3	8.4	8.4	9.0	9.1	9.2	9.3	9.4										
% conversion	69.5	72.1	72.7	75.0	72.9	77.1	84.2	85.5	82.7	83.3										
% selectivity to dimers	74.9	77.0	78.6	79.5	78.7	70.1	73.9	74.8	71.0	70.2										
% selectivity to trimers	0.0	0.0	0.0	0.0	0.0	0.0	0.0	0.0	0.0	0.0										
% selectivity to others	25.1	23.0	21.4	20.5	21.3	29.9	26.1	25.2	29.0	29.8										

3. 1-Hexene over ASA catalyst

Reaction conditions and reference:	1-Hexene feed, ASA catalyst, 50-210 °C, 40 bar and WHSV of 0.5 g/g.h; Figure 5-12																		
	50 °C						75 °C								100 °C				
TOS (days)	0.6	0.7	0.8	0.9	1.0	1.1	1.6	1.7	1.7	1.8	1.9	2.0	2.0	2.6	2.7	2.8	2.9	3.0	
% conversion	11.1	16.0	16.3	17.0	21.7	23.7	16.6	28.6	33.4	35.8	36.9	39.2	41.2	47.5	66.1	70.8	71.4	76.3	
% selectivity to dimers	97.3	98.0	98.0	98.1	98.1	98.2	98.7	97.2	95.5	95.4	94.9	97.8	97.4	97.9	88.6	85.1	93.5	82.8	
% selectivity to trimers	1.8	1.5	1.4	1.3	1.4	1.4	0.7	2.2	4.0	4.1	4.7	1.8	2.2	1.6	9.9	13.1	4.5	15.4	
% selectivity to others	0.9	0.5	0.6	0.6	0.5	0.4	0.6	0.5	0.5	0.5	0.5	0.4	0.4	0.5	1.5	1.8	1.9	1.8	
	125 °C			150 °C			160 °C			170 °C				180 °C					
TOS (days)	3.6	3.7	3.8	4.6	4.8	5.0	5.7	5.8	6.0	6.6	6.7	6.8	6.9	7.0	7.6	7.7	7.8	7.9	8.0
% conversion	78.3	81.2	82.7	85.2	87.4	90.5	93.1	88.6	88.4	94.4	94.0	86.3	88.0	86.8	86.8	87.8	88.2	88.9	87.5
% selectivity to dimers	80.3	79.7	81.2	75.3	74.3	66.6	61.2	58.8	60.5	52.8	57.6	70.0	60.0	62.3	62.3	61.9	60.3	57.3	63.1
% selectivity to trimers	17.5	18.3	16.7	20.8	21.0	25.1	27.7	31.2	28.3	24.9	22.2	23.1	21.1	27.3	27.3	29.1	29.0	25.8	24.1
% selectivity to others	2.1	2.0	2.1	3.2	4.0	5.7	11.1	9.1	11.0	18.0	20.1	6.8	18.9	10.3	10.3	8.5	8.8	16.4	12.7
Reaction conditions and reference:	1-Hexene feed, ASA catalyst, 50-210 °C, 40 bar and WHSV of 0.5 g/g.h; Figure 5-12																		
	190 °C					200 °C				210 °C									
TOS (days)	8.6	8.8	8.9	9.0	9.0	9.7	9.8	9.9	10.6	11.0	11.6								
% conversion	85.0	84.1	86.1	86.2	35.6	36.8	70.4	78.1	83.6	91.3	81.2								
% selectivity to dimers	69.5	68.1	55.6	55.6	88.3	74.9	63.0	60.1	56.8	56.3	63.6								
% selectivity to trimers	7.4	8.7	23.1	19.8	2.2	6.0	9.1	11.0	13.0	5.6	1.6								
% selectivity to others	22.7	23.1	21.2	24.6	9.5	19.1	27.9	28.9	30.2	38.1	34.8								

4. 1-Octene over ASA catalyst

Reaction conditions and reference:	1-Octene feed, ASA catalyst, 150 °C, 40 bar and WHSV of 0.5 g/g.h; Figure 5-13																		
TOS (days)	0.8	1.0	1.9	2.9	3.1	3.9	4.8	5.1	5.2	5.8	6.1	6.2	7.1	8.0	8.9	9.7	10.4	10.7	11.4
% conversion	90.8	90.9	91.1	88.2	88.9	88.5	88.6	88.2	88.3	88.3	87.3	86.1	86.5	86.5	86.5	85.6	84.6	85.3	85.4
% selectivity to dimers	65.3	66.7	68.3	71.5	70.0	71.6	69.3	70.0	69.6	67.5	70.2	77.6	71.8	73.0	71.7	74.1	81.4	72.4	71.8
% selectivity to trimers	24.3	24.7	23.1	22.1	22.4	20.9	23.6	23.3	23.5	25.7	22.9	15.3	21.5	20.4	21.7	18.7	11.4	21.3	22.1
% selectivity to others	10.0	8.5	7.7	6.4	7.5	7.4	7.1	6.7	6.8	6.6	6.9	7.1	6.7	6.6	6.6	7.1	7.2	6.3	6.0

Reaction conditions and reference:	1-Octene feed, ASA catalyst, 150 °C, 40 bar and WHSV of 0.5 g/g.h; Figure 5-13 (continued)																		
TOS (days)	11.7	12.4	12.5	12.8	13.4	13.6	13.7	14.4	14.7	15.6	16.6	17.4	17.8	18.4	18.7	19.4	19.7	20.4	20.7
% conversion	85.0	85.7	85.5	85.4	85.1	85.8	85.8	86.5	86.0	84.6	84.8	84.8	85.0	84.7	84.9	84.8	84.9	84.3	82.8
% selectivity to dimers	71.1	72.6	71.1	73.4	77.7	72.0	71.8	70.0	71.5	79.0	73.4	73.4	72.5	75.3	73.5	76.7	73.6	75.6	75.0
% selectivity to trimers	23.1	21.1	22.8	20.3	15.5	21.6	21.9	23.6	22.0	13.8	20.1	20.3	21.2	18.4	20.2	16.6	20.4	18.3	19.5
% selectivity to others	5.8	6.3	6.0	6.3	6.8	6.3	6.1	6.3	6.4	7.2	6.4	6.3	6.3	6.4	6.3	6.6	5.9	6.1	5.5
TOS (days)	21.5	21.7	23.5	24.2	24.5	25.1	25.4	26.1	26.5	27.1	27.4	28.1	28.3	29.2	30.0	30.6	31.6		
% conversion	82.8	82.1	83.5	83.9	84.8	85.0	85.0	84.0	82.6	83.0	83.3	83.6	83.3	84.0	83.9	83.0	82.6		
% selectivity to dimers	76.1	78.7	76.0	76.4	73.5	74.1	74.1	73.6	75.7	75.3	74.4	75.9	76.1	73.3	74.8	78.0	76.2		
% selectivity to trimers	18.5	15.7	17.8	17.2	20.2	18.8	18.8	20.5	18.5	18.8	19.8	17.9	18.0	21.0	19.1	15.8	18.1		
% selectivity to others	5.4	5.7	6.1	6.3	6.3	7.1	7.1	6.0	5.8	5.9	5.8	6.1	5.9	5.7	6.1	6.2	5.6		

Reaction conditions and reference:	1-Octene feed, ASA catalyst, 150 °C, 40 bar and WHSV of 0.5 g/g.h; Figure 5-14						
TOS (days)	0.9	1.0	1.1	1.7	2.1	2.8	4.6
% conversion	59.0	59.5	60.5	65.3	66.5	68.5	68.4
% selectivity to dimers	90.9	90.6	90.8	89.2	89.4	89.9	89.4
% selectivity to trimers	0.0	0.1	0.1	1.5	0.1	0.2	0.7
% selectivity to others	9.1	8.6	9.0	8.0	10.5	9.9	9.9